Catalytic Hydroliquefaction of Lignin to Value-Added Chemicals

Ghafarnejad Parto, Soheila

Publication date:
2018

Document Version
Publisher's PDF, also known as Version of record

Catalytic Hydroliquefaction of Lignin to Value-Added Chemicals

Dissertation

To obtain

The Degree of Doctor of Philosophy

Technical University of Denmark

Department of Chemical and Biochemical Engineering

Soheila Ghafarnejad Parto

April 2018

Supervision by

Professor Anker Degn Jensen

Associate Professor Jakob Munkholt Christensen

Lars Saaby Pedersen

Abstract

Despite the high potential of lignin as a source of renewable aromatics, it is mainly treated as a low value product due to its recalcitrant character. The goal of this PhD study was to degrade lignin to fuels and higher value chemicals. To this end, lignin was dispersed in a solvent and treated at elevated temperature in the presence of a catalyst and under hydrogen pressure. Mainly conversion of lignosulfonate, as one of the major types of commercial lignin, was investigated. Lignosulfonate was provided by its world leading supplier, Borregaard A/S.

The role of solvent in degradation of lignosulfonate was evaluated in ethylene glycol and ethanol media at 250 ˚C using Ni based catalysts and 50 bar hydrogen. A similar yield of liquefied products was obtained by catalytic conversion in ethanol and ethylene glycol, being 31 and 32 wt%, respectively. It was observed that the solvent clearly affects the products of the degradation. The oil fractions from depolymerization in ethanol had lower molecular weight compared to the oil products obtained in ethylene glycol medium, indicating higher degree of degradation of liquefied products in ethanol. On the other hand, ethylene glycol showed superior activity in inhibiting condensation reactions and char formation; 16 and 46 wt% THF soluble and THF insoluble fractions were obtained from catalytic conversion of H-LS in ethanol, while those numbers from conversion in ethylene glycol medium were 45 and 23 wt%, respectively. Formation of char was only observed in ethanol medium. No effect was observed by changing the support material, which indicates that only Ni sites are active in hydrogenolysis of lignosulfonate. The presence of NiS in the spent catalyst was confirmed by X-ray crystallography and ion coupled plasma (ICP). It was suggested that Ni/NiS sites may catalyze the reaction via a sulfur removal cycle.

Lignosulfonate was further subjected to a reductive catalytic degradation over an alumina supported NiMo catalyst (provided by Haldor Topsøe A/S) in ethanol medium at 310 ˚C. A high oil yield and low char yield of 88 and 15 wt% were obtained, respectively, with catalyst: lignin: solvent ratio of 2 g: 10 g: 100 ml. The role of ethanol was prominent for the stabilization of reactive intermediates, which was catalyzed in the presence of NiMo. Simultaneous deoxygenation and desulfurization reactions took place in the presence of catalyst. The oxygen and sulfur content in the oil fraction obtained after 4 hours reaction time were 11.2 and 0.1 wt%, indicating considerable deoxygenation and desulfurization compared to the lignosulfonate feed (O: 30.8 wt%, S: 3.1 wt%), suggesting that this oil fraction can be used as a fuel additive or further be upgraded. It was noticeable that despite the high yields of degraded compounds in the presence of catalyst, the liquefied fractions were mainly within the range of dimers and oligomers. The reusability of the catalyst without any pretreatment was confirmed for at least two times.

In a further series of experiments, direct conversion of beech wood was targeted over a sulfided NiMo/Al_2O_3 catalyst (provided by Haldor Topsøe A/S) in ethanol medium at 300 ˚C. Biomass was converted into monomers and dimers, derived from lignin, and light hydrocarbons, originating from cellulose and hemicellulose. The main identified monomers were 4-propyl guaiacol (PG) and 4-propyl syringol (PS) with total monomer yield of 18.1 wt%

based on the Klason lignin content in beech wood. Studies of the influence of reaction temperature indicated that at 200 ˚C, the process targets only the lignin with a monomer yield of 12.1 wt% based on the Klason lignin content, while the holocellulose is conserved. The highest monomer yield of 20.0 wt% based on the Klason lignin content was obtained at 260 ˚C, indicating that the optimum temperature required for degradation of lignin fractions to monomers is within 200-260 ˚C. The direct conversion of biomass with high yield of lignin monomers showed promise compared to a two-step procedure involving isolation of lignin by the organosolv method and subsequent conversion of organosolv lignin. Here, a monomer yield of only 4.3 wt% was detected from conversion of organosolv lignin at 300 ˚C. Moreover, the oil from direct biomass conversion possessed a lower molecular weight compared to the oil from conversion of organosolv lignin.

Resumé

På trods af lignins store potentiale som kilde til bæredygtigt producerede aromatiske kemikalier betragtes lignin stadig som et produkt af lav værdi. Dette er på grund af lignins modstandsdygtighed over for nedbrydning til de aromatiske byggesten. Målet for dette PhD-projekt var at nedbryde lignin til brændstofkemikalier og kemikalier af højere værdi. For at opnå dette mål blev lignin dispergeret i et solvent og udsat for forhøjede temperaturer under et forhøjet tryk af brint. Der blev fokuseret på omdannelsen af lignosulfonat (LS), som en af de primære kommercielle lignintyper. Lignosulfonaten kommer fra Borregaard A/S, som er den ledende globale leverandør af lignosulfonat.

Solventets rolle i nedbrydningen af lignosulfonat blev undersøgt i ethylenglykol (EG) eller ethanol (EtOH) ved 250 °C med brug af en Ni-baserede katalysatorer og 50 bars brinttryk. Udbytterne af væskeformige lignin-derivater var meget ens i ethanol og ethylenglykol, nemlig 31 hhv. 32 vægt%. Det observeredes at solventet har en mærkbar effekt på nedbrydningsprodukterne. Oliefraktionerne fra depolymerisering i EtOH havde en laverer molvægt end olieprodukter dannet i EG mediet, hvilket indikerer en større grad af nedbrydning af de væskeformige produkter i EtOH. På den anden side viser EG sig bedre til at inhibere kondensationsreaktioner og kuldannelse. De THF-opløselige og THF-uopløselige produktandele var 16 hhv. 46 vægt% efter nedbrydning af H-LS i ethanol. Til sammenligning var værdierne fra omdannelse i ethylenglykol 45 hhv. 23 vægt%. Dannelsen af kul blev kun observeret med ethanol som solvent. Der blev ikke observeret nogen effekt af at ændre bærermaterialet for Ni katalysatoren, hvilket indikerer at kun Ni spiller en rolle i hydrogenolysen af lignosulfonat. Tilstedeværelsen af NiS i den brugte katalysator bekræftedes af røntgenkrystallografi og ion coupled plasma (ICP) spektroskopi. Det foreslås at Ni/NiS katalyserer nedbrydningsreaktionen via en cyklus hvor svovlfjernelse spiller en rolle.

Derudover blev lignosulfonat underkastet en reduktiv katalytisk nedbrydning over en alumina-båren NiMo katalysator (leveret af Haldor Topsøe A/S) i ethanolsolvent ved 310 °C. Der blev opnået et højt olieudbytte og et lavt kuludbytte på 88 hhv. 15 vægt% med et katalysator:lingnin:solvent forhold på 2 g:10 g:100 mL. Ethanol spillede en væsentlig rolle i stabiliseringen af de reaktive intermediære, og disse stabliserende reaktioner med ethanol synes også at være karalyseret af NiMo katalysatoren. Samtidig forløb der deoxygenerings- og afsvovlingsreaktioner under tilstedeværelse af katalysatoren. Indholdet af ilt og svovl i oliefraktionen opnået efter 4 timers reaktionstid var 11.2 hhv. 0.1 vægt%, hvilket indikerer betragtelig afiltning og afsvovling sammenlignet med den oprindelige lignosulfonat (O: 30.8 vægt%, S: 3.1 vægt%). Dette tyder på, at oliefraktionen kan anvendes som brændstof-additiv eller opgraderes yderligere til højkvalitets brændstof. Det var tydeligt, at på trods af de høje udbytter af nedbrudte specier, så bestod de væskeformige fraktioner fortrinsvis af specier i dimer- og oligomer-størrelse. Muligheden for at genbruge katalysatoren uden forbehandling blev bekræftet med mindst 2 gentagelser.

En yderligere forsøgsserie undersøgte den direkte omdannelse af birketræ over en sulfideret NiMo/Al_2O_3 katalysator (leveret af Haldor Topsøe A/S) i ethanolsolvent ved 300 °C.

Det observeredes at biomassens lignin blev omdannet til monomerer og dimerer, og derudover dannedes lette kulbrinter fra cellulosen og hemicellulosen. De primære identificerede monomerer var 4-Propyl guaiacol (PG) og 4-Propyl syringol (PS) med et samlet monomer-udbytte på 18.1 vægt% baseret op Klason ligninindholdet i birketræet. Undersøgelser af reaktionstemperaturens indflydelse indikerede at ved 200 °C omdannes kun ligninen og reaktionen gav et monomerudbytte på 12.1 vægt% baseret på Klason ligninindholdet, hvorimod cellulosefraktionerne er bevare. Det højeste monomerudbytte på 20.0 vægt% baseret på Klason ligninindholdet blev opnået ved 260 °C, hvilket indikerer at den optimale temperatur for nedbrydning af biomassens lignindel til monomerer er i temperaturområdet 200 -260 °C. Den direkte omdannelse af biomasse med et højt udbytte af lignin-monomerer er en lovende rute sammenlignet med 2-trins processer hvor ligninen først isoleres med organosolv-metoden og hvor organosolv-ligninen efterfølgende omdannes. Med denne metode blev der kun observeret et monomerudbytte på 4.3 vægt% ved 300 °C. Derudover havde olieproduktet fra den direkte biomasseomdannelse en lavere molekylevægt end olien fra omdannelse af organosolv lignin.

Preface and Acknowledgements

This PhD project has been funded equally by Technical University of Denmark (DTU) and BioValue platform, which includes Haldor Topsøe A/S and Borregaard. The project has been mainly conducted in the research center of Combustion and Harmful Emission Control (CHEC), Department of Chemical and Biochemical Engineering, DTU.

My special thanks and gratitude go to my PhD supervisor, Professor Anker Degn Jensen whose immense knowledge and experience in the research field has been the greatest asset to the project. It has been a great honor for me to work in his research team and learn from him. I was fortunate to have his insightful guidelines along my PhD and writing my thesis. His office was always open for me for scientific discussions. I would also like to thank my co-supervisor, Associate Professor. Jakob Munkholt Christensen, for his enthusiasm to mentor the project and widen my perspective in the subject. His scientific contribution in this thesis has been reflected in every chapter of this work. Lars Saaby Pedersen from Haldor Topsøe A/S is greatly thanked for co-supervising this project, giving feedbacks, and providing me analytical instruments at the company.

Haldor Topsoe A/S having a stake in the outcome of this research, openly allocated its resources to support this work. Peter Wiwel from the company R&D was very supportive and helpful in facilitating the use of the analytical facilities at the company. The eye-opening discussions we had on analyzing different materials made the tedious tasks smooth and efficient. Asger Baltzer Hansen is profoundly thanked for being instrumental in obtaining meaningful and accurate results from GC×GC analysis. I am so grateful for the great expertise he genuinely offered.

Most of this PhD was focused on catalytic conversion of lignosulfonate. My gratitude goes to Freddy Tjosås from Borregaard A/S, Norway for sharing his deep knowledge in the specifications of lignosulfonate, participating in the tele meetings and giving feedbacks.

I would like to thank the technicians at CHEC, who smooth the daily struggles with the lab work for the PhD students. My special thanks go to Anders Kjersgaard. Ander’s fun-loving personality along with his technical expertise came to support the lab tests when something went wrong with the setup.

I had the chance to share office with Assistant Professor Martin Høj. I am grateful for all the eye opening scientific discussions we had.

When I started my PhD studies at CHEC, I was surprised how the colleagues were supportive. I would like to thank Joachim Bachmann Nielsen, who has been very helpful in introducing me the laboratory and the setup and also relative analytical apparatus. When it comes to scientific supports, and also for the friendly chats, it is difficult to mention only a few names, so I would like to thank all my colleagues at CHEC. After long hours in the lab, when I was back to my office, it was heartwarming to see their office lights were ON. It reminded me that the hard work is the price we all pay for our enthusiasm and ambitions.

When I set off to leave my home country, Iran, and pursue my dreams, it was the support of my parents and my brother and sister who gave me the strength to overcome my fears. My parents always supported me and respect my decisions no matter what. Thanks to all of you who are always there for me in my difficulties and happiness.

I would like to have a word with my baby on the way: I am sorry if I unintentionally put you under stress over the last few months writing the thesis. The only thing that now I can think of is the moment I am keeping you in my arms.

Last but not least, my profound appreciation goes to my best life-long friend, Hassan, my husband, for his genuine and sincere support all the way from the beginning of this journey. You always kept me motivated even when you were in another continent. Thank you.

Soheila (Sonia) Ghafarnejad Parto

April 2018

List of Publications & Conference Contributions

Articles in Peer-Reviewed Journals

Soheila Ghafarnejad Parto, Jakob Munkholt Christensen, Lars Saaby Pedersen, Freddy Tjosås, and Anker Degn Jensen, *"Solvothermal conversion of lignosulfonate assisted by Ni catalyst: Investigation of the role of ethanol and ethylene glycol as solvents"*, to be submitted, 2018

Soheila Ghafarnejad Parto, Jakob Munkholt Christensen, Lars Saaby Pedersen, Freddy Tjosås, Asger Baltzer Hansen, Christian Danvad Damsgaard, Cristiano Spiga, Daniel Bo Larsen, Jens Øllgaard Duus, and Anker Degn Jensen, *"Liquefaction of lignosulfonate in supercritical ethanol using alumina supported NiMo catalyst: Analysis of the products and parameter study"*, to be submitted, 2018

Soheila Ghafarnejad Parto, Emma K. Jørgensen, Jakob Munkholt Christensen, Lars Saaby Pedersen, Daniel Bo Larsen, Jens Øllgaard Duus, and Anker Degn Jensen, *"One-pot catalytic conversion of beech wood and organosolv lignin over NiMo/Al_2O_3"*, to be submitted, 2018

Conference Contributions

Soheila Ghafarnejad Parto, Jakob Munkholt Christensen, Lars Saaby Pedersen, Freddy Tjosås, and Anker Degn Jensen, *"Solvothermal conversion of technical lignins over NiMo catalyst"*, Poster presentation at European Congress on Catalysis, EUROPACAT, 2017, Florence, Italy

Soheila Ghafarnejad Parto, Jakob Munkholt Christensen, Lars Saaby Pedersen, Freddy Tjosås, and Anker Degn Jensen, *"Solvothermal depolymerization of lignosulfonate"*, Oral presentation at Green Chemistry & Engineering Conference, 2017, Reston, USA

Soheila Ghafarnejad Parto, Jakob Munkholt Christensen, Lars Saaby Pedersen, Freddy Tjosås, and Anker Degn Jensen, *"Catalytic liquefaction of lignin to value-added chemicals"*, Oral presentation at Workshop on the Use of Lignocellulosic Biomass, 2016, Odense, Denmark

Soheila Ghafarnejad Parto, Jakob Munkholt Christensen, Lars Saaby Pedersen, Freddy Tjosås, and Anker Degn Jensen, *"Catalytic liquefaction of lignin to value-added chemicals"*, Poster presentation at the 2nd Lund Symposium on Lignin and Hemicellulose Valorisation, 2015, Lund, Sweden

Soheila Ghafarnejad Parto, Jakob Munkholt Christensen, Lars Saaby Pedersen, Freddy Tjosås, and Anker Degn Jensen, *"Catalytic conversion of lignin to value-added products: A review"*, Poster presentation at Catalysis: Fundamentals and Practice, 2015, Liverpool, England

Contents

List of Figures

List of Tables

Abbreviations

AR	Argon
BAS	Brønsted acid site
CEN	Carbon effective number
CO	Carbon monoxide
CoMo	Cobalt molybdenum
CR	Carbohydrate retention
DCO	Decarbonylation/ Decarboxylation
DDO	Direct deoxygenation
DEG	Diethylene glycol
DHE	Dihydroeugenol
DHE-OH	4-(3-hydroxypropyl)-2-methoxyphenol
DL	Delignification
DMDS	Dimethyl disulfide
DMPP	2,6-dimethoxy-4-propyl-phenol
DMSO	Dimethyl sulfoxide
EA	Ethyl guaiacol
EG	Ethylene glycol
EtOH	Ethanol
GC	Gas chromatography
GCV	Gross calorific value
GGGE	Guaiacyl glycerol beta guaiacyl ether
HDN	Hydrodenitrogenation
HDO	Hydrodeoxygenation
HDS	Hydrodesulfurization
Helium	He
HHV	High heating value
H-LS	Sulfonic acid lignosulfonate
HYD	Hydrogenation
ICP-EOS	Inductively coupled plasma-optical emission spectroscopy
i-EuOH	Isoeugenol

LAS	Lewis acid site
LFDE	Lignin first delignification
MCH	Methylcyclohexane
Mi-EuOH	Methoxyisoeugenol
Min	Minute
Mw	Weight average molecular weight
Mn	Number average molecular weight
MS	Mass spectrometer
Na-LS	Sodium lignosulfonate
NiMo	Nickel molybdenum
PA	Propyl guaiacol
PDI	Poly dispersity index
Pr-OH	Propanol
RRF	Relative response factor
SEC	Size exclusion chromatography
STM	Scanning tunneling microscopy
TCD	Thermal conductivity detector
TEG	Triethylene glycol
TEM-EDX	transmission electron microscopy energy-dispersive X-ray spectroscopy
THF	Tetrahydrofuran
TPD	Temperature programmed desorption
TPR	Temperature programmed reduction
TTEG	Tetraethylene glycol
2-Me-THF	2-Methyl tetrahydrofuran

Chapter 1:

Introduction

1. Introduction

The growth of the global population and depletion of the fossil-based fuels, beside the environmental effects of the greenhouse gasses, drives interest towards sustainable and carbon-neutral resources for energy supply [1]. Conversion of biomass is one of the main approaches for development of the renewable and non-fossil based fuels and chemicals [2]. The potential resources of biomass should not affect the food crops of the human and animals and also must not result in environmental degradation [3]. Agricultural waste products, sugar cane bagasse, wheat straw and rice stalk are some of the non-edible suitable biomass resources for the conversion to fuels and chemicals [3].

Lignocellulose constitutes the major part of biomass [4]. The cell walls of the lignocellulose is composed of carbohydrate polymers (cellulose and hemicellulose) and aromatic polymer (lignin) (see Figure 1) [3]. The content of the three constituents in the biomass vary depending on the source and the age of the plant. However, a typical distribution 35–50% cellulose, 20–35% hemicellulose, and 10–25% lignin is found in many plant species [5]. Cellulose and hemicellulose are conventionally used in pulp and paper industry. Moreover, new applications such as production of bio-fuel and chemicals from holocellulose are recently developed [6], [7]. Despite the high potential of lignin as a source of aromatic chemicals, it is mainly isolated from cellulose and hemicellulose as a low value by-product in paper industry and bio-ethanol production (regarded as ‘technical lignin’) and is mostly burned for the energy supply [8], [9]. In such treatments, the main focus is on extraction of high quality cellulose and hemicellulose, while lignin is significantly transformed during pretreatment [10]; some of the facile bonds in lignin structure such as C-O bonds are cleaved while more stable C-C bonds are formed [9], [11].

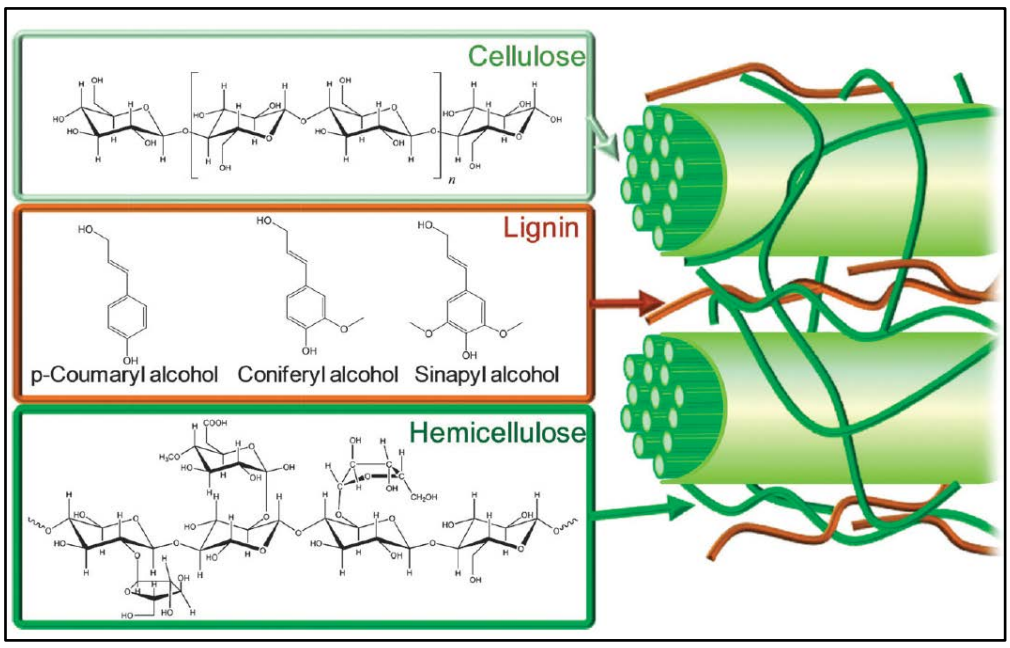

Figure 1 The main constituents of lignocellulosic biomass [6]

The current commercial applications of lignin are mainly limited to binder, dispersant or composite [12], owing to the presence of functional groups such as phenolic hydroxyl and carboxylic acids and possessing colloidal properties [13]. Vanillin is one of the commercial products from lignin; about 15% of the world vanillin supply is produced from oxidation of lignin [14]. Borregaard is the main producer of vanillin from lignosulfonate (a type of technical lignin produced from sulfite pulping) [15]. There are variety of chemicals and fuels that can be obtained from lignin through various conversion processes, which require an intensive research and the development effort in order to make them economically viable. Table 1 lists the most important chemicals which have high potential to be produced from lignin in near future and presents the current technology, production complexity and their market value [16].

Table 1: Chemicals and fuels from lignin with good industrialization potential [16].

Lignin derived product	Current technology status	Production complexity	Market volume
BTX* and higher alkylates	Medium	Medium	No data
Cyclohexane and styrene	Low	Medium-high	High
Ethanol and mixed alcohols	Low	High	High
Phenol	Medium	Medium	High
Aromatic and aliphatic acids	Low	High	High
Formaldehyde-free binders	Medium-high	Medium-high	High
Vanillic acid	Medium	Medium	No data
Mixed liquid fuels	Medium	Medium	High
Polymers and composites	Low-medium	Medium	No data
Carbon fiber	Low-medium	Medium-high	High

* BTX: Benzene, toluene and xylene

Conversion of technical lignin to higher value chemicals and fuels is possible via methods such as oxidation, gasification, pyrolysis and solvolysis [17], [18]. Oxidation of lignin results in formation of products with higher oxygen content, which is not favorable if production of fuel is of interest. Gasification of lignin to syngas and further synthesis of chemicals such as methanol or Fischer-Tropsch fuels are energy intensive [19]. The thermochemical conversion methods are well illustrated in Figure 2 [20]. Lignin decomposes over a broad temperature range due to the various oxygen- and carbon-carbon functional groups in its structure with different thermal stabilities [21]. The decomposition of lignin initiates at relatively low temperatures, i.e., 150-275 °C by dehydration of hydroxyl groups followed by cleavage of α- and β- aryl ether linkages at 150 to 300 °C [22]. Cleavage of the aliphatic side chain from aromatic ring occurs around 300 °C while C-C linkages between lignin structural units break at higher temperatures around 370-400 °C. Pyrolysis and catalytic cracking (catalytic pyrolysis) require high temperatures [23]. Moreover, the pyrolysis suffers from extensive gas formation and production of unstable acidic liquid products [23]. The liquefaction methods in the presence of solvent are favorable as the operational temperatures are relatively moderate [24] and the liquid products are more stable compared to the pyrolysis liquid products, due to their lower acidity [25]. Water and organic solvents (the process is attributed as solvolysis) are among those vastly investigated [26]–[39]. If the solvolysis is assisted with the presence of a

catalyst in a reductive medium (hydroconversion), the process results in selective degradation of lignin and formation of stable monomers [20] which shows promises for monomer production among other methods.

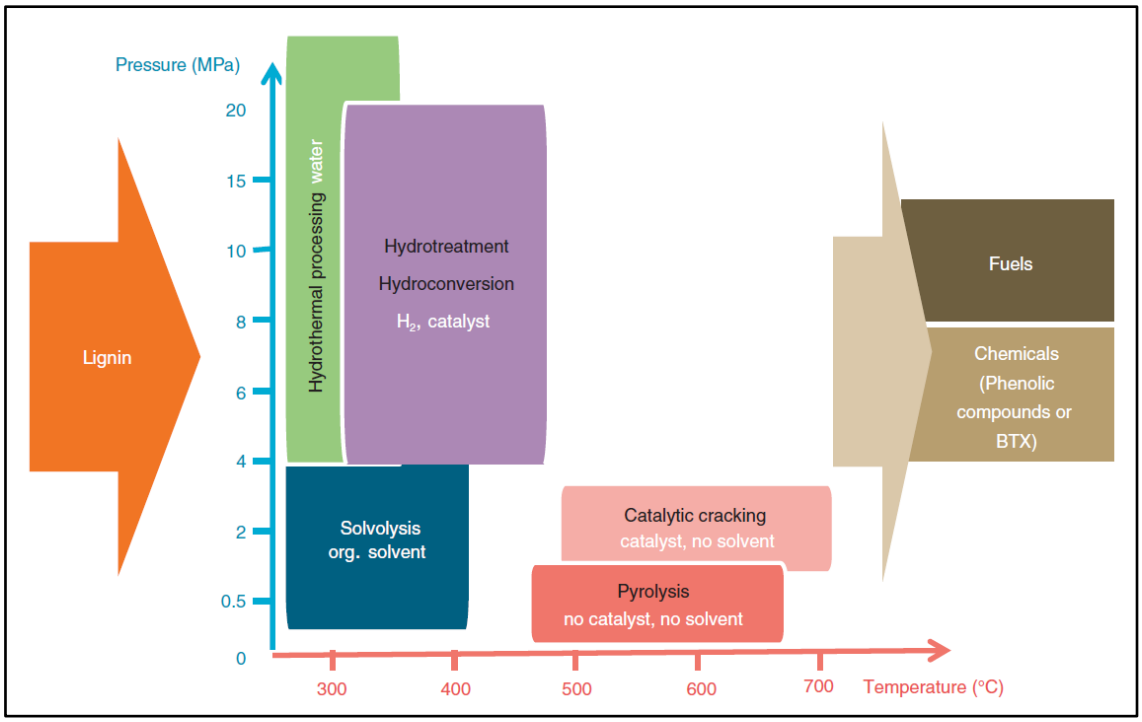

Figure 2 Thermochemical conversion approaches to obtain high value added fuels and chemicals from lignin [20].

Besides the abovementioned methods for conversion of technical lignin, an approach recently gained interest is direct conversion of biomass and degradation of lignin in the presence of a solvent, while the cellulose and hemicellulose remain nearly untouched [10], [19], [40], [41]. This method is attributed as early-stage catalytic conversion of lignin (ECCL) or lignin-first biorefining process. The holocellulose produced by this method is suitable for further utilization with conventional methods such as fermentation and enzymatic hydrolysis [42], [43].

1.1. Outline of the thesis

The focus of this Ph.D study is on reductive conversion of lignin in a solvent assisted with a heterogeneous catalyst. Catalytic conversion of lignin and biomass in different solvents and in the presence of a wide range of catalysts were reviewed. Based on the literature study and initial experiments, a depolymerization method was developed. Amongst different types of technical lignin, conversion of lignosulfonate was studied, which is rarely discussed in the literature. Effect of solvent (ethanol and ethylene glycol) and the role of catalysts (supported Ni and NiMo) were studied in detail and reaction mechanisms based on the results were proposed. Besides conversion of lignin, one-pot direct conversion of biomass without any pretreatment was studied, using the method developed for conversion of lignin. The conversion

of biomass was investigated with the lignin first biorefining vision, and was extended to conversion of all biomass constituents including lignin, cellulose and hemicellulose. The outlines of this thesis are summarized as follows:

Chapter 2: The structure of lignin and the available technical lignins are presented and the recent publications regarding depolymerization of lignin and biomass in the presence of different solvents and catalysts are discussed.

Chapter 3: A detailed description of the experiments, setup and the workup procedure applied are elaborated. Moreover, the description of the analytical techniques and evaluation of the liquid, solid and gaseous products are provided.

Chapter 4: Conversion of lignosulfonate in the absence and presence of Ni based catalysts in ethanol and ethylene glycol solvents was investigated, and based on the results the role of solvent on inhibiting condensation reactions was elaborated.

Chapter 5: Conversion of lignosulfonate in the presence of hydrotreating $NiMo/Al_2O_3$ catalyst in ethanol was studied and the necessity of pre-sulfidation of catalyst was investigated. A parameter study was conducted evaluating the effect of reaction temperature, reaction time and catalyst loading.

Chapter 6: Conversion of beech wood in the presence of hydrotreating $NiMo/Al_2O_3$ catalyst in ethanol was studied and the effect of reaction temperature on the degradation of lignin, cellulose and hemicellulose was evaluated. Additionally, one-pot conversion of biomass was compared with the two-step extraction of organosolv lignin and its successive conversion, with the main focus being on lignin degradation.

Chapter 7: The concluding remarks and the future outlook are presented.

Appendices: The supplementary information for chapters 4-6 are presented.

Chapter 2:

Literature Review on Catalytic Conversion of Lignin and Biomass

2. Literature review on catalytic conversion of lignin and biomass

In this chapter, a detailed description of lignin and different types of technical lignin is given. Moreover, this chapter deals with the literature regarding catalytic solvolysis of lignin and biomass to fuels and fine chemicals.

2.1. Lignin: Structure and types of technical lignin

Lignin is one of the main constituents of lignocellulosic biomass. The composition, molecular weight and quantity of lignin in different plant sources vary significantly. Softwoods has relatively high lignin content (27-33%) whereas hardwoods and grasses have lower lignin content (18-25% and 17-24%, respectively) [16], [44]. Lignin is constituted of random polymerization of three phenol derivatives called monolignols: *p*-coumaryl alcohol (M1H), coniferyl alcohol (M1G) and sinapyl alcohol (M1S) [44]. Each monolignol produces *p*-hydroxyphenyl, guaiacyl, and syringyl residues in the polymer shown in Figure 3. Heterogeneity of lignin structure is a result of different concentration of monolignol residues which differs with the plant source [21]. In softwood, G structure is the dominant structure, while in the hardwood both G and S groups are present [3], [21], [45]. Monolignols are connected via C-C and C-O bonds. The structure of lignin and the main bonds are depicted in Figure 4 [46]. The most abundant bond in lignin is β-O-4, with 45-50 % in softwood and more than 60 % in hardwood [47], which is a carbon-oxygen bond between a *p*-hydroxy moiety and the β-end of a propenyl group [44]. α-O-4 and 4-O-5 linkages with 4-9 % and 6-7 % content are the other important ether linkages in the structure of lignin [47].

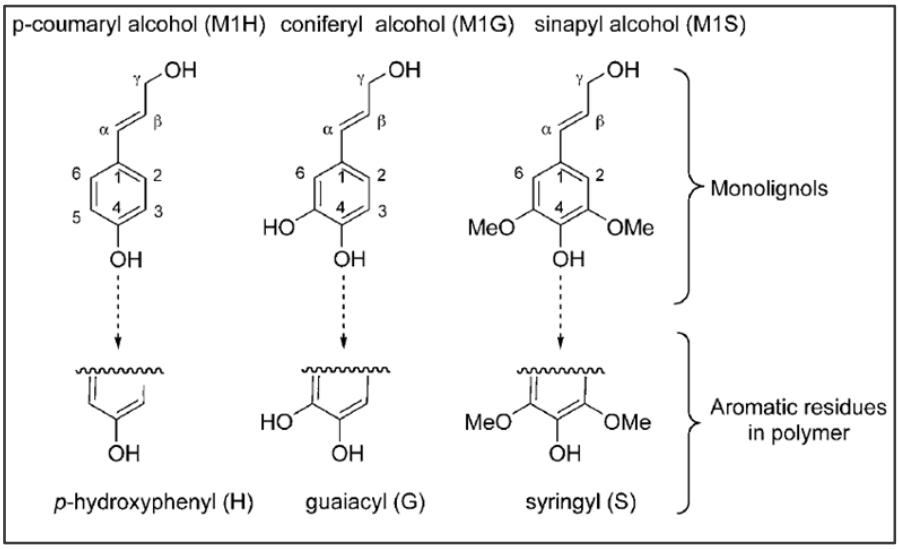

Figure 3 Monolignol monomers and aromatic residues in the polymer [44].

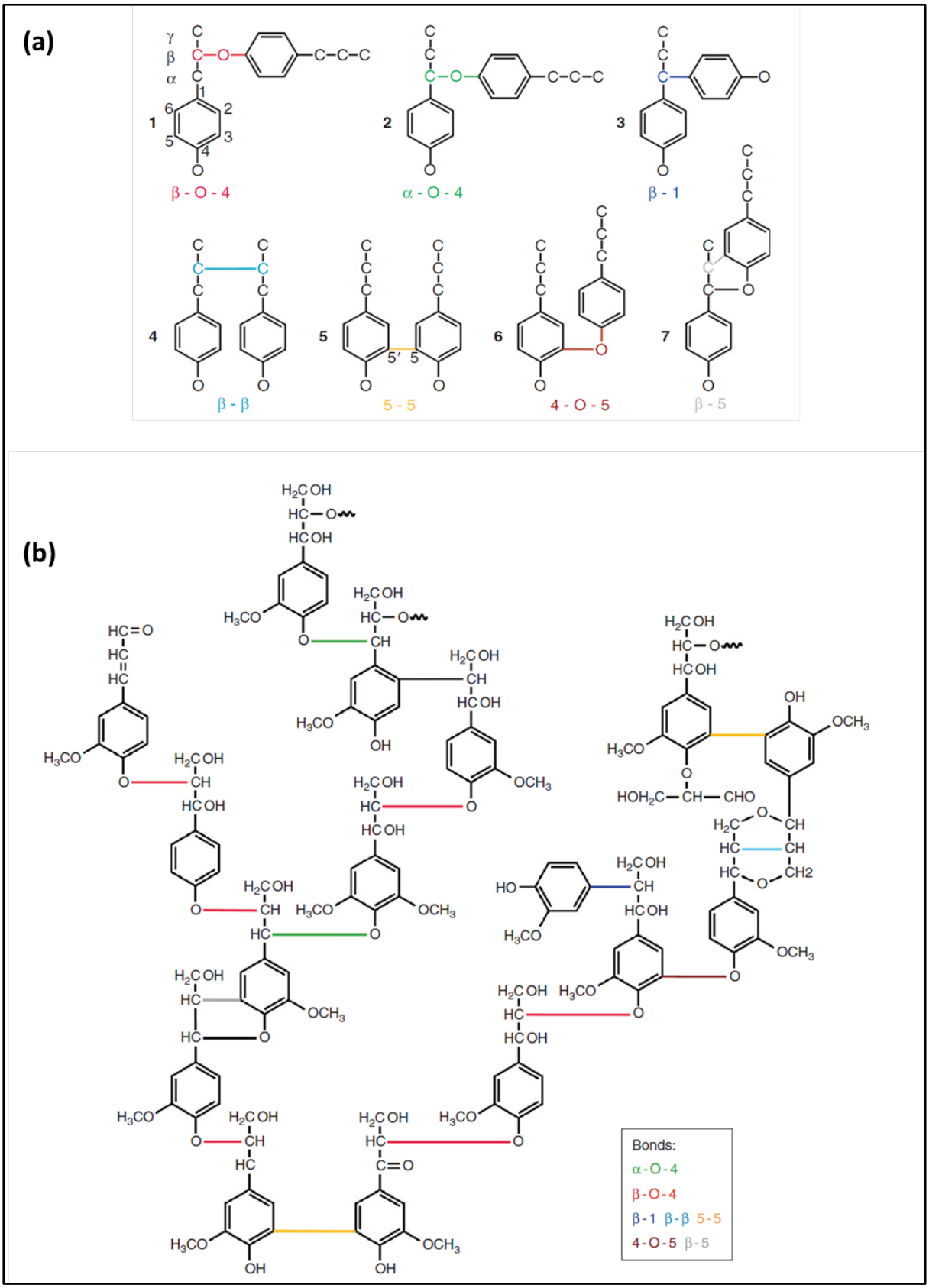

Figure 4 (a) The main linkages in the structure of lignin, (b) A proposed structure of lignin [46].

One of the main challenges in the exploiting lignin is its unclearly defined structure [22]. Besides, there are many different pretreatment methods based for extraction and isolation of lignin from biomass. In different wood treatment conditions, native lignin is treated under relatively severe conditions, resulting in cleavage of more facile bonds such as C-O ether bonds [48] and formation of new bonds, mostly stable C-C bonds [3], [11]. As a result, the physical and chemical properties of technical lignin is different than native lignin. *Kraft lignin*, *lignin sulfonate (lignosulfonate)*, *organosolv lignin* and *soda lignin* are some of the main types of technical lignin, which are described in section 2.1.1 to 2.1.5. There are other types of technical lignins for instance *hydrolysis lignin*, *explosion lignin* and *ionic liquid lignin*, which are not elaborated upon in this chapter, as they are less conventional compared to the other types.

2.1.1. Kraft Lignin

The kraft or sulfate process is the main pulping process with the lignin production being around 85% of the total lignin production [11], [49]. In kraft processing, wood is treated with a Na_2S/NaOH solution in the temperature ranges of 155-175 °C for a few hours through which the lignin-carbohydrate linkages are cleaved and thiol groups are formed [2]–[4], [50]. During kraft pulping, lignin is degraded mostly by the cleavage of β and α aryl ether bonds, whereas the 5-5 linkages are highly resistant over the treatment [47]. The condensation reactions may occur during kraft pulping, results in the formation of stable bonds such as C-C linkages, which are more frequent in the kraft lignin than the original lignin [11], [51]. By reaction of hydrosulfide ion with α-carbon and further nucleophilic attacks of hydrosulfide to β-carbon an episulphide structured compound is formed (Figure 5) [49]. Kraft lignin is retrieved by precipitation and neutralization of black liquor with acidic solution through self-aggregation of lignin [45].

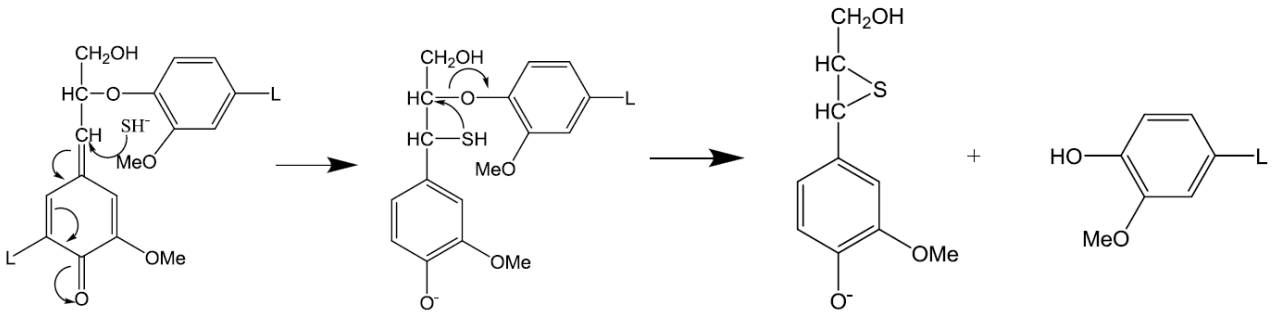

Figure 5 Cleavage of β-O-4 linkage in the kraft pulping process [49]

The molecular weight of kraft lignin is within 2500 to 39000 g/mol and its sulfur content is around 1.5-3 wt% [45]. Kraft pulp mills are basically developed based on the combustion of black liquor for the production of electricity and process steam of the mills and only a small portion (around 2%) is devoted to applications such as dispersant, emulsifier, ion exchange resins and production of chemicals such as DMSO and aliphatic acids [11], [45], [52]. It is argued that due to efficiency improvement of kraft pulp mills, the mills may produce an excess amount of energy relative to their consumption, which represents the necessity of valorization of lignin for economic viability of pulping industries [45]. MeadWestvaco and Metso Corporation are the main producers of kraft lignin [36], [45], [49].

2.1.2. Sulfonate lignin (Lignosulfonate)

Lignin sulfonate or lignosulfonate is produced as a by-product of the sulfite pulping process with annual production of about 1 million ton as dry mass [13]. About 80 years ago, sulfite pulping was the dominant industrial method for the production of lignin [45]. Sulfite process takes place by digestion of wood at 120-180 °C in the aqueous solution of sulfite or bisulfite salt of sodium, ammonium, magnesium or calcium [11]. In the sulfite process The side chain of the phenyl propane unites are hydrolytically cleaved, sulfonated, and dissolved as lignin sulfonate [11]. This lignin has both hydrophobic and hydrophilic features [53]. The main reaction of lignosulfonate formation in sulfite pulping process is illustrated in Figure 6 [45] and the main sulfite pulping conditions are presented in Table 1 [44].

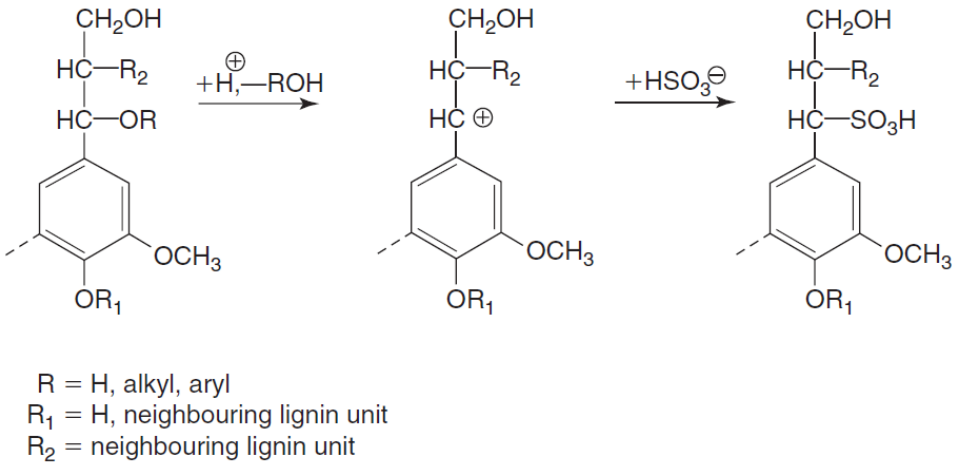

Figure 6 Main reaction scheme for lignosulfonate formation during acid sulfite pulping [45], [54].

Lignosulfonate generally contains 4-8 wt% sulfur mainly in the form of sulfonate groups present on the aliphatic side chain (the degree of sulfonation is about 0.4 to 0.5 per phenylpropanoid unit) which makes it water soluble [45]. Molecular distribution of lignosulfonate is very wide [55] and it has a higher average molecular weight (1000 to 150,000) compared to kraft lignin with a broad polydispersity index [1] around 6-8 [45], [49]. Lignosulfonate has applications such as suspension stabilizer of concrete mixture, stabilizer of immiscible liquids such as asphalt emulsion, animal food binder, adhesive and moisture retaining agents [2], [4], [13], [44]. Vanillin, which is produced by oxidation of lignin over cupper based catalysts, is a high value product from lignosulfonate [14], [56].

[1] The Polydispersity Index (*PDI*) is a measure of the distribution of molecular mass in a polymer. *PDI* is defined as:

$$PDI = Mw/Mn$$

Where M_w is the weight average molecular weight and M_n is the number average molecular weight.

Table 1 Sulfite pulping conditions [44]

Process	Reactive agents	pH	Temperature [°C]
Acid sulfite	SO_2/HSO_3^-	1-2	125-145
Bisulfite	HSO_3^-	3-5	150-175
Neutral sulfite	HSO_3^-/SO_3^{2-}	6-7	150-175
Alkaline sulfite/anthraquinine	Na_2SO_3	9-13	50-175

Even though production of lignin by sulfite process is overtaken by kraft pulping process, there are some stable industrial plants producing 8% of the total lignin production through sulfite process; *Borregaard LignoTech* is the leading producer of lignosulfonate, producing more than 500,000 metric tons (dry basis) [45]. In the Borregaard process $Ca(HSO_3)_2$ is mainly used as the pulping solution [57]. Their lignin products are fermented, double fermented, ultrafiltered and oxidized based on calcium, sodium or ammonium as the counter ion [45]. The degree of sulfonation in lignosulfonate produced by Borregaard varies from 0.17 to 0.65 sulfonate groups per phenyl propane unit [45]. The second largest producer of lignosulfonate is *Tembec* with products mainly in sodium, ammonium and magnesium lignosulfonate forms [45]. Although the company produces lignosulfonate of high value, a considerable portion of the products are dedicated for the energy supply, depending on the energy cost and market condition [45]. *La Rochette Venizel*, *Nippon Paper*, *Cartiere Burgo* and *Domsjo* are the other manufacturers of lignosulfonate [45].

2.1.3. Soda lignin

Soda pulping has been mainly developed for non-wood fibers and annual crops such as flax, bagasse and wheat straw [45]. The first commercial production of soda pulping achieved in 1851, making it the first industrial pulping method. Nowadays, about 5% of the total pulp production is produced by soda pulping [11]. The soda pulping is similar to kraft pulping to some extent, which includes cleavage of β and α aryl ether bonds, while it uses a sulfur free cooking liquor. The pulping process involves heating the fibrous biomass in a pressurized reactor to 150-170 °C in the presence of alkali solution, mostly sodium hydroxide with pH of 11-13 [22], [45]. Cleavage of a β-O-4 linkage is depicted in Figure **7**. Under the alkaline condition, an ether bonds is cleaved via involvement of the hydroxyl groups in the α or γ carbons, resulting in the formation of epoxide compound which is further converted to glycol [45]. Similar to kraft process, recovery of soda lignin occurs through acid precipitation.

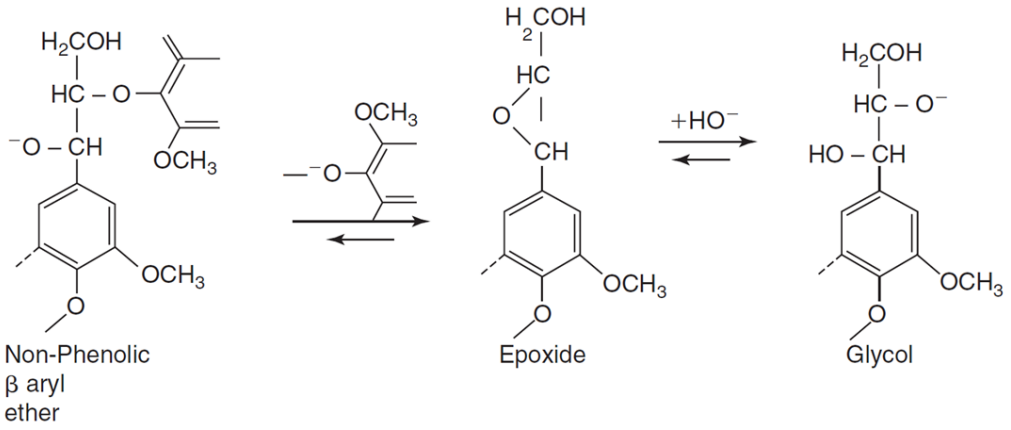

Figure 7 Main reactions in the formation of soda lignin [45], [58].

Soda lignin is sulfur free, water-insoluble and contains low ash and sugar content [45]. The structure is considered to be closer to the structure of lignin in nature, compared to kraft and sulfite lignin [13]. The average molecular weight of the soda lignin ranges from 6,900 to 8,500 and its polydispersity is about 3 [45]. The main applications of soda lignin are as dispersants, animal food additive and production of phenolic resins [13]. GreenValue SA with the production capacity about 10 000 ton per year is the main producer of soda lignin which exploits non-wood biomass sources [45]. Northway Lignin Chemical is the other producer of soda lignin.

2.1.4. Organosolv lignin

Organosolv lignin is produced by treatment of biomass with a mixture of organic solvent and water at 150-200 °C followed by acidic precipitation [11]. Sulfur free structure, high chemical purity and low molecular weight are the distinctive features of organosolv lignin which makes it a very good candidate for valorization [11], [53]. Lignin is released through hydrolytic cleavage of aryl ether linkages. Methanol, ethanol, butanol, phenol, ethylene glycol, acetic acid, acetone and formic acid are some of the main organic solvents for the extraction of lignin [13], [52]. Applying solvents with higher boiling points lowers process pressure, however, further solvent recovery by distillation might be a challenging task [11]. Alcell, Acetosolv, Organocell and ASAM are some of the commercial processes for production of organosolv lignin [11], [59]. Organocell pulping process, which is an alkali-catalyzed process, is basically developed for delignification of softwood biomass; first, wood chips are impregnated with 50% methanol solution at 170-190 ˚C and further the partially delignified chips are exposed to 35% methanol solution containing sodium hydroxide at 170 ˚C [11]. In Alcell process, 50% ethanol solution is applied as solvent for delignification of hardwood biomass in a series of extractors at 190 ˚C and 28 bar [11], [36]. Alcell lignin is highly soluble in acetone, THF and ethyl acetate [11].

2.1.5. Comparison of different technical lignins

General features of each lignin are presented in Table 2. High abundance of kraft lignin and lignosulfonate, besides their lower price compared to the other types of lignin, make them

very interesting raw materials for conversion to high-value chemicals and fuels. Water solubility of lignosulfonate facilitates its conversion in hydrothermal and solvothermal conditions. However, it should be noted that the presence of sulfur in the structure of kraft lignin and lignosulfonate is one of the main challenges in conversion of these types of lignin in the presence of a heterogeneous catalyst [11]. Organosolv lignin and soda lignin are sulfur free and have relatively lower molecular weight and represent the most similar structure to the native lignin [53]. However, the cost of solvent recovery [52] and the lack of access to biomass in all seasons are the drawbacks of each lignin type, respectively. In the next section, solvolytical depolymerization of different types of technical lignin is reviewed.

Table 2 General features of different lignin types [4], [17].

Lignin	Sulfur [wt%]	Water solubility	M_w [g/mol]	Advantages
Kraft lignin	1-3	insoluble	2500-39000	The most abundant lignin, low price
Lignosulfonate	4-8	soluble	1000-150000	The second abundant lignin, low price
Soda lignin	0	insoluble	6900-8500	Sulfur free, low ash and sugar content
Organosolv lignin	0	insoluble	500-5000	Highly pure, no ash, sulfur free, low molecular weight

2.2. Solvothermal conversion of technical lignin

In this section solvothermal conversion of technical lignin and the relevant publications are discussed. In a solvolysis process, the liquefaction is achieved in the presence of a solvent such as water, methanol, ethanol, propanol, cyclohexane and co-solvents such as formic acid and tetralin. The presence of a polar organic solvent improves depolymerization while may prohibit repolymerization of monomers and dimers [60]. The cleavage of the lignin polymer is usually facilitated in the presence of a catalyst. Transition metal catalysts and hydrotreating catalysts such as NiMo and CoMo are extensively investigated for conversion of lignin [33] and summarized in many review articles [47], [52], [61]–[63] and therefore, the solvolysis of lignin over these catalysts are elaborated here.

2.2.1. Transition metal catalysts for conversion of lignin

Transition metal based catalysts are greatly used in petrochemical industry in the processes such as methanation, steam reforming, methanol synthesis, Fischer Tropsch and hydrogenation of olefins [64]. Due to the presence of unoccupied *d* orbital in their electron configuration, they are able to have variable oxidation states which make them active for catalytic applications. Among different transition metal catalysts, Ni based catalysts are industrially used for a wide range of applications such as hydrogenation and steam reforming [65]. Concerning conversion of lignin and the representative model compounds, nickel catalyst are tested by many research groups [33], [51], [66]–[70]. Moreover, copper, molybdenum, platinum, palladium and ruthenium based catalysts are being investigated for conversion of lignin [37], [71]–[76]. In this section, some interesting findings such as the role of solvent and the degradation mechanisms for solvolysis of lignin using transition metal catalysts are presented.

Warner et al. [30] investigated solvolytic depolymerization of home-extracted organosolv lignin in supercritical methanol using a range of porous metal oxides such as $CuMgAlO_x$, $MnMgAlO_x$ and $ZnMgAlO_x$ at 310 ˚C with catalyst: lignin: methanol ratio of 100 mg: 100 mg: 3 ml. According to the results, the highest lignin conversion of 48 wt% was obtained over $C_{20}MgAl_x$ catalyst after 1 hour reaction time, with 25 wt% yield of methanol-soluble products [30]. In the absence of Cu, char formation was observed indicating that Cu prohibited condensation reactions [30]. Their observation is aligned with those from the group of Hensen; they studied conversion of soda lignin over Cu based catalysts supported on $MgAlO_x$, in detail [31], [77]–[79]. A higher monomer yield of 17 wt% was observed over $CuMgAlO_x$ catalyst (Table 3, Entry 1) compared to $PtMgAlO_x$ catalyst (Table 3, Entry 3, monomer yield of 6 wt%) and $NiMgAlO_x$ (Table 3, Entry 4, monomer yield of 4 wt%) in ethanol at 300 °C [31]. Moreover, the yield of THF soluble solid fraction was higher over Cu based catalyst.

Table 3 Results of the degradation of soda lignin at 300 °C and 4 hours (catalyst: lignin: solvent ratio of 500 mg: 1000 mg: 20 ml), 10 bar N_2 (loaded at RT) [31].

Entry	Catalyst	Solvent	Monomers [wt %]	THF soluble LR[(a)] [wt %]	THF insoluble LR [wt %]	Char [wt %]
1	$CuMgAlO_x$	EtOH	17	73	18	0
2	$CuMgAlO_x$	MeOH	6	57	39	1
3	$PtMgAlO_x$	EtOH	6	43	22	0
4	$NiMgAlO_x$	EtOH	4	51	11	17

(a) LR: Lignin residue

Ethanol showed superior performance in prohibition of repolymerization reactions compared to methanol as lower amount of THF insoluble products were observed from depolymerization in ethanol (Table 3, Entry 1 & 2) [31]. According to Huang et al. [78] ethanol acts as a capping agent, stabilizes the highly reactive phenolic intermediates by O-alkylation of the hydroxyl groups and C-alkylating of the aromatic rings [78]. Formaldehyde can be produced from methoxy groups and from γ-carbon in alkyl side chains in lignin [78]. Reaction of the *in-situ* produced formaldehyde with phenol produces phenolic oligomers and polymers [78]. Ethanol reacts with formaldehyde and forms higher alcohol and esters over $CuMgAlO_x$ catalyst via Guerbet reactions and esterification [78]. The role of ethanol in stabilization of reactive fragments and inhibiting repolymerization reactions over $CuMgAlO_x$ catalysts is shown in Figure 8.

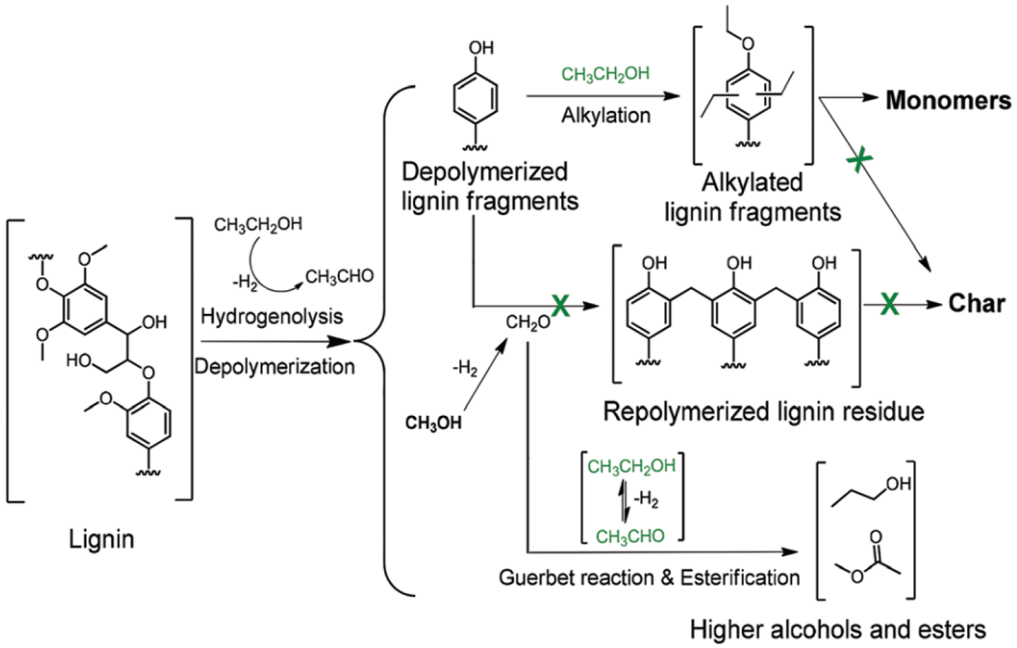

Figure 8 Repolymerization suppression in ethanol medium via alkylation, Guerbet reaction and esterification over $CuMgAlO_x$ catalyst [78].

It was shown that Guerbet and esterification reactions were more important than alkylation in suppressing char formation [77]. Huang et al. [77] investigated the role of support material on the conversion of soda lignin in supercritical ethanol at 340 ˚C and 4 hours. Mainly C_{4+} ethers were detected as products from reaction with ethanol over Cu/Al_2O_3 (with the most acidic features), indicating alkylation reactions were catalyzed by acid sites on the surface of alumina. When $Cu_{20}MgAl$ (with (Cu+Mg)/Al ratio of 4.2, as the most basic catalyst) was used, higher alcohol and higher esters were the main products indicating that Guerbet reactions and esterifications were catalyzed on the basic catalyst. Char formation was only observed on Cu_{20}/Al_2O_3. On the other hand, no char was observed when Cu/MgO was used, which highlighted the importance of end-capping reactive fractions such as formaldehyde on the basic sites [77]. Huang et al. [79] observed higher yield of monomers when the partial pressure of the *in-situ* produced hydrogen was increased. The monomer yield increased from 20 wt% at 340 ˚C in a 50 ml autoclave with 1 g lignin, 0.5 g $Cu_{20}MgAl_x$ and 20 ml of ethanol to 30 wt% in a 100 ml autoclave with the same amount of lignin and catalyst, while the solvent volume was increased to 40 ml, which was attributed to the higher partial higher pressure of hydrogen formed by ethanol reforming.

Organosolv lignin (500 mg) was reductively converted over Ni/Al-SBA-15 catalyst (150 mg) in methylcyclohexane solvent (15 ml) to cycloalkanes with a selectivity of 99% at 300 ˚C and 8 hours [80]. The solvent used for degradation of lignin greatly affects the selectivity of the compounds in the presence of Ni based catalysts [66]. Wang and Rinaldi [66] investigated the role of solvent on degradation of diphenyl ether model compound and lignin in the presence of Raney Ni catalyst. Four main group of solvents were evaluated: Protic solvents with Lewis basicity (methanol, ethanol, 2-propanol, 1-butanol, 2-butanol and tert-butanol), protic solvents

without Lewis basicity (Hex-F-2-PrOH), aprotic polar solvents (ethyl acetate, tetrahydrofuran (THF), 2-methyltetrahydrofurane (2-Me-THF), and 1,4-dioxane) and aprotic nonpolar solvents (methylcyclohexane (MCH), decaline and n-heptane). The conversion and the selectivity of the reaction products are presented in Table 4.

Table 4 Conversion of diphenyl ether and the selectivity of the compounds 2-7. Reaction condition: 2.9 mmol diphenyl ether, 100 mg Raney Ni, 15 ml solvent, 90 ˚C, 50 bar H_2 (loaded at RT), 2.5 hours [66].

Solvent	Conversion %	2	3	4	5	6	7
Methanol	12.4	13.7	0	25.7	32.3	16.8	11.5
Ethanol	33.0	11.8	0.3	10.7	26.7	33.6	16.9
2-Propanol	72.7	15.0	1.9	1.6	15.4	40.5	25.6
Hex-F-2-PrOH	100	0	67.3	0	0	16.6	16.1
1-Butanol	32.0	9.3	0.7	9.2	22.5	36.8	21.5
2-Butanol	55.1	15.4	0.8	10.3	18.0	32.1	23.4
t-Butanol	21.7	20.4	1.4	18.4	17.2	21.4	21.2
Ethyl acetate	47.0	21.0	1.8	8.1	15.7	30.1	23.3
THF	29.6	15.5	0	14.2	25.3	27.6	17.4
2-Me-THF	61.1	24.1	1.7	2.9	12.8	34.4	24.1
1,4-dioxane	17.8	24.5	0	24.1	22.0	13.3	16.1
n-Heptane	99.0	9.6	36.5	0	1.5	27.5	24.9
Decaline	99.6	6.3	41.4	0	0	26.6	25.7
MCH	100	0	55.4	0	0	22.8	21.8

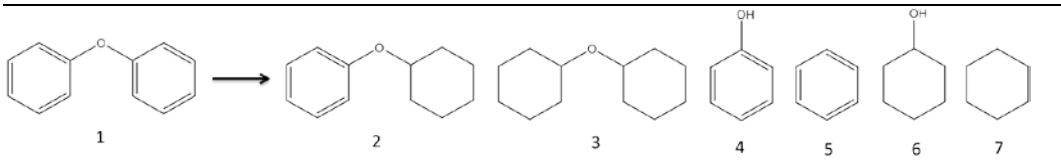

A reversed correlation was reported between the conversion of the diphenyl ether and solvent Lewis basicity (shown in Figure 9) [66]. They suggest that solvents with higher Lewis basicity adsorb on the Ni active sites and may inhibit hydrogenolysis and hydrogenation activity of catalyst. Adsorption of alcohol solvents on the Ni sites inhibit activity of the catalyst, however, the coverage of the catalyst with alkoxy groups decreases by increasing the size of the alcohol chain, as evidenced by higher conversion in 1-butanol than methanol, despite similar Lewis basicity [66]. Besides the effect of solvent on the conversion of diphenyl ether, the product distribution was greatly affected by nature of the solvent [66]. While non-polar solvents such as methyl cyclohexane favored formation of saturated products, protic solvents and polar aprotic solvents favored formation of unsaturated compounds. Lewis basic solvents such as methanol, 1,4-dioxane and THF resulted in lower rates of hydrogenation [66].

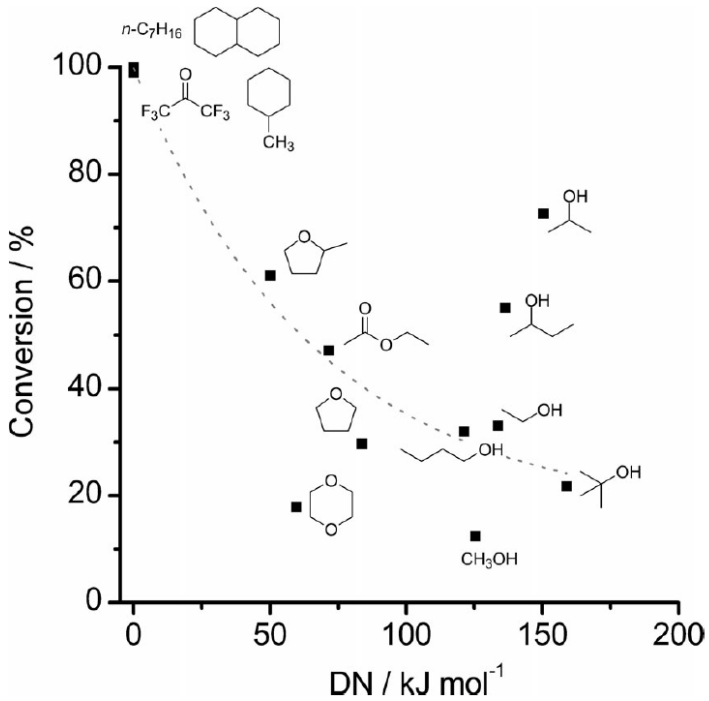

Figure 9 Conversion of diphenyl ether vs. the Lewis basicity of the solvents (described by the donor number DN) over Raney nickel catalyst. Reaction condition: 2.9 mmol diphenyl ether, 100 mg Raney Ni, 15 ml solvent, 90 ˚C, 50 bar H_2 (loaded at RT), 2.5 hours [66].

Tetralin is known as a hydrogen donor solvent. Under thermal conditions, tetralin deforms through the mobile carbon-hydrogen bonds to produce naphthalene and hydrogen radicals, as illustrated in Figure 10 [81]. Conversion of organosolv lignin (20 g) in the presence of tetralin (250 ml) under 10 bar H_2 pressure at temperature range of 370-410 °C and in the presence of 5 wt% nickel-tungsten catalyst (1 g) was investigated by Thring and Breau [82]. By increasing the severity of the reaction (increasing time and the reaction temperature from 15 min and 370 °C to 60 min and 410 °C), the conversion of lignin increased from 5% to 50%, while residue content considerably decreased [82]. Syringols and guaiacols were the predominant products at lower temperature and lower reaction time, while demethoxylated compounds such as phenol, catechol and their alkyl derivatives were predominant in reaction at 410 °C and 60 min, indicating that demethoxylation occurred by increase of the reaction temperature and reaction time [82].

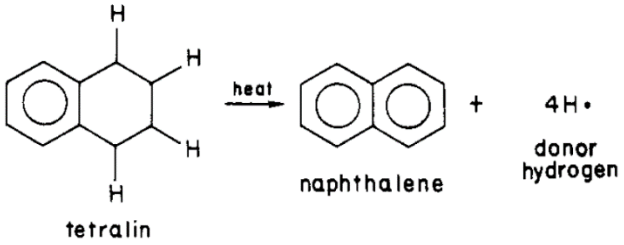

Figure 10 Hydrogen radical formation by tetralin degradation [81].

Catalytic conversion of model compounds is investigated in order to understand the reaction pathways. In a work from Lercher group, hydrothermal cleavage of aryl ethers, representing β-O-4, α-O-4 and 4-O-5 linkages was investigated over Ni/SiO_2 catalyst in water at 120 ˚C and 6 bar H_2 pressure [83]. The proposed reaction pathways are shown in Figure 11 [83]. They observed that cleavage of C-O-C in β-O-4 occurred at the position of aliphatic carbon resulting in the formation of phenol and ethylbenzene (Figure 11, a). Phenol further experienced hydrogenation and cyclohexanol was formed. Amongst the model compounds, α-O-4 is very unstable [83]. High reaction rate of the resembling model compound (1017 $mol.mol_{Ni(surf)}^{-1}.h^{-1}$) was reported in the presence of 0.03 g catalyst (one tenth of the catalyst mass used for conversion of β-O-4), which was considerably higher than the reaction rate of β-O-4 (13 $mol.mol_{Ni(surf)}^{-1}.h^{-1}$) [83]. Both bond dissociation energy (BDE) and activation energy accounted for higher reaction rate of α-O-4. BDE of α-O-4 is 218 kJ/mol, which is lower than BDE of β-O-4 (289 kJ/mol) while activation energy of α-O-4 is lower than β-O-4 (72 kJ/mol vs. 86 kJ/mol). Similar to β-O-4, bond cleavage took place through aliphatic C-O bond (Figure 11, b). Phenol and toluene were produced, however, by further hydrogenation of phenol, cyclohexanol and cyclohexane were formed to some extent [83].

Rather different cleavage route was reported for 4-O-5 resembling compounds (Figure 11, c) [83]. Two major routes were reported: hydrogenolysis of diphenyl ether to cyclohexanol and benzene, and hydrolysis of diphenyl ether to two molecules of phenol, which were further hydrogenated to cyclohexanol. Hydrogenation of diphenyl ether to cyclohexyl phenyl ether was the other pathway occurred to minor extent, with benzene and cyclohexane being the ultimate products [83]. Though the BDE of 4-O-5 was higher than β-O-4 (314 kJ/mol vs. 289 kJ/mol, the turn over frequency (TOF) of the former was higher than the later (26 h^{-1} vs. 13 h^{-1}), attributed to distinctive cleavage of the bonds in 4-O-5: While C-O bond cleavage in β-O-4 and α-O-4 was through Ni catalyzed hydrogenolysis, C-O cleavage in 4-O-5 occurred via parallel hydrolysis and hydrogenolysis [83].

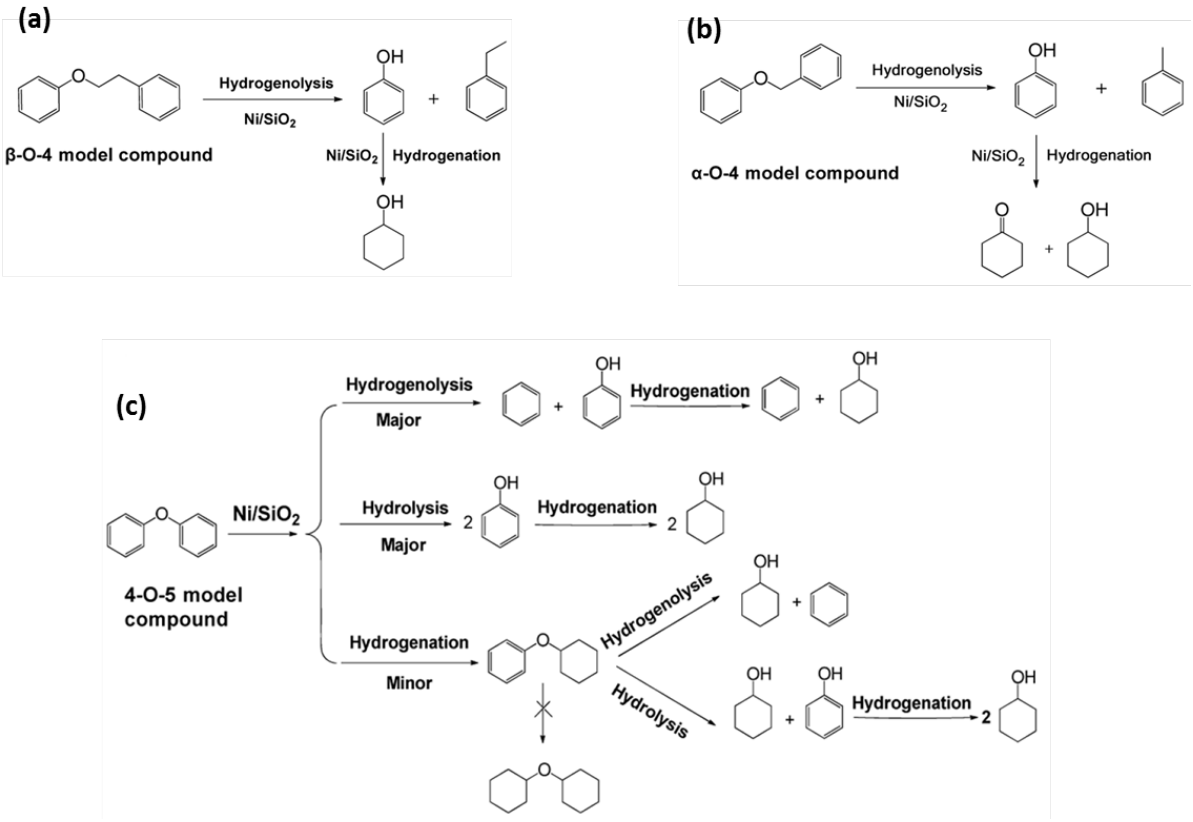

Figure 11 Reaction of β-O-4, α-O-4 and 4-O-5 model compounds over Ni/SiO_2 catalyst in water at 120 ˚C. Reaction condition: 0.01 mol model compound, 0.3 g catalyst (0.03 g for reaction of α-O-4) and 80 ml water, 6 bar H_2 pressure [83].

Support material influenced the degradation of lignin over Ni based catalysts. In another work by Lercher et al. [68] degradation of organosolv lignin was investigated over 20-21 wt% Ni supported on SiO_2 and zeolites (HBEA and HZSM-5) in a batch reactor using hexadecane as solvent at 250 and 320 ˚C. The liquid phase was composed of C_5-C_{14} naphthenes and water. According to the results (shown in Table 5), higher yields of hydrocarbons were obtained over Ni/HBEA and Ni/HZSM-5 attributed to the presence of Brønsted acid sites, catalyzing dehydration of intermediately formed alcohols. The products in the oil phase from Ni/SiO_2 catalyst test was composed of 20 wt% monocyclic alcohols (such as cyclohexanol and its alkyl substituents) and 80 wt% monocyclic alkanes (such as cyclohexane and its alkyl derivatives). The formation of cyclic alkanes was attributed to the dehydration of alcohols on the Lewis acid sites of the Ni/SiO_2.The product in liquid phase from reaction over Ni/HZSM-5 and Ni/HBEA were 90 wt% monocyclic alkanes and 10 wt% bicyclic alkanes and 83 wt% monocyclic alkanes and 17 wt% bicyclic alkanes, respectively. By increasing degradation temperature to 320 ˚C, 96 wt% conversion of organosolv lignin over Ni/HBEA was reported.

Table 5 Results of catalysts acidity measurements and the yield of the reaction products over Ni based catalysts. Reaction condition: 1 g lignin, 0.5 g catalyst, 100 ml hexadecane, 20 bar H_2 (Loaded at RT), 250 ˚C, 6 h [68].

Catalyst	Catalyst acidity ($\mu molg^{-1}$)		Gas phase [wt%]	Liquid phase [wt%]	Solid residue [wt%]	Unconverted lignin
	BAS	LAS				
Ni/SiO_2	-	39	4.1	23 ± 2	31 ± 5	25
Ni/HZSM-5	36	91	5.5	28 ± 2	26 ± 5	18
Ni/HBEA	19	71	6.8	35 ± 4	22 ± 5	12

Lercher and colleagues [68] proposed a mechanism for degradation of organosolv lignin in the presence of Ni based catalysts, shown in Figure 12. According to them, degradation of organosolv lignin occur by hydrogenolysis of aryl alkyl ether bonds (pathway A), and formation of phenolic intermediate fractions [68]. The subsequent saturation of intermediated phenolic compounds followed by dehydration of *in-situ* formed cyclic alcohols on the Brønsted acid sites (fast pathways of B, C & D) and hydrogenolysis (slow pathway of E) yield to cyclic alkenes. The cyclic alkenes were subsequently hydrogenated. Undesirable repolymerization reactions simultaneously occur (pathway F), which take place with lower rates by increase of reaction temperature.

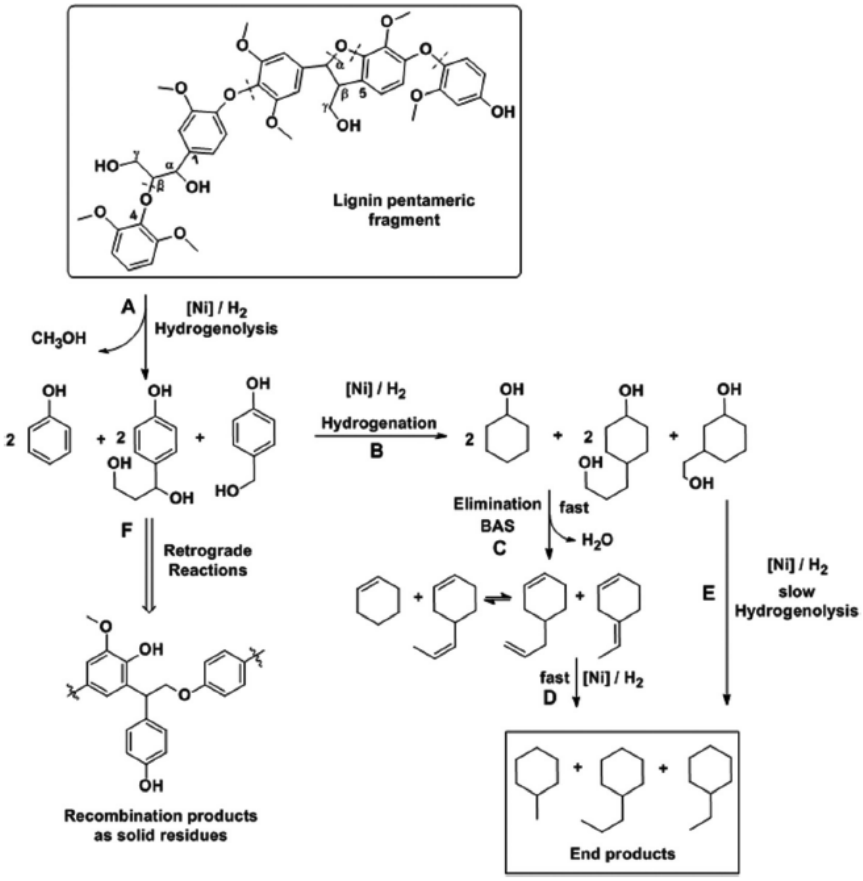

Figure 12 A proposed reaction pathway by Lercher et al. [68] for degradation of organosolv lignin and hydrodeoxygenation (HDO) of the *in-situ* formed fragments on the Ni based catalyst.

Sulfur is a known as a poison for transition metal catalysts [48]. Mortensen et al. [84] investigated effect of sulfur in 10 vol% guaiacol in 1-octanol (as bio-oil model compound) on the activity of Ni/ZrO_2 catalyst at 250 °C and total pressure of 100 bar. A 0.3 vol% 1-octanethiol (0.05 wt% sulfur in the feed) was added to the feed as sulfur source. While the conversion of 1-octanol and guaiacol were 100% and a degree of deoxygenation of 90-92% was reported in the absence of 1-octanethiol, addition of sulfur decreased the conversion drastically and after 12 hours no conversion was observed. They argued that by sulfur poisoning of the catalyst, both hydrogenation and deoxygenation reactions were stopped through formation of non-active nickel sulfide phase [84].

Yuan et al. [85] investigated depolymerization of kraft and organosolv lignin in supercritical acetone over 5 wt% Ru/C, 5 wt% Ru/Al_2O_3, 10 wt% Ni/Al_2O_3, 10 wt% Ni/AC and NiMoW based industrial catalyst (named FHUDS-2) at 300-350 ˚C under 100 bar H_2 pressure and 1 hour reaction time. In each test, 30 g lignin was converted in a batch reactor over 1.5 g catalyst (3 g FHUDS-2 was loaded due to its lower metal loading) and 150 ml of acetone. The average molecular weight of the kraft lignin and organosolv lignin were 10200 g/mol and 2600 g/mol, respectively. In non-catalytic tests, severe condensation reactions took place evidenced by increasing the Mw of the products of kraft lignin (DKL, yield of 70 wt%) and the products of organosolv lignin (DOL, yield of 100 wt%) compared to the original feedstock (shown in Figure 13) [85]. In all catalytic tests, the yields of DKL and DOL fractions were higher than 94.5 wt%. As can be seen in Figure 13, the molecular weight of different fractions decreased drastically in catalytic reactions, indicating the role of catalyst on degradation. The catalysts used were suitable for degradation of both types of lignins, with Ru/C and FHUDS-2 being the most effective catalysts on degradation. The molecular weight of the DKL and DOL in the presence of Ru/C were lower compared to Ru/Al_2O_3, attributed to the condensation reactions in the presence of acidic alumina support.

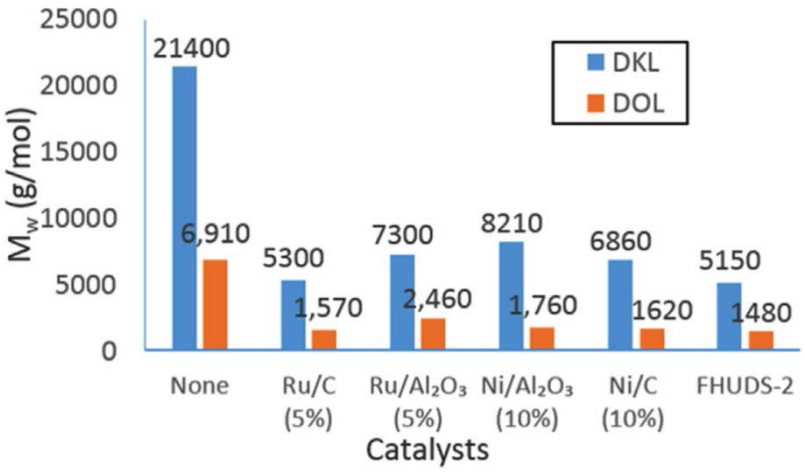

Figure 13 Molecular weight of DKL and DOL fractions at 300 ˚C. Reaction condition: 30 g lignin: 1.5 g catalyst (3 g FHUDS-2), 150 ml acetone, 100 bar H_2 (loaded at RT), 1 hour [80].

Yuan et al. [85] observed that the temperature had a great effect on the yields and molecular weight distribution of the degraded fractions (see Figure 14). While the temperature

increased from 300 to 325 ˚C over Ru/C catalyst, the yield of DKL increased while the solid yield decreases, attributed to the higher rate of degradations and increase of solubility of lignin at higher temperatures. On the other hand, the molecular weight of DKL showed a decreasing trend by increasing reaction temperature, and experienced a significant decrease from 300 to 325 ˚C, indicating that temperatures higher than 300 ˚C were required for suppression of condensation reactions. The yields of DOL and its molecular weight did not considerably changed by increasing reaction temperature, as it initially had low molecular weight and high solubility in acetone. This indicated that low temperatures of 250-275 ˚C were sufficient for degradation of organosolv lignin [85].

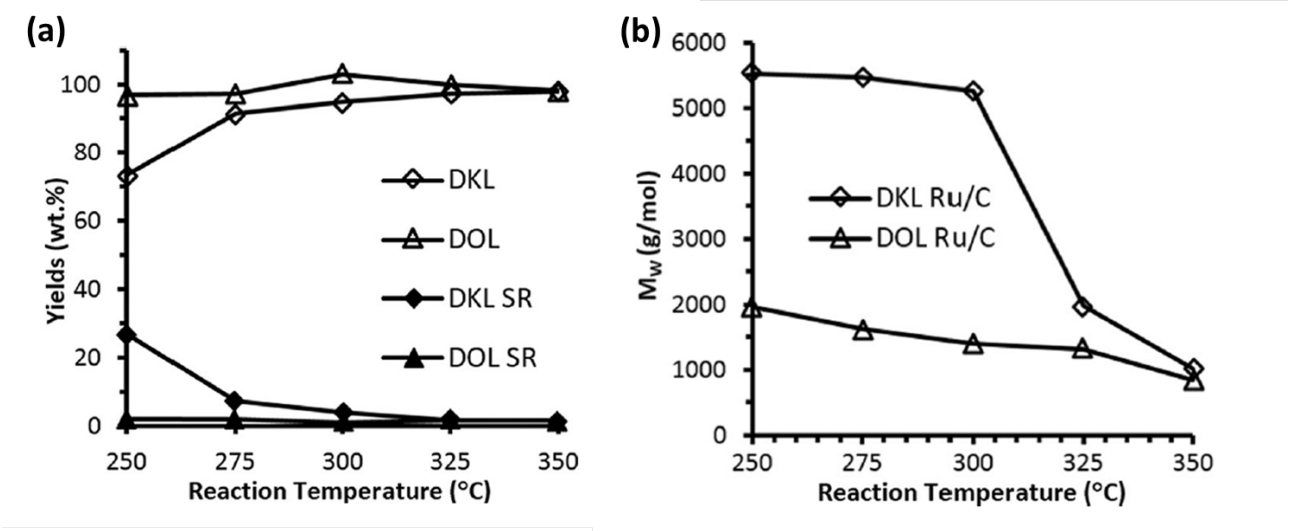

Figure 14 Yields of the liquid and solid fractions from conversion of kraft and organosolv lignin and the molecular weight of the liquid phases vs. reaction temperature over Ru/C catalyst. Reaction condition: 30 g lignin: 1.5 g catalyst, 150 ml acetone, 100 bar H_2 (loaded at RT), 1 hour [85].

Ma et al. [35] investigated ethanolysis of kraft lignin in the presence of carbon supported α-molybdenum carbide catalyst at 280 °C and 6 hours. Aliphatics (yield of 82 wt%) including C_6 alcohols and C_8-C_{10} esters and aromatics including arenes, phenol and benzyl alcohols were formed without formation of char or tar [35]. An overall yield of 1.64 g product per gram of lignin was obtained by utilizing carbon supported α-MoC catalyst, indicating excessive solvent incorporation in the presence of catalyst [35]. The initial hydrogen pressure reversely affected the yield of liquid products (LP25) including esters, alcohols and aromatics, shown in Figure 15 [35]. Ma et al. [35] suggested that increase of the initial hydrogen content from 0 to 40 bars suppressed the chemisorption of ethanol on the catalyst surface due to the inhibition effects of the gas-phase hydrogen, resulting in a reduction on the yield of aromatic compounds.

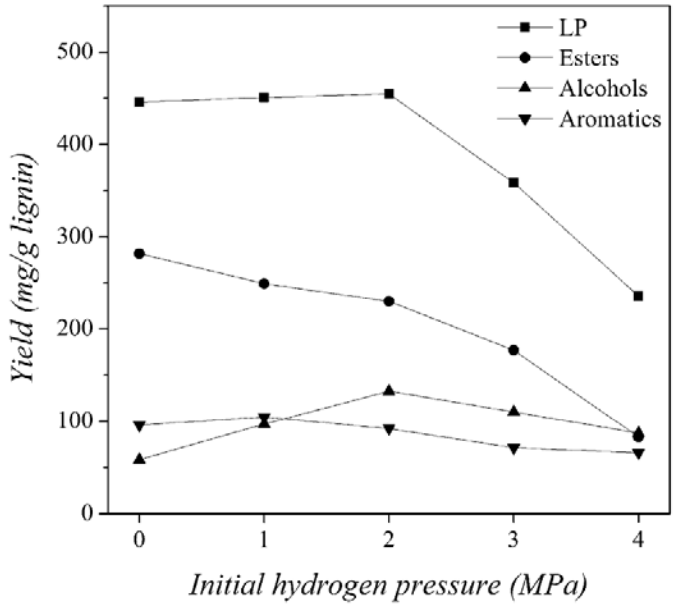

Figure 15 Effect of initial hydrogen loading on the yield of liquid products (LP25), esters, alcohols and aromatic compounds. Reaction condition: 0.5 g α-MoC_{1-x}/AC catalyst, 1 g kraft lignin, 100 ml ethanol. 280 ˚C and 6 hours [35].

2.2.2. Hydrotreating NiMo and CoMo catalysts

Nickel molybdenum (NiMo) and cobalt molybdenum (CoMo) are traditional hydrotreating catalysts, normally supported on alumina [86]. These catalysts are primarily developed for sulfur removal via hydrodesulfurization (HDS) and nitrogen removal via hydrodenitrogenation (HDN) [87], [88]. Conversion of lignin and the representing model compounds is investigated using NiMo and also CoMo catalysts [89]–[95]. In these catalysts, Co and Ni are promoter agents that donate electrons to the active sites of molybdenum, presumably by weakening the bonds between molybdenum and sulfur, lowering sulfur coordination and providing vacant sites [96]. The presence of promoter results in structural, morphological and electronic changes and increases the catalyst activity for HDS [97], [98].

In MoS_2 catalyst, a sandwich pattern of one layer of molybdenum atoms between two layers of sulfur is proposed [99]. It is suggested that the edge sites of the catalyst are active for HDO and HDS [98]. In fully sulfided state, MoS_2 has a triangular morphology. Lauritsen et al. [100] synthesized Co and Ni promoted MoS_2 catalysts on a single crystal Au(111) surface to obtain highly dispersed catalyst particles and evaluated the morphology with scanning tunneling microscopy (STM) images. According to STM analysis, the morphology of the nanoclusters of MoS_2 transfers from triangular to truncated morphologies by formation of CoMoS (shown in Figure 16, a). Regarding NiMoS catalyst, two types of Ni-Mo-S clusters form: A truncated triangular morphology (type A, similar to CoMoS) and a dodecagonal-like nanocluster (type B) (Figure 16, b & c). CoMoS and the type A NiMoS clusters are decorated in the edge with unprompted and fully sulfided edges (MoS_2) and Ni- and Co-substituted edges with sulfur coverage of 50%. The type B NiMoS contains three types of terminating edges: Fully Ni substituted NiMoS $(\bar{1}010)$ in larger cluster, partially Ni substituted NiMoS $(10\bar{1}0)$, and NiMoS with high-index $(11\bar{2}0)$.

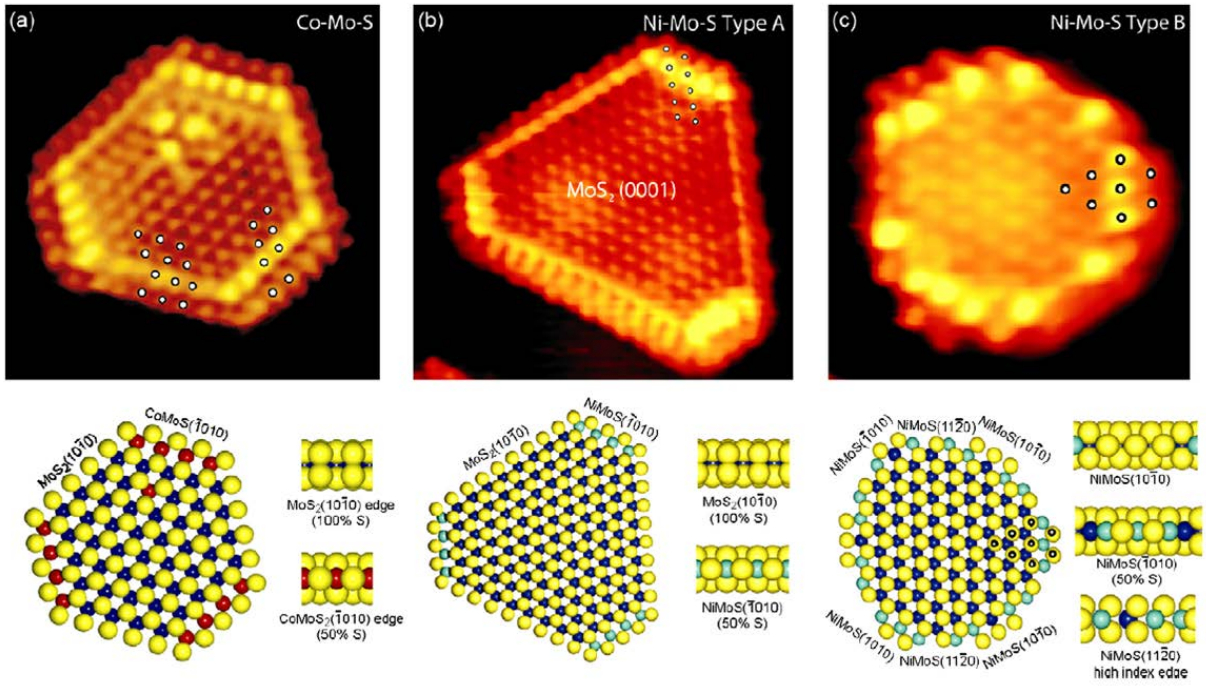

Figure 16 STM images of (a) CoMoS, (b) type A NiMoS and (c) type B NiMoS supported on Au(111) and ball model of catalysts (top and side views) based on density functional theory (DFT) calculations [98].

The NiMo and CoMo catalysts are primarily in oxide form, and should be sulfided to gain activity. The sulfidation is normally conducted in the presence of H_2S, or alternatively with a sulfiding agent such as dimethyl disulfide (DMDS) at 300-400 ˚C. According to texier et al. [101], at temperatures higher than 230 ˚C, DMDS reductively decomposes to methane and H_2S according to Eq. 1

$$CH_3\text{-}S\text{-}S\text{-}CH_3 + 3H_2 \longrightarrow 2CH_4 + 2H_2S \qquad \text{Eq. 1}$$

The presence of sulfur source in catalytic conversions using NiMo and CoMo catalysts is required in order to keep catalyst activity. This is advantageous when conversion of kraft lignin and lignosulfonate is targeted, as these technical lignins contain sulfur. Mortensen et al. [102] investigated the stability of Ni-MoS_2/ZrO_2 catalyst during HDO of phenol in 1-octanol at 280 ˚C. According to their results, addition of sulfur was necessary for keeping the activity of the catalyst via sulfur vacancies when HDO is taking place. Both H_2S and H_2O compete for the catalyst active sites. In the absence of sulfur, the edge sulfur atoms can be replaced by oxygen [102].

Narani et al. [32] investigated conversion of kraft lignin (containing 1.6 wt% sulfur) with NiMo and CoMo catalyst at 320 ˚C with initial hydrogen pressure of 35 bar for 8 hours and catalyst: lignin: solvent loading of 0.25 g: 1 g: 30 ml methanol. The catalyst was sulfided *in-situ* by addition of 0.1 g DMDS. NiMo showed higher activity for degradation of lignin than CoMo: The yield of methanol degraded oil over CoMoS/AC was 41 wt% while that number for NiMoS/AC was 57 wt%. The yield of monomers using different catalysts is shown in Figure

17. By exchanging Mo with W, the methanol soluble oil of 62 wt% over oxide catalyst ($NiWO_x$/AC) and 82 wt% over sulfide catalyst (S-NiW/AC) were reported. The highest monomer yield of 28.5 wt% was reported over S-NiW/AC catalyst (Figure 17) [32]. It was suggested that the catalyst with neutral or basic features favor degradation of lignin. The ammonia desorption of 18.4, 44.5 and 77.0 µmol/g_{cat} were detected for NiW/AC, NiMo/AC and CoMo/AC catalysts, indicating that NiW/AC and CoMo/AC were the least and the most acidic catalysts [32]. Sulfide NiW/AC catalyst showed higher activity in degradation of kraft lignin compared to oxide catalyst [32]. A char yield of 8 wt% was reported over oxide NiW/AC, while no char was observed over sulfide catalyst. They observed 40% methanol soluble oil yield over S-NiW supported on ZSM-5 (acidic support) with formation of 30 wt% char, which indicated that condensation reactions were catalyzed on the acidic sites of the catalyst [32]. The catalysts supported on ML (MgO-La_2O_3), MC (MgO-CeO_2) and MZ (MgO-ZrO_2) showed basic features, with the methanol soluble oil yields being 82, 75 and 68 wt% [32].

Narani et al. [32] suggested that external source of hydrogen is required for activity of NiMo catalyst. In the absence of molecular hydrogen and reaction in nitrogen medium, a methanol soluble oil yield of 22 wt% over NiMoS/AC was reported, with considerably lower yields of monomers (6.5% vs. 14.5% in the presence of hydrogen) indicating the effect of molecular hydrogen on inhibiting condensation reactions or enhancing the rate of lignin depolymerization.

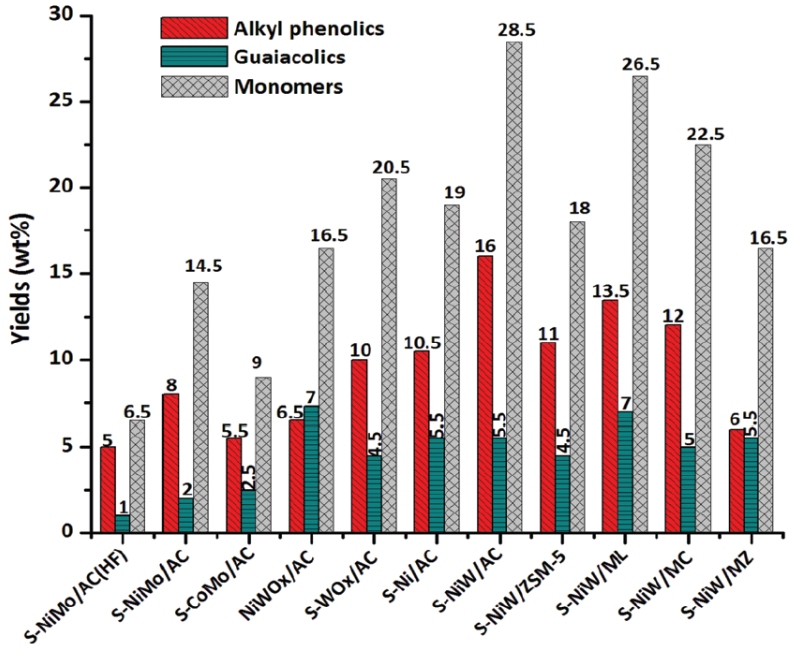

Figure 17 The yields of monomers including alkyl phenolics and guaiacolics from conversion of kraft lignin over sulfide and oxide NiMo, sulfide WO_x, sulfide Ni and sulfide NiW supported on a range of materials including activated carbon (AC), ZSM-5, MgO-La_2O_3 (ML), MgO-CeO_2 (MC) and MgO-ZrO_2 (MZ). S-NiMo/AC(HF) represents the reaction in th absence of hydrogen. 0.25 g catalyst, 1 g kraft lignin, 30 ml methanol, 35 bar H_2, 320 ˚C, 8 hours [32].

Joffres et al. [103] investigated conversion of protobind 1000 lignin (soda lignin) over alumina supported NiMo catalyst in a batch reactor at 350 ˚C and 5 hours. In each test 30 g lignin was reacted in 70 g tetralin medium with/without 3 g pre-sulfided $NiMo/Al_2O_3$ catalyst and 16 µl DMDS (for keeping the sulfidation satate of catalyst) under 80 bar H_2 pressure. The conversions, losses and the yields of different fractions with and without catalysts and at the time of t0 (the experiment stopped when the temperature reached the set point) are shown in Figure 18. A conversion of 27 wt% was observed at t0, with the liquid yield being 24 wt%. The time required to reach to t0 was 14 minutes. Compared to the starting lignin, the HSQC NMR analysis of the residual lignin from t0 reaction indicated that the lignin experienced transformations during heating the reactor to the set point, as the signals corresponding to β-O-4 linkage and methoxy groups were disappeared while bonds such as β-5 were formed. The presence of catalyst increased the oil yields compared to non-catalytic conversion after 5 hours reaction time. The main identified compounds in the liquid phase were phenols, aromatics, naphthenes and alkanes. By evaluation of liquid and solid fractions with different analytical techniquies including HSQC NMR, P NMR and FTIR, the following reactions were proposed occurring in the presence of catalyst after 5 h: Dehydroxylation of aliphatic OH groups, decarboxylation of carboxylic acids, saturation of aliphatic double bonds, demethoxylation of syringyl and guaiacyl units and cleavage of ether bonds.

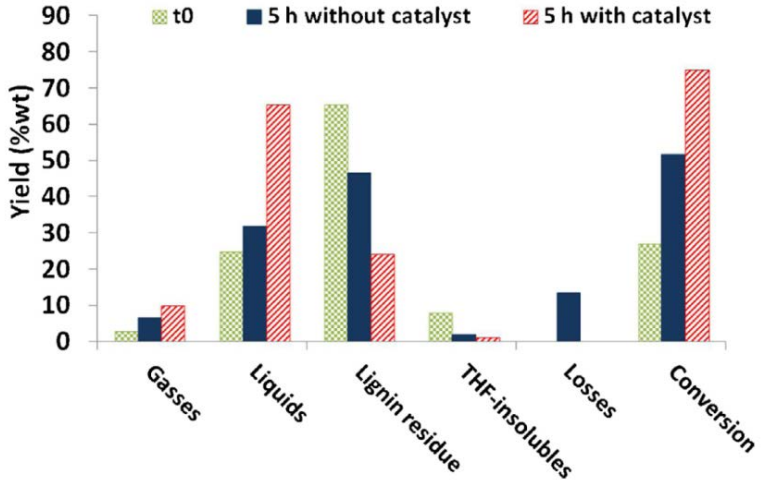

Figure 18 The conversion and the yields of different fractions from conversion of soda lignin over $NiMo/Al_2O_3$ in tetralin solvent in the absence and presence of catalyst. t0 represents a catalytic tests which was stopped when the temperature reached the set point. Reaction condition: 30 g lignin: 0/ 3 g pre-sulfided catalyst: 70 g tetralin at 350 ˚C and 5 hours [103].

In another work, Joffres et al. [104] expanded the reaction time to 0, 1, 5, 14 and 28 hours. It was observed that by increasing reaction time to 28 h, the conversion and the liquid yield increased to 87 and 71 wt%, respectively, and the lignin residue yield decreased to 11.4 wt%. The evaluation of the products present in the liquid phase indicated that the yields of methoxy phenols, dimethoxy phenols and benzenediols quickly decreased while the yield of phenols increased continuously (shown in Figure 19). The yields of compounds such as paraffins, naphthenes and aromatics increased over different reaction times, reaching to 13.3 wt% based on the lignin loading.

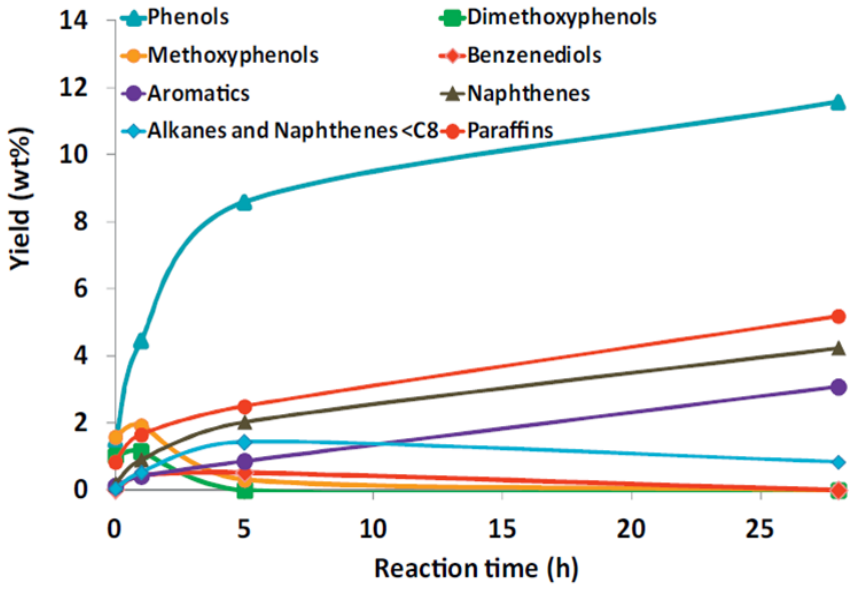

Figure 19 The yields of demethoxyphenols, methoxyphenols, benzenediols, phenols, light hydrocarbons, paraffins, naphtenes and aromatics over different reaction times. Reaction condition: 30 g lignin: 3 g pre-sulfided catalyst $NiMo/Al_2O_3$: 70 g tetralin at 350 ˚C [104].

Two step catalytic conversion of kraft lignin (sulfur content of 1.64 %), Alcell organosolv lignin and lignin from sugarcane bagasse (sulfur content of 1.53 %) was studied by Jongerious et al. [105]. In this method, lignin was first treated under liquid phase reforming (LPR), where 1 g of lignin was liquefied in a batch reactor over 0.5 g 1 wt% Pt/Al_2O_3 catalyst in a solution, comprised of 25 ml 1 M NaOH in water and 25 ml ethanol, at 225 ˚C and 58 bar argon (Ar) with a reaction time of 2 hours. The product of their LPR process was almost solid free, attributed to the solubility of lignin in alkaline solutions. The identified monomers from LPR reaction of organosolv and kraft lignin were mainly composed of alkyl and propanol substituted guaiacol and syringol-type compounds. They further upgraded an amount of 500-800 mg of the oil obtained from LPR in a HDO with 50 mg $CoMo/Al_2O_3$ or Mo_2C/CNF catalysts and 7.5 g dodecane solvent at 300 ˚C and hydrogen pressure of 50 bar for 4 hours. They observed solid products from HDO reaction, which were possibly unreacted lignin fractions that were not soluble in dodecane [105].

The yields of the monomers from LPR and LPR+HDO processes for three types of lignin are shown in Figure 20. In the LPR reaction products, the identified monomeric compounds from the hardwood organosolv lignin were composed of 58% tris-oxygenated syringol-like molecules while 59% bis-oxygenated monomers were detected from conversion of softwood kraft lignin. Considering the grass type bagasse lignin, 42% bis-oxygenated and 38% mono-oxygenated phenolic were among the monomers which were consistent with the nature of the biomass and abundance of syringyl, guaiacyl and p-coumaryl units. The yield of monomers from conversion of oil from organosolv and kraft lignin over $CoMo/Al_2O_3$ catalyst decreased to 6% and 6%, respectively, which was lower than the monomer yields from LPR process. The decrease of the monomer yields was partially attributed to the removal of oxygen. The

monomer yield for bagasse lignin oil was 5%. Noticeably, formation of oxygen free compounds such as benzene, toluene and xylene was only observed after HDO reaction [105]; amongst the identified monomers, 25%, 15% and 20% of the compounds were oxygen free in the products from organosolv, kraft and bagasse lignin. Similar reaction mixture was observed from HDO over Mo_2C/CNF catalyst, where 9%, 7% and 6% monomer yields were observed from organosolv, kraft and bagasse lignin [105].

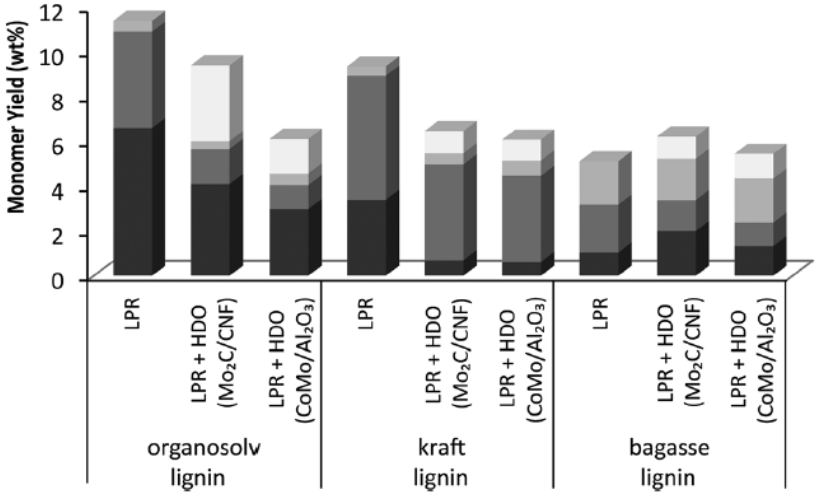

Figure 20 Yield of the monomeric products after LPR and LPR+HDO reactions. LPR reaction condition: 1 g lignin: 0.5 g 1 wt% Pt/Al_2O_3: 25 ml 1 M NaOH in water and 25 ml ethanol, at 225 ˚C, 58 bar Ar, 2 hours. HDO reaction condition: 500-800 mg oil from LPR: 50 mg $CoMo/Al_2O_3$ or Mo_2C/CNF catalysts: 7.5 g dodecane, at 300 ˚C, 50 bar H_2, 4 hours. White: oxygen free products, light gray: mono-oxygenated products, dark gray: products containing two oxygen functionalities, black: products with three or more oxygen functionalities [105].

Grilc et al. [39] investigated the role of solvents on hydrodeoxygenation of liquefied wood samples over oxide $NiMo/Al_2O_3$ catalyst at 300 ˚C and 1 hour in a slurry reactor. Tetralin, phenol, 2-propanol, pyridine, m-cresol, anthracene, cyclohexanol and xylene were the solvents evaluated. In each test, the reactor was loaded with 200 ml reaction mixture (oil: solvent ratio of 1:3 containing 7.5 wt% catalyst based on the mass of solvolysis oil). The pressure inside the reactor was kept at 80 bar with a flow of 1NL/min of fresh hydrogen. The liquefied wood samples were obtained by liquefaction of sawdust in a mixture of glycerol and diethylene glycol (1:1 Mass basis) containing 3 wt% p-toluenesulfonic. Therefore, the liquefied oil contained 0.9 wt% sulfur. The reaction products were composed of a tar residue (filterable while dissolved in ethanol or THF), liquid phase (including reaction products and solvent), condensed fraction (mainly water produced from HDO reactions and light hydrocarbons) and gas phase [39]. The yields of different fractions and the gross calorific value (GCV, MJ/kg) of the liquid phase are shown in Figure 21. Amongst different solvents, tetralin showed promises for HDO reactions over NiMo catalyst. The highest GCV and the lowest yield of tar were observed in tetralin, indicating that the *in-situ* produced hydrogen from tetralin inhibited the condensation reaction of reactive fragments. Almost similar yields were observed in 2-propanol and anthracene. The highest yield of tar was observed in these solvents, indicating

that condensation reactions were not inhibited by the solvents. However, the GCV of the oil from anthracene was the highest amongst the others. The yield of tar phase was relatively low in phenol and m-cresol suggesting that the solvent were capable of end-capping the reactive fragments. The yield of condensed phase was lower in phenol, attributed to the inferior HDO activity compared to m-cresol. The yields in cyclohexanol and xylene were within the same range; however the yield of tar fraction was higher in cyclohexanol. The highest yield of condensed fractions in pyridine solvent indicated the role of solvent in extensive hydrocracking reactions and degradation to light products.

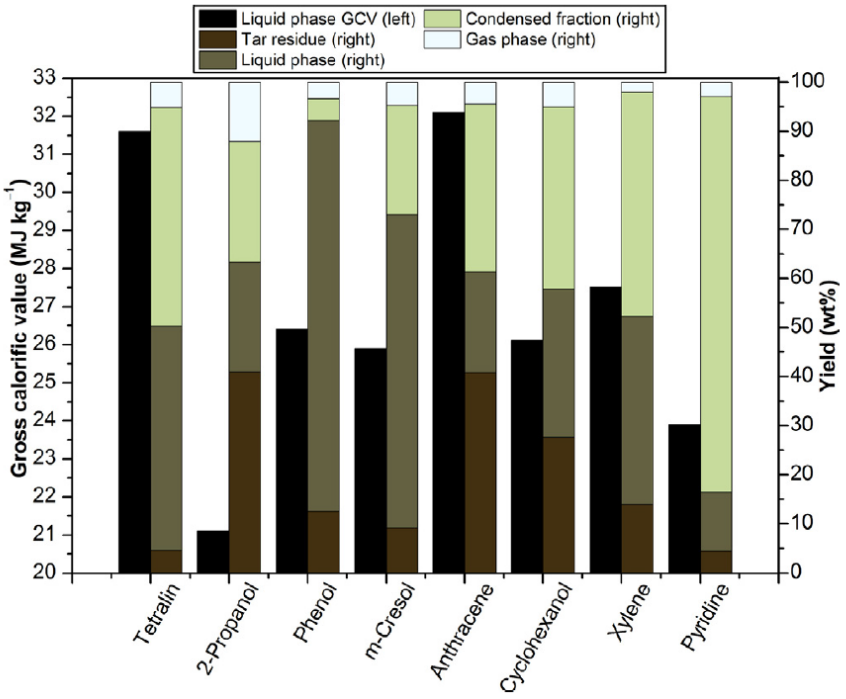

Figure 21 The yields of different fractions and GCV of liquid phases from hydrotreating liquefied oil over oxide NiMo catalyst. 200 ml reaction mixture (oil: solvent ratio of 1:3 containing 7.5 wt% catalyst based on the mass of solvolysis oil), 300 ˚C, 80 bar H_2, 1 hour [39].

Promotion of MoS_2 catalyst affects the reaction pathways. Raybaud et al. [106] investigated deoxygenation activity of unsupported Ni-promoted MoS_2 (by varying Ni/Mo ratio) for conversion of ethyl heptanoate in a fixed bed reactor at 250 ˚C and H_2/feed ratio of 350 Nl/l (equivalent to hydrogen partial pressure of 1.44 MPa in the reactor). The feed was composed of 6 wt% ethyl heptanoate in dodecane. While in the absence of Ni promoter, MoS_2 was highly selective for HDO and formation of C_7 hydrocarbons, both HDO and decarboxylation/decarbonylation (DCO) pathways were taking place over Ni promoted MoS_2 catalyst. As shown in Figure 22, by increase of Ni/Mo ratio, the selectivity increased towards DCO products. According to Raybaud et al. [106] the required energy for hydrogenation of C=O and cleavage of C-OH were lower over NiMoS catalyst compared to MoS_2. They elaborated on the role of Ni through two pathways: Ni in NiMoS form promoted hydrodeoxygenation reactions whereas Ni in Ni monosulfide enhanced decarbonylation reactions.

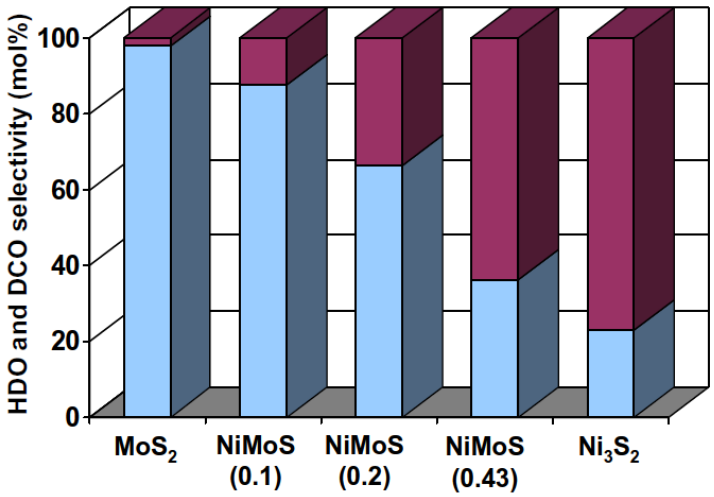

Figure 22 HDO and DCO selectivity during conversion of 6 wt% ethyl heptanoate in dodecane over sulfide catalysts with different Ni/Mo molar ratio at 250 ˚C and H_2/feed ratio of 350 Nl/l. Blue: HDO mol %, Purple: DCO mol % [106].

Zhang et al. [91] investigated cleavage of β-O-4 over NiMo catalyst in alcohol solvent (methanol) and in the presence of H_2 at 180 ˚C, using different model compounds including β-O-4-A (with alcohol functional group attached to C_α) and β-O-4-K (with C_α=O bond). According to their results, the cleavage of C_β-OPh was not influenced by BDE value. The functional group attached to the C_α atom had a great impact on cleavage of C_β-OPh bond [91]. The BDE of β-O-4-A and β-O-4-K are 274.0 and 227.8 KJ/mol, respectively. However, the results of conversion of these compounds in 1 hour reaction time showed 69 and 20% conversion, with 33 and 14% ether bond cleavage in each compound. They showed that the presence of hydrogen was necessary for cleavage of C_β-OPh bond since only 1% conversion of β-O-4-A was reported in Ar atmosphere [91]. They proposed that conversion of β-O-4-A took place through the following steps:

- Dehydroxylation of C_α-H bond on the acid sites of catalyst and generation of carbocation intermediate $PhCH^{\delta+}CH_2OPh$
- $PhCH^{\delta+}CH_2OPh$ transformed into $PhCH.CH_2OPh$ radical through receiving electron on catalyst redox cycle
- C_β-OPh was cleaved (BDE of C_β-O in $PhCH.CH_2OPh$ form is lower than the original form) and the *in-situ* formed radicals reacted with H_2 or methanol on hydrogenation sites resulting in formation of phenols, arenes and other ethers

They suggested that Mo might be the redox site whereas hydrogenation sites could be MoS_x or NiMo for conversion of β-O-4-A (see Figure 23) [91].

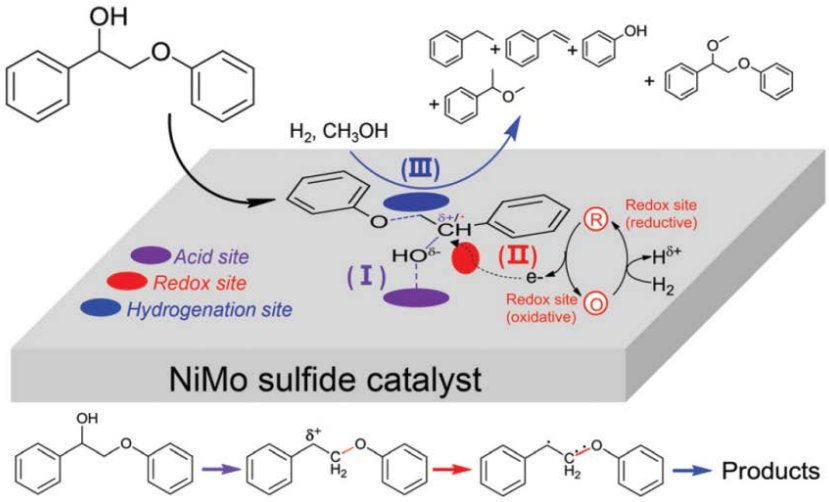

Figure 23 The proposed mechanism for cleavage of β-O-4-A model compounds over sulfided NiMo in alcohol solvent [91].

HDO of lignin derived products results in formation of low oxygen containing products with a better miscibility with hydrocarbon fuels [107]. High degree of oxygen removal with the least possible hydrogen consumption is one of the main challenges in the HDO reactions [56]. Hydrodeoxygenation of guaiacol in the presence of supported and unsupported CoMoS catalyst was investigated by Bui et al. [87] at 300 °C and at a hydrogen pressure of 40 bar. Catechol and phenol were observed as primary products. The proposed reaction pathway is presented in Figure 24. According to Bui et al. [87], HDO could occur either via direct deoxygenation route (DDO) or through the hydrogenation (HYD) route. Thus, benzene formation possibly occurred by direct C-O cleavage from phenol while cyclo-alkane and cyclo-alkenes formation occurred by hydrogenation of the aromatic ring through HYD pathway [87].

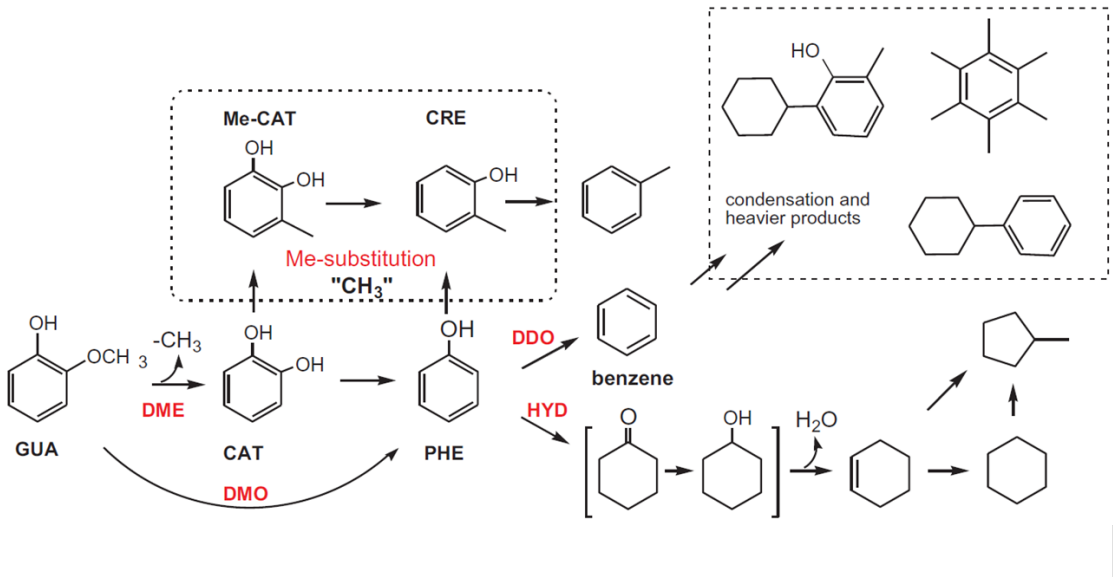

Figure 24 General reaction scheme for guaiacol conversion over transition metal sulfide catalyst under H_2 pressure [87].

84% conversion of guaiacol in the presence of $CoMoS/Al_2O_3$ catalyst at 300 ˚C, 50 bar H_2 pressure and 4 h reaction time was observed by Jongerius et al. [88]. Phenol, anisole, catechol, methylated products and hydrogenated products were reported as the main products of the conversion with selectivity of 34%, 3%, 11%, 19% and 3%, respectively. In a similar study, Laurent et al. [108] investigated hydrodeoxygenation of guaiacol over sulfided $CoMo/\gamma\text{-}Al_2O_3$ and $NiMo/\gamma\text{-}Al_2O_3$ catalysts at a total pressure of 70 bar and 300 °C. Guaiacol conversion of 10% was observed without catalyst while the conversion increased up to 57% and 65% in the presence of CoMo and NiMo catalysts, respectively. Catechol, phenol and trace amounts of benzene and cyclohexane were detected as products while methylated products were not observed [108].

2.2.3. Catalytic conversion of lignosulfonate

The numbers of studies on reductive conversion of lignosulfonate are limited [109]–[111]. There are two main challenges associated with lignosulfonate valorization. Sulfur poisoning of the heterogeneous catalyst active sites and contamination of the lignin derived products with sulfur. Since a significant focus of this thesis is on conversion of lignosulfonate, the relevant studies on conversion of this lignin are summarized here.

Horacek et al. [111] investigated conversion of 5 wt% aqueous solution of sodium lignosulfonate in the presence of 2 g alumina supported NiW, NiO (with Ni loading of 2.5, 5, 10 and 15 wt%) and NiMo catalysts (with loading of 7 wt% NiO and 4, 7 and 10 wt% MoO_3) in a tubular flow reactor at 320 ˚C and hydrogen flow of 2 Nml/min and F/W of 1 h^{-1}. Prior to each experiment, the catalysts were reduced at 350 ˚C for 1 h in hydrogen flow of 5 Nml/min and pressure of 130 bar. Using GC-MS analysis, they found guaiacol as the primary product in all conditions. Para-substituted guaiacols, such as 2-methoxy-4-methylphenol, p-ethyl guaiacol, 2-methoxy-4-propyl phenol, 1-(4-hydroxy-3-methoxyphenol)-2-propane, 4-hydroxyl-3-methoxybenzeneacetic acid as well as other alkyl phenols were the other identified compounds (shown in Figure 25).

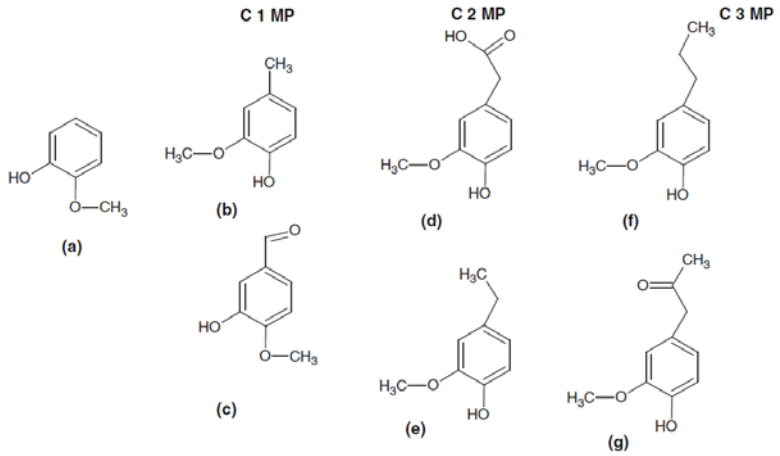

Figure 25 The main products identified from conversion of sodium lignosulfonate over Alumina supported NiW, NiO and NiMo catalysts. (a) guaiacol, (b) 2-methoxy *p*-cresol, (c) 3-hydroxy-4-

methoxybenzaldehyde, (d) 4-hydroxy-3-methoxy benzeneacetic acid, (e) *p*-ethyl guaiacol, (f) *p*-propyl guaiacol, and (g) 2-propanone, 1-(4-hydroxy-3-methoxyphenyl) [111].

The highest yield of 1.8 wt% guaiacol was reported over 10 wt% NiO catalyst while this number slightly decreased to 1.5 wt% over NiMo catalyst with MoO_3 loading of 10 wt%. Better performance over NiO compared to NiMo and NiW was reported to be due to hydrogenolytic activity of nickel at temperatures above 200 ˚C. They suggested that nickel promotes cleavage of C-C and C-O linkages in lignin structure and the primary products (C1-C3 methoxyphenols). A plausible reaction pathway for decomposition of sodium lignosulfonate was proposed (shown in Figure 26). However, Horacek et al. [111] did not discuss if the sulfur in the feedstock lead to catalyst deactivation [111].

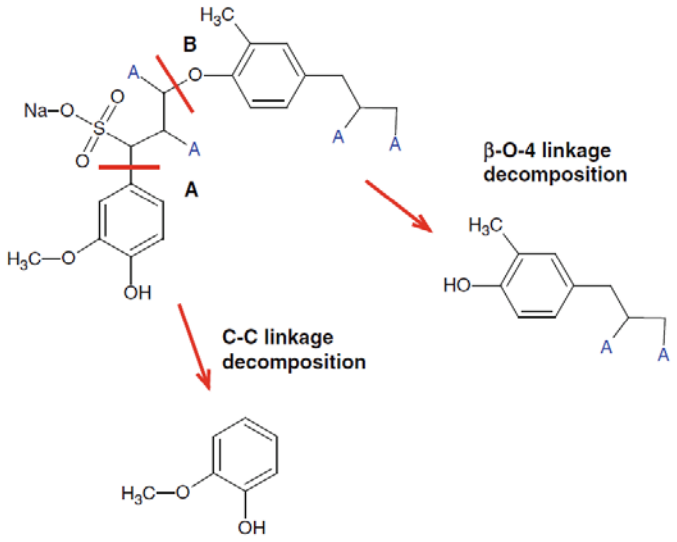

Figure 26 Reaction pathways for catalytic decomposition of sodium lignosulfonate [111].

Song et al. [110] reported catalyst screening for depolymerization of lignosulfonate in ethylene glycol at 200 ˚C and 50 bar hydrogen pressure (see Figure 27). While no conversion was observed in the absence of catalyst, less than 20 conversion of lignin was reported in the presence of zeolite and zeolite-based catalysts [110]. Raney catalysts (Cu, Fe and Co), precious metals (Pd/AC, Ru/AC and Pt/AC) and transition metal catalysts (Cu/AC and Ni/MCM-41) were the other group of the catalysts investigated; conversion of 10-40% and selectivity of 60-80% towards 4-propyl-guiacol (PA) and 4-ethyl-guiacol (EA) was reported over these catalysts. Ni-based catalysts demonstrated conversion higher than 60 wt% and selectivity of 75-95% for alkyl-substituted guaiacols. Opposite to Horacek et al. [111], Song et al. [110] proposed that the nickel based catalysts do not have C-C cleavage activity, since aromatic dimers and aliphatic C-C bonds were detected in the products. According to Song et al. [110], C-O-C and C-OH bonds in the structure of lignosulfonate were hydrogenolyzed through reaction with H^* (formed by dissociation of H_2) over Ni(0) sites. The C-S decomposition over catalyst resulted in formation of NiS species. Song et al. [110] argued that by further reaction of NiS with H^*, the catalyst was regenerated and sulfur left the catalyst in form of H_2S. They stated that reductive atmosphere was required for keeping the activity of the catalyst.

Investigating reusability of catalyst demonstrated that the conversion decreased from 68% to 30% after using the catalyst for three times. However, by regeneration in hydrogen for 2 hours in ethylene glycol, the conversion increased to 72% [110].

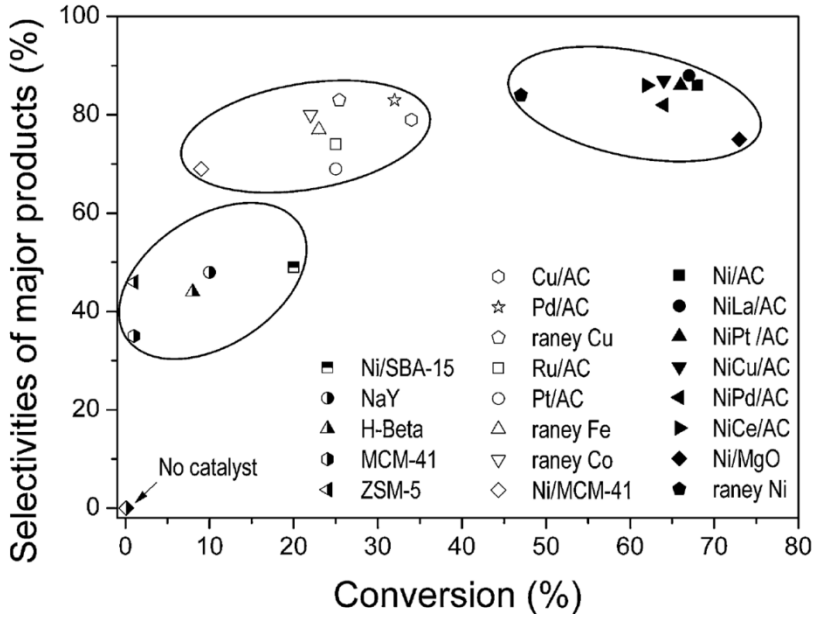

Figure 27 Conversion of lignosulfonate over various catalysts in ethylene glycol as solvent. 0.2 g catalyst, 2 g sodium lignosulfonate: 120 ml ethylene glycol, 200 ˚C, 50 bar H_2 [110].

Shu et al. [109] tested hydrogenolysis of sodium lignosulfonate over noble metal and metal chloride Lewis acid catalyst in methanol. The reaction condition was 0.5 g Na-LS, 1 mmol metal chloride, 0.1 g 5 wt% noble metal and 40 ml methanol in a 100 ml batch autoclave and 30 barg H_2 pressure loaded at 280 ˚C for 5 hours. The sulfur content of Na-Ls was 5.05 wt%. They obtained aliphatic alcohol and aromatic monomers as liquefied products. While addition of Pd/C catalyst increased the degradation slightly from 64.4 % in non-catalytic condition to 69.3 wt%, the considerable boost was reported by conversion in Pd/C and CrCl3 mixture, where the degradation increased to 83.9% with the yields of aliphatic alcohols and monomers being 5.3 and 8.5 wt%, respectively, attributed to the presence of metallic acidic catalyst and electronegativity of Cl^- as hydrogen bonding acceptor and nucleophilic reagent [109].

2.2.4. Summary of solvothermal conversion of technical lignin

In the literature, it was reported that the reaction medium has a great influence on the degradation of lignin. Solvents with high Lewis basicity may adsorb on the catalyst active sites and inhibit adsorption of lignin degraded fragments. Moreover, formation of saturated compounds can occur in a non-polar solvent while unsaturated compounds may be formed in a polar solvent. The performance of ethanol in degradation of lignin was elaborated in the literature; Ethanol inhibits condensation reactions by suppressing reactive fragments via esterification and alkylation. Among different heterogeneous catalysts, Ni and Cu based catalysts and also hydrotreating NiMo catalyst showed good performance on degradation of

lignin and stabilization of reaction products. Formation of oxygen free aromatics was reported over NiMo and CoMo catalysts.

2.3. Solvothermal conversion of biomass

In the conventional pulp industries, extraction of cellulose from biomass is the main target; therefore the remaining lignin is composed of highly cross-linked phenolic groups formed via C-C bond formations which, depending on the pulping process, may contain sulfur. An alternative approach is the direct catalytic conversion of biomass; in this approach, either whole biomass in converted [112] or lignin is fractionized (mainly in the presence of a catalyst) while cellulose and hemicellulose is almost conserved. The later process is attributed as 'early-stage catalytic conversion of lignin (ECCL)' or 'lignin-first biorefining' [40]. The lignin derived products by this method show high selectivity towards a few number of monomers [19], [43], [113], whereas in the conversion of technical lignin, obtaining monomers with high selectivity remains as a challenge.

Brand et al. [114] investigated non-catalytic degradation of lignocellulosic constituents including cellulose, xylose (as representative of hemicellulose) and lignin in supercritical ethanol and nitrogen atmosphere. Conversion of cellulose significantly increased from 11.6% to 93.8% by increasing the reaction temperature from 265 to 350 ˚C (shown in Figure 28, a) [114]. The cellulose liquefaction was associated with formation of light hydrocarbons, water and gaseous fractions. They observed weak temperature dependence on the lignin conversion; the lignin conversion increased marginally from 45% at 293 ˚C to 51.9% at 350 ˚C, indicating that lignin is the most recalcitrant wood constituent in biomass (Figure 28, b). Xylose was almost completely converted with the conversion of 98.1% at 265 ˚C, indicating that hemicellulose is the most facile constituent of biomass [114].

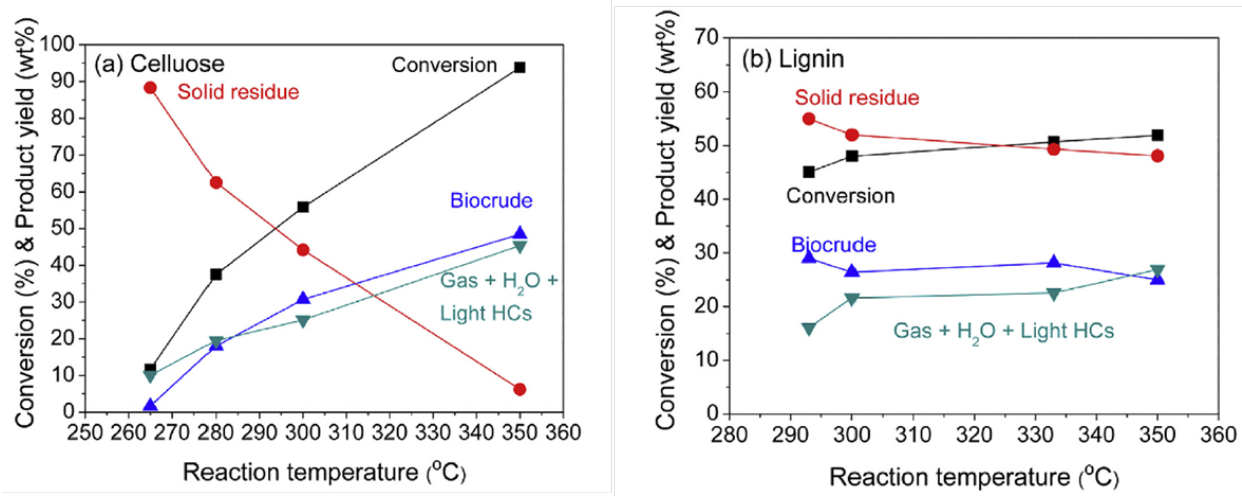

Figure 28 Conversions and product yields from liquefaction of (a) cellulose and (b) lignin over different reaction temperatures. Reaction condition: 6 g substrate: 60 ml ethanol, 20 bar N_2 (loaded at RT), 30 minutes [115].

Yamazaki et al. [115] observed that longer chain alcohols were capable of decomposition of beech wood in shorter reaction time. They converted 150 mg Japanese beech in 4.9 ml

alcohol at 275 and 350 ˚C. Under similar condition, 90% liquefaction of wood was achievable at 350 ˚C and 30 minutes in methanol and ethanol, while it took 20, 10 and 3 minutes to obtain the same degree of liquefaction in 1-propanol, 1-butanol and 1-octanol. The higher rates of liquefaction in longer chain alcohols was attributed to higher solubility of the higher molecular weight compounds in these alcohols [115].

Addition of a catalyst showed great effect on lignin degradation. Ferrini et al. [116] investigated conversion of poplar wood (containing 30% lignin) in the presence of Raney Ni catalyst in 2-propanol/H_2O (70/30 %, vol/vol) solvent at 160-220 ˚C for 3 hours. An overview of this catalytic refining process is presented in Figure 29. Wang et al. [117] have previously showed that Raney Ni catalyst in PrOH is an excellent medium for hydrogenolysis of aryl-aryl and aryl alkyl ethers [117]. Lignin was degraded in catalytic biorefining method to liquefied products, whereas in the absence of catalyst (organosolv extraction) lignin was retrieved as solid matter (Figure 29, b) [116]. Moreover, the obtained holocellulose (cellulose and hemicellulose) was reported as a compatible raw material for the production of glucose and xylose by enzymatic hydrolysis. Ferrini et al. [116] reported bio-oil and holocellulose yields of 25 wt% and 71% at 180 ˚C, respectively, corresponding to 63% delignification. By increasing temperature to 220 ˚C, the degree of delignification increased to 87% while the molecular weight of the bio oil shifted toward lower values. The easily separated catalyst (by magnetic force) was usable at least for 8 times. They proposed that acetone, which was the major by-product of the reaction, could be hydrogenated to 2-PrOH in a separated small reactor to boost the economy of the process [116].

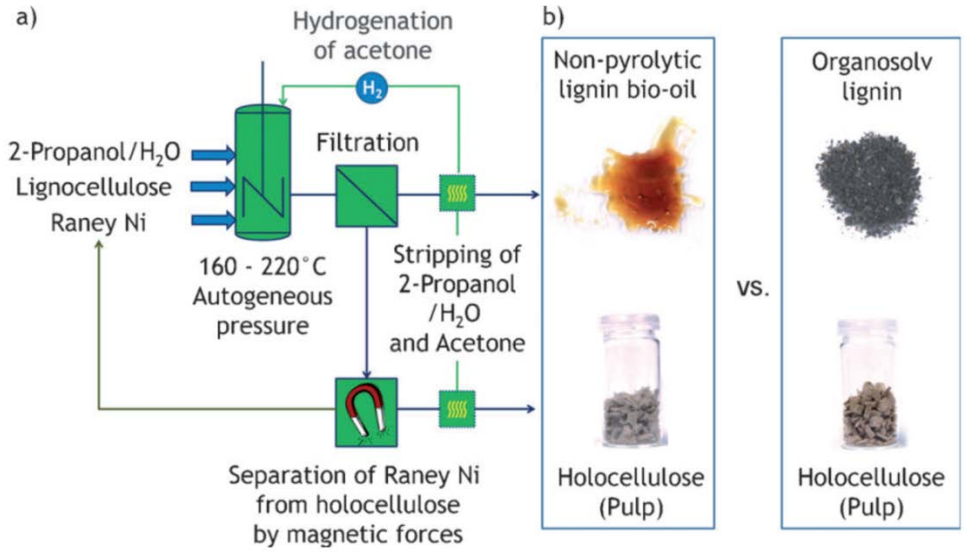

Figure 29 (a) Schematic representation of the catalytic biorefining method for treatment of poplar wood over Raney Ni catalyst in 2-propanol/H_2O (70/30 %, vol/vol) solvent. Reaction condition: 16 g wood: 10 g catalyst: 140 ml solvent, 160-220 ˚C, 3 hours. (b) Visual comparison of the products obtained by catalytic biorefining and organosolv process [116].

Fractionation of birch wood was investigated over Ru/C catalyst in methanol medium and hydrogen pressure [43]. In a typical run, 2 g birch wood was converted over 0.3 g 5% Ru/C catalyst in 40 ml methanol at 250 ˚C with initial hydrogen loading of 30 bar. A delignification of 92 % was achieved at this temperature. The total yield of monomers was 52% with 4-propyl guaiacol and 4-propyl syringol being the main monomers. The retrieved pulp, containing cellulose and hemicellulose, were subsequently converted into sugar polyols in a tungstosilicic acid and water mixture in the presence of a Ru/C catalyst under hydrogen pressure at 190 ˚C [43]. In another work, the same group tested conversion of birch sawdust in the presence of 0.2 g Ni/Al_2O_3 catalyst (21 wt% Ni) in a similar reaction condition [113]. A delignification of 90%, with phenolic monomer yield of 40% was reported with 70% selectivity towards 4-n-propanolguaiacol and 4-n-propanolsyringol as the main monomers [113]. Comparing the monomer types observed from the same type of biomass over Ru/C and Ni/Al_2O_3 catalysts elucidated the role of catalyst [43], [113]. According to Van Den Bosch et al. [113] the solvent was greatly involved in lignin fragmentation and depolymerization to phenolic compounds while the catalyst was mostly involved in stabilization of reactive fragments via hydrogenation of unsaturated side chains. A simplified mechanism of lignin fractionation and the role of catalyst and solvent is shown in Figure 30.

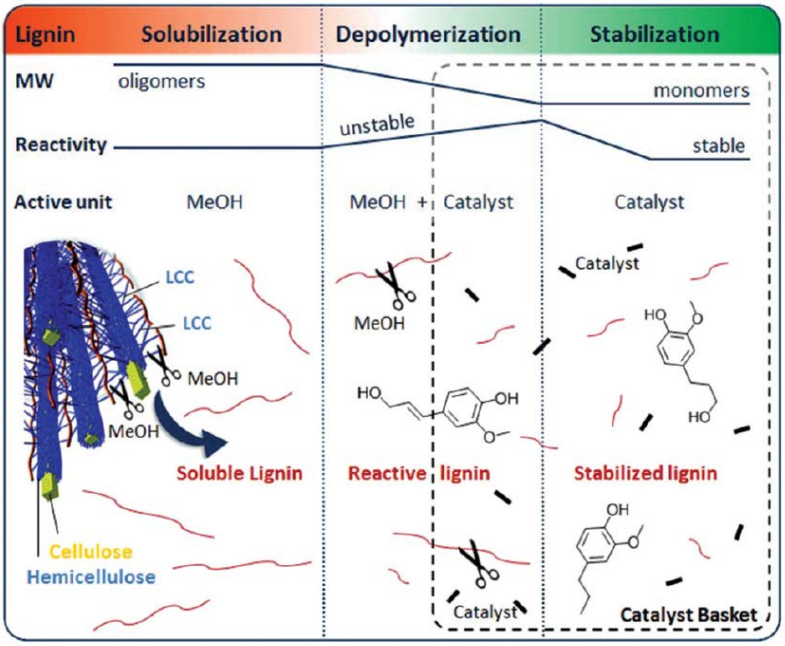

Figure 30 A proposed mechanism on the role of solvent and catalyst in fractionation of lignin in methanol medium [113].

Schutyser et al. [41] investigated the effect of solvent on the fractionation of birch wood over Pd/C catalyst. Bio-based solvents such as methanol, ethanol, 2-propanol, 1-butanol, ethylene glycol, THF, 1,4-dioxane, hexane and also water were investigated. An empirical descriptor was introduced as 'lignin first delignification' (LFDE), which was defined as delignification (DL) × carbohydrate retention (CR). The number closer to 100% indicated better performance of solvent in fractionation of lignin and conserving helocellulose [41]. A

correlation was reported between the solvent polarity (Reichardt parameter, E_T^N) and the delignification, shown in Figure 31. They observed that the delignification was the highest in water, while it decreased as the carbon number in alcohol increased. The delignification was lower in cyclic ethers, THF and 1,4-dioxane while the lowest delignification was observed in the n-hexane, being apolar solvent [41]. Their results were consistent with those from Song et al. [33] where they tested conversion of birch sawdust (2 g) over 0.2 g Ni/C catalyst in the presence of 40 ml solvent at 200 ˚C, 6 h reaction time and 1 atm argon. Some of the investigated solvents were methanol, ethanol, iso-propanol, 25% glycerol + water solution, 1,4-Dioxane, and cyclohexane. A lignin conversion of 54% was reported in methanol, which decreased to 48 and 50% in ethanol and ethylene glycol [33]. Reaction in i-PrOH and glycerol solution resulted in lower conversion of 27 and 16%, respectively. No conversion was reported in cyclohexane solvent, attributed to lack of solvent in hydrogen production and also dissolubility of lignin in the solvent, which was aligned with the low yield of phenolics reported by Schutyser et al. [41]. Despite solubility of lignin in 1,4-Dioxane, only conversion of 15% was observed attribute to the lack in hydrogen production [33].

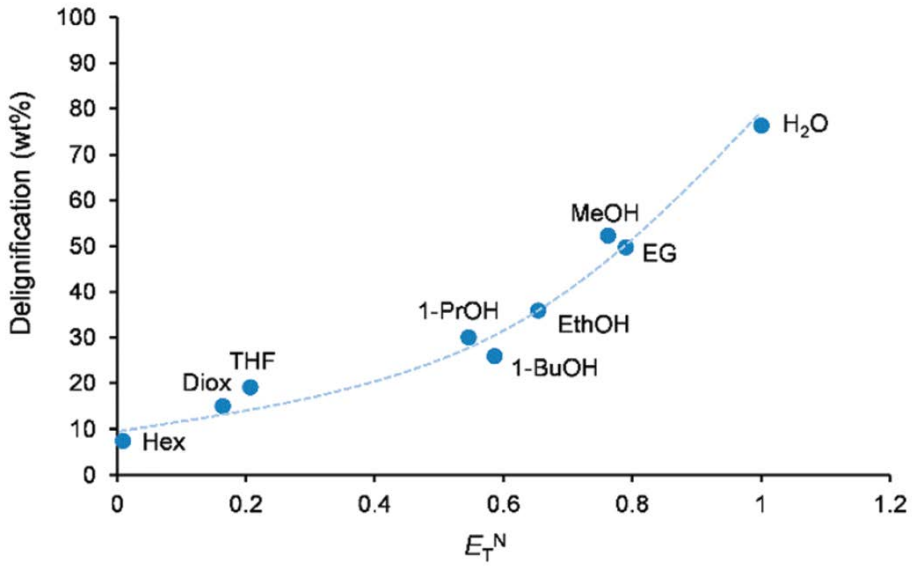

Figure 31 Delignification from conversion of birch sawdust vs. solvent polarity. Reaction condition: 2 g feedstock, 0.2 g 5% Ni/C, 40 ml solvent, 30 bar H_2 (loaded at RT), 200 ˚C, 3 hours [41].

Despite higher delignification observed in water, Schutyser et al. [41] showed that water also solubilized the carbohydrate fractions, which was unfavorable. The yields of lignin derived monomers and the retention of holocellulsoe (presented by C5 and C6 sugars) using different solvents is shown in Figure 32. The carbohydrate retention was almost similar in the other solvents, while LFDE was higher for methanol and ethylene glycol, making them the proper solvents [41].

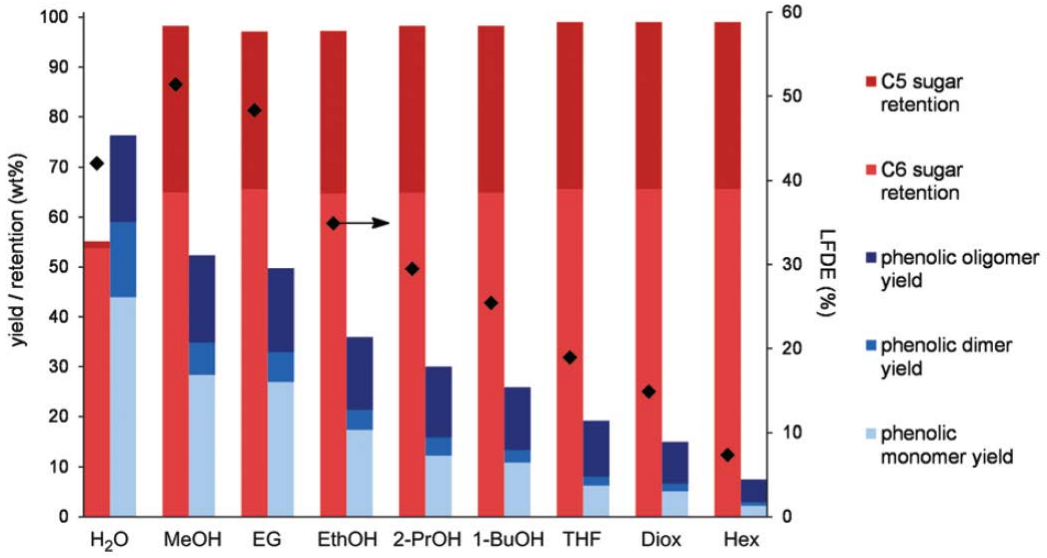

Figure 32 Yield of lignin derived phenolics and the carbohydrate retention from conversion of birch sawdust. 2 g feedstock, 0.2 g 5% Ni/C, 40 ml solvent, 30 bar H_2 (loaded at RT), 200 ˚C, 3 hours.

Klein et al. [69] followed the work from Song et al. [33] over 5-10 wt% Ni /AC catalysts and expanded the biomass feedstock to poplar and eucalyptus wood. The conversion conditions were based on the method from Song et al. [33] with biomass to catalyst ratio of 1.0 g: 0.05 g. However, Klein et al. [69] obtained lignin oil yields within the range of 10-30 wt%, which was lower compared to those from Song et al. [33] (54% conversion of lignin to liquid products). The yields of monomers obtained by Klein et al. [69] and their distribution is shown in Figure 33, and the results from Song et al. [33] are shown for comparison. They speculated that the incompatible results with those from Song et al. [33] might originate from variation of biomass composition based on the region and the season [69].

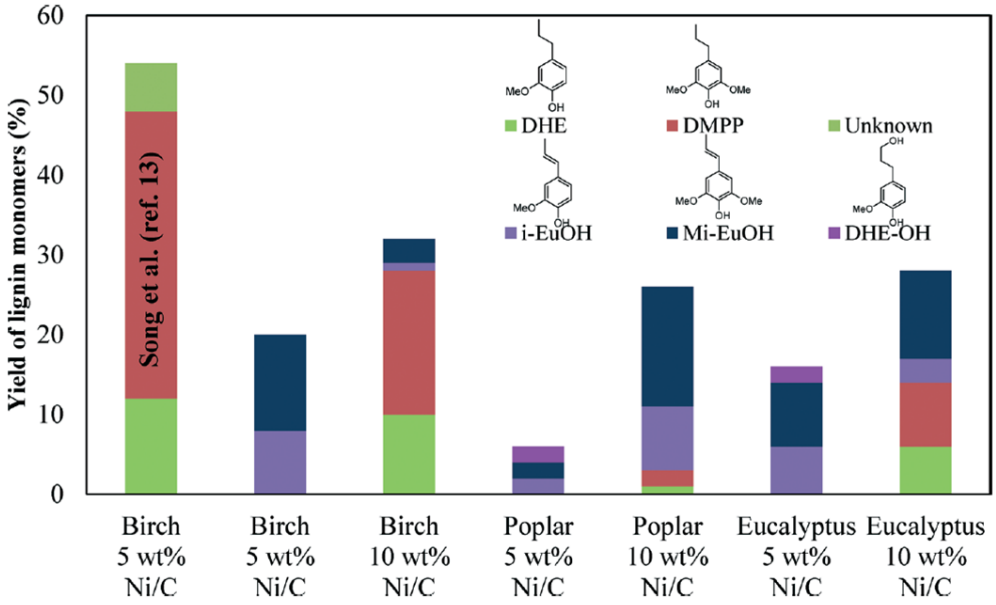

Figure 33 Results from conversion of different biomass over Ni/AC catalyst. 1 g feedstock, 0.05 g (5 wt%) or 0.1 g (10 wt%) catalyst, 200 ˚C, 2 bar N_2 and 6 hours. DHE: dihydroeugenol, DMPP: 2,6-dimethoxy-4-propyl-phenol, i-EuOH: isoeugenol, Mi-EuOH: methoxyisoeugenol, DHE-OH: 4-(3-hydroxypropyl)-2-methoxyphenol [69].

In an interesting approach, Sun et al. [118] fractionized pine lignocellulose over copper-doped porous metal oxide catalyst in methanol at 140-220 ˚C. The structure of the main lignin derived monomers and the proposed reaction mechanism for cleavage of β-O-4 is shown Figure 34. The highest monomer yield of 13% was reported at 220 ˚C, with the selectivity for dihydroconiferyl alcohol (1G), 4-propyl guaiacol (2G) and 4-ethyl guaiacol (3G) compounds being 61, 33 and 6%, respectively. Furthermore, they treated the solid residue (unreacted holocellulose and catalyst) from the first step with fresh methanol at 320 ˚C and obtained a colorless methanol soluble fraction containing mainly aliphatic alcohols, ethers and ester [118]. They proposed that cleavage of β-O-4 occurred via dehydrogenation and formation of ketone intermediate, followed by hydrogenolysis of C_β-O bond, hydrogenation and dehydration or hydrogenolysis of the formed intermediate [118].

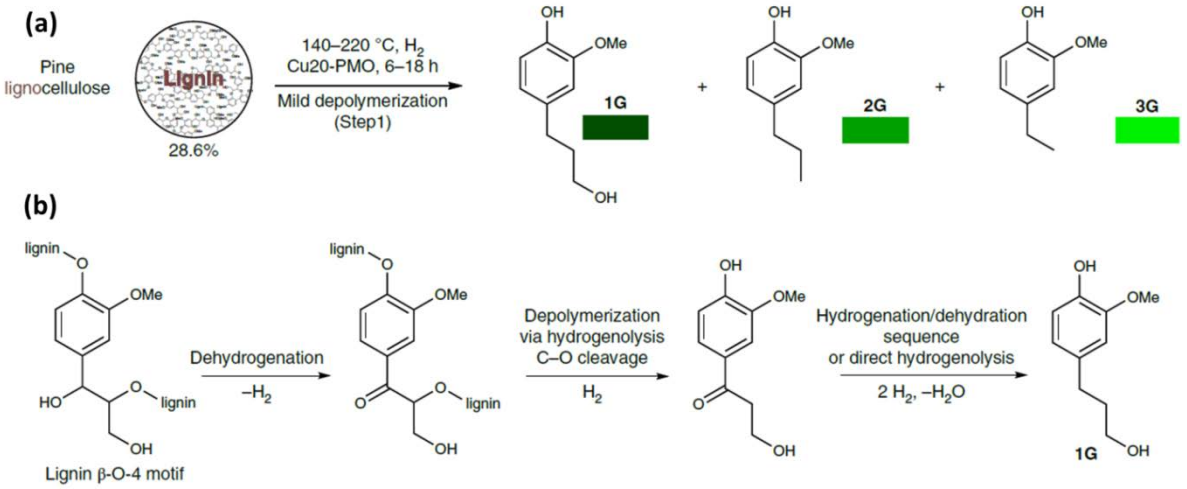

Figure 34 (a) The structure of the main monomers obtained from conversion of pine wood in methanol and over Cu_{20}-PMO catalyst. (b) The proposed reaction mechanism. Reaction condition: 0.2 g catalyst, 1 g biomass, 10 ml methanol, 40 bar H_2, 18 hours [118].

Xia et al. [119] investigated conversion of whole biomass over $Pt/NbOPO_4$ in cyclohexane solvent at 190 ˚C. An amount of 0.2 g biomass was treated over 0.2 g catalyst in 6.46 g cyclohexane with initial hydrogen pressure of 50 bar and reaction time of 20 hours. The direct conversion of birch sawdust resulted in formation of 13.1 wt% hexane, 10.2 wt% pentane and 4.8 wt% alkylcyclohexans from cellulose, hemicellulose and lignin, respectively, with the total alkane yield being 28.1 wt% [119]. It was suggested that catalytic activity involved in conversion of biomass was originating from Pt, Nb and acidic sites to facilitate C-O bond cleavage and hydrodeoxygenate reactive fragments [119].

Li et al. [120] investigated one pot catalytic conversion of birch wood (1 g) over 0.4 g Ni-W_2C/AC catalyst (4% Ni, 30% W_2C) in water (100 ml) at 235 ˚C and 60 bar H_2. Ethylene glycol and other diols (with the total yield of 70.6%) were formed from hydrolysis of cellulose and hemicellulose, while lignin was converted to phenolics including guaiacyl propanol, syringyl propanol, guaiacyl propane and syringyl propane, (with the total yield of 36.9%). By changing the reaction medium to methanol and ethylene glycol, the monomer yields further increased to 42.2 and 46.5, which was attributed to higher solubility of lignin and hydrogen in methanol and ethylene glycol. This is consistent with the results from Schutyser et al. [41], where only conversion of lignin was targeted. According to Li et al. [120] the lignin content and the type of biomass affect the liquefaction of biomass over Ni-W_2C/AC (see Table 6). The increase in the lignin content imposed hardship in degradation of both lignin and carbohydrate. Conversion of birch, poplar, ashtree and basswood with lignin content lower than 20% resulted in phenols and diol yields higher than 30 and 70%, respectively. Considering degradation of beech and xylosma with 23-25% lignin, the yields of phenols and diols decreased to approximately 26-29% and 58-62%. By further increase in the lignin content in pine wood and yate over 30%, the yield of phenols and diols considerably decreased to about 10% and 31-43%, indicating that by increase in the lignin, the degradation and cracking process become recalcitrance. The grass type biomass (bagasse and corn stalk) had lower yield of monomers

and diols compared to the wood type biomasses with similar lignin contents. Despite relatively low lignin content in corn stalk, the phenol and diol yields were 20.6 and 20.9%, respectively. Almost similar phenol yield was observed from conversion of bagasse, however, the dioal yield was higher (59.6%) [120]. Their observation was consistent with those from Van Den Bosch et al. [43]: The conversion of birch wood and poplar wood over 5% Ru/C catalyst in methanol resulted in 93 and 86% delignification, with the monomer yields of 50 and 41%, respectively, while the conversion of miscanthus grass resulted in delignification and monomer yield of 63 and 27%, respectively [43].

Table 6 The lignin content and the yield of phenols and diols from conversion of different biomass types over Ni-W_2C/AC catalyst at 235 ˚C. Reaction condition: 1 g biomass, 0.4 g catalyst, 100 ml water, 60 bar H_2, 4 hours [120].

Biomass	Lignin %	Total phenols %	Total diols %
Corn stalk	12.9	20.6	20.9
Birch	19.8	36.9	70.6
Poplar	14.8	32.4	75.1
Basswood	15.1	37.3	71.0
Ashtree	17.8	40.5	75.6
Beech	25.3	26.1	57.8
Xylosma	23.0	29.3	61.9
Bagasse	13.5	23.4	59.6
Pine	33.6	10.1	43.5
Yate	30.9	10.9	30.6

Positive effects were reported by Schutyser et al. [41] using wet biomass; 70 wt% delignification was reported from fractionation of 2 g birch wood in 40 ml ethylene glycol containing 2 g water (simulating 50 wt% wet biomass) over Pd/C catalyst at 200 ˚C, while in the absence of water the delignification was about 50 wt% [41]. In a work by Ferrini et al. [116] the degradation of poplar wood in the presence of Raney Ni catalyst at 180 ˚C in pure 2-PrOH and 2-PrOH/MeOH (10:1, vol/vol) resulted in the delignification of 40 and 43% respectively, while in the presence of water as co-solvent (2-PrOH/H_2O, 70/30 %, vol/vol) the delignification increased to 63% indicating that the presence of water in the solvent mixture improves the delignification and yield of the bio oil, most likely by water facilitating the transport of liquor into the wood pellets and further extraction of lignin [116].

2.3.1. Summary of solvothermal conversion of biomass

Lignin first biorefining approach has gained interest in the literature, with the main focus being degradation of lignin to monomers and conserving holocellulose. It was reported that addition of a catalyst greatly effects on the stabilization of lignin derived products and the type of monomers. The role of solvent was demonstrated to be in fractionation of lignin. If preserving the holocellulose fraction is aimed, polar solvents such as methanol and ethylene glycol were shown to be good candidate while water with high polarity can undesirably solubilize cellulose and hemicellulose.

Chapter 3:

Experimental Work

3. Experimental work

Conversion of lignin and biomass were conducted in a Parr 4566 series batch reactor and the products were carefully analyzed using different analytical techniques. The description of the setup, the chemicals used and different analysis are presented in this chapter.

3.1. Setup description

The reactor used for the experiments and its schematic is shown in Figure 35. The setup is composed of autoclave (volume: 300 ml) and an overhead stand, both made of Hastelloy C steel with maximum temperature and pressure viability of 350 ˚C and 200 barg, respectively. The fixed top of the reactor is equipped with a magnetic drive stirrer to ensure sufficient stirring inside the reactor in a speed range of 0-700 rpm. Sealing of the autoclave to the overhead stand is assured by using PTFE gasket. Heat is supplied by a heater, which surrounds the autoclave. Cooling water is supplied by VWR RC-10 chiller in order to provide adequate cooling in the reactor and also cooling magnetic stirrer during the experiments. The temperature inside the reactor is measured by a thermocouple inserted into the reactor and is connected to a Parr 4840 series controller. Pressure in the reactor is readable by a pressure gage placed in the fixed top. Gas is introduced into the reactor through a needle valve on the fixed top. Nitrogen is supplied by in-house gas distribution system while hydrogen is supplied by a gas cylinder. Gas pressure is adjustable through a back pressure valve and a further needle valve. The discharge of the gas phase is possible via a valve on the fixed top. The setup and accessories and cooling system is placed in a fume cabinet.

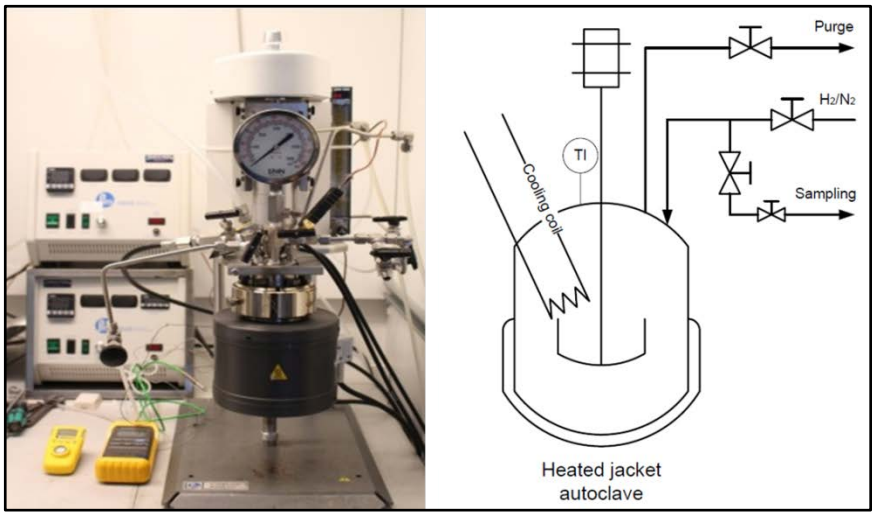

Figure 35 Parr 4566 series batch reactor and schematic of the setup

3.2. Feedstocks and Chemicals

The solvents used were ethanol (VWR, 99.9%) and ethylene glycol (Sigma-Aldrich, 99.8%). Other chemicals including the gases for GC analysis were of analytical grade. Spruce based sodium lignosulfonate (Na-LS) was provided by Borregaard A/S. The Na-LS contained 7.3 and 0.01 wt% Na and K, respectively. According to Mortensen et al. [102], potassium is detrimental to the HDO activity of supported NiMoS, and sodium is expected to have a similar

effect. In order to avoid any potential interactions of sodium with Ni and NiMoS active sites, the Na^+ and K^+ were exchanged with H^+ ions using Amberlite 120 H ion-exchange resin. In the ion-exchange procedure, 100 g Na-LS was dissolved in 1600 ml deionized water containing 68.2 g resin. The solution was stirred for 2 hours at room temperature. After 2 hours, the lignosulfonate solution and the resin were separated by decanting. The ion-exchange process was repeated using fresh resin until the pH of the solution decreased to 1.4 [121]. The ion-exchanged form of lignosulfonate is denoted H-LS. Thereafter, the H-LS was retrieved by evaporation of water from the lignosulfonate solution in an oven at 50 ˚C, overnight. After the ion-exchange, the amount of Na and K decreased to 0.1 and 0.001% on the dry matter, respectively.

The specifications of H-LS including C, H, S, O, humidity and ash content, weight average and number average molecular weight (Mw and Mn, respectively) and the atomic ratios of O/C and H/C are presented in Table 7. The corresponding polydispersity of H-LS based on the Mw and Mn values was determined as 4.9.

Table 7 Specifications of protonated lignosulfonate (H-LS).

	Molecular weight g/mol		**Composition wt%**						**Atomic ratio**	
	Mw	Mn	C	H	O	S	Humidity	Ash	O/C	H/C
H-LS	9400	1900	61.1	4.4	30.8	3.1	2.5	0.6	0.38	0.86

Nordic beech wood with particle size of 600 µm was used in the tests for conversion of biomass. The composition of beech wood constituents is presented in Table 8. The carbon, oxygen, hydrogen and nitrogen content of beech wood were determined to be 53.03, 41.00, 5.83 and 0.14 wt% (on dry and ash free matter basis). The oxygen content was determined by difference. No sulfur was detected in the beech wood likely because the sulfur content in beech wood was lower than the detection limit of the elemental analyzer.

Table 8 The composition of beech wood constituents.

Feedstock	**Total sugars**	**Glucan**	**Xylan**	**Klason lignin**	**Acid soluble lignin**	**Ash**	**Extractives**
Content wt%	60.7	39.9	17.6	20.8	3.1	0.5	3.2

Organosolv lignin was extracted from the same beech wood by an organosolv extraction according to a method from Wang et al. [80]. 50 g beech wood was treated with 300 ml water/ethanol solution (1:1, vol:vol) in Parr 4575 series reactor at 178 ˚C under nitrogen atmosphere for 3.3 h,. After the extraction, the soluble fraction (mainly lignin) was separated from solid cellulose and hemicellulose residues by filtration, followed by solvent removal via evaporation. The solid phase remaining unevaporated was regarded as ‘organosolv lignin’. The mass balance however revealed that the extracted solid phase was composed of 72.5 wt% lignin (assuming all lignin was dissolved.) mixed with 27.5 wt% other fractions mostly extracted hemicellulose. The carbon, hydrogen and oxygen content of the obtained organosolv lignin was determined 56.4, 6.2 and 37.6 wt%, respectively, whereas no nitrogen was detected.

3.3. Catalyst

In the experiments using Ni based catalyst (Chapter 4), the 5.0 wt% Ni/SiO_2, Ni/AC, Ni/ZrO_2 and $Ni/\gamma–A_2O_3$ catalysts were prepared by incipient wetness impregnation method using nickel nitrate hexahydrate ($Ni(NO_3)_2.6.H_2O$) as precursor. The supports were SiO_2 (Saint-Gobain, 250 m^2/g), AC (Sigma-Aldrich, 600 m^2/g), ZrO_2 (Saint-Gobain, trace monoclinic, 146 m^2/g) and $\gamma–A_2O_3$ (Saint-Gobain, 254.7 m^2/g). All catalysts were crushed, sieved to 150-300 µm and reduced before use. The Ni/SiO_2 catalyst was reduced for 2 hours in Parr 4566 series autoclave at 1 atm, 350 ˚C with H_2 flow of 1 Nl/min. A quantity of 1 g of Ni/AC, Ni/ZrO_2 and $Ni/\gamma–Al_2O_3$ catalysts were reduced ex-situ using a Quantachrome iQ_2 apparatus with H_2 flow for 2 hours at 600 ˚C, followed by passivation in 1% O_2 and 99% N_2 at room temperature. The passivated catalysts were reactivated prior to use in Parr 4566 series autoclave with a H_2 flow of 1 Nl/min for 2 hours at 400 ˚C.

Commercial alumina supported NiMo catalyst provided by Haldor Topsøe A/S was used in Chapter 5 and 6. In chapter 5, the commercial NiMo is regarded as NiMo-I. The catalyst was crushed, sieved to 150-300 µm. For studies on the sulfidation of catalyst by TEM analysis, an in-house alumina supported NiMo sample was prepared (regarded as NiMo-II). The support was γ-Al_2O_3 from Saint-Gobain with a surface area of 254.7 m^2/g. The catalyst was prepared by successive incipient wetness impregnation stages: First the support was impregnated with Mo using an aqueous solution of ammonium molybdate tetrahydrate ($(NH_4)_6Mo_7O_{24}.4H_2O$), from Sigma-Aldrich with purity ≥ 99%, as precursor. The precursor solution was added dropwise to the support while stirring to ensure a homogenous precursor distribution. The water was evaporated in an oven at 50 ˚C, overnight. Ni was then added in a second impregnation step, using an aqueous solution of nickel nitrate hexahydrate ($Ni(NO_3).6H_2O$), from Sigma-Aldrich with purity of 99.999%. The in-house synthesized catalyst was calcined by heating to 500 ˚C at a rate of 5 ˚C/min in 2.5 L/min flow of 20 vol% O_2 and 80 vol% N_2 and holding at this temperature for 3 hours. The Mo and Ni content of the calcined catalyst was measured by ICP analysis to 12.8 and 2.3 wt%, respectively, which corresponds to Ni/Mo molar ratio of 0.3. This molar ratio is recognized as optimal value for HDS activity [122]. The sulfur content after pre-sulfidation of the home-synthesized NiMo-II catalyst was 10.0 wt% as determined by ICP analysis, corresponding to the formation of MoS_2, NiS and Ni_2S_3. The NiMo oxide catalyst was pre-sulfided prior to use in a Parr 4566 series reactor; the pre-sulfidation was achieved using 1 ml dimethyl disulfide (DMDS) in a reductive atmosphere (1 g oxide catalyst, 30 bar H_2, loaded at RT) at 400 ˚C, overnight.

3.4. Depolymerization reactions

In all the experiments, once the materials were transferred into the autoclave, the reactor was sealed and flushed with N_2 for at least three times. Subsequently, the reactor was flushed with H_2 and then pressurized to specified H_2 pressure at RT. The reactor was then heated to the desired temperature while stirring. Stirring was important to avoid that lignin deposited at the reactor bottom and was exposed to high temperature in the absence of solvent and catalyst causing severe charring. Once the set point temperature was reached, the reaction time was started. The reaction time for most of the experiments was 3 hours, except for a few

experiments in chapter 5, where the effect of reaction time was evaluated. At the end of the experiment, the reaction was stopped by quenching the reactor in an ice bath. As soon as the temperature inside the reactor reached ambient, gas samples were collected using Tedlar gas bags. Before opening the reactor, the gas phase was discharged and the reactor was flushed with N_2. The material and the quantities in each chapter are presented below:

3.4.1. Depolymerization reactions presented in chapter 4

In a typical run, 7.5 g lignosulfonate, 0/0.75 g catalyst and 75 ml of solvent were transferred into the reactor. The loaded H_2 pressure into the reactor was 50 bar at RT and the depolymerization reactions were conducted at 250 ˚C.

3.4.2. Depolymerization reactions presented in chapter 5

The experiments were conducted with typically 1 g catalyst, 10 g lignin (H-LS), and 100 ml solvent. The reactor was charged with 26 bar H_2 at RT, then the reactor was heated to the desired temperature (260, 290, 300, 310 ˚C). The catalyst was used in oxide form in most of the experiments, however, in a few experiments the catalyst was used pre-sulfided. The effect of sulfur addition during reaction was studied in an experiment by adding 1 ml DMDS to the reaction medium.

3.4.3. Liquefaction of biomass presented in chapter 6

The catalytic conversion of biomass was studied using 1 g oxide catalyst (which was pre-sulfided prior to use) commercial NiMo catalyst, 10 g biomass and 100 ml solvent. 0.5 ml DMDS, corresponding to H_2S partial pressure of 1.8 bar at 300 ˚C, was added in order to maintain the sulfide state of the catalyst. The reactor initially was charged with 26 bar H_2 at RT.

3.5. Workup procedure

The solid and the liquid products of the reactions were separated by vacuum filtration over a pre-weighed filter paper. The filter cake was washed with 100 ml ethanol to ensure removal of the liquefied products. The filtrate and ethanol used for rinsing the cake were collected. The solid phase was dried overnight at 60 ˚C. The solid phase was comprised of spent catalyst, ash, and char. In the experiments in chapter 4, when ethanol was used as solvent, and also the experiments in chapter 5 and 6, the heavy and light fractions in the liquid phase were separated using rotary evaporator at 35 ˚C, 5 mbar pressure and a rotation rate of 130 RPM. Ethanol and the light products were evaporated (light phase), and a thick liquid phase remained unevaporated, regarded as ‘oil’ (heavy liquid phase). During the workup procedure, the masses of different fractions and the mass of added ethanol for washing the solid phase were carefully measured. A mass loss of 6-15 wt% was observed during the workup procedure, mainly in the filtration step.

An extensive product extraction procedure was applied in the experiments in chapter 4, when ethylene glycol was used as solvent since evaporation of ethylene glycol was not practical due to its high boiling point (197.3 ˚C). Solid phase was isolated from the liquid phase in a procedure described for ethanol experiments. Subsequently, the liquid product fraction was

diluted with water in a separation funnel followed by addition of ethyl acetate. The funnel was then shaken vigorously. The aqueous phase and the organic phase were separated; the water phase in the bottom layer and the organic phase on the top. It was expected that unreacted ethylene glycol and the ethanol used for washing were transferred to the aqueous phase while the liquefied organic compounds were in the oil phase. Extraction was repeated three times to ensure complete separation of the products. In the next step, the lignin degradation products were isolated from ethyl acetate using rotary evaporation.

The yield of the oil fractions was calculated based on the dry and ash free (DAF) feedstock (Eq. 2). The organic solid mass originating from feedstock was calculated by subtraction of mass of ash and loaded catalyst from the total solid mass obtained from filtration. The solid yields were calculated using Eq. 3.

$$\text{Oil yield} = \frac{m_{Oil}}{m_{DAF\ feedstock}} \cdot 100 \qquad \text{Eq. 2}$$

$$\text{Solid yield} = \frac{m_{Solid\ residue} - m_{Ash} - m_{Catalyst}}{m_{DAF\ feedstock}} \cdot 100 \qquad \text{Eq. 3}$$

In chapter 4, the selectivity of the monomers in the oil fractions was determined by Eq. 4.

$$\text{Selectivity to monomers} = \frac{m_{\ Monomer\ determined\ by\ GC-FID}}{m_{Oil\ fraction}} \cdot 100 \qquad \text{Eq. 4}$$

In the experiment presented in chapter 4, the solid phase obtained from each test was fractionized by dissolving in THF. It was assumed that char, catalyst and ash were insoluble in THF. The solid phase was dispersed in 100 ml THF followed by stirring for 30 minutes at room temperature. Next, the solutions were filtered using vacuum filtration. The 'THF insoluble solid', collected on the filter paper, was dried overnight. The filtrate phase 'THF soluble solid' was recovered by evaporation of THF. The yield of each fraction was calculated using Eq. 5 and 6, respectively.

$$\text{THF insoluble solid yield} = \frac{m_{THF\ insoluble\ solid} - m_{Ash} - m_{Catalyst}}{m_{DAF\ lignosulfonate}} \cdot 100 \qquad \text{Eq. 5}$$

$$\text{THF soluble solid yield} = \frac{m_{THF\ soluble\ solid}}{m_{DAF\ lignosulfonate}} \cdot 100 \qquad \text{Eq. 6}$$

In the experiment on liquefaction of biomass (chapter 6), the conversion of biomass or organosolv lignin was calculated as in Eq. 7. The content of the sugar derived light products were determined according to Eq. 8. The relative area basis percentages of light products were measured by GC-FID analysis of the light fractions and the water content in the light phase was determined by Karl-Fischer titration. The monomer yields in the oil fractions from conversion of biomass were determined based on Klason lignin, using Eq. 9, while the monomer yields from conversion of organosolv lignin were determined based on the DAF Organosolv lignin, using Eq. 10.

$$\text{Conversion} = \left(1 - \frac{m_{Solid\ fraction} - m_{Ash} - m_{Catalyst}}{m_{DAF\ biomass}}\right) \cdot 100 \quad \text{Eq. 7}$$

$$\text{Light products yield} = \frac{(m_{Light\ fraction} - m_{Water})}{m_{Sugars\ in\ biomass}} \cdot \text{Area \%}_{\text{Light product}} \quad \text{Eq. 8}$$

$$\text{Monomer yield}_{\text{biomass}} = \frac{m_{Monomer}}{m_{Klason\ lignin\ in\ biomass}} \cdot 100 \quad \text{Eq. 9}$$

$$\text{Monomer yield}_{\text{organosolv lignin}} = \frac{m_{Monomer}}{m_{DAF\ Organosolv\ lignin}} \cdot 100 \quad \text{Eq. 10}$$

3.6. Characterizations and analytical techniques

3.6.1. Catalyst characterization

Some specifications of Ni based catalysts used in chapter 4 were determined using TPR, CO chemisorption, NH_3-TPD and XRD that are described below:

Temperature programmed reduction (TPR) analysis was performed in order to investigate the reducibility of Ni $(NO_3)_2$ species using a Quantachrome iQ_2 apparatus. The consumption of H_2 was measured using a Hiden QGA mass spectrometer. The catalyst was flushed with 40 Nml/min of helium (He) for 25 minutes followed by heating from room temperature to 350 ˚C (Ni supported on SiO_2) or 600 ˚C (Ni supported on AC, γ-Al_2O_3 and ZrO_2) at a rate of 2 ˚C/min with H_2 flow of 40 Nml/min and then maintaining at this temperature for 4 hours. The consumption of H_2 is indicative of catalyst reduction and the end of H_2 consumption is taken as evidence of complete reduction.

Catalyst metal dispersion was measured by carbon monoxide (CO) chemisorption. The metal dispersion represents the percentage of the available metal atoms (N_s) to the total metal atoms (N_T) [123]. Similar to TPR, a Quantachrome iQ_2 apparatus was used and CO was measured by TCD detector. Prior to chemisorption, the catalyst was properly reduced at the required temperature for 2 hours, followed by cooling to 30 ˚C by 40 Nml/min He flow. The titration was conducted at 30 ˚C by pulse injection of 279 µl CO into the He flow and measuring the CO uptake. The results were used to calculate the Ni particle size. It should be emphasized that the nickel carbonyl generated in this procedure can cause harm to the TCD detector filament.

The acidity of Ni/SiO_2, Ni/ZrO_2 and Ni/γ-Al_2O_3 was determined by temperature programmed desorption of ammonia (NH_3-TPD). An amount of 0.1 g of each sample was heated to 500 ˚C in He flow of 25 Nml/min and then cooled to 100 ˚C. Thereafter, the samples were saturated with 50 Nml/min NH_3 flow for 2 hours. TPD was then conducted by heating the sample to 500 ˚C at a heating rate of 10 ˚C/min in He flow of 25 NmL/min. A thermal conductivity detector (TCD) was used for measuring the desorbed NH_3 with the acidity equated to the desorbed amount of NH_3 [123]. The peak in the temperatures lower than 200 ˚C is

considered as weak acid sites, whereas the peak at higher temperature is considered as strong acidity region.

The X-Ray diffraction (XRD) of fresh and spent catalysts was recorded with a Huber G670 powder diffractometer using Cu (Kα1) radiation. Measurements were performed in the range of 3-100 degrees with a step size of 0.005 and total measurement duration of 60 minutes. The software used for crystal identification was Crystallographica Search-Match (by Oxford Cryosystems Ltd.) with the ICDD PDF4 powder diffraction database.

Inductively coupled plasma-optical emission spectroscopy (ICP-OES) was used for quantification of the Ni, Mo and S content in NiMo-II catalyst samples. The samples were melted together with potassium pyrosulfate, dissolved in a solution of water and HCl and analyzed with optical emission spectroscopy. The sulfur content in the NiS catalyst (chapter 4) were determined in a similar way. The results are presented in chapters 4 and 5.

In chapter 5, the NiMo catalysts prepared in-house (NiMo-II) were analyzed with transmission electron microscopy energy-dispersive X-ray spectroscopy (TEM-EDX) analysis. The pre-sulfided NiMo-II catalyst before reaction, spent pre-sulfided NiMo-II after the reaction at 310 ˚C, and also spent non pre-sulfided NiMo-II after the reactions were all analyzed with TEM-EDX analysis. The samples were dispersed on a grid and mounted on an FEI single tilt holder. The TEM images were obtained using FEI Tecnai T20 G2 S-TEM microscope operating at 200 keV. The EDX spectra were acquired with an Oxford X-max silicon-drift detector (SDD) with an active area of 80 mm^2.

3.6.2. Analysis of the feedstocks and products

The content of organic carbon, hydrogen, sulfur and nitrogen in lignosulfonate, biomass, oil and solid fractions were analyzed using a EuroVector EA 3000 CHNS analyzer. The measurement is done by the combustion of 1 mg encapsulated samples at 980 ˚C and further quantification of CO_2, H_2O, N_2 and SO_2 by GC-TCD. The oxygen percentage was calculated by subtraction of C, H, N, S and ash content of each sample.

The sulfur content in the oil fractions was measured by ICP-OES. The samples were prepared by dilution of a weighed amount of oil samples in ethanol.

The ash content of H-LS, beech wood and also solid residues was determined by combusting an aliquot in an oven at 600 ˚C. The solid residues from catalytic experiments were mixed with spent catalyst. It was assumed that catalyst is not combustible and is left with the ash after the combustion.

The molecular weight distribution of lignin, solid and oil fractions was evaluated using size exclusion chromatography (SEC). SEC was performed using an Agilent 1100 series HPLC equipped with a UV-vis detector. A polymer Standard Service Company Polarsil pre-column (50 × 8 mm, 5 µm) and column (300 × 8 mm, 5 µm) were used. A 90/10 wt% DMSO/water solution containing 0.05 M LiBr was used as solvent. The samples were dissolved in the solvent with a concentration of approximately 2 mg/ml. The column oven temperature was set to 80

˚C to facilitate the elution of solvent. 10 µl of sample was injected for each analysis and the elution flow rate was set to 1 ml/min. Phenol (Mw: 94 g/mol) and 4-propyl guaiacol (Mw: 166 g/mol), guaiacylglycerol beta guaiacyl ether (GGGE) (Mw: 320 g/mol) and tannic acid (Mw: 1701 g/mol) were used as representative standards for lignin monomers, dimers and polymers. It was expected that only lignin derived fractions were detected by the UV-vis detector, at 280 nm, which is the wavelength suitable for detection of aromatic species.

The oil and light fractions were analyzed using a Shimadzu QP 2010 Ultra GC-MS-FID apparatus equipped with a Supelco Equity 5 column. Identification and quantification of the samples was performed by a mass spectrometer and flame ionization detector (FID), respectively. A weighed amount of oil samples were diluted in 10 ml ethanol for analysis. The initial temperature for the GC column was set to 40 ˚C and the column was heated to 250 ˚C with a heating rate of 10 ˚C/min and kept at this temperature for 5 minutes. A split ratio of 90 was used in the injection section. The MS scanning was set to a range of 30 to 400 m/z and the MS was intentionally turned off between 2.4 to 4 minutes in order to avoid saturation by the high concentration of ethanol. Product identification was performed using the NIST 08 library. A weighed quantity of phenol was added to the oil samples as external standard. The 'relative response factor' method [124] was used for quantification of the compounds in the oil; the relative response factor (RRF) of guaiacol, 4-methyl guaiacol, 4-ethyl guaiacol and 4-propyl guaiacol was obtained using commercial standards (according to Eq. 11). C_s and A_s are the concentration and the area of standards and C_i and A_i are the concentration and the area of the compound i. The RRF of the compounds such as ethyl vanillate, 4-propyl syringol, phenol 2-methoxy-4-(2-proponyl) and phenol, 2, 6-dimethoxy-4-(2-propenyl) was determined using effective carbon number (ECN) method [125].

$$RRF = \frac{Cs \cdot Ai}{Ci \cdot As} \qquad \text{Eq. 11}$$

In chapter 5, the oil phases from non-catalytic and catalytic reactions were analyzed with GC×GC analysis. The samples were analyzed on a LECO Pegasus GC×GC-TOFMS equipped with two columns: The first column was a 25 m × 0.25 mm i.d. and 0.25 µm film of ZB-1701 connected to a second column which was a 1.5 m × 0.18 mm i.d. and 0.18 µm film of Rtx-5. The oven temperature of the first column was set to 40 ˚C for 2 minutes, then heated to 300 ˚C with a heating rate of 5 ˚C/min and was kept at 300 ˚C for 5 minutes. The second oven had an offset of 5 ˚C from first column. Pulsed split with split ratio 25 and pressure of 20 psi for 2 minutes was applied. The carrier gas was helium with constant flow of 1.5 mL/min. The modulation time was 8 seconds throughout the run. The MS acquisition was acquired with mass range of 41-441 m/z at 100. The ion source temperature was set to 225 ˚C. The MS plots were analyzed using LECO ChromaTOF software, version 4.50.

An Agilent 7890A series gas chromatography equipped with a TCD detector was used for identification and quantification of gaseous products. After each experiment, when the temperature inside the reactor reached ambient temperature, a sample of the gas phase was collected in a Tedlar bag for GC analysis. The gas injection into the GC was achieved using a

fixed pressure pump. The gas flow was further split into two lines. He and Ar were used as carrier gases. H_2 was analyzed with an arrangement of a 6 ft Haysep Q and 5 Å molecular sieve columns, where Ar was the carrier gas. The gases N_2, O_2, CO, CO_2, CH_4, C_2H_4 and C_2H_6, were detected in the He line with 3 ft Haysep Q, HP-Plot and 5 Å molecular sieve columns; The calibration curves were created using certified gas mixtures from AGA. The moles of each gas were calculated by the gas distribution in the gas phase measured by the GC and the pressure in the cooled autoclave assuming ideality.

The heteronuclear single quantum coherence nuclear magnetic resonance (HSQC NMR) experiments on the oils were performed on a 400 MHz Bruker Ascend magnet with an Avance II console and equipped with a Prodigy cryoprobe, at 400.13 MHz for ^{1}H and 100.61 for ^{13}C using the standard Bruker pulse sequence. The samples were prepared by dissolving them in DMSO-d_6 as solvent. The experiments were recorded with a sweep width of 12 ppm in ^{1}H and 2048 points and 256 increments in the indirect dimension (^{13}C) covering 165 ppm. The delay for magnetization transfer delay was calculated to be optimal for a one-bond coupling for 145 Hz. Data were processed and plotted using Mnova software.

Chapter 4

Solvothermal Conversion of Lignosulfonate Assisted by Ni Catalyst

4. Solvothermal conversion of lignosulfonate assisted by Ni catalyst

Among the relevant studies on catalytic conversion of lignosulfonate, Song et al. [110] recently reported 68 wt% conversion over 10 wt% Ni/AC catalyst in ethylene glycol at 200 ˚C under hydrogen atmosphere with product selectivity being 75-95% for alkyl-substituted guaiacols, which is very promising yield of monomeric units [110]. They observed higher conversion of lignosulfonate in ethylene glycol than in ethanol medium (a conversion of 21 wt% in ethanol) [110]; however, the role of solvent on the depolymerization mechanism was not elaborated upon. The degradation medium has a great impact on the depolymerization of lignin and stabilization of degraded fragments. Ethylene glycol is a good solvent for dissolution of lignin through formation of H-bonding between EG and hydroxyl groups in the lignin [126]. Furthermore, ethylene glycol has been reported to act as an end capping agent, preventing repolymerization [127]. On the other hand, Huang et al. [78] demonstrated that as a solvent for lignin degradation, ethanol can suppress undesirable condensation reactions through alkylation and esterification with degraded lignin fragments and by stabilization of reactive compounds such as formaldehyde.

In this chapter the results of our investigation on the conversion of lignosulfonate over Ni based catalysts in ethanol and ethylene glycol are presented. The products fractions are carefully evaluated in order to understand the solvent effect on depolymerization and inhibiting condensation reactions. The sulfur in the structure of lignosulfonate arise challenges for using a heterogeneous catalysts. We also investigated the sulfur tolerance of Ni catalyst.

4.1. Catalyst

5 wt% Ni catalysts supported on SiO_2 was prepared by incipient wetness impregnation. A nickel dispersion of 14.7 % was measured by CO titration, which corresponds to an approximate catalyst particle size of 7.5 nm. One step reduction of Ni/SiO_2 catalyst at 350 ˚C was confirmed by TPR. In order to understand the role of support material on the catalyst activity, Ni supported on AC, ZrO_2 and γ-Al_2O_3 were prepared. The particle size of Ni/AC and Ni/γ-Al_2O_3 catalysts was estimated 14.8 and 32.5 nm, respectively (Table 9). However, the CO titration and therefore particle size estimation of Ni/ZrO_2 was not achievable due to severe deposition of nickel carbonyl in the TDC detector. The acidity of Ni/SiO_2, Ni/ZrO_2 and Ni/γ-Al_2O_3 catalysts were measured using NH_3-TPD, while Ni/AC was assumed to be neutral. According to NH_3 desorption measurements, catalysts with a range of acidity were synthesized: The NH_3 desorbed content increased in order of 55, 373 and 601 µmol/g_{cat} for Ni/SiO_2, Ni/ZrO_2 and Ni/γ-Al_2O_3 catalysts. The temperature in which NH_3 was desorbed from Ni/ZrO_2 was within the range of strong acidity while those for Ni/SiO_2 and Ni/γ-Al_2O_3 were in the range of weak acidity.

Table 9 The particle size and acidities of the 5 wt% nickel based catalysts

Catalyst	Particle size [nm]	NH_3 desorbed [µmol/g_{cat}] weak	NH_3 desorbed [µmol/g_{cat}] strong

Ni/SiO_2	7.5	55 (at 152 ˚C)	-
Ni/AC	14.8	N.A.	N.A.
Ni/ZrO_2	N.A.	-	373 (at 225 ˚C)
$Ni/\gamma\text{-}Al_2O_3$	32.5	602 (at 184 ˚C)	-

4.2. Solvothermal conversion of lignosulfonate

The oil and solid yields from conversion of H-LS with and without catalyst in ethanol and ethylene glycol solvents are presented in Table 10.

Table 10 The yields of the oil and solid fractions from conversion of H-LS over Ni/SiO_2 catalyst. Reaction condition: 0/0.75 g catalyst, 7.5 g H-LS, 75 ml solvent, initial H_2 loading of 50 bar at RT, 250 ˚C, 3 hours.

Ethanol medium					
Entry	**Catalyst**	**Oil yield wt%**	**Solid phase wt%**		
			THF insoluble	THF soluble	Total
1	Non-Catalytic	16	60	10	70
2	Ni/SiO_2	31	46	16	62
3*	Ni/SiO_2	47	30	9	39
Ethylene glycol medium					
Entry	**Catalyst**	**Apparent/ Estimated Oil yield wt%**	**Solid phase wt%**		
			THF insoluble	THF soluble	Total
4	Non-Catalytic	89/ 20	6	74	80
5	Ni/SiO_2	93/ 32	23	45	68

* Reaction temperature of 300 ˚C

The oil and solid yields from non-catalytic conversion of H-LS in supercritical ethanol were 16 and 70 wt%, respectively (Table 10, Entry 1). A poor mass balance was obtained which was mainly due to severe solid deposition in the internal surface of the autoclave and the stirring compartment, accompanied by loss of solid products during the workup procedure. The oil yield increased to 31 wt% by catalytic conversion of H-LS in ethanol medium, while solid yield decreased to 62 wt% (Table 10, Entry 2). The higher yield of liquefied oil products in the presence of a catalyst is likely due to hydrogenolysis of facile bonds such as C-O over Ni active sites [110] and the role of catalyst in stabilization of the reactive fragments. Van den Bosch et al. [113] elaborated the role of Ni/Al_2O_3 mainly as stabilization of reactive lignin fragments and inhabitation of repolymerization during delignification of birch sawdust in methanol. By addition of catalyst the yield of THF insoluble fraction decreased from 60 wt% in the absence of catalyst to 46 wt%, and the yield of THF soluble fraction increased from 10 wt% to 16 wt% in catalytic condition. The physical appearance of the solid phase changed noticeably by addition of catalyst. The solid residues in non-catalytic reactions were large lumps, while small solid particles were obtained after catalytic reaction. This difference may be affected by grinding action of the catalyst particles on the char under the stirring. The yield of the liquefied products are highly influenced by reaction temperature [109]; 47 wt% oil yield was obtained

by conversion of H-LS over Ni/SiO_2 catalyst at 300 ˚C in ethanol (Table 10, Entry 3) and the total solid yield decreased to 39 wt%. The higher oil yields were likely through increase of the thermal cracking rates at higher temperatures [27] and also increase of the end-capping alkylation reactions compared to repolymerization reactions [31].

A more complex workup procedure using extraction with water and ethyl acetate was applied for isolation of liquefied products from EG. It was assumed that organic compounds were extracted in ethyl acetate phase. Ethyl acetate was later evaporated using rotary evaporation. However, after its evaporation, excessive oil contents of 6.7 and 7.0 g were obtained from non-catalytic and catalytic tests, respectively (corresponding to 'apparent' oil yields of 89 and 93 wt%), which were considerably higher than the expected mass of oil fractions from degradation of lignin. Solid yields of 80 and 68 wt% were obtained in the absence and presence of catalyst, respectively. It was speculated that the extra mass observed in the liquid phase was either due to poor separation of the solvent (EG) from products or extensive solvent incorporation to the lignin fragments, which is elaborated later. The yield of the oil fractions from conversion of H-LS in EG were therefore approximated as everything not accounted for by the solid fractions ('Estimated' oil yields). Similar to reaction in the ethanol medium, the yield of liquefied fraction increased over the catalyst (Table 10, Entry 4 and 5). The estimated oil yield of 32 wt% obtained over Ni/SiO_2, which was very similar to the yield in the EtOH medium. Only 8 wt% THF insoluble fraction was observed in non-catalytic condition, however, this number increased to 23 wt% over catalyst.

By contrast, Song et al. [110] reported 68 and 21 wt% conversion of sodium lignosulfonate in EG and EtOH over Ni/AC at 200 ˚C, respectively. They further observed 78 wt% conversion from reaction of Na-LS in EG at 240˚ C. Unlike Song et al. [110], we observed almost similar yields of 31 and 32 wt% of the degraded fractions (oil yield) in both solvents. There may be several reasons for the differences between our work and Song et al. [110]. The origin of lignin and the number of -O- and -OH bonds influences its thermal degradation [59] and dissolution in solvents [126]. In the work by Song et al. [110] , the biomass from which the lignosulfonate was extracted was not stated, so there may be differences in the feedstocks. Moreover, they had loadings of 0.2 g catalyst, 2 g lignosulfonate and 120 ml solvent. The excess amount of solvent to lignin ratio compared to our reaction conditions (7.5 g lignin, 75 ml solvent) may affect the conversion. They used lignosulfonate with sodium ions as counter ion to sulfonate group, while the lignosulfonate we investigated was in sulfonic acid form. The SO_3H groups can acid-catalyze the reaction [128], which may be the reason for higher conversion we observed in EtOH medium compared to their result. Lignosulfonate is highly soluble in EG, while its solubility in EtOH is limited [129]. Some unconverted lignosulfonates may remain soluble in EG after the reaction which then may result in overestimation of the conversions. A workup procedure suitable for separation of degraded products and unreacted lignin from solvent seems critical for accurate analysis.

4.2.1. Evaluation of the products and comparison between ethanol and ethylene glycol as reaction media

The cleavage of facile bonds such as C-O aryl ethers present in the structure of lignin results in the formation of reactive monomeric and dimeric intermediate radicals [127]. Repolymerization reactions and non-selective formation of stable C-C bonds induced by radicals can suppress the degradation and results in formation of char. Condensation of phenolic groups originating from lignosulfonate and aldehydes are reported [128]. Formation of C-C bonds can be inhibited by reaction of the solvent with the radicals. In order to elaborate on the role of each solvent, the liquefied products were analyzed with GC-MS equipped with FID detector. The chromatograms of the oil fractions obtained over Ni/SiO_2 are presented in Appendix A, Figure A1 and Figure A2. Monomer yields (base on DAF lignin) of 3.6 and 4.0 wt% were quantified from non-catalytic and catalytic conversion in EtOH presented in Table 11. The monomer yields from non-catalytic and catalytic degradation in EG were 1.2 and 0.8 wt%, which were lower compared to the monomer yields in EtOH. The observed yields of monomers indicate that the oil fractions are mainly composed of larger oligomers. In the work by Song et al. [110] 75-95% selectivity for alkyl-substituted guaiacols from conversion of sodium lignosulfonate in EG at 200 ˚C was reported. However, evaluating our oil fractions using GC-MS-FID results, it was observed that only a small fraction of the oil phases were comprised of monomers, and therefore, the high selectivity reported by Song et al. [110] could not be reproduced in our work.

Table 11 The selectivity of monomers in the oil fractions from non-catalytic and catalytic conversion of H-LS based on GC-MS-FID analysis, and total monomer yields base on DAF lignin. Reaction condition: 0/0.75 g catalyst, 7.5 g H-LS, 75 ml solvent, initial H_2 loading of 50 bar at RT, 250 ˚C, 3 hours.

Experiment	Selectivity %			Monomers yield wt%
	Guaiacols & substituted guaiacol	Aromatic esters	Total	
EtOH, Non-catalytic	10.9	11.8	22.7	3.6
EtOH, Ni/SiO_2	6.6	6.3	12.9	4.0
EG, Non-catalytic	5.8	-	5.8	1.2
EG, Ni/SiO_2	2.6	-	2.6	0.8

In the oil from conversion of H-LS in EtOH, guaiacol and substituted guaiacol and aromatic esters were the two main groups of identified compounds with guaiacol (selectivity of 8.6% in the absence of catalyst and 5.3% over Ni/SiO_2) and ethyl vanillate (selectivity of 10.3% in the absence of catalyst and 5.6% over Ni/SiO_2) being the primary compounds. Structure of guaiacol and ethyl vanillate is shown in Figure 36. Compounds such as 4-methyl guaiacol, 4-ethyl guaiacol and 4-propyl guaiacol were identified in trace amounts. Formation of guaiacol and alkyl substituted guaiacols can take place via hydrogenolysis of C-O-C bonds involving phenyl propane units such as such as β-O-4 and α-O-4 [130]. The cleavage of β-O-4 is reported to occur in temperature range of 200-300 ˚C in different solvents [27]. Formation of ethyl vanillate was reported from degradation of Alkali lignin at 250 ˚C over vanadium sulfide catalyst [131]. The aromatic esters were possibly produced by reaction of in-situ

produced aromatic carboxylic acids from degradation of lignosulfonate and ethanol. According to the GC-MS results, esterification occurs in ethanol medium in both non-catalytic and catalytic reactions, resulting in stabilization of reactive fragments. Sulfonic acid groups present in the structure of H-LS catalyze esterification reactions [132]. Esterification reactions are favored for enhancement of bio-oil quality as carboxylic acids groups decrease the stability of oil and makes the oil more acidic [133]. Esterification between ethanol and acids increases at supercritical condition [134]. Guaiacol was the primary monomeric product from degradation of lignin in the EG medium and corresponded to selectivity of 5.8 and 2.6 wt% in the oil phases from non-catalytic and catalytic conditions, respectively.

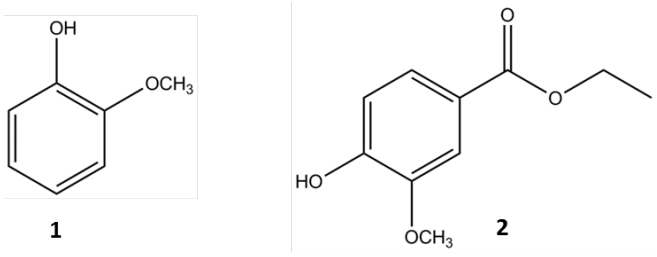

Figure 36 The main identified compounds in the oil fractions by GC-MS analysis: (1) Guaiacol, (2) Ethyl vanillate

The stability of the solvent is critical for an economically viable bio-refinery. The GC-MS-FID analysis of the light fractions from reaction in EtOH detected 99.4% EtOH (Area basis) as the major compound. Formation of trace amounts of 3-methyl 1-pentanol, 1,1 diethoxy ethane and 2-ethoxy 1-propanol was detected from self-reaction of EtOH molecules and esterification. The GC analysis of the gas phase detected negligible amounts of CO_2 and CH_4 from both non-catalytic and catalytic conversion of lignosulfonate. This observation indicates that EtOH was relatively stable at the reaction conditions.

The high apparent yields of liquid phase from reactions in EG were not to a large extent originating from poor extraction of EG as only 6 and 10 wt% EG was detected in the oil phases from non-catalytic and catalytic reactions, using GC-MS-FID. Rather the high yield is due to conversion of EG to higher glycols; the GC-MS analysis of the oil fractions indicated extensive formation of diethylene glycol (DEG), triethylene glycol (TEG), tetraethylene glycol (TTEG), and compounds such as diethylene glycol ethyl ether, which account for the extra oil mass. A blank test in the absence of lignin was conducted in order to evaluate self-reaction of EG over Ni/SiO_2 catalyst. Only ethylene glycol and trace amounts of 2-methoxy 1, 3 dioxolane were detected from blank test, which indicated formation of higher glycols was associated with the presence of H-LS or its degradation products. A likely explanation for the EG conversion in the presence of H-LS is the acid catalysis from H-LS protons. Self-reaction of EG under acidic conditions and formation of DEG and TEG are reported [134], [135]. The H^+ originated from SO_3H in the structure of H-LS can catalyze such reactions [128], which possibly initiated EG self-reactions. As shown in Figure 37, protonation of EG can take place by introduction of H^+ from SO_3H unit in the lignosulfonate structure. By nucleophilic attack of the adjacent EG molecule, a DEG is formed through dehydration. Formation of TEG and higher glycols follows

a similar mechanism. The reaction of EG is not limited to self-reaction. EG reacts with reactive lignin intermediates via end-capping reactions [41]. Moreover, reaction between carboxyl groups produced in-situ from degradation of lignin and ethylene glycol results in the formation of esters and ketones [136]. However, apart from guaiacol, we could not detect other products from reaction of H-LS degraded compounds and EG, which is probably because these compounds were too large to pass the GC column and reach the detector.

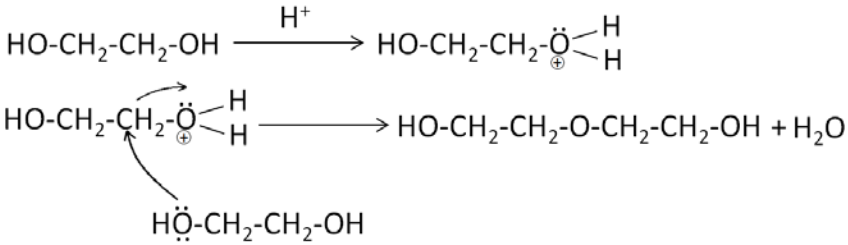

Figure 37 Acid catalyzed self-reaction of ethylene glycol to form diethylene glycol ether.

Although GC is a robust method for analysis of chemicals, most of the lignin degradation compounds are not volatile at the conventional GC analysis conditions and will thus not be detected. Size exclusion chromatography (SEC) is a useful technique for determination of the molecular weight distribution of the liquefied fractions. The SEC of the oil fractions obtained from non-catalytic and catalytic degradation of lignosulfonate confirmed the formation of lower molecular weight compounds compared to the starting feedstock (Figure 38). We used phenol, GGGE and tannic acid as standards. The corresponding peak position for each standard is shown for comparison. According to the elution pattern of the oil fractions, the majority of the degraded compounds had molecular weights that ranged from dimers to oligomers. This is consistent with the GC analysis of the oil fractions, showing relatively low yields of monomers. The SEC of the oil fractions from EtOH tests showed a bimodal pattern (see Figure 38). The oil from catalytic conversion in EtOH showed a larger shoulder in higher molecular weight fractions (lower retention times) compared to oil produced without a catalyst. The elution of non-catalytic oil produced in EG medium showed a slightly broader molecular weight distribution compared to oil formed in the presence of a catalyst. Comparing the molecular weight distributions of the oil in the two different solvents indicates that the oil fractions from EtOH medium had much smaller molecular weight compared to the oils in EG. Schutyser et al. [41] observed formation of higher molecular weight lignin oligomers in ethylene glycol than in other solvents including ethanol, water and methanol from conversion of birch sawdust over Pd/C catalyst at 200 ˚C. This may be due to the end-capping reactions between EG and higher glycols with lignin fragments. Both EG and EtOH solvents can perform end-capping of formed radical fragments. They react with –OH and –COOH groups in the degraded fractions via different reactions including formation of hydrogen bonds and esterification. EG with two hydroxyl groups most likely links two smaller fragments into a larger one while EtOH with one hydroxyl group reacts with only one radical fragment. Thus, conversion in EG leads to oils with larger molecular weight. Taking into account the SEC and GC-MS-FID results of the oil fractions, it is concluded that catalytic role has been more pronounced in formation of dimers

and oligomers, perhaps by inhibiting condensation of larger fragments, whereas the monomer yields has not been increased by a catalyst.

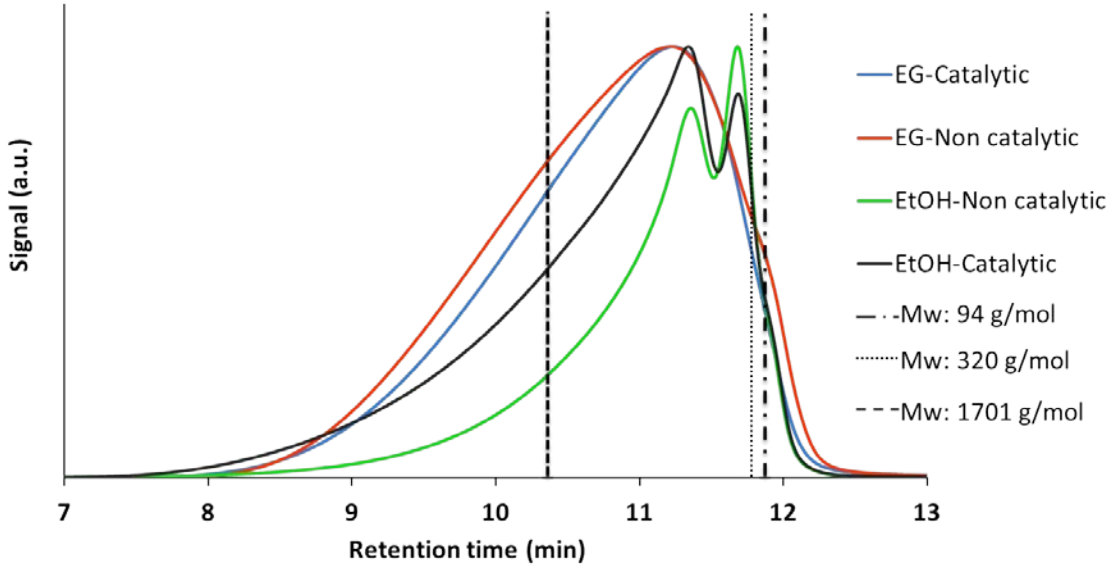

Figure 38 SEC analysis of non-catalytic and catalytic oil products from conversion of H-LS in EtOH and EG media. Reaction condition: 0/0.75 g Ni/SiO_2 catalyst, 7.5 g H-LS, 75 ml solvent, initial H_2 loading of 50 bar at RT, 250 ˚C, 3 hours.

A strong odor of sulfur in the light and oil fractions was an indication of the presence of sulfur. The ICP analysis detected 0.38 and 0.73 wt% sulfur in the oil from catalytic conversion of H-LS in EtOH and the liquid products from EG test (Apparent oil), respectively. This indicates that the oil would need further desulfurization to become a viable fuel. The considerably higher sulfur content in the oil from EG test might be because of the reaction of EG with reactive intermediate, stabilizing them, and inhibiting further cleavage of C-S bonds.

The solid phases were fractionized into THF soluble and THF insoluble compounds and analyzed with SEC analysis. However, the THF insoluble fraction from the EtOH test was not soluble in the 90/10 wt% DMSO/water solution, used as solvent for SEC analysis. This observation indicates that the THF insoluble fraction from EtOH medium was composed of highly crosslinked carbonaceous fragments. The SEC analyses of the solid phases from catalytic conversion of H-LS in both solvents are shown in Figure 39. The molecular weight distribution of the THF soluble fraction from the EtOH medium practically overlays on the SEC of H-LS, which suggests that this phase is largely composed of unreacted lignosulfonate. Moreover, formation of higher molecular weight fractions compared to H-LS in the left shoulder confirms condensation reactions building larger structures. The THF soluble fraction from EG medium shows lower molecular weight compared to THF insoluble fraction, which is consistent with its solubility in THF. As EtOH is less efficient for end-capping, the solid is a combination of highly cross-linked carbonaceous char phase and H-LS that has undergone little or no conversion (THF soluble) whereas EG as a better end-capping agent gives a solid that is a mixture of mid-size depolymerization products. It has been observed that EG can react

with in-situ produced formaldehyde from cleavage of β-O-4 and β-5 [127], and inhibits phenol formaldehyde condensation reactions, and suppresses char formation.

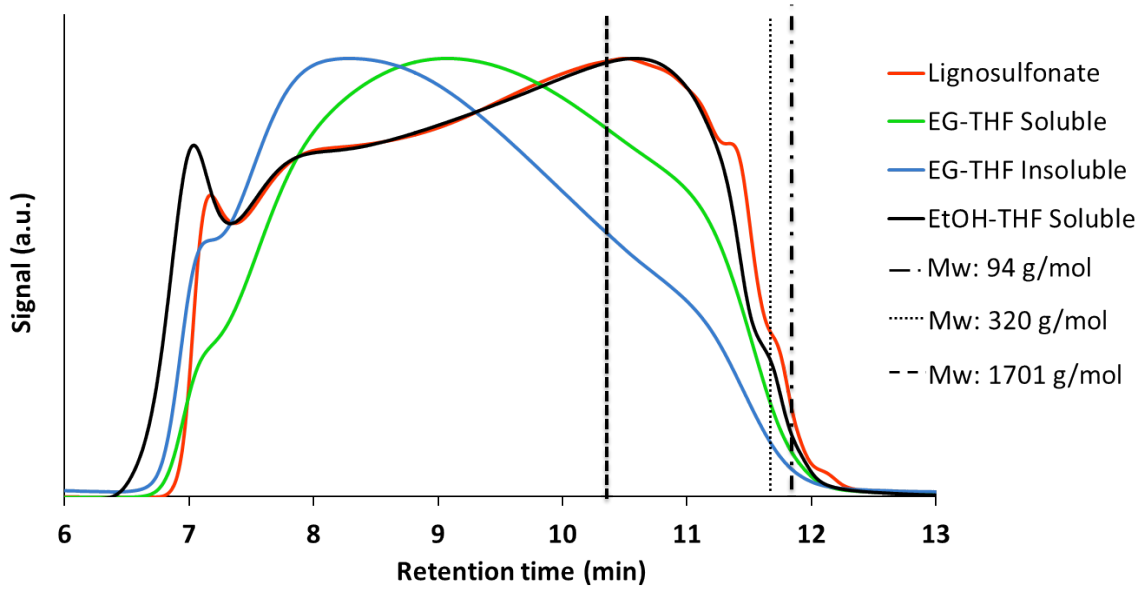

Figure 39 SEC analysis of the solid phases from catalytic conversion of H-LS in EtOH and EG mediums. Reaction condition: 0.75 g Ni/SiO_2 catalyst, 7.5 g H-LS, 75 ml solvent, initial H_2 loading of 50 bar at RT, 250 ˚C, 3 hours.

It was observed that the content of THF insoluble phase from reaction of H-LS in EG increased from 6 wt% in non-catalytic condition to 23% in the presence of a catalyst (Table 10, Entry 4 & 5). The GC analysis of the liquid fractions indicated that the relative areas of DEG, TEG and TTEG compared to EG increased in the presence of catalyst, which indicated that isomerization of EG was catalyzed over Ni/SiO_2. The lower –OH density of these compounds compared to EG may have inhibited end-capping and be the reason for the higher THF insoluble fractions in the catalytic condition. Mu et al. [137] investigated dissolution of Alkali lignin in EG and poly ethylene glycol at 140 ˚C. While lignin was fully soluble in EG, only 5 wt% lignin- poly ethylene glycol solution was reported due to low density of hydroxyl groups [137].

The elemental composition of oil and solid phases were also determined. Van Krevelen diagrams were plotted based on atomic O/C and H/C ratios. The H/C and O/C ratios for H-LS and the oil fractions are shown in Figure 40. Deoxygenation and hydrogenation was clearly observed in the oil fractions in an EtOH medium. The oil from catalytic tests had a lower O/C ratio compared to the non-catalytic oil, which indicated the role of a catalyst on removal of oxygen most likely by hydrodeoxygenation. The O/C ratio in the oil from a catalytic test at 300 ˚C was lower compared to the oil obtained at 250 ˚C, indicating increased oxygen removal at higher temperatures. Also note that the oil yield at 300 ˚C was significantly higher (47 wt%) than at 250 ˚C (31 wt%), see Table 10.

The oil fractions from EG tests were a mixture of liquefied lignin derivatives incorporated by EG, and also DEG, TEG, TTEG and higher glycols. Therefore, the presented O/C and H/C atomic ratios for these fractions are representing the whole mixture and not only the liquefied lignin fraction, and the fact that H/C and O/C ratios are higher in oil from conversion of H-LS in EG than in the original H-LS will reflect this solvent incorporation and solvent conversion. Using the Dulong formula [134], the higher heating value (HHV) of H-LS was determined as 21.4 MJ/kg. This number increased in the oil fractions from conversion of H-LS in non-catalytic and catalytic conditions in EtOH medium to 25.6 and 26.6 MJ/kg. The liquid fractions from conversion of H-LS in EG (which contains EG and higher glycols) in non-catalytic and catalytic condition had HHVs of 25.3 and 23.4 MJ/kg, respectively.

The Van Krevelen diagram of the solid phases confirmed the decrease in O/C content in solid residues from both solvents, which was more pronounced in the solid residue from EG. The H/C content in the solid fractions from EG medium slightly increased compared to H-LS which may be through incorporation of higher glycols to large fractions.

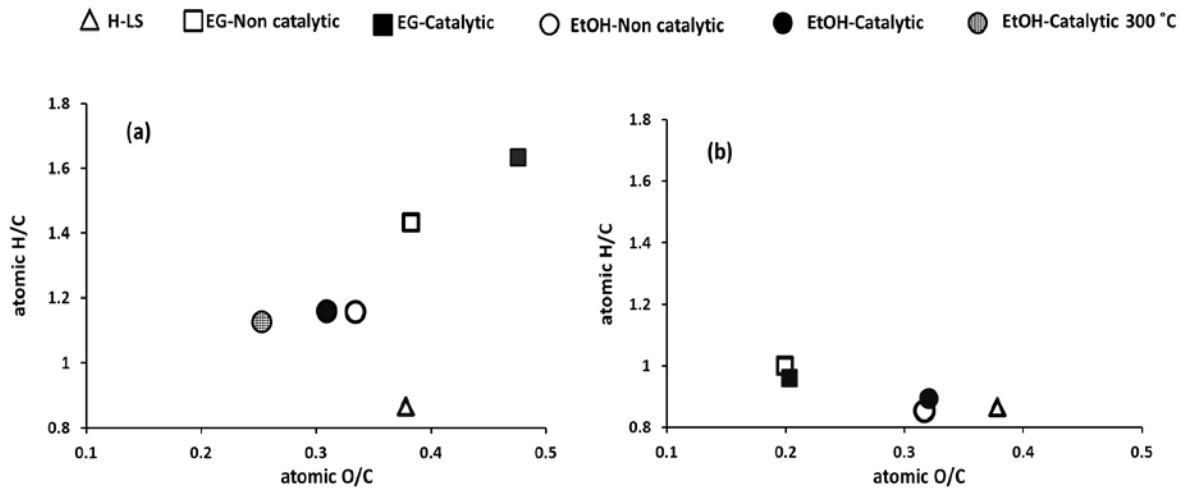

Figure 40 Van Krevelen diagrams of (a) oil and (b) solid fractions from conversion of H-LS in EtOH and EG mediums. Reaction condition: 0/0.75 g catalyst, 7.5 g H-LS, 75 ml solvent, initial H_2 loading of 50 bar at RT, 250 ˚C (except for conversion of H-LS in EtOH at 300 ˚C), 3 hours.

The presented results clearly indicated differences in performance of EG and EtOH as solvents for conversion of sulfonic acid lignosulfonates. At the reaction condition, thermal cleavage of ether bonds occurred and resulted in formation of monomeric and dimeric reactive fragments. By reaction of solvent with the degraded compounds, these were stabilized and prohibited from further degradation/condensation. There are advantages and disadvantages associated with each solvent. Feasibility studies can further clarify superiority of either of solvents for conversion of lignosulfonate. The performances of the solvents are summarized as follows:

- EtOH remained almost intact at the reaction conditions. The GC-MS analysis showed that EG to a significant extent was converted to higher glycols via self-reaction. Depending on the value of the liquefied products from EG conversion, the conversion

of EG to higher glycols may be unfavorable. However, it should be noted that conversion of EG was acid catalyzed by H^+ from sulfonate group. It is possible that the stability of EG can be improved by utilizing non-acid forms of lignosulfonate such as Na-LS. In support of this, although at lower temperature than applied here, Schutyser et al. [41] stated that EG remained stable during conversion of birch sawdust over Pd/C catalyst at 200 ˚C.

- The isolation of the oil from EtOH is simple and may be done by distillation. On the contrary, separation of reaction products in the EG medium is very challenging due to the high boiling point of EG and also partial solubility of EG in conventional solvents used for extraction of products.
- The products from reaction in EtOH, alkyl substituted guaiacols and aromatic esters, can be used as a source of value-added chemicals. The O/C atomic ratio of the oil from EtOH reaction decreased to 0.31 while the H/C increased to 1.16. However, if applications such as fuel additives are considered, further hydrodeoxygenation reactions are necessary. The oil fraction from EtOH tests had lower molecular weight distribution compared to the oil from EG medium. The liquefied compounds in EG were mixed with EG and higher glycols. The mixture may be directly used for applications such as functional gels and additive for lubricant [136], [137].
- EG is a better end-capping agent in preventing C-C bond formations. The presence of THF and DMSO insoluble solid fractions from EtOH tests indicated that the end-capping reactions between EtOH and reactive fractions were less efficient compared to EG. The solid residues left from reaction in EG can possibly be recycled in a continuous process and degraded to lower molecular weight compounds, while degradation of the solid char residue from EtOH medium could require severe reaction conditions or different processes such as pyrolysis or gasification. The char residue can also be burned for the energy supply.
- EtOH is in a supercritical condition at 250 ˚C. The operational pressure in EtOH tests rose up to 155 bar while the pressure in EG tests was up to 78 bar. Obviously, a lower pressure is favorable from industrial equipment design point of view. It is beneficial to optimize the process condition by reduction of initial hydrogen loading and ethanol to lignosulfonate ratio.

4.3. Effect of the catalyst support on the degradation of lignosulfonate

The effect of the support material on the catalytic behavior of Ni based catalysts was investigated by using Ni catalyst supported on SiO_2, AC, ZrO_2 and γ-Al_2O_3 (the specifications of the catalysts are presented in Table 9). The catalytic tests were conducted in EtOH medium due to easier workup procedure. The oil and solid yields from reaction of H-LS over Ni/AC, Ni/ZrO_2 and Ni/γ-Al_2O_3 are presented in Table 12, Entry 1-3. The oil yields were almost similar up to 34 wt%, despite the nature of support and associated acidity. The oil yield from conversion of H-LS over Ni/AC (the inert support) was 34 wt% which was almost similar with 33 wt% oil yield over Ni/γ-Al_2O_3 catalyst (possessing acidity). The SEC analysis of the oil fractions from conversion of H-LS over Ni deposited on different support materials showed similar molecular weight distribution (Shown in Appendix A, Figure A3). Moreover, similar

results were observed from elemental analysis of the oil phases. Furthermore, using merely support as catalyst was evaluated using AC and SiO_2 (Table 12, Entry 4-5), where oil yields almost similar to the oil yield from non-catalytic condition (around 15-18 wt%, see Table 10 and Table 12) were observed. Considering all the evidences, we conclude that catalyst carrier most probably was not involved in catalytic degradation of lignosulfonate and the presence of an active phase like Ni was required.

Table 12 The oil and solid yields from conversion of H-LS over Ni based catalyst in EtOH. Reaction condition: 0.75 g catalyst, 7.5 g lignin, 75 ml solvent, initial H_2 loading of 50 bar at RT, 250 ˚C, 3 hours.

Entry	Catalyst	Oil yield wt%	Solid yield wt%
1	Ni/AC	34	60
2	Ni/ZrO_2	34	69
3	$Ni/\gamma\text{-}Al_2O_3$	33	67
4	AC	15	76
5	SiO_2	18	67
6	Ni/SiO_2 (Sulfided)	33	52
7	Ni/SiO_2*	30	60

*Spent catalyst from reaction of H-LS in EtOH in the presence of Ni/SiO_2

4.4. Working state of Ni based catalyst

Sulfur is a known poison for Ni catalyst [138], and sulfur-poisoning may occur during the conversion of the sulfur containing feedstock. XRD analysis of solid residue from catalytic conversion of H-LS over Ni/SiO_2 in EtOH confirmed presence of a NiS phase (Shown in Appendix A, Figure A4). The XRD pattern of the detected NiS peaks is in agreement with literature [84], [139]. The NiS phase detected by XRD analysis of the spent catalyst is likely formed through cleavage of C-S bond in lignosulfonate and adsorption of sulfur on Ni active sites. The presence of sulfur in the spent Ni/SiO_2 catalyst residues was also confirmed by ICP analysis. In order to observe whether sulfur deposition affects cracking activity of catalyst, a batch of Ni/SiO_2 catalyst was deliberately sulfided in the presence of DMDS; 0.75 g of catalyst was treated with 10 ml DMDS at 400 ˚C overnight. The autoclave was initially loaded with 30 bar H_2 pressure (RT). The presence of NiS was confirmed by XRD analysis on the sulfided catalyst. This catalyst was tested for conversion of H-LS at standard reaction condition without any further reduction (Table 12, Entry 6). Surprisingly, an oil yield of 33 wt% was observed which was almost similar to the oil from fresh Ni/SiO_2 catalyst. This observation indicated that either the catalytic activity is not affected by the presence of sulfur and formation of NiS, or NiS is partially regenerated during the reaction. Narani et al. [32] also reported activity of a sulfided Ni/AC catalyst for conversion of kraft lignin, where 70 wt% methanol soluble oil was obtained at 320 ˚C. Song et al. [110] argued that Ni metal is active for hydrogenolysis of ether bonds. They reported that NiS phases were regenerated to catalytically active Ni sites in reductive medium by desorption of sulfur in form of H_2S [110]. We treated the NiS/SiO_2 catalyst in a blank test (without lignin) in the presence of EtOH at 250 ˚C and 50 bar H_2 (RT) to see whether NiS can react to the metallic Ni. The ICP analysis confirmed presence of sulfur in the catalyst after reductive EtOH treatment with S/Ni molar ratio of 0.71. This is lower than

a full NiS stoichiometry. It is not possible to make conclusions about the surface state of the catalyst on the basis of ICP, but the results indicate that the catalyst remains at least partly non-sulfided under reaction conditions and is able to exert some catalytic effect in this state. Understanding the exact mechanism of the catalytic activity is complex. Based on our observations, results from Song et al. [110] and the literature, herein we propose the following potential routes on the activity of Ni/NiS sites:

- The sulfur in the structure of lignosulfonate or in the depolymerized fractions adsorbs on Ni via cleavage of C-S bond and forming NiS. A sulfur removal cycle may simultaneously take place where the adsorbed S may desorb in form of compounds such as H_2S [110].
- Maxted et al. [140] reported that while sulfur in high molecular weight organosulfur compounds adsorbs on catalytic sites, the carbon chain can inhibits adsorption of other reactants in the adjacent sites [140]. By adsorption of sulfur from lignosulfonate or partially degraded oligomers on catalytic active sites, the carbonic chain may therefore have steric effects and possibly hinder formation of new NiS bonds. The adsorbed organosulfur then may be degraded via hydrogenolysis on the covered active sites and desorb, followed by successive adsorption of an organosulfur compound.

4.4.1. Catalyst reusability

The reusability of spent Ni/SiO_2 catalyst was tested in EtOH. It was not possible to separate the catalyst from the char from the former experiment and therefore we used the total solid residue (char + catalyst) from reaction of Ni/SiO_2 (Table 10, Entry 2) as catalyst and assumed that the char would not react further or catalyze reaction. The solid residue was treated with hydrogen prior to use, in a way similar to the standard tests. An oil yield of 30 wt% was observed (Table 12, Entry 7) which is almost similar to the 31 wt% oil yield over fresh Ni/SiO_2. The SEC analysis of the oil fraction from catalytic reuse test was also consistent with the molecular weight distribution of oil obtained with fresh catalyst (Shown in Appendix A, Figure A5). This confirms the reusability of the catalyst.

4.5. Conclusion

The liquefaction of lignosulfonate in its acid form (H-LS) in ethanol and ethylene glycol media was investigated in the absence or presence of Ni/SiO_2 catalyst, and the solid and liquid products were analyzed in detail. The yields of liquefied fractions were almost similar in the two solvents (31 wt% in EtOH and 32 wt% in EG). Monomer yields of 0.8-4.0 wt% were obtained while SEC analysis indicated that the products in the oil fractions were mainly dimers and oligomers. The molecular weight distribution of oil from conversion in EtOH medium showed formation of lower molecular weight compounds compared to the oil from conversion of H-LS in EG medium. The solid residue from EtOH tests was mainly char. Char formation was to a greater extent inhibited in EG medium by end-capping reaction and suppression of repolymerization by reactive compounds. EtOH was relatively stable in the reaction conditions whereas EG was significantly converted to DEG, TEG and TTEG. The oligomerization of EG

is catalyzed by H^+ from the SO_3H groups in the lignosulfonate structure. No effect was observed from the catalyst support material for Ni supported on AC, SiO_2, ZrO_2 and γ-Al_2O_3. The oil yields obtained were almost similar for all four catalysts. The formation of a NiS phase in the spent catalyst from conversion of H-LS in EtOH medium was confirmed by XRD and ICP analysis. The catalyst remained partially active despite formation of NiS.

Acknowledgement

Leonhard Schill for is thanked for conducting ammonia desorption analysis. Providing the catalyst support material by Saint Gobain is appreciated.

Chapter 5:

Solvothermal conversion of lignosulfonate assisted by NiMo catalyst

5. Solvothermal conversion of lignosulfonate assisted by NiMo catalyst

Hydrotreating NiMo and CoMo catalyst have gained interest in solvothermal conversion of biomass and lignin. A recent patent reported [141] successful conversion of biomass in digestive solvents such as ethanol and ethylene glycol over supported catalysts comprised of S, Mo/W, and Co, Ni or a mixture of them at 180-300 ˚C. Cattelan et al. [76] observed higher yields of aromatics from conversion of kraft lignin in the presence of an MoS_2 based catalyst compared to non-catalytic conversion in supercritical ethanol at 280 ˚C under nitrogen atmosphere: The yield of aromatic compounds increased from 10.2 wt% to 17.8 wt% in the presence of catalyst [76] Cattelan. Joffres et al. [103], [104] observed cleavage of β-O-4 and α-O-4 bonds in reductive degradation of wheat straw soda lignin over $NiMoS/Al_2O_3$ at 350 ˚C in tetralin solvent.

We investigated conversion of lignosulfonate over alumina supported NiMo in ethanol medium. The quality of liquid, solid and gaseous compounds was comprehensively evaluated and the role of solvent and also its consumption was elaborated. Additionally, we studied the effect of reaction parameters such as reaction temperature, reaction time, catalyst loading and reusing the catalyst to maximize the yield of the liquefied fractions. Furthermore, we investigated the necessity of pre-sulfidation of the NiMo catalyst for conversion of the lignosulfonate. It was intended to observe whether the catalyst can be sulfided in-situ by sulfur present in lignosulfonate, or it must be sulfided prior to use to gain the cracking, HDO and HDS activity.

5.1. Depolymerization of lignosulfonate

The results from conversion of H-LS are summarized in Table 13. The reproducibility was confirmed by repeating a few selected experiments. A high yield of 67±2 wt% oil phase was obtained from conversion of H-LS over NiMo-I catalyst at 310 ˚C (Table 13, Entry 1). The catalyst was used in its oxide form, and it was assumed that it may get sulfided in-situ by reaction with sulfur from lignosulfonate. This will be discussed later based on the results from NiMo-II catalyst. The yield of solid fraction was 38 ± 2 wt%. Noticeably, the sum of solid and oil yields exceeded 100 %, most likely due to solvent incorporation. The observed oil yield is amongst the highest yields reported from one-pot mild solvothermal conversion of lignin [92], [111]; Oregui-Bengoechea reported maximum oil yield of 65 wt% from conversion of rice-straw lignin in ethanol/formic acid solution over sulfated alumina supported NiMo catalyst at higher temperature of 340 ˚C [92].

Table 13 Results from conversion of H-LS. Reaction condition: 0/1 g NiMo-I catalyst, 10 g lignin, 100 ml ethanol, 26 bar H_2 (loaded at RT).

Entry	Catalyst: Pre-Sulfided/ Oxide	Catalyst mass [g]	Reaction time [h]	T [˚C]	Oil yield wt%	Solid yield wt%
1	Oxide	1	3	310	67	38
2	Non-Catalytic	0	3	310	26	77
3 [(a)]	Oxide	1	3	310	45	64
4	Non-Catalytic	0	3	260	17	81
5	Oxide	1	3	260	29	72
6	Pre-Sulfided	1	3	260	46	56
7 [(b)]	Oxide	0.5	3	310	76	24
8 [(b)]	Pre-Sulfided	0.5	3	310	76	25
9 [(c)]	Pre-Sulfided	1	3	260	44	51
10	Pre-Sulfided	1	3	290	53	45
11	Pre-Sulfided	1	3	300	62	40
12	Oxide	1	1	310	53	49
13	Oxide	1	2	310	61	42
14	Oxide	1	4	310	79	25
15	Oxide	0.5	3	310	57	47
16	Oxide	2	3	310	88	15
17	Oxide	3	3	310	87	16
18 [(d)]	Spent catalyst	N.A	3	310	65	35
19 [(e)]	Spent catalyst	N.A	3	310	61	36

(a) Experiment in N_2 atmosphere (8 bar N_2 loaded in room temperature), (b) 0.5 g catalyst, 5 g lignin, 50 ml solvent, (c) With addition of 1 ml DMDS in the reactor, (d) Reusing catalyst from Entry 1, (e) Reusing catalyst from Entry 18.

The sulfidation state of NiMo catalyst after reaction of H-LS was assessed using TEM and EDX. At a similar reaction condition (310 ˚C & 3 h, no DMDS addition), H-LS was reacted over the oxide home-synthesize NiMo-II catalyst and the TEM and EDX images were obtained. Also, the TEM and EDX images of fresh pre-sulfided NiMo-II and pre-sulfided NiMo-II after reaction (spent catalyst, reaction with H-S at 310 ˚C & 3 h, no DMDS addition) were obtained as reference. The MoS_2 slabs were clearly visible in the TEM images of the fresh pre-sulfided NiMo-II (Figure 41, a) and the spent pre-sulfide NiMo-II (Figure 41, b). Regarding the spent non pre-sulfided NiMo-II (Figure 41, c), linear features were detected which were consistent with MoS_2 slabs, however, in a less developed state compared to the pre-sulfided NiMo-II catalyst samples. The EDX analysis of the spent non pre-sulfide NiMo-II showed a homogenous distribution of Ni, Mo and S (Shown in Figure 42). 10.0 wt% sulfur was determined by ICP in the sulfided home-synthesized NiMo-II catalyst, which is sufficient to convert Mo and Ni atoms to the sulfide state. Taking into account TEM and EDX results, we therefore conclude that the catalyst was sulfided in-situ from the sulfur present in the structure of lignin. In some EDX images, accumulation of Ni and S was observed (shown in Appendix B, Figure B1), which is most likely due to formation of Ni_3S_2 along with NiMoS [142].

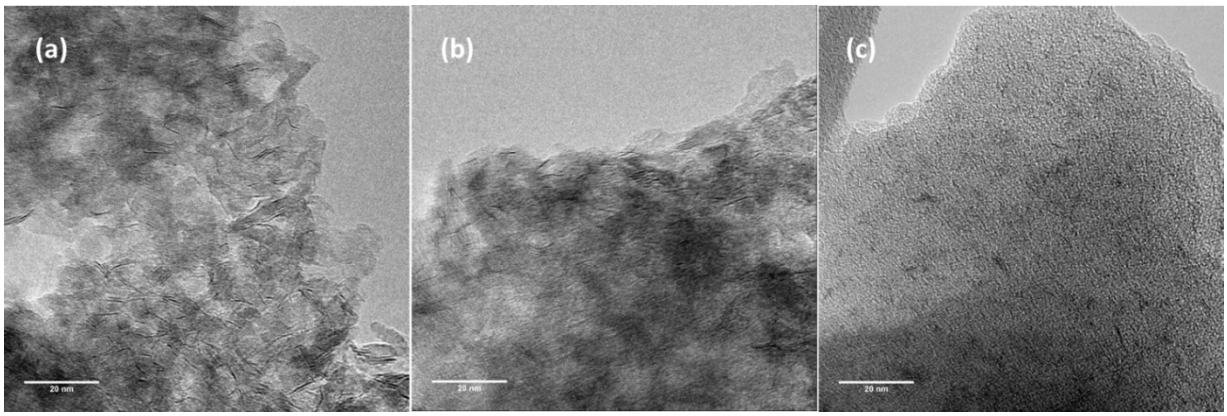

Figure 41 TEM images of (a) Fresh pre-sulfide NiMo-II, (b) Spent pre-sulfided NiMo-II, (c) Spent non pre-sulfided NiMo-II. Reaction condition: 1 g NiMo-II catalyst, 10 g lignin, 100 ml ethanol, 26 bar H_2 (loaded at RT), 3 hours.

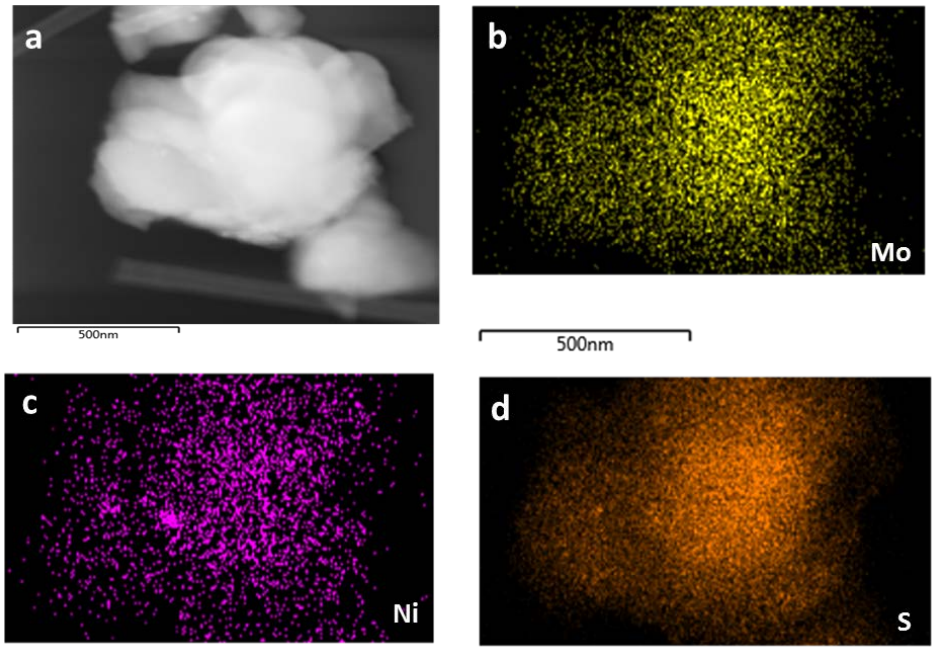

Figure 42 (a) TEM image of spent non pre-sulfided NiMo-II catalyst, EDX mapping of (b) Mo, (c) Ni and (d) S in spent non pre-sulfided NiMo-II catalyst from reaction of H-LS at 310 ˚C. Reaction condition: 1 g NiMo-II catalyst, 10 g lignin, 100 ml ethanol, 26 bar H_2 (loaded at RT), 3 hours.

The role of catalyst was studied by conversion of H-LS in the absence of catalyst (Table 13, Entry 2). The presence of the catalyst clearly promoted the formation of liquefied fragments. Only 26 wt% oil was obtained in the absence of the catalyst compared to 67 wt% with the catalyst. Conversely, the solid fraction was 77 wt% in the absence of the catalyst versus 38 wt% when the catalyst was present. The oil and solid fractions from non-catalytic and catalytic tests were comprehensively evaluated in order to determine the differences.

5.1.1. Evaluation of the oil fractions

The oil fractions were analyzed with GC-MS analysis (Figure 43).The structures of the main compounds identified with the mass spectrometer are shown. Here it should be considered that only the compounds that were sufficiently volatile to pass through the column at GC conditions were identified with the MS. The GC analysis therefore only covers the lowest size range of the products. Guaiacol, alkylated guaiacols and ethyl vanillate comprised the main identified compounds in the oil from the non-catalytic tests (See Figure 43, a). Guaiacol and alkyl substituted guaicols are expected compounds from degradation of spruce based lignin; spruce lignin is mainly composed of coniferyl alcohol units (G-Lignin) [143]. Formation of Guaiacol and its variations can be attributed to the cleavage of β-O-4 bonds [144]. Formation of ethyl vanillate may take place by formation of vanillic acid from cleavage of ether bonds and esterification with the ethanol.

Noticeably, the identified compounds in the oil from catalytic conversion were different from the compounds in the absence of catalyst (Figure 43, b).Three main groups of compounds were identified in the oil fraction obtained over alumina supported NiMo-I: alkyl phenols, alkoxy alkyl phenols and alkoxy alkyl benzene. The selectivity to mono-oxygen containing compounds was more than 50 % (area basis), whereas all compounds in the oil fraction from non-catalytic test contained at least two oxygen atoms. This implies a deoxygenation activity of the catalyst on the di-oxygenated species. The presence of alkyl ether bonds was pronounced in the monomers of the catalytic oil. Horacek and co-workers [111] observed guaiacol and guaiacol derivatives from conversion of 5 wt% aqueous solution of lignosulfonate over alumina supported NiMo catalyst at 320 ˚C in a continues flow reactor. The difference between the products observed in our work and the work from Horacek et al. [111] exhibits the role of ethanol in C- and O alkylation of reactive intermediate [78], catalyzed over NiMo/Al_2O_3 catalyst.

Moreover, the oil fractions from non-catalytic and catalytic conversion of H-LS at 310 ˚C were qualitatively analyzed with GC×GC analysis for identification of the main compound groups in the oil fractions (Figure 44). Guaiacol and alkyl guaiacols (methyl, ethyl and propyl substituted guaiacol) and catechol and alkyl catechols (methyl, ethyl substituted catechols) were the major identified compounds in the oil fraction obtained in the non-catalytic condition, whereas alky phenols, alkyl benzenes and alkyl catechols were identified compound groups in the catalytic oil. Ethanol incorporation in form of alkylation was clearly observed over the catalyst, where formation of bis and tert alkyl compounds were observed. Oxygen free compounds such as alkyl benzene were only detected in the oil from catalytic conversion of H-LS. Deoxygenation and alkylation reactions in the presence of the catalyst were therefore confirmed by GC×GC, which is consistent with the GC-MS results. Vanillic acid derivative were the other identified group in non-catalytic condition, while the intensities corresponding to this group considerably decreased in the catalytic oil, presumably by deoxygenation activity of the catalyst in removing the carboxyl groups. Moreover, vanillin derivatives with a low intensity were detected in the oil from non-catalytic condition only.

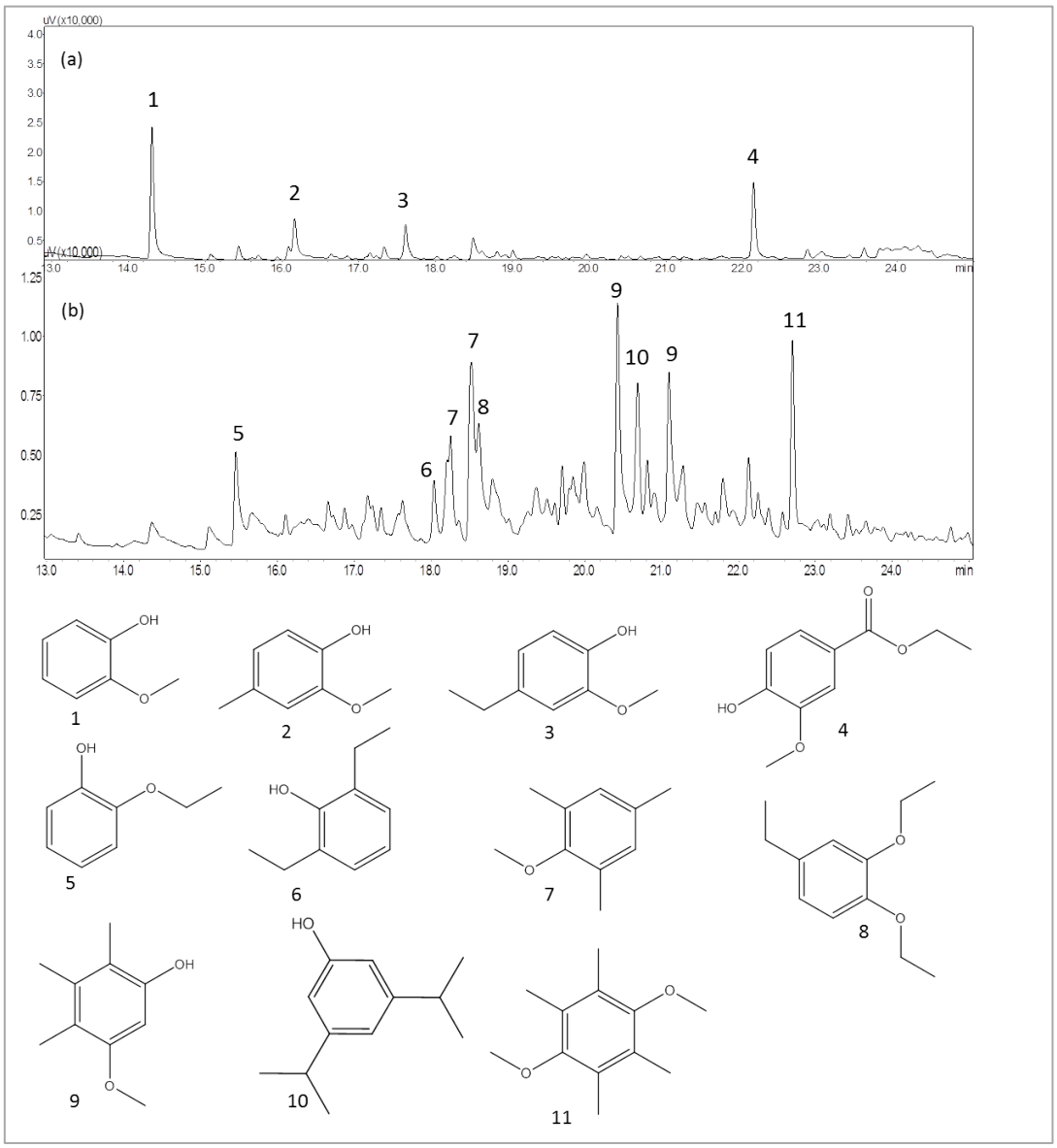

Figure 43 GC-MS analysis of the oil fraction from conversion of H-LS at 310 ˚C (a) non-catalytic, (b) over NiMo-I catalyst. Reaction condition: 0/1 g catalyst, 10 g lignin, 100 ml ethanol, 26 bar H_2 (loaded at RT), 3 hours.

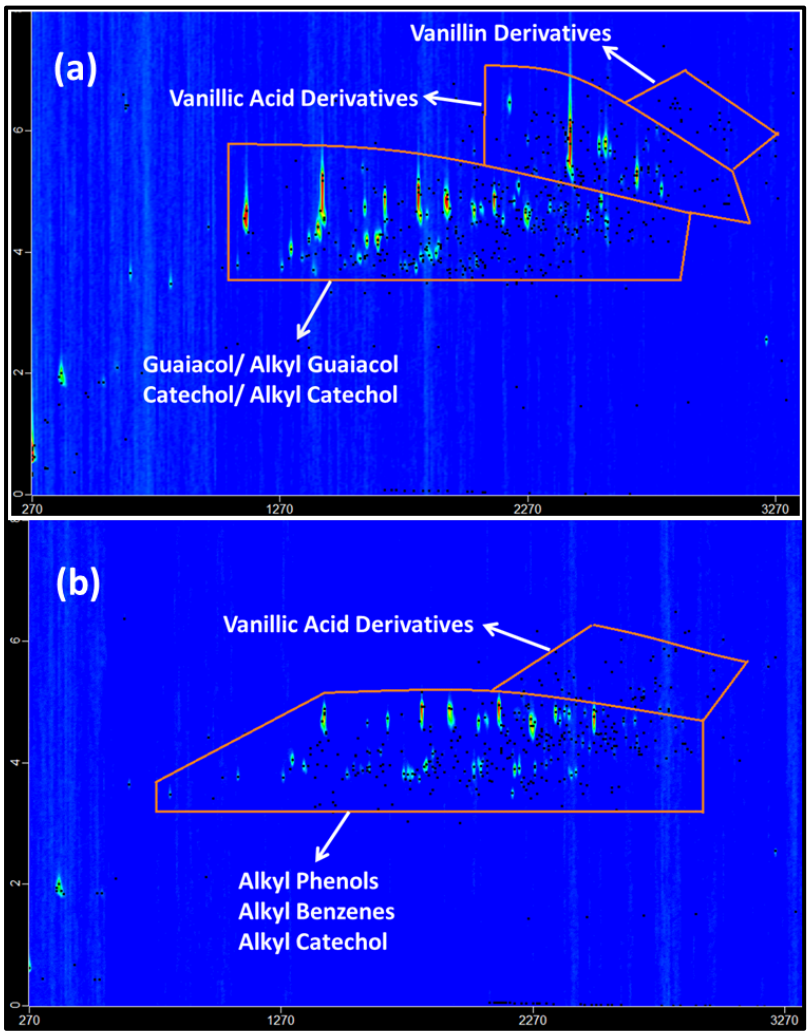

Figure 44 GC×GC analysis of the oil fractions from (a) non-catalytic and (b) catalytic test over NiMo-I at 310 ˚C. Reaction condition: 0/1 g catalyst, 10 g lignin, 100 ml ethanol, 26 bar H_2 (loaded at RT), 3 hours.

The size exclusion analyses (SEC) of non-catalytic and catalytic oils are shown in Figure 45. Moreover, the SEC of H-LS is shown for comparison. The retention times of phenol, GGGE and tannic acid are shown as standards. Surprisingly, the conversion of H-LS over NiMo catalyst did not result in formation of compounds with higher degree of depolymerization. Both oil fractions had the same retention time ranges. The oil from non-catalytic test showed a bimodal elution, while the oil from the catalytic condition had a more uniform molecular weight distribution. The main peaks in both oil samples had elution times with the range of dimers to oligomers. However, the catalytically produced oil had a greater fraction of larger compounds. The formation of higher fraction of monomers perhaps requires higher reaction temperature to scissor highly stable C-C bonds. The potential reasons for the similar sizes of the oil fractions are elaborated later with the mechanism of lignin degradation.

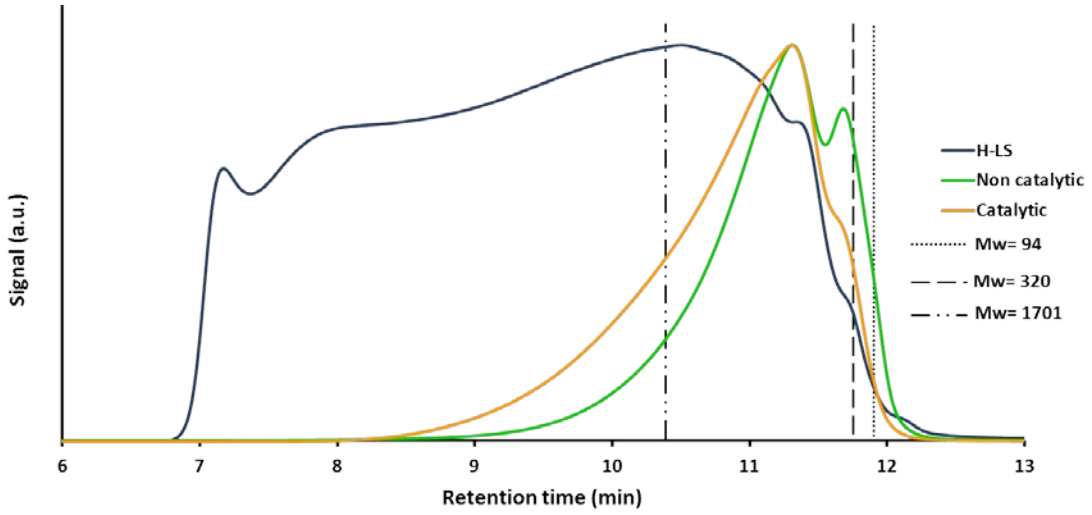

Figure 45 SEC analysis of H-LS, oils from non-catalytic and catalytic conversion at 310 ˚C. Reaction condition: 0/1 g NiMo-I catalyst, 10 g lignin, 100 ml ethanol, 26 bar H_2 (loaded at RT), 3 hours.

The SEC analysis of the oil fractions from non-catalytic and catalytic tests confirmed that the oil fractions consisted of mainly dimers and oligomers and a minor concentration of monomers. However, we only detected monomers by the GC technique. In order to get a better insight into the functional groups in the oil fractions, HSQC NMR was utilized. The NMR analysis of the oil fractions from non-catalytic and catalytic reactions over NiMo-II at 310 ˚C are shown in Figure 46. The aliphatic, aromatic and the signals corresponding to the side chains are specified, according to the literature [145], [146]. The prominent inter-connecting units in the structure of lignin such as β-O-4 and α-O-4 were not detected, indicating that the degradation in the absence and presence of catalyst resulted in the cleavage of these bonds. Compared to the non-catalytic oil, a pronounced decrease in methoxy protons (δ_C/δ_H 56.2/3.75), relative to the aromatic protons, was observed in oil products from catalytic conversion. In agreement with the GC-MS results, this indicates the catalytic hydrogenolysis and deoxygenation of methoxy groups. Additionally, 9 times more CH_4 was evolved in the catalytic test which is consistent with the hydrogenolysis of -OCH_3 to CH_4. A decrease in γ-protons (δ_C/δ_H 62.9/3.76, 61.3/4.27), the alcohol neighboring protons, was observed in catalytically produced oil. This indicated the removal of the hydroxyl group on the aliphatic carbon in the presence of the catalyst. Higher intensities in the aliphatic region were detected in the oil from catalytic conversion which corresponds to CH_3/CH in α position connected to an aromatic ring and is consistent with the observed ethanol alkylation reactions catalyzed over NiMo catalyst.

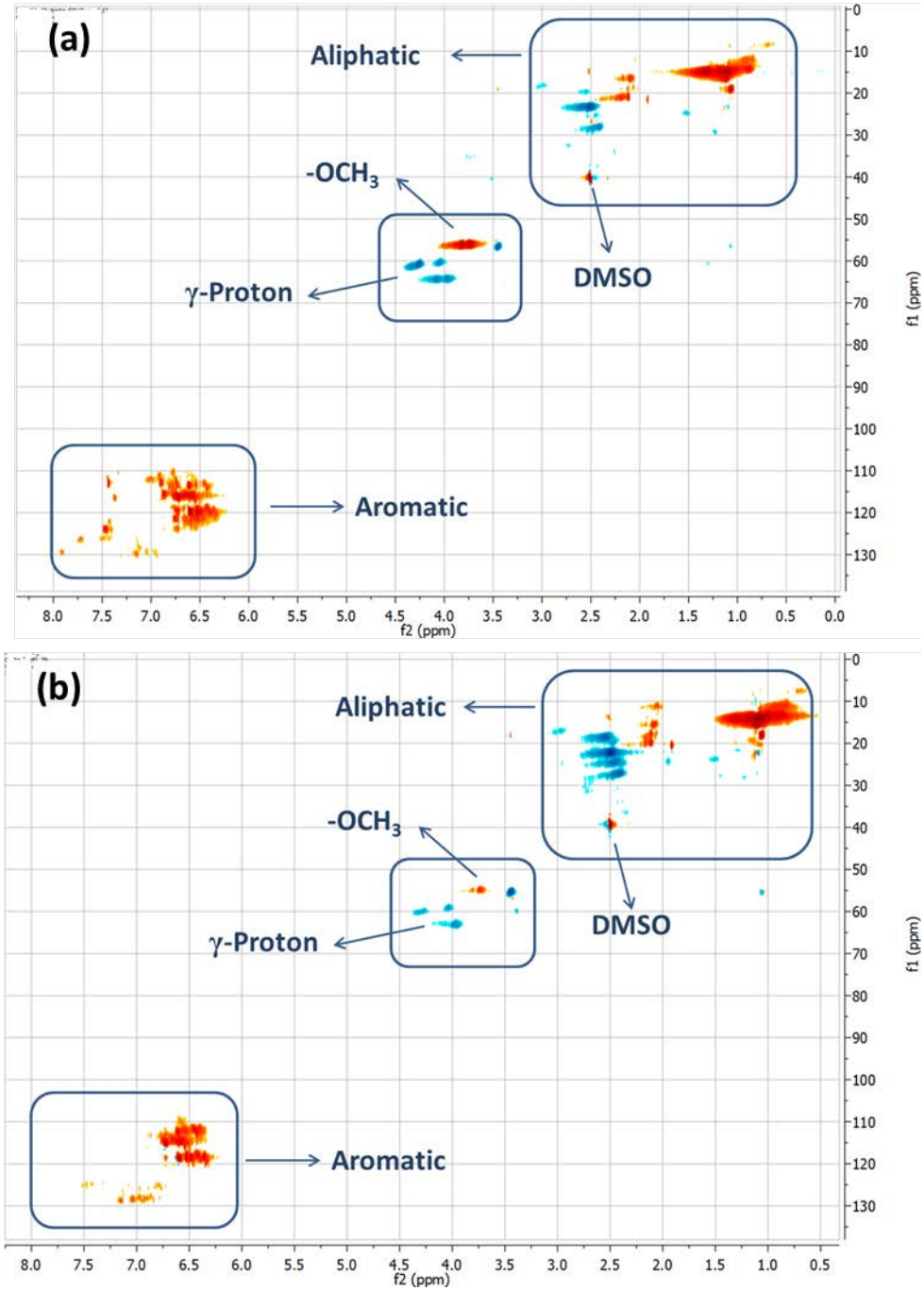

Figure 46 HSQC NMR of the oil fractions from (a) non-catalytic oil, (b) catalytic over NiMo-I at 310 ˚C. Reaction condition: 0/1 g catalyst, 10 g lignin, 100 ml ethanol, 26 bar H_2 (loaded at RT), 3 hours.

The elemental analysis of the lignin and oil samples is shown in Table 14. The higher heating values (HHVs) were calculated using the Dulong formula [134]. The oxygen content of the non-catalytic oil fraction (Table 14, Entry 2) was 23.3 wt%, compared to 30.8 wt% for the H-LS, indicating that the deoxygenation took place even in the absence of catalyst. This is in agreement with the observations of Nielsen et al.[25], where deoxygenation was reported in non-catalytic conversion of enzymatically hydrolyzed lignin in ethanol at 250-450 ˚C. Higher degree of deoxygenation was observed over NiMo-I catalyst (Table 14, Entry 3), where the

oxygen content decreased to 11.4 wt%. The HHV in the oil obtained over NiMo-I catalyst was calculated to be 36.5 MJ/kg similar to that of butanol (HHV of 36.6 MJ/kg) [147]. Surprisingly, the sulfur content of the oil from non-catalytic test was 0.25 wt%, which was lower than in the oil from catalytic test, 0.43 wt%. However, the sulfur content of the catalytic oil can be reduced to 0.1 wt% by prolonging the reaction time to 4 h, which is elaborated later.

Table 14 Elemental analysis and the HHV values of H-LS and the oil fractions from non-catalytic and catalytic conversion of H-LS at 310 ˚C. Reaction conditions: 0/1 g catalyst: 10 g lignin: 100 ml ethanol, 26 bar H_2 (loaded at RT) except for the test in N_2 atmosphere, 3 hours.

Entry	H-LS/Oil	Catalyst	C wt%	O wt%	H wt%	S wt%	Atomic O/C	Atomic H/C	HHV (MJ/kg)
1	H-LS	-	61.1	30.8	4.4	3.1	0.38	0.86	21.4
2	Oil	Non-catalytic	69.9	23.2	6.7	0.25	0.25	1.14	29.0
3	Oil	NiMo-I	80.1	11.4	8.0	0.43	0.11	1.20	36.5
4	Oil*	NiMo-I	79.9	11.3	8.4	0.29	0.11	1.27	37.1

* Oil produced in N_2 atmosphere (8 bar N_2 loaded at RT)

The role of hydrogen on degradation of lignin was studied by catalytic conversion of H-LS in N_2 atmosphere (8 bar at room temperature). Here, oil and solid yields of 45 and 64 wt% were detected, respectively (Table 13, Entry 3). The oil yield in N_2 atmosphere was lower than the oil yield in H_2 atmosphere (45 vs. 67 wt%). Similarly, Narani et al. [32] observed 22 wt% methanol soluble oil from conversion of kraft lignin over NiMoS/AC in the absence of H_2, while the oil yield increased to 53 wt% in the presence of 35 bar of hydrogen (loaded at RT). The elemental composition of the oil in N_2 atmosphere showed similar features to the oil from H_2 (Table 14, Entry 4). It is speculated that the in-situ ethanol derived hydrogen can be involved in hydrogenolysis and reductive deoxygenation reactions. The formation of hydrogen from ethanol in nitrogen atmosphere was confirmed by GC analysis. The NMR analysis (shown in Appendix B, Figure B2) indicated that the catalyst was capable of demethoxylation under nitrogen pressure, within the same degree as under hydrogen pressure. However, the decrease of γ-protons did not progress to the same extent in nitrogen atmosphere, perhaps due to lower partial pressure of hydrogen. Therefore, it is concluded that higher partial pressure of hydrogen positively affects the liquefaction reactions likely by stabilization of reactive radicals.

Based on the results from characterization of the oil fractions using different analytical technique, the following mechanism is suggested: The similar molecular weight distribution ranges observed by SEC analysis of the oil fractions from non-catalytic and catalytic conditions indicates that the depolymerization reactions are possibly not affected by catalyst. Moreover, the HSQC NMR analysis of the oils confirmed absence of prominent interconnecting units in the structure of lignin such as β-O-4 in non-catalytic and catalytic conditions, and aligned with SEC results indicates that degradation reactions possibly occur via thermal cracking and ethanolysis. Highly reactive intermediates produced from depolymerization undergo fast condensation reactions, unless the reactivity is suppressed by end-capping reactions [113]. In the presence of catalyst, stabilization of radical fragments takes place via ethanol alkylation reactions, resulting in higher liquefaction yield [78]. Moreover, the role of catalyst is noticeable on deoxygenation reactions via reductive removal of hydroxyl and methoxy groups.

5.1.2. Evaluation of the solid fractions

The solid products were isolated using filtration. In catalytic reactions, the solid residue consisted of organic matters and ash originating from lignin and spent catalyst. The physical appearance of the solid fractions from non-catalytic and catalytic conditions (Table 13, Entry 1 and 2) is shown in Appendix B, Figure B3. While the solid residue in the absence of catalyst consisted of large agglomerated lumps, the solid residue from the catalytic reaction had much smaller particles of more uniform size, presumably due to grinding action of the catalyst particles on the char under the stirring. The elemental composition of the solid residues from non-catalytic and catalytic conversion of H-LS is shown in Table 15. The solid from non-catalytic test had a higher carbon content than the solid from catalytic conversion whereas the chemical composition of the solid from catalytic condition possessed very similar composition to H-LS (Table 15, Entry 1). However, getting insight in the molecular weight distribution of the solid phases was not achievable due to their insoluble character in 90/10 wt% DMSO/water (solvent used for SEC analysis, in which H-LS is completely soluble). Therefore, it was concluded that both solid fractions were produced from condensation reactions. The higher oxygen content in the solid from catalytic condition compared to the non-catalytic solid, suggest that it probably experienced a lower degree of condensation.

Table 15 Elemental analysis and the HHV values of H-LS and the solid fractions from non-catalytic and catalytic conversion of H-LS at 310 ˚C. Reaction condition: 0/1 g catalyst: 10 lignin: 100 ml ethanol, 26 bar H_2 (loaded at RT), 3 hours.

Entry	H-LS/ Solid	Catalyst	C wt%	O wt%	H wt%	S wt%	Atomic O/C	Atomic H/C	HHV (MJ/kg)
1	H-LS	-	61.1	30.8	4.4	3.1	0.38	0.86	21.4
2	Solid	Non-catalytic	76.4	17.8	4.8	0.94	0.17	0.75	29.5
3	Solid	NiMo-I	65.3	30.0	4.7	N.A	0.34	0.87	17.8

5.1.3. Pre-sulfidation of catalyst

It was interesting to evaluate whether there are advantages from pre-sulfidation of the catalyst with respect to the products distribution. To this end, a number of tests were conducted using the oxide and pre-sulfided catalyst at 260 and 310 ˚C (results are shown in Figure 47). H-LS was tested in a non-catalytic reaction at 260 ˚C as a benchmark to compare non-catalytic and catalytic results at this temperature. Without catalyst, the oil and solid yields of 17 and 81 was obtained at 260 ˚C (Table 13, Entry 4). By addition of catalyst at 260 ˚C in the oxide form (Table 13, Entry 5), the oil yields increased to 29 wt%, while the solid yield decreased to 72 wt%. Moreover, by reaction of H-LS over pre-sulfided NiMo at 260 ˚C (Table 13, Entry 6) the oil yield increased to 46 wt%, while the solid yield decreased to 56 wt%, which indicated that pre-sulfidation of NiMo was advantageous for reaction at 260 ˚C to acquire higher catalytic activity.

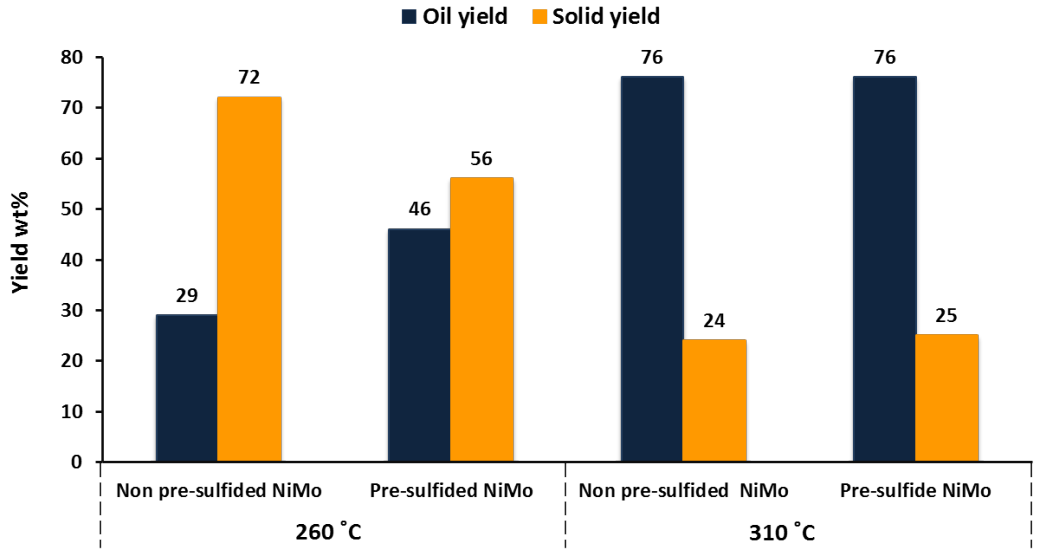

Figure 47 Oil and solid yields from degradation of H-LS with non pre-sulfided NiMo-I and pre-sulfided NiMo-I at 260 and 310 ˚C. Loading at 260 ˚C: 1 g catalyst, 10 g H-LS, 100 ml ethanol. Loading at 310 ˚C: 0.5 g catalyst, 5 g H-LS and 50 ml ethanol. 26 bar H_2 (loaded at RT), 3 hours.

At 310 ˚C the oil yield was 76 wt% over both the oxide and sulfide catalyst (Table 13, Entry 7 & 8, respectively) and the solid yields were also similar of above 25 wt%. In these experiments, the loading of catalyst, lignin and solvent in the experiments at 310 ˚C were cut by half, in order to avoid overpressure when using the pre-sulfided NiMo. It is interesting to observe that the oil yields increased under these conditions (compared to 67 wt% in standard reaction condition), which probably was due to higher partial pressure of hydrogen and also the variations in the density of supercritical ethanol and solubility of lignin. The oil fractions from non pre-sulfided and pre-sulfided NiMo tests at 310 ˚C were analyzed with GC-MS analysis. The identified monomers and the selectivity were very similar (shown in Appendix B, Table B1). We therefore, concluded that opposite to the tests at 260 ˚C, there was no effect in terms of the oil and solid yields at 310 ˚C over non pre-sulfided and pre-sulfided catalyst. However, the gas phase analysis indicated a major difference, where larger amount of gaseous products were formed for the pre-sulfided catalyst (shown in Figure 48). The concentration of ethane in the gas phase from the test using the pre-sulfided NiMo was more than twice of that in the gas phase from reaction over non pre-sulfided catalyst. A similar trend was observed for all gases except for C_2H_4, which was converted over the pre-sulfided catalyst to the alkane (C_2H_6). This was consistent with the rapid initial pressure increase over the pre-sulfided catalyst. This initial gas formation most likely occurred from the solvent and stopped when the catalyst surface was covered with the lignin decomposition products. For the non pre-sulfided catalyst, however, the sulfidation and initial lignin breakdown occurred simultaneously and therefore much less active free sites were available for solvent consumption in the early stages of the experiment.

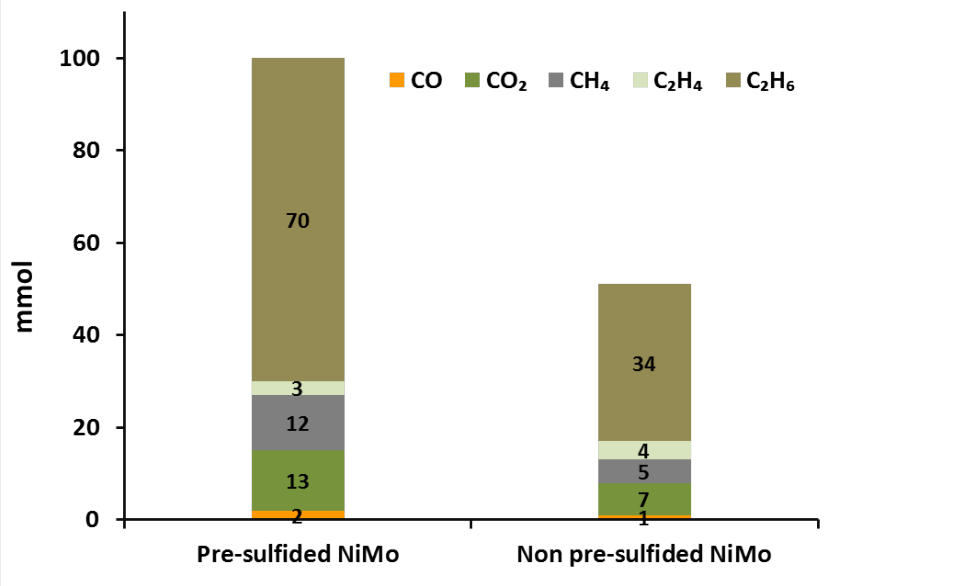

Figure 48 Gas phase analysis from conversion of H-LS over non pre-sulfided and pre-sulfided catalyst at 310 ˚C. Reaction condition: 0.5 g catalyst, 5 g H-LS, 50 ml ethanol. 26 bar H_2 (loaded at RT), 3 hours.

It is therefore suggested that at 310 ˚C, the *in-situ* sulfidation by sulfur present in H-LS is kinetically fast throughout 3 hours reaction time, and therefore pre-sulfidation has negligible effect on the liquefaction yields, while at 260 ˚C, the sulfidation is kinetically progressing with lower rates and therefore pre-sulfidation of catalyst is advantageous in increasing the oil yields. Hereafter, the catalytic experiments at 310 ˚C were conducted using NiMo-I catalyst without pre-sulfidation, unless specified.

The presence of sulfur source in catalytic conversions using NiMo and CoMo catalysts is required in order to keep catalyst activity. According to Mortensen et al. [102] when hydrodeoxygenation of phenol takes place, both H_2S and H_2O compete for the catalyst active sites [102] and in the absence of sulfur, the edge sulfur atoms can be replaced by oxygen. We assumed that instead of co-feeding a sulfur source, the sulfur present in the structure of lignin can keep sulfur vacant sites active. In a test, 1 ml of DMDS was added to the reactor for conversion of H-LS over pre-sulfided NiMo at 260 ˚C (Table 13, Entry 9), to ensure sufficient partial pressure of H_2S inside the reactor. Almost similar results to the test in the absence of DMDS were observed, which indicated that the sulfidation state of catalyst was kept by organic sulfur from lignosulfonate.

5.2. Parameter study

5.2.1. Effect of reaction temperature

The effect of reaction temperature on the degradation of H-LS was elaborated by expanding the reaction temperatures to 290 (Table 13, Entry 10) and 300 ˚C (Table 13, Entry 11). The catalysts for the tests at 290 and 300 ˚C were pre-sulfided to ensure catalytic activity. The oil and solid yields from conversion of H-LS and the atomic H/C and O/C ratios are shown

in Figure 49. The rise in oil yield, increase in H/C ratio and decrease in O/C ratio illustrate the increase in lignin degradation and hydrodeoxygenation reactions with increase in temperature. The partial pressures of CO and CO_2 in the gas phase from catalytic reaction at 260 ˚C were 1.08 and 1.7 bar, while at 310 ˚C the pressure were 1.4 and 2.3 bar, respectively, indicating the prominent role of temperature on cleavage of C-O bond, decarbonylation and decarboxylation. The oil yield increased relatively more when the temperature increased from 290 to 300 ˚C ($\Delta(\text{oil yield}/\Delta T) = 0.9$ wt%/℃). The temperature required for high rate of degradation and cleavage of stable C-C and C-O bonds depends on the type of biomass and treatment method. Yuan et al. [85] observed an increase of the depolymerization over 5% Ru/C in acetone for kraft lignin when the reaction temperature increased from 250 to 275 ˚C. However, they did not observe the same trend for organosolv lignin, as it originally had lower molecular weight distribution and much better solubility in ethanol at lower temperatures [85]. The increase of the oil yield from 300 to 310 ˚C occurred with slop of $\Delta(\text{oil yield}/\Delta T) = 0.5$ wt%/℃.

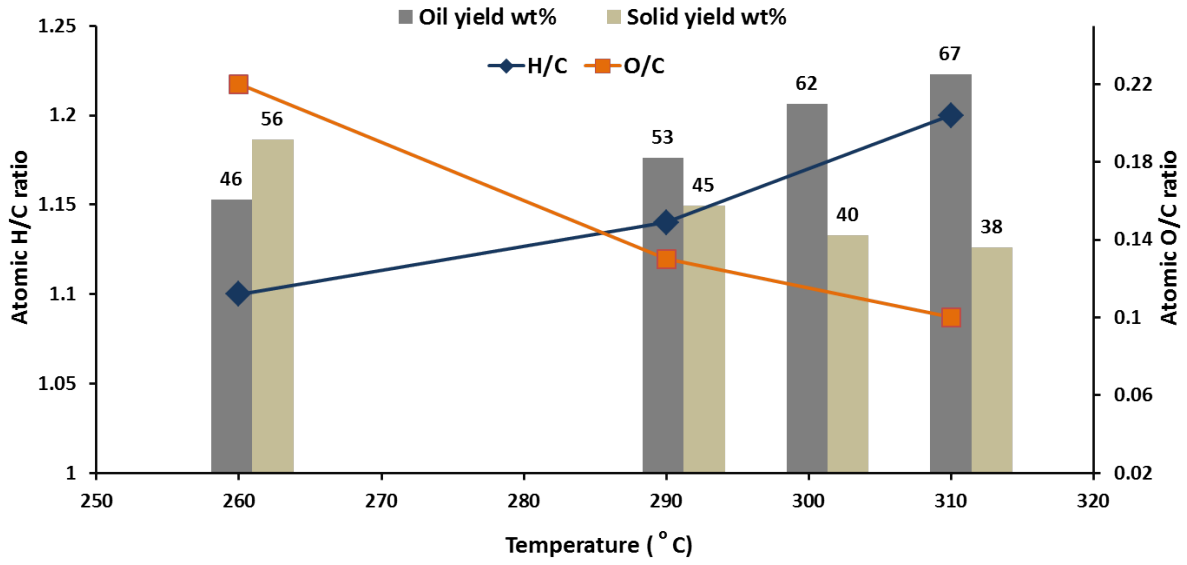

Figure 49 The oil and solid yields and atomic H/C and O/C ratios as function of temperature. Reaction condition: 1 g catalyst: 10 g lignin: 100 ml ethanol, 26 bar H_2 (loaded at RT), 3 hours.

Surprisingly, the SEC analysis of the oil fractions at 260 and 310 ˚C showed similar molecular weight distribution range (Shown in Appendix B, Figure B4). Though the oil yield obtained at 310 ˚C was higher than the yield at 260 ˚C, the degree of depolymerization is limited to the specific molecular weight distribution. These observations indicate that at higher temperatures more degradation occurred, however, the degradation progressed only to a certain size range centered in the dimer to oligomer range, and little degradation to monomers took place.

5.2.2. Effect of the reaction time

The effect of reaction time was studied by varying it from 1 to 4 hours at 310 ˚C (Table 13, Entries 12-14). The oil and solid yields from these tests are shown in Figure 50. The oil yield increased from 53 wt% after 1 h reaction time to 79 wt% after 4 h and the solid yield decreased from 49 wt% after 1 h reaction to 25 wt% after 4 h.

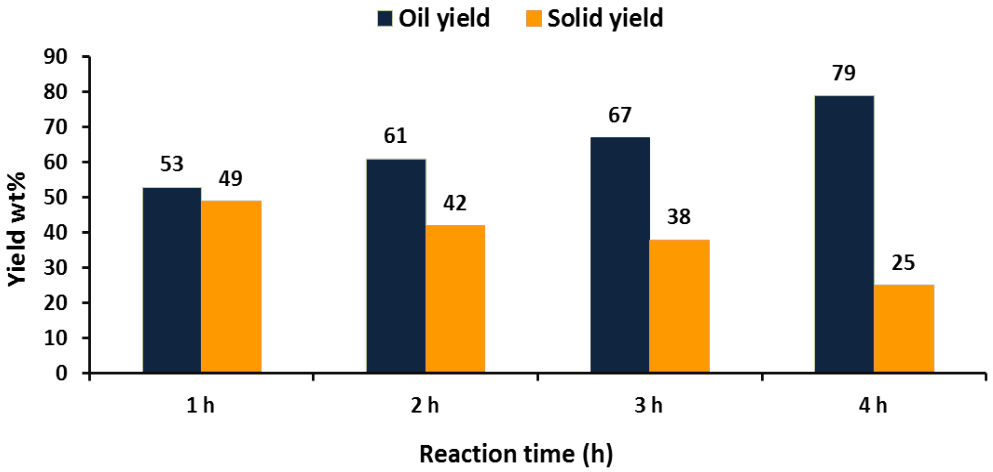

Figure 50 The oil and solid yields as a function of reaction time. Reaction condition: 1 g catalyst: 10 g lignin: 100 ml ethanol, 26 bar H_2 (loaded at RT).

The elemental analysis and the atomic O/C and H/C ratio in the oil fractions are presented in Table 16. The atomic O/C ratio gradually decreased by increasing the reaction time. The NMR analysis of the oil fractions indicated that demethoxylation occurred progressively (shown in Appendix B, Figure B5-B7). In addition, a gradual increase in the partial pressure of methane indicated that hydrogenolysis continued throughout the reaction. However, the decrease of methoxy groups levelled off after three hours. Decrease of γ-protons was observed for 3 hours, while it increased slightly after 4 hours, which might be due to uncertainties of the measurements. The gas phase analysis indicated that CO content was nearly constant in different reaction time and CO_2 content increased by increase of reaction time from 1 h to 2 h, but flattened by further increase of reaction time. This observation indicates that decarbonylation and decarboxylation reactions progressed in the early stages of the reactions. The sulfur content, determined by ICP analysis, decreased from 0.5 wt% after 1 h reaction to 0.1 wt% after 4 hours, which if compared to the lignosulfonate with 3.1 wt% sulfur content, indicates 97% sulfur removal in the oil fraction after 4 hours. This is expected since the NiMoS is an efficient HDS catalyst.

Table 16 Elemental analysis of the oil fractions from conversion of H-LS in different reaction time. Reaction condition: 1 g catalyst: 10 g lignin: 100 ml ethanol, 26 bar H_2 (loaded at RT).

Reaction time [h]	C wt%	H wt%	S wt%	O wt%	Atomic O/C	Atomic H/C	HHV (MJ/kg)
1	73.7	7.3	0.5	18.4	0.19	1.19	32.1
2	78.8	7.5	0.5	13.2	0.12	1.15	35.0
3	80.1	8.0	0.4	11.4	0.11	1.20	36.5
4	80.6	8.0	0.1	11.2	0.10	1.20	36.7

The oil fractions were analyzed by GC-MS. In the oil fraction from 1 h test, guaiacol and ethyl vanillate (shown in Figure 43, compounds no.1 & 4) were the main compounds detected which shared similarities with non-catalytic oil fraction. Almost similar compounds were detected in the oil fraction obtained after 2 hours. However in the oil from 3 hours reaction time, the guaiacol and ethyl vanillate peaks disappeared and instead, peaks corresponding to alkyl phenols, alkoxy alkyl phenol and alkoxy alkyl benzene were detected (Shown in Figure 43). Similar compounds were detected in the oil after 4 hours, indicating that demethoxylation and alkylation progressed over time. Narani et al. [32] observed that during conversion of kraft lignin, by prolonging the reaction time from 4 h to 8 h, guaiacol and substituted guaiacols transformed to alkyl phenols while the oil yield increased from 40 to 82 wt%. In our experiments 79 wt% oil is achievable with a considerably shorter reaction time of 4 hours and the oil is comprised mainly of alkyl phenolic and alkoxy alkyl benzene compounds.

The molecular weight distribution of the oil fractions after 2 ,3 and 4 hours reaction time indicated a similar pattern (detected by SEC analysis), while the oil fraction from 1 hour reaction time showed formation of slightly lower moleculare weight oil (shown in Appendix B, Figure B8). Similar to the observations on the reaction temperature, it was observed that the molecular weight distribution of the oil did not decrease by increasing the reaction time; further decrease of the molecular weight of the oil fraction may require more severe conditions compared to the employed condition.

5.2.3. Effect of the catalyst loading

The effect of catalyst mass was investigated by varying the loading of catalyst with a fixed amount of lignin (10 g). The solid and oil yields are shown in Table 13 (Entries 15-17). The oil yield increased from 57 to 88 wt% by increasing catalyst mass from 0.5 g to 2 g and the solid yield decreased from 47 wt% to 15 wt%. However, by increasing the catalyst mass from 2 g to 3 g no further increase of the oil yield was observed. At this stage, the conversion of the original lignin seems to have stopped and the remaining solid was likely a highly cross-linked char from e.g. repolymerization and therefore the oil yield did not change further as this solid could not be converted. The SEC analysis showed almost similar elution pattern, except for the oil from 0.5 g catalyst test. This phase was composed of smaller molecular weight fractions (shown in Appendix B, Figure B9). Similar to what was observed by increasing the reaction temperature and reaction time, further degradation of dimers and oligomers to monomers did not occur even with the highest catalyst loading. This supports the proposed mechanism for lignin degradation.

5.3. Catalyst reusability

Catalyst reusability is a critical factor for catalytic processes. The spent catalyst from catalytic conversion of H-LS was mixed with solid char residue. Separation of the catalyst from the char was not possible; therefore, we used the entire solid residue fraction from a standard reaction experiment (Table 13, Entry 1) as a catalyst for a subsequent experiment, without any pretreatment. The oil yields decreased slightly from 67 wt% to 65 wt% and 61 wt%, by reusing catalyst for the first and second time (Table 13, Entry 18-19) which may be due to the loss of catalyst in workup procedure. Moreover, coke may have formed on the catalyst. Considering the reasonably high oil yields, it was concluded that catalyst is reusable for at least two times without any pretreatment.

5.4. Ethanol consumption

Lignin degradation via ethanolysis (or generally solvolysis) may be economically favorable if solvent can be conserved and recycled. Solvent consumption in lignin solvolysis is rarely discussed in the literature. Recently, Nielsen and co-workers [148] elaborated on solvent consumption in un-catalyzed conversion of biorefinery lignin using methanol, ethanol, propanol and butanol as solvent. Along with the reactions for stabilizing the lignin fragments, ethanol may react with itself to higher alcohols, esters, aldehydes, ethers and hydrocarbons [77], undergo self-condensation reactions to form light fractions and degrade to gaseous compounds [148]. The incorporation of ethanol to aromatic compounds is favorable in a sense that it increases the energy density of the oil fraction. Ma et al. [35] observed 164 wt% oil yield from ethanolysis of kraft lignin over α-MoC_{1-x}/AC at 280 ˚C, which indicated considerable ethanol incorporation.

In order to evaluate solvent consumption to the light and gas phases, a non-catalytic and a catalytic control test in the absence of lignosulfonate at 310 ˚C was conducted and the light and gas phases were compared. The detail of the gas phase analysis is shown in the Appendix B, Table B2. It was observed that in the non-catalytic ethanol control test and lignin test, 3 and 12 mmol C_2^+ gases (mainly C_2H_6 but also including C_2H_4, C_3H_6, C_3H_8 and n-C_4H_{10}) were formed, indicating that both solvent decomposition and hydrogenolysis of C-C bonds of alkyl side chains in lignosulfonate contribute to formation of them. The same trend was observed for CO, CO_2 and CH_4. However, it was not possible to distinguish the degree of conversion of lignin and solvent individually. The formation of gaseous compounds in the presence of catalyst increased considerably. The light phases from control and lignin tests were analyzed with GC-MS. The water content in the light phases was determined using Karl-Fischer titration and the quantities of ethanol and light fractions were determined based on GC areas and considering the water content in each sample. Similar to the gas composition, distinguishing between water produced from deoxygenation of lignin fragments and ethanol conversion was not possible. The detail of the identified and quantified compounds in the light phases is shown in Appendix B, Table B3.

The ethanol consumption is evaluated by considering the conserved ethanol amount, the yields of water and light products in the light phase and yield of gas phase and comparing to the initially loaded ethanol. A mass loss was observed that may be due to deposition of light phases in the internal walls of the setup overhead. The degradation of lignin to gas and light phases and formation of water from deoxygenation of lignin were neglected. The content of each fraction is shown in Figure 51. It was observed that in the presence of lignin, ethanol was partially converted to the light products, water and gas phase. Further process optimizations such as initial ethanol loading are required to decrease the extent of ethanol consumption for the economy of the process. Noticeably, ethanol consumption was considerably higher in the absence of lignin, which indicated that referring to the control tests is not accurate enough for evaluation of solvent consumption in lignin conversion processes. The presence of lignin therefore inhibited the consumption of ethanol to some extent. The coverage of catalyst active sites by lignin degradation products was most probably the reasons for the lower consumption of ethanol in the presence of lignin, which is desirable as it inhibits solvent loss to gaseous or light fractions.

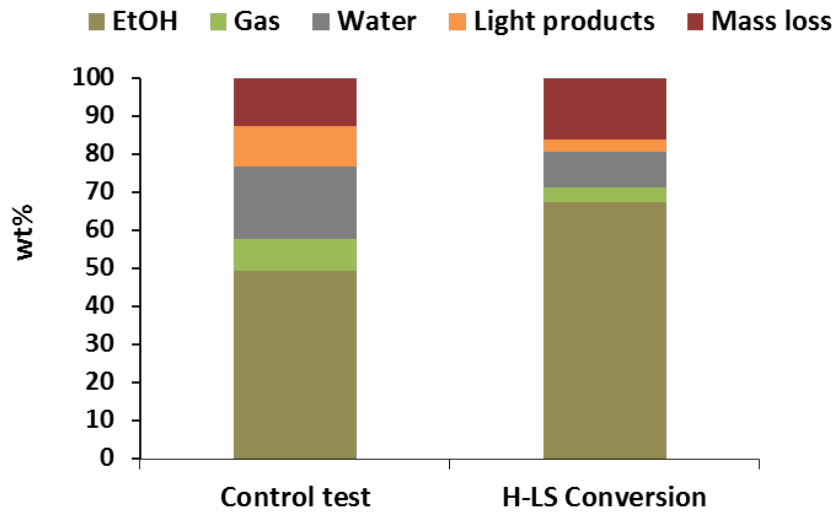

Figure 51 The ethanol content and the yields of gas, water and light products based on the initial ethanol loading for ethanol control test and lignin conversion at 310 ˚C. Reaction condition: 1 g catalyst: 0/10 lignin: 100 ml solvent, 26 bar H_2 (loaded at RT), 310 ˚C, 3 hours.

Conclusion

Lignosulfonate was successfully degraded in the presence of alumina supported NiMo catalyst at temperature ranges of 260-310 ˚C in ethanol. The presence of catalyst resulted in a considerable increase of the liquefied fractions, which is attributed to stabilization of reactive compounds with reductive ethanol incorporation over catalytic sites. 67 wt% oil yield was obtained from conversion of H-LS at standard reaction condition at 310 ˚C (1 g catalyst: 10 g lignin: 100 ml solvent, Initial H_2 loading of 26 bar, 3 hours). It was observed that at 310 ˚C, *in-situ* activation by formation of the more active sulfide NiMoS catalyst was achievable by deposition of sulfur from the lignosulfonate. However, pre-sulfidation of the catalyst is required at lower temperatures e.g. 260 ˚C. The yield of liquefied fraction increased to 88 wt% from conversion by doubling the catalyst loading at 310 ˚C. The reusability of the catalyst with only a minor loss in the oil yield without any pretreatment was confirmed for at least two times. Ethanol was partially consumed in the solvolysis process via incorporation to the reaction products, which is favorable, and unfavorable conversion to light products and gaseous fractions, which is undesirable.

Acknowledgement

NMR Center at Chemistry department, DTU is acknowledged for access to the 400 MHz spectrometer. Providing the catalyst support material by Saint Gobain is appreciated.

Chapter 6:

Catalytic conversion of beech wood and organosolv lignin over $NiMo/Al_2O_3$

6. Catalytic conversion of beech wood and organosolv lignin over $NiMo/Al_2O_3$

Early-stage catalytic conversion of lignin is a method based on mild liquefaction of lignin to a handful of chemicals while leaving the holocellulose nearly unchanged [10], [43], [149]. Lignin in birch sawdust was successfully fractionized to 4-propyl guaiacol and 4-propyl syringol with total monomer yield of 52% at 250 ˚C in methanol over a Ru/C catalyst in the presence of hydrogen [43], while conversion of the same biomass over Pd/C and Ni/Al_2O_3 led to formation of 4-propanol guaiacol and 4-propanol syringol [41], [113]. The solvent was greatly involved in lignin fragmentation and depolymerization while the catalyst was mostly responsible for stabilization of reactive fragments via hydrogenation of unsaturated side chains [113]. Similarly, solvent assisted one-pot catalytic conversion of whole biomass to monomers and light hydrocarbons was recently studied [79], [115], [120]. Using the one-pot conversion method, a conversion of 28 wt% was reported from conversion of birch wood over $Pt/NbOPO_4$ catalyst in cyclohexane at 190 ˚C, with the formation of alkyl cyclohexane, pentane and hexane as products derived from lignin, hemicellulose and cellulose [119]. The role of the catalyst was to perform HDO of the fragments released into the solvent [119].

The results of one-pot conversion of beech wood and evaluation of the effect of reaction temperature from 200 to 300 ˚C are presented in this chapter. The conditions were selected to convert only the lignin and altered to convert all the biomass constituents and obtain high overall conversion of the biomass. A commercial $NiMo/\gamma\text{-}Al_2O_3$ catalyst was used with ethanol as solvent and in presence of hydrogen, with the aim to obtain both degradation and hydrodeoxygenation. The direct conversion of the lignin in whole biomass to lignin monomers was compared with a two-step procedure involving organosolv extraction of the lignin and subsequent catalytic conversion.

6.1. One-pot conversion of beech wood

One-pot conversion of raw beech wood in ethanol over commercial sulfided $NiMo/\gamma\text{-}Al_2O_3$ catalyst at 300 ˚C resulted in 99 wt% conversion of the biomass. 44 wt% liquefied heavy phase (oil) was obtained which was mainly composed of lignin degradation fractions and some compounds originating from cellulose and hemicellulose. The lignin content was selectively fractionized to 4-propyl guaiacol (PG) and 4-propyl syringol (PS), accompanied by formation of 4-ethyl guaiacol, 1,2,3-trimethoxy-5-methyl, benzene and 5-sec-butyl-1,2,3-benzenetriol, with the total monomer yield of 18.1 wt% (shown in Table 17, Entry 1). Formation of substituted syringol and guaiacol species are expected as beech wood lignin is mainly composed of guaiacyl and syringyl units (G and S unites) [47] connected mostly via β-O-4 bonds. The light fraction contained compounds from holocellulose; the hemicellulose and cellulose were mainly converted to C5-C6 ketones and furans from cleavage of glucoside bonds and also were converted to ethers and ester from reaction of holocellulose originating compounds with the ethanol (the identified compounds are presented in Appendix C, Table C1).

The lignin derived monomers can directly be used as chemicals, or alternatively, be upgraded via reactions such as functionalization and conversion to compounds such as aromatic amines [118]. The light products from the holocellulose fraction may be used as a fuel additive, or upgraded by hydrodeoxygenation. Our results are considerably different from previous results in the literature [150]. Grilc et al. [150] reported about 25% unconverted wood from conversion of 20 g beech sawdust in 80 g tetralin in a slurry reactor over 2 g sulfided $NiMo/Al_2O_3$ under 50 bar hydrogen pressure at a constant gas flow of 1 NL/min at 300 ˚C in 60 min. The researchers reported that by further increasing the temperature to 350 ˚C and reaction time up to 160 min, the content of insoluble residue (containing char) increased to 20 wt% [150], while in our process no char was formed and almost full conversion of biomass was obtained within 3 hours. According to Grilc et al. [150], the increase of the insoluble residue simultaneously occurred with decrease of hydrodeoxygenated oil products, suggesting that the oil fraction was the precursor of the charring. In the literature, char formation is attributed to the condensation reactions of insolubilized carbohydrates [151], which compete with wood liquefaction. The difference between our results and the literature [150] highlights the superior performance of ethanol in solubilization of aromatic monomers and carbohydrate fractions possibly via end-capping the radicals fragments by esterification. Moreover, cleavage of C-O bonds by ethanolysis and subsequent etherification may explain our char free products [148]. Consistent results were observed by duplication, which supported the reproducibility of the results.

The role of the catalyst was evaluated by conversion of beech wood in the absence of catalyst. A high conversion of 86 wt% was obtained in the non-catalytic condition (Table 17, Entry 2), indicating that liquefaction of lignin and degradation of holocellulose was nearly independent of the catalyst. The unconverted biomass was possibly constituted of cellulose. Amongst biomass constituents, cellulose is the most difficult to degrade owing to its crystalline structure [79]. In the absence of catalyst, complete degradation of holocellulose in ethanol requires a temperature of 350 ˚C [114]. An oil yield of 50 wt% was obtained in the absence of catalyst with monomer yield of 10.8 wt%. Compared to the non-catalytic condition, hydroxyl groups in the light products were removed in the presence of a catalyst; compounds such as propanoic acid, 2-hydroxy-ethyl esters and butanoic acid, 2-hydroxy ethyl ester were transformed to propanoic acid ethyl ester and butanoic acid ethyl ester in the presence of catalyst.

Table 17 The conversions, oil and solid yields and the yields of the monomers in the oil fractions from conversion of beech wood at 300 ˚C. 0/1 g $NiMo/Al_2O_3$ catalyst: 10 g beech wood, 100 ml ethanol, 26 bar H_2 (loaded at RT), 3 hours.

Entry	Catalytic/ Non-catalytic	Conversion wt%	Oil yield wt%	Solid yield wt%	Monomer yield wt%		
					PG	PS	Total
1	Catalytic	99	44	1	5.6	8.7	18.1
2	Non-catalytic	86	50	14	1.4	3.7	10.9

The SEC analysis of the oil fractions from non-catalytic and catalytic conversions are shown in Figure 52. The retention time ranges corresponding to the elution of 4-propyl guaiacol and tannic acid are shown for comparison. The largest peak in the oil from catalytic conversion

of beech wood was within the retention time of 4-propyl guaiacol. This indicates that the catalytic oil was mainly comprised of compounds within the size range of monomers and dimers. The SEC of the non-catalytic oil showed greater amount in the left shoulder, indicating that this oil fraction contained higher molecular weight compounds compared to the catalytic oil. Considering that fractionation of lignin occurs even in the absence of catalyst, next to the higher yield of monomers and the lower molecular weight of the aromatic compounds in the catalytic oil, it is suggested that the catalytic role is prominent in stabilization of lignin derived fragments and inhibiting condensation reactions [113]. Moreover, the high conversion of beech wood of 99 wt% over the catalyst may be due to a synergistic effect of the *in-situ* produced water from HDO reactions and its interactions with carbohydrates (8.7 g water was detected in the light fraction from catalytic conversion at 300 ˚C). Higher conversion of biomass in the presence of water as an additive is reported [116], [151]: Water provides better interaction with wood components and transfers solvent to the structure of holocellulose, which results in increased conversion rate of biomass. While about 10% unconverted wood was reported from conversion of pine wood in guaiacol medium at 310 ˚C, less than 5% solid residue was obtained by conversion in guaiacol/water (8:1 w/w) solution [151], which supports the role of water in solubilization and hydrolysis of biomass.

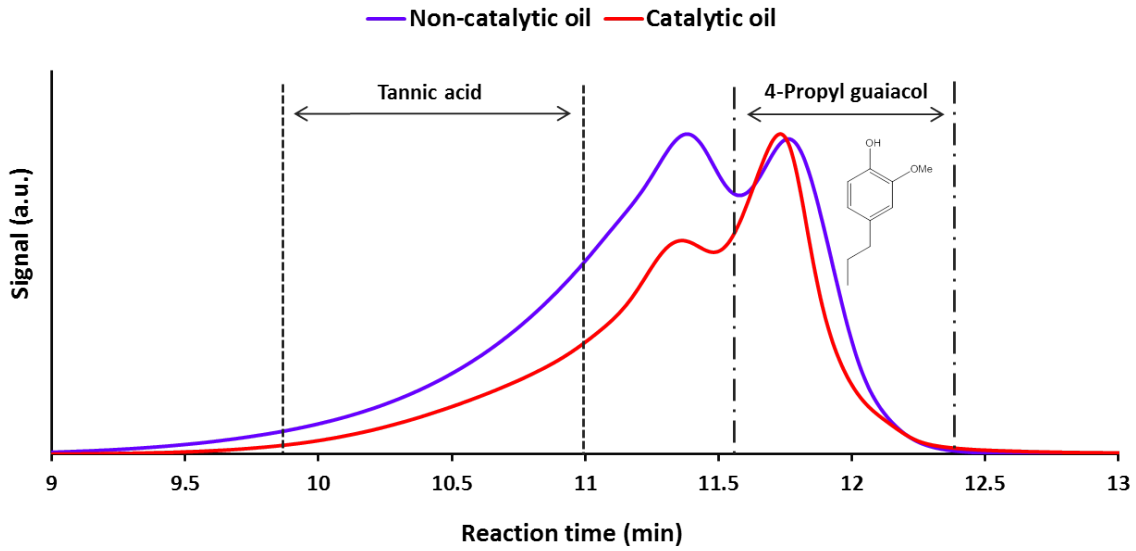

Figure 52 SEC of the oil fractions from non-catalytic and catalytic conversion of beech wood in ethanol medium at 300 ˚C. 0/1 g $NiMo/Al_2O_3$ catalyst, 10 g beech wood, 100 ml ethanol, 26 bar H_2 (loaded at RT), 3 hours.

6.1.1. Effect of the reaction temperature

The effect of reaction temperature on the degradation of biomass constituents was studied by catalytic conversion of beech wood at 200, 260 and 280 ˚C, and the results were compared

with those at 300 ˚C. The conversions, oil and solid yields and the yields of the lignin derived monomers (based on Klason lignin) at different reaction temperatures are shown in Table 18. In these experiments the sum of the yields of light products, water and gas were determined by difference (light phase). By increasing the temperature from 200 ˚C to 300 ˚C, the conversion increased from 21 wt% to 99 wt% (Table 18). The solid phases retrieved after each test possessed a fibrous texture at 200, 260 and 280 ˚C indicating that the wood structure was preserved to some extent. The solid yield decreased significantly when raising the temperature from 260 to 280 ˚C. The oil yields increased from 20 wt% at 200 ˚C (corresponding to a lignin conversion of 99 wt%, if only Klason lignin is converted) to 44 wt% at 300 ˚C. On the other hand, the yields of light products, water and gas phases increased from 1 wt% to 55 wt% by increasing the temperature from 200 to 300 ˚C. The increase in the yield of light, water and gas is mainly due to conversion of ethanol, increased thermal cracking of carbohydrates, increased HDO reactions and formation of gaseous compounds. The evolution of oil and light fractions are elaborated below.

Table 18 The conversions and the yields of oil, solid and light phase and monomers from conversion of beech wood over $NiMo/Al_2O_3$ at different reaction temperatures. 1 g catalyst: 10 g beech wood, 100 ml ethanol, 26 bar H_2 (loaded at RT), 3 hours.

Entry	T [˚C]	Conversion wt%	Solid yield wt%	Oil yields wt%	Light phase wt%*	Monomer yield wt%			PS/ PG
						PG	PS	Total	
1	200	21	78	20	1	1.0	2.2	12.1	2.2
2	260	51	49	29	22	5.6	11.3	20.0	2.0
3	280	87	14	41	46	5.4	9.8	18.8	1.8
4	300	99	1	44	55	5.6	8.7	18.1	1.5

* Light phase: Light products + water + gas

6.1.1.1. Degradation of lignin

The total lignin content of the investigated beech wood is 23.9 wt%. However, the observed oil yields increased up to 44 wt% at 300 ˚C, indicating that degradation products from holocellulose fraction were also present in the oil. Thus, comparing the degree of degradation of lignin based on the oil yields is not realistic. We, therefore, considered the monomer yields as a mean of comparison for lignin degradation. The lignin degradation to monomers increased by increasing the reaction temperature from 200 ˚C to 260 ˚C. The total monomer yield increased from 12.1 wt% at 200 ˚C to 20.0 wt% at 260 ˚C, while it slightly decreased to 18.8 and 18.1 wt% at 280 and 300 ˚C, respectively. These results suggest that lignin is extracted from holocellulose at lower temperature of 200 ˚C. However, major degradation to monomers requires higher temperature evidenced by the highest monomer yield at 260 ˚C. The results indicate that an optimum monomer yield may be obtainable between 200-260 ˚C. This is aligned with the observations of Schutyser et al. [41] where the monomer yields (relative to maximum possible monomer yield, see ref [41] for details) from conversion of birch sawdust in methanol increased from nearly 30% at 200 ˚C to almost 50% at 250 ˚C over Pd/C catalyst and 3 hours reaction time with catalyst: biomass: solvent ratio of 0.2 g: 2 g: 40 ml. At higher temperature of 280 and 300 ˚C, general degradation of hemicellulose and cellulose occurred,

which is consistent with the increase in formation of light products, water and gaseous compounds with increase of reaction temperature.

The ratio of sinapyl: coniferyl: coumaryl alcohol units in beech wood was estimated 40: 56: 4 [152], [153]. However, we observed higher yields of 4-propyl syringol compared to 4-propyl guaiacol in all the oil fractions. Noticeably, the ratio of PS to PG content decreased from 2.2 at 200 ˚C to 1.5 at 300 ˚C, converging towards the theoretical S/G. Compared to coniferyl alcohol units, sinapyl alcohol are more involved in formation of β-O-4 linkages, while coniferyl alcohol units form more C-C bonds than sinapyl alcohol units [7]. Therefore, the decrease of S/G by increase of reaction temperature may be attributed to the cleavage of more stable bonds such as C-C bonds attached to the coniferyl alcohols.

The formation of PG and PS compounds is attributed to cleavage of prevalent β-O-4 bonds. Zhang et al. [91] proposed that cleavage of a β-O-4 over sulfided NiMo occurs via removal of the hydroxyl group from C_α position on the catalyst acid sites followed by formation of a radical intermediate and subsequent hydrogenolysis of the C-O bond. The catalytic cleavage of bonds is expected to occur on thermally liquefied fragments as solid-solid interactions between biomass and catalyst is not expected. The obtained propyl substituted products in our study seem to support the pathway proposed by Zhang et al. [91] (Figure 53). The GC-MS analysis of the oil from reaction at 200 ˚C indicated the presence of phenol 2-methoxy-4-(2-propenyl) and phenol, 2, 6-dimethoxy-4-(2-propenyl) compounds with rather high quantities (monomer yield of 8.9 wt%). However, these compounds disappeared by increase of the reaction temperature to 260 ˚C, indicating that saturation of alkyl side chains of the aromatics took place at higher temperatures.

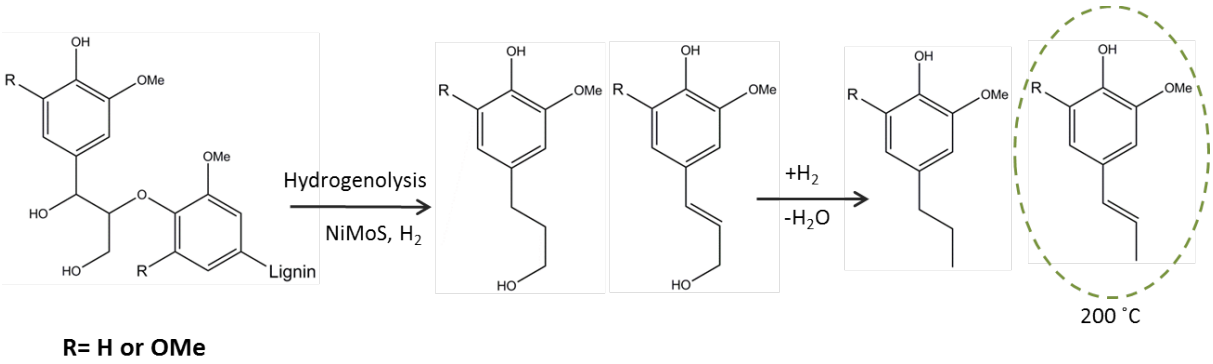

Figure 53 Proposed mechanism [91] for cleavage of β-O-4 bonds present in the structure of beech wood lignin over sulfided NiMo/Al_2O_3 (NiMoS) catalyst at 200-300 ˚C.

In order to assess the quality of the oil phases and evaluate the degree of hydrodeoxygenation, elemental analysis was conducted. The detailed elemental analysis is presented in Table C2, Appendix C. 2.7 wt% sulfur was detected in the oil fraction obtained at 200 ˚C, which is attributed to the contamination from DMDS derived products. The sulfur content further decreased to 1.3 and 1.0 wt% at 260 and 300 ˚C, which is consistent with the increased oil yields at higher temperatures. No sulfur was detected in the oil at 280 ˚C, most probably due to the measurement errors. The representative Van Krevelen diagram is shown

in Figure 54 and the atomic O/C and H/C ratio of beech wood is shown for comparison. Deoxygenation and hydrogenation is observed in the oil fractions: Lower atomic O/C and slightly higher H/C ratio was observed in the oil fraction at 200 ˚C compared to the catalytic oil at 260˚ C, perhaps due to co-presence of holocellulose derived compounds in the oil from 260 ˚C. Slightly higher atomic H/C ratio was observed in the oil obtained at 280 ˚C compared to the oil at 300 ˚C, possibly due to the analysis uncertainties. The greatest HHV of 27.4 MJ/kg (using Dulong formula [134]) was determined for the oil from 280 ˚C.

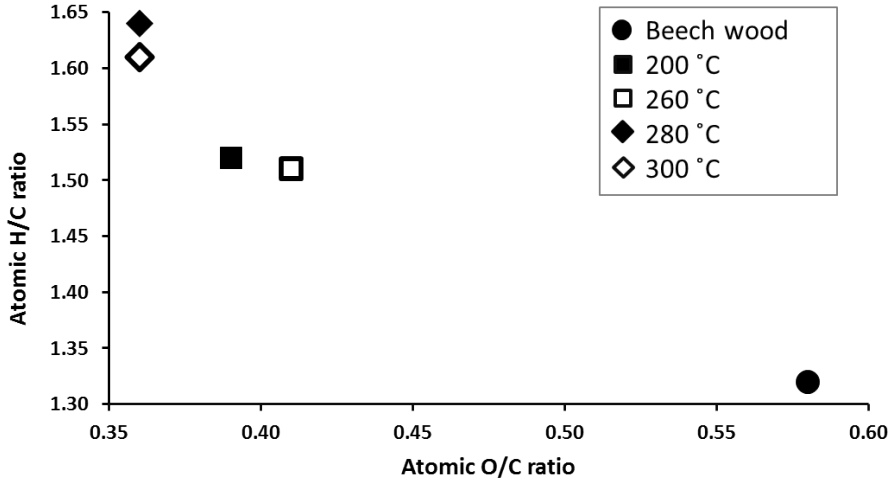

Figure 54 Van Krevelen diagram representing atomic H/C and O/C ratio of beech wood and the oil fractions from conversion of beech wood over sulfided $NiMo/Al_2O_3$ at different reaction temperatures. 1 g catalyst: 10 g beech wood, 100 ml ethanol, 26 bar H_2 (loaded at RT), 3 hours.

6.1.1.2. Light fraction and degradation of cellulose and hemicellulose

The light phase obtained at each reaction temperature was comprised of ethanol, light products (see Table C1 in Appendix C) and water. Ethanol was partially consumed during the reaction and also degraded to the light products and gaseous compounds. The light products in each experiment were therefore products coming from holocellulose and solvent. The content of ethanol, water and light products and the percentage of converted ethanol based on ethanol input at each temperature are summarized in Table 19. Ethanol was the dominating product in the light fraction at all temperatures, but its concentration decreased progressively from 98.0 wt% at 200 ˚C to 77.6 wt% at 300 ˚C, associated with formation of light products and water formation from hydrodeoxygenation and ethanol dehydration reactions. Noticeably, ethanol was a stable solvent at 200 ˚C and even 260 ˚C with ethanol conversion being 0.3 and 4.3 wt%, respectively, while its conversion increased to 11.1 and 18.5 wt% at 280 and 300 ˚C. Conversion of solvent is of economical concern and with ethanol conversions obtained at different reaction temperatures, the lower temperatures of 200 and 260 ˚C are favored for solvent conservation.

Table 19 The content of ethanol, water and light products in the light fractions from converison of beech wood and ethanol conversion over sulfided $NiMo/Al_2O_3$ at different reaction temperatures. 1 g catalyst: 10 g beech wood, 100 ml ethanol, 26 bar H_2 (loaded at RT), 3 hours.

T (˚C)	200	260	280	300
Water wt%	1.9	5.0	8.5	10.6
Light products wt%	0.1	2.2	6.7	11.8
Ethanol wt%	98.0	92.8	84.8	77.6
Ethanol conversion wt%	0.3	4.3	11.1	18.5

Some of the light compounds such as furans and cyclopentane originated from biomass only, while compounds like esters and alcohols were products of both ethanol and holocellulose fractions. Blank experiments without wood at 280 and 300 ˚C indicated that ethanol reacted more severely in the absence of biomass. In the presence of biomass, the biomass degradation products probably cover the catalyst active sites, partially, and hinder the ethanol degradation. Thus, using the blank tests results as a mean to distinguish and quantify the biomass and ethanol conversion products does not provide the correct picture. The yields of a few compounds that were solely products of biomass conversion are presented in Table 20 for evaluation of cellulose and hemicellulose conversions. The yields were determined based on the sugar content in the biomass. The structure of the compounds is shown in the Appendix C, Figure C2.

Table 20 The yields of the sugar derived compounds from conversion of beech wood over sulfided $NiMo/Al_2O_3$ at different reaction temperatures. 1 g catalyst: 10 g beech wood, 100 ml ethanol, 26 bar H_2 (loaded at RT), 3 hours.

Compound	200 ˚C wt%	260 ˚C wt%	280 ˚C wt%	300 ˚C wt%
Ketones				
2-Pentanone	0.00	0.18	1.43	2.47
2-Octanone	0.00	0.00	0.00	0.39
2-Methyl cyclopentanone	0.01	0.20	1.48	2.16
2-Ethyl cyclopentanone	0.00	0.05	0.78	1.11
Furan				
Dimethyl furan	0.08	0.17	0.83	2.84
Ester				
Pentanoic acid ethyl ester	0.00	0.26	1.16	1.47
Ether				
2-Ethoxypentane	0.00	0.00	0.11	0.58
Alcohol				
1-Nonanol	0.00	0.00	0.19	0.77

The formation of the selected compounds was very limited at 200 ˚C, indicating that at this temperature most of the cellulose and hemicellulose fractions were conserved. A 20 wt% oil yield was obtained at this temperature, which is consistent with the lignin content of the biomass (20.9 wt% Klason lignin) and with solid residue yield of 78 wt%. Considering the very low yields of sugar derived fractions, the oil fraction is expected to be mostly lignin derived products. However, by increasing the reaction temperature to 260 ˚C, 2-pentanone, 2-ethyl cyclopentanone, and pentanoic acid ethyl ester were formed and concentration of 2-methyl

cyclopentanone and dimethyl furan increased, indicating degradation of the holocellulose fraction. At 280 ˚C, 2-ethoxy pentane and 1-nonanol were also detected. 2-octanone was only detected at 300 ˚C. The yield of 2-pentanone, 2-methyl cyclopentanone and dimethyl furan reached over 2 wt% at 300 ˚C. These results confirm that by increasing the reaction temperature the holocellulose fractions were converted to the valuable light products and partially to the gaseous compounds.

Formation of gaseous compounds increased by increase of reaction temperature; 0.31, 0.96, 1.84 and 2.62 g gas was determined from reactions at 200, 260, 280 and 300 ˚C (shown in Figure 55). The gas phase at 200 ˚C was mainly comprised of hydrogen; however, by increasing temperature to 260 ˚C, the content of C_2H_4, C_2H_6, CO and CO_2 gases increased. The formation of CO and CO_2 is attributed to the removal of carbonyl and carboxyl groups, respectively, while formation of C_2H_4 and C_2H_6 were most likely due to degradation of solvent and light products and possibly to a less extent via cracking reactions of the side chains of the biomass constituents.

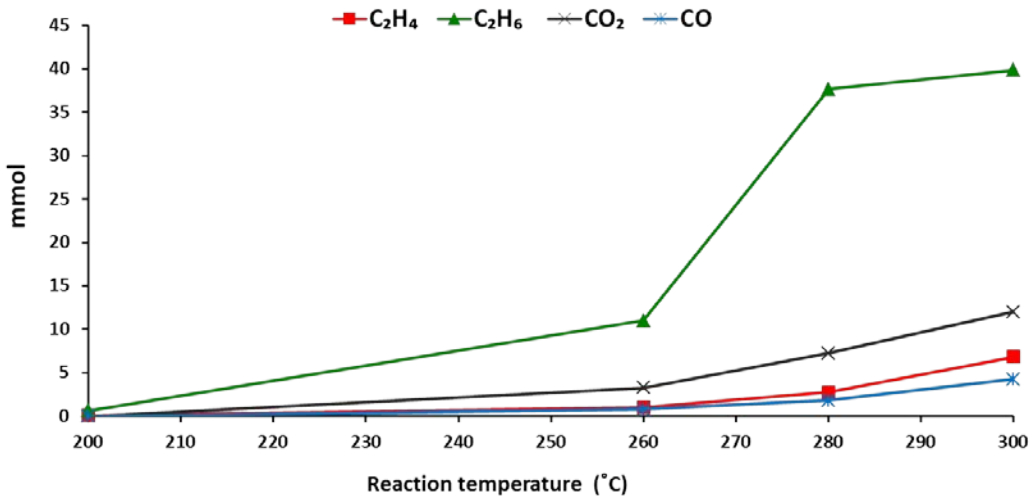

Figure 55 The main compounds in the gas phase from conversion of beech wood over sulfided $NiMo/Al_2O_3$ over different reaction temperatures. 1 g catalyst: 10 g beech wood, 100 ml ethanol, 26 bar H_2 (loaded at RT), 3 hours.

The evaluation of oil, light and gaseous fractions indicate that at 200 ˚C, ethanol and holocellulose are conserved and mainly lignin is converted. This reaction temperature can be employed if the ECCL strategy is of interest. However, the lower yield of monomers compared to the higher temperatures indicated that this temperature was not sufficient for obtaining high monomer yields. By further increasing the reaction temperature, the yield of lignin derived monomers increased and cellulose and hemicellulose conversion was observed. Considering the significant increase in conversion between 260 and 280 ˚C (51 and 87 wt%) and the gas formation within the same temperature range, it is assumed that this temperature range is necessary for carbohydrates constituents degradation. Our method is versatile for either ECCL at temperatures between 200 and 260 ˚C, with the highest monomer yield, or full conversion

of biomass at 300 ˚C with a total oil yield of 44 wt% containing 29.6 wt% oxygen. The oil fraction should however be deoxygenation and desulfurization for applications such as fuels.

6.2. Direct conversion of beech wood vs. organosolv pretreatment and lignin conversion

Organosolv is a pretreatment method where sulfur free and comparatively low molecular weight lignin is obtained while the remaining pulp is a good feedstock for enzymatic processes [7]. The lignin obtained by organosolv treatment is relatively pure compared to the other types of technical lignin [154]. In order to assess the susceptibility of organosolv lignin to conversion to liquid products and compare it with direct conversion of raw biomass, organosolv lignin was extracted. The organosolv lignin however had a carbohydrate impurity of 27.5 wt%.

In the absence of catalyst, a conversion of 62 wt% was observed with an oil yield of 41 wt%. In the presence of catalyst, almost complete conversion of organosolv lignin was achieved at 300 ˚C, with an oil yield of 86 wt% and a solid yield of 2 wt%. The high conversion indicates that the lignin produced in organosolv treatment is degradable under the catalytic reaction conditions. However, a low monomer yield of 4.3 wt% was detected in the oil phase. The main identified compound was mainly PS with a yield of 2.3 wt%, which was significantly lower than the yield in the direct conversion of biomass (8.7 wt%). Despite high conversion of organosolv lignin, the molecular weight distribution of the oil showed that its degree of depolymerization was considerably lower than the oil from direct conversion of beech wood (see Figure 56). The molecular weight distribution of organosolv lignin is shown for comparison. The physical appearance of the oil fraction obtained from direct conversion of biomass also showed a better fluidity, which is aligned with the lower molecular weight of the oil fraction.

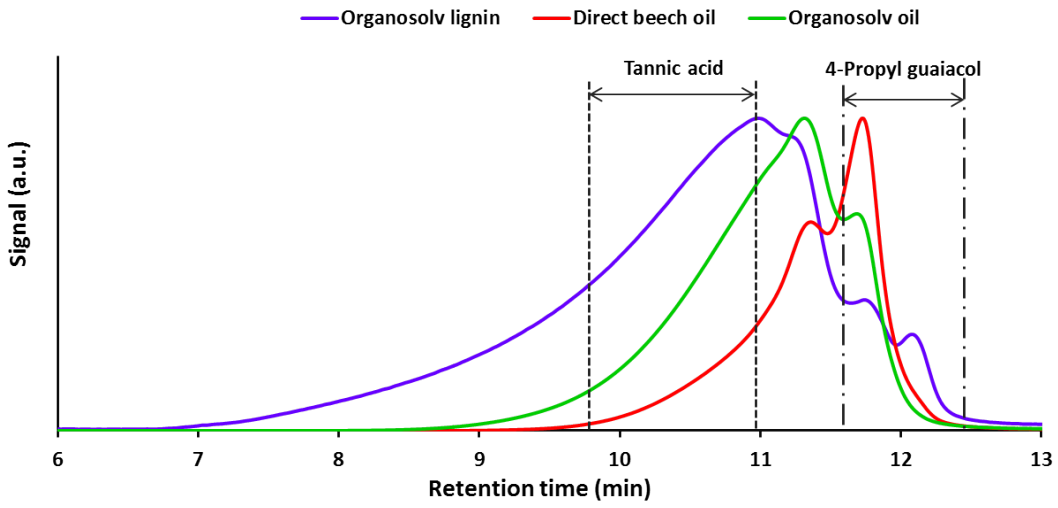

Figure 56 SEC of organosolv lignin and the oil fractions from direct conversion of beech wood and organosolv lignin over sulfided $NiMo/Al_2O_3$ at 300 ˚C. 1 g catalyst: 10 g feedstock, 100 ml ethanol, 26 bar H_2 (loaded at RT), 3 hours.

The HSQC NMR of organosolv lignin and the oil fractions from conversion of organosolv lignin and direct conversion of biomass (at 300 ˚C) were acquired for evaluation of the

chemical units present. The representative C and H signals of interconnecting β-O-4, phenylcoumaran (containing β-5 and α-O-4 bonds) and resinol (containing β-β and γ-O-α bonds) were determined according to the literature [135], [146], [155], [156]. The HSQC NMR of the aliphatic side in organosolv lignin (shown in Figure 57, a) indicated the presence of β-O-4 bonds with both G and S units (Aα: 4.82/71.9 ppm, Aβ: 4.09/85.9 ppm), phenylcoumaran units (Bα: 5.43/86.9 ppm, Bβ: 45/53.1 ppm) and resinol units (Cα: 4.63/84.9 ppm, Cβ: 3.03/53.5 ppm, Cγ: 3.76/71.0 ppm) and methoxy groups (3.75/56.2 ppm). Both G and S units were detected in the aromatic side of organosolv lignin (Figure 57, b). However, these units disappeared in the HSQC-NMR of the oil fractions from conversion of organosolv lignin (Figure 57, c) and beech wood (Figure 57, d), indicating that β-O-4 bonds were fully broken under the employed reaction conditions, with the possibility of cleavage of phenylcoumaran and resinol units, as depolymerization of these units requires cleavage of both C-O and C-C bonds [116]. The signals corresponding to methoxy groups were considerably lower in the oil fractions indicating HDO activity of the sulfided NiMo catalyst, as expected [102]. Despite removal of β-O-4 bonds in the oil fractions, the formation of larger molecular weight oil from organosolv lignin compared to the oil from direct conversion of biomass was most probably due to the presence of stable C-C bonds, possibly formed by transformations that the native lignin experienced during extraction via organosolv treatment. Our results are aligned with those from Sun et al. [118] where lower monomer yields and higher yields of oligomers were observed from conversion of organosolv lignin compared to conversion of biomass over Cu_{20}-PMO catalyst at 180 ˚C. Therefore, we conclude that direct conversion of biomass is promising compared to conventional pretreatment of biomass and subsequent conversion of lignin.

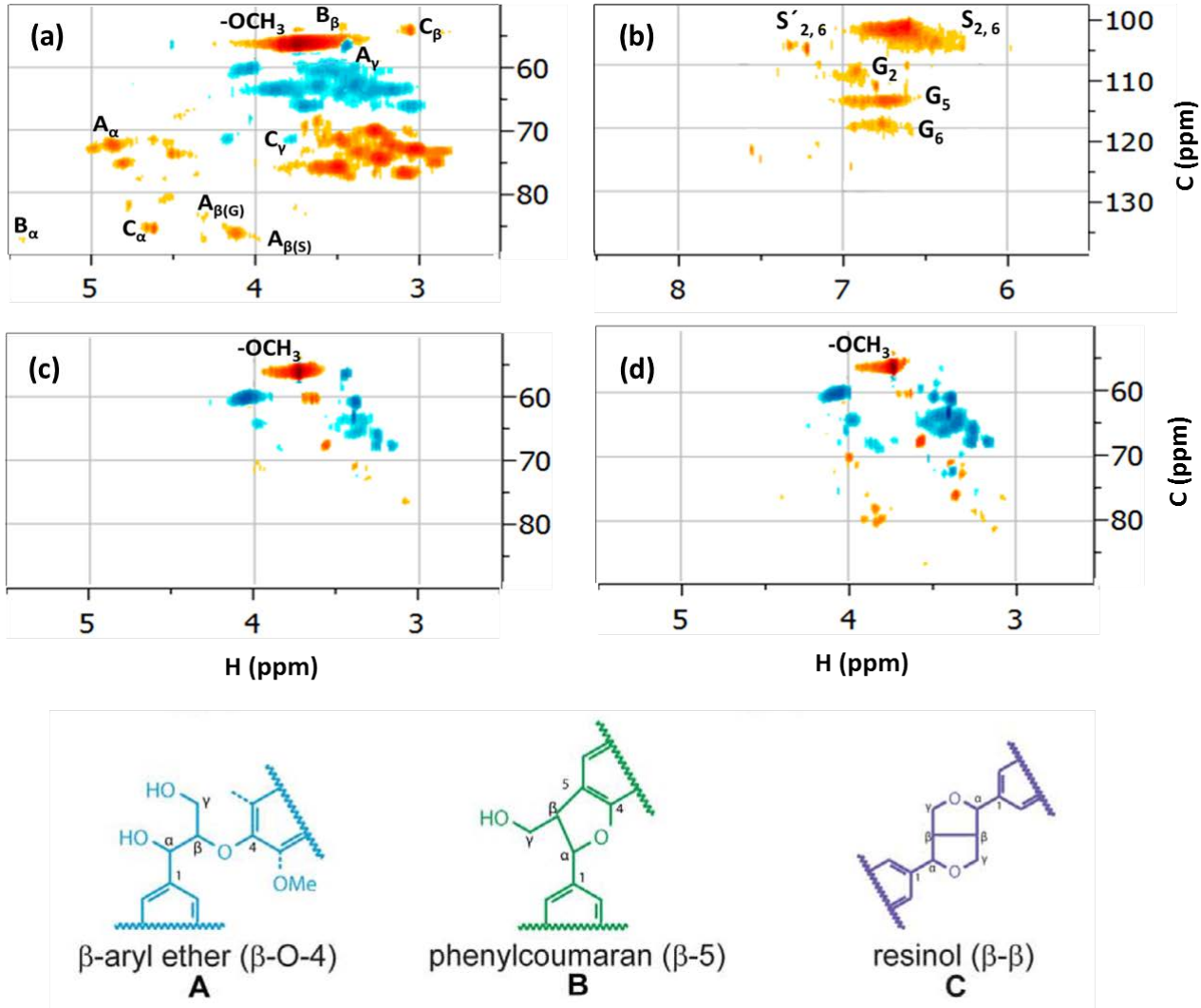

Figure 57 HSQC NMR analysis of (a) side chain signals of organosolv lignin, (b) aromatic signals of organosolv lignin and the side chain signals of oil fractions from conversion of (c) organosolv lignin and (d) beech wood over sulfided NiMo/Al_2O_3 at 300 ˚C. 1 g catalyst: 10 g feedstock, 100 ml ethanol, 26 bar H_2 (loaded at RT), 3 hours. The structure of β-aryl ether, phenylcoumaran and resinol are adapted and modified from [155].

Conclusion

The direct conversion of beech wood over sulfided $NiMo/Al_2O_3$ catalyst in ethanol solvent was studied at 300 ˚C. A high monomer yield of 18.1 wt% (relative to the Klason lignin content of 20.8 wt%) was observed with 4-propyl guaiacol and 4-propyl syringol being the major compounds. The molecular weight distribution of the oil indicated formation of compounds mainly within the range of monomers and dimers. The cellulose and hemicellulose fractions were completely converted to ketones, furans, alcohols, esters, ethers and aldehydes. The lignin derived monomers can be used as chemical building blocks, while the holocellulose derived compounds can further be upgraded by hydrodeoxygenation to serve as fuel. A study of the influence of reaction temperature indicated that at 200 ˚C mainly lignin was converted leaving the holocellulose untouched. By increasing the temperature to 260, 280 and 300 ˚C also the holocellulose fractions were progressively converted and at 300 ˚C essentially all biomass was converted to liquid or gaseous products with a total oil yield of 44 wt% and oxygen and sulfur content of 29.6 wt% and 1.0 wt%, respectively. Further deoxygenation and possibly desulfurization is required for utilizing this oil fraction as a fuel. Ethanol conversion, which is of economic concern, was practically zero at 200 ˚C, but it was increasingly converted at 260, 280 and 300 ˚C. The direct conversion of biomass is a versatile approach for production of chemical building blocks and high value chemicals. The direct conversion of biomass was compared with a two-step process where the lignin was first extracted by the organosolv method and then converted in ethanol. The two step method resulted in a slightly lower total oil yield (87 wt%) and a considerably lower yield of monomers (4.3 wt%) and a larger molecular weight distribution of the oil. This indicates that organosolv lignin contained stable C-C bonds and its recalcitrance was a result of transformations in the organosolv process. These findings highlight the superiority of the direct conversion method versus the conventional pretreatment methods.

Acknowledgement

NMR Center at Chemistry department, DTU is acknowledged for access to the 400 MHz spectrometer.

Chapter 7:

Summary and concluding remarks

7. Summary and concluding remarks

Solvothermal conversion of lignin is a promising approach which if assisted with a heterogeneous catalyst may result in relatively high yield of monomers. Among different types of technical lignin, solvothermal conversion of lignosulfonate was investigated in this PhD thesis using Ni based and commercial NiMo catalysts at moderate temperatures of 250-310 ˚C. The experiments were conducted in a batch reactor in the presence of a solvent and hydrogen. After each test, different product fractions were evaluated using various analytical techniques. The following are some of the main findings in this study:

It was observed that reaction medium greatly effects on the product distribution. Ethanol and ethylene glycol were evaluated as reaction media for conversion of lignosulfonate over Ni based catalysts in chapter 4. Both solvents can be produced from bio-based processes and therefore degrading lignin using them supports an integrated green biorefinery. The result showed that yield of oil fraction was nearly independent of the reaction medium. However, the compounds were of lower molecular weight in ethanol. Therefore, if obtaining lower molecular weight compound is intended, ethanol is a better solvent. The degraded oil can be directly used as a fuel additive or alternatively upgraded in a further cracking/hydrotreating process. Surprisingly, no char was observed in the reaction products in ethylene glycol, which indicated that this solvent had a better performance in inhibiting condensation reactions. In conversion of lignin, condensation reactions occur simultaneously with degradation. A good solvent should suppress the activity of the reactive fragments and inhibit char formation. The higher density of hydroxyl group in ethylene glycol is presumably the main contributor in suppressing char formation. It was however not possible to select a solvent as the one with better performance since both solvents showed pros and cons, and therefore a feasibility study is required for selecting the solvent by considering the type of feedstock and availability of solvent for a potential lignin valorization process.

In chapter 5, it was shown that lignosulfonate can be successfully converted over $NiMo/Al_2O_3$ in ethanol at 260-310 ˚C. A high oil yield of 88 wt% was observed at 310 ˚C from conversion of 10 g lignin in the presence of 2 g catalyst in a relatively short reaction time of 3 hours. Comparing the type of product in the absence and presence of catalyst, it was shown that depolymerization reactions were mostly from thermolysis types and what makes the catalytic process superior, is the role of catalyst in inhibiting condensation reactions of the depolymerized reactive fragments and also HDO and HDS. It was observed that catalyzed over NiMo, ethanol stabilizes the phenolics by alkylation reactions and inhibits condensation reactions. NiMo catalyst is a conventional hydrotreating catalyst that is widely used in petrochemical industry. The catalyst is developed over the years and optimized for the applications in petrochemical industries, and therefore by using this type of catalyst for conversion of lignin, the challenges of production of a stable catalyst are avoided. The good performance of this catalyst brings the conversion of lignin one step closer to industrial conversion step. A parameter study was conducted evaluating the effect of reaction time, reaction temperature and catalyst loading and was shown that the catalyst is reusable for at least two times. However, it should be emphasized that the product of the liquefaction of

lignosulfonate over NiMo were not selective to specific monomers, and if production of chemicals is intended an upgrading process may be required.

Lignin first biorefining method was the other strategy evaluated in this PhD (chapter 6). The method relies on fractionation of lignin in biomass and leaving holocellulose unconverted. The main superiority of the method is that the lignin derived products are extracted in form of mainly monomers and dimers, which in contrast to the conversion of technical lignin, shows high selectivity to a few number of monomers. Beech wood was converted over NiMo catalyst in ethanol medium at 200- 300 ˚C. It was observed that mainly lignin was degraded at 200 ˚C, with high selectivity to 4-propyl syringol and 4-propyl guaiacol while by increasing temperature to 300 ˚C hemicellulose and cellulose were progressively being converted. This method is flexible as either lignin conversion or whole biomass conversion can be attempted. Moreover, the method showed promises compared to two step extraction of lignin with organosolv process and further conversion of it, where lower yields of monomers was obtained. The complex structure of lignin experiences transformations during pulping process and other pretreatments such as those in the production of bio-ethanol and organosolv process, and becomes more recalcitrance towards degradation as a result of formation of stable C-C bonds.

7.1. Outlook

The results obtained in this PhD study provide insight in degradation of lignin with the main focus on lignosulfonate and also conversion of beech wood.

The high yields of oil fractions over NiMo catalyst were promising. However, understanding the reaction mechanism in the molecular level is challenging as lignin is a complex polymer. A detailed study using model compounds over NiMo catalyst can enlighten the mechanism and be useful for modeling the degradation.

The conversion of lignin over NiMo catalyst can be combined with a further upgrading process in order to obtain higher yields of monomers with higher selectivity. The upgrading is normally conducted in the presence of stable solvent such as dodecane and depending on the targeted compounds, a variety of hydrogenation and deoxygenation catalysts can be used.

Though good results were obtained from conversion of beech wood, this method is still in its early stage of evaluations and should be expanded to the other types of biomass and other catalytic systems. In this method ethanol is used as solvent, which itself degrades in the presence of catalyst and form light compounds that can also be obtained from cellulose and hemicellulose. Therefore, it remains as a challenge to distinguish ethanol derived products from those from conversion of biomass. The evaluation of whole system in terms of the products yield and economy is not possible unless the products can be distinguished. Therefore, a great focus should be devoted on developing methods for product evaluation. Solvent consumption should be minimized by altering lignin to ethanol loading, catalyst loading and reaction time. This is not only of concern for conversion of biomass, but also for conversion of technical lignin.

Bibliography

Bibliography

[1] Q. Bu, H. Lei, A. H. Zacher, L. Wang, S. Ren, J. Liang, Y. Wei, Y. Liu, J. Tang, Q. Zhang, and R. Ruan, "A review of catalytic hydrodeoxygenation of lignin-derived phenols from biomass pyrolysis," *Bioresour. Technol.*, vol. 124, pp. 470–477, 2012.

[2] P. Mousavioun, "Properties of Lignin and Poly(hydroxybutyrate) Blends," Queensland University of Technology, 2011.

[3] W. O. S. Doherty, P. Mousavioun, and C. M. Fellows, "Value-adding to cellulosic ethanol: Lignin polymers," *Ind. Crops Prod.*, vol. 33, no. 2, pp. 259–276, 2011.

[4] M. Kleinert, J. R. Gasson, and T. Barth, "Optimizing solvolysis conditions for integrated depolymerisation and hydrodeoxygenation of lignin to produce liquid biofuel," *J. Anal. Appl. Pyrolysis*, vol. 85, no. 1–2, pp. 108–117, 2009.

[5] F. H. Isikgor and C. R. Becer, "Lignocellulosic biomass: A sustainable platform for production of bio-based chemicals and polymers," *Polym. Chem.*, vol. 6, no. 25, pp. 4497–4559, 2015.

[6] D. M. Alonso, S. G. Wettstein, and J. A. Dumesic, "Bimetallic catalysts for upgrading of biomass to fuels and chemicals," *Chem. Soc. Rev.*, vol. 41, no. 24, pp. 8075–8098, 2012.

[7] A. Alzagameem, B. El Khaldi-Hansen, B. Kamm, and M. Schulze, "Lignocellulosic Biomass for Energy, Biofuels, Biomaterials, and Chemicals," in *Biomass and Green Chemistry: Building a Renewable Pathway*, S. Vaz Jr., Ed. Cham: Springer International Publishing, 2018, pp. 95–132.

[8] X. Zhou, "Conversion of kraft lignin under hydrothermal conditions," *Bioresour. Technol.*, vol. 170, pp. 583–586, 2014.

[9] A. Berlin and M. Balakshin, "Industrial lignins: Analysis, properties, and applications," in *Bioenergy Research: Advances and Applications*, Elsevier, 2014, pp. 315–336.

[10] T. Renders, S. Van Den Bosch, S. Koelewijn, and W. Schutyser, "Lignin-first biomass fractionation : the advent of active stabilisation strategies," *Energy Environ. Sci.*, vol. 10, pp. 1551–1557, 2017.

[11] P. Azadi, O. R. Inderwildi, R. Farnood, and D. a. King, "Liquid fuels, hydrogen and chemicals from lignin: A critical review," *Renew. Sustain. Energy Rev.*, vol. 21, pp. 506–523, 2013.

[12] D. Areskogh, J. Li, G. Gellerstedt, and G. Henriksson, "Structural modification of commercial lignosulphonates through laccase catalysis and ozonolysis," *Ind. Crops Prod.*, vol. 32, no. 3, pp. 458–466, 2010.

[13] A. Vishtal and A. Kraslawski, "Challenges in industrial applications of technical lignins," *BioResources*, vol. 6, no. 3, pp. 3547–3568, 2011.

[14] A. W. Pacek, P. Ding, M. Garrett, G. Sheldrake, and A. W. Nienow, "Catalytic conversion of sodium lignosulfonate to vanillin: Engineering aspects. part 1. effects of

processing conditions on vanillin yield and selectivity," *Ind. Eng. Chem. Res.*, vol. 52, no. 25, pp. 8361–8372, 2013.

[15] H.-R. Bjørsvik and F. Minisci, "Fine Chemicals from Lignosulfonates. 1. Synthesis of Vanillin by Oxidation of Lignosulfonates," *Org. Process Res. Dev.*, vol. 3, no. 5, pp. 330–340, 1999.

[16] J. E. Holladay, J. F. White, J. J. Bozell, and D. Johnson, "Top Value-Added Chemicals from Biomass Volume II - Results of Screening for Potential Candidates from Biorefinery Lignin," 2007.

[17] M. P. Pandey and C. S. Kim, "Lignin Depolymerization and Conversion: A Review of Thermochemical Methods," *Chem. Eng. Technol.*, vol. 34, no. 1, pp. 29–41, 2011.

[18] S. Kang, X. Li, J. Fan, and J. Chang, "Hydrothermal conversion of lignin: A review," *Renew. Sustain. Energy Rev.*, vol. 27, pp. 546–558, 2013.

[19] Z. Cao, M. Dierks, M. T. Clough, I. B. D. De Castro, and R. Rinaldi, "A Convergent Approach for a Deep Converting Lignin-First Biorefinery Rendering High-Energy-Density Drop-in Fuels A Convergent Approach for a Deep Converting Lignin-First Biorefinery Rendering High-Energy-Density Drop-in Fuels," *Joule*, vol. 2, pp. 1–16, 2018.

[20] B. Joffres, D. Laurenti, N. Charon, A. Daudin, A. Quignard, and C. Geantet, "Thermochemical Conversion of Lignin for Fuels and Chemicals: A Review," *Oil Gas Sci. Technol. – Rev. d'IFP Energies Nouv.*, vol. 68, no. 4, pp. 753–763, 2013.

[21] G. Brunner, "Processing of Biomass with Hydrothermal and Supercritical Water," in *Supercritical Fluid Science and Technology*, vol. 5, 2014, pp. 395–509.

[22] S. Laurichesse and L. Avérous, "Chemical modification of lignins: Towards biobased polymers," *Prog. Polym. Sci.*, vol. 39, no. 7, pp. 1266–1290, 2014.

[23] A. Prakash, R. Singh, B. Balagurumurthy, T. Bhaskar, A. K. Arora, and S. K. Puri, "Thermochemical Valorization of Lignin," in *Recent Advances in Thermochemical Conversion of Biomass*, Elsevier B.V., 2015, pp. 455–478.

[24] S. Huang, N. Mahmood, M. Tymchyshyn, Z. Yuan, and C. C. Xu, "Reductive de-polymerization of kraft lignin for chemicals and fuels using formic acid as an in-situ hydrogen source," *Bioresour. Technol.*, vol. 171, pp. 95–102, 2014.

[25] J. B. Nielsen, A. Jensen, L. R. Madsen, F. H. Larsen, C. Felby, and A. D. Jensen, "Noncatalytic Direct Liquefaction of Biorefinery Lignin by Ethanol," *Energy & Fuels*, vol. 31, pp. 7223–7233, 2017.

[26] T. D. H. Nguyen, M. Maschietti, T. Belkheiri, L. E. Åmand, H. Theliander, L. Vamling, L. Olausson, and S. I. Andersson, "Catalytic depolymerisation and conversion of Kraft lignin into liquid products using near-critical water," *J. Supercrit. Fluids*, vol. 86, pp. 67–75, 2014.

[27] S. Cheng, C. Wilks, Z. Yuan, M. Leitch, C. Xu, and C. Charles, "Hydrothermal degradation of alkali lignin to bio-phenolic compounds in sub/supercritical ethanol and

water-ethanol co-solvent," *Polym. Degrad. Stab.*, vol. 97, no. 6, pp. 839–848, 2012.

[28] K. Okuda, M. Umetsu, S. Takami, and T. Adschiri, "Disassembly of lignin and chemical recovery - Rapid depolymerization of lignin without char formation in water-phenol mixtures," *Fuel Process. Technol.*, vol. 85, no. 8–10, pp. 803–813, 2004.

[29] H. Pińkowska, P. Wolak, and A. Złocińska, "Hydrothermal decomposition of alkali lignin in sub- and supercritical water," *Chem. Eng. J.*, vol. 187, pp. 410–414, 2012.

[30] G. Warner, T. S. Hansen, A. Riisager, E. S. Beach, K. Barta, and P. T. Anastas, "Depolymerization of organosolv lignin using doped porous metal oxides in supercritical methanol," *Bioresour. Technol.*, vol. 161, pp. 78–83, 2014.

[31] X. Huang, T. I. Korányi, M. D. Boot, and E. J. M. Hensen, "Catalytic depolymerization of lignin in supercritical ethanol," *ChemSusChem*, vol. 7, no. 8, pp. 2276–2288, 2014.

[32] A. Narani, R. K. Chowdari, C. Cannilla, G. Bonura, F. Frusteri, H. J. Heeres, and K. Barta, "Efficient catalytic hydrotreatment of Kraft lignin to alkylphenolics using supported NiW and NiMo catalysts in supercritical methanol," *Green Chem.*, vol. 17, no. 11, pp. 5046–5057, 2015.

[33] Q. Song, F. Wang, J. Cai, Y. Wang, J. Zhang, W. Yu, and J. Xu, "Lignin depolymerization (LDP) in alcohol over nickel-based catalysts via a fragmentation-hydrogenolysis process," *Energy Environ. Sci.*, vol. 6, no. 3, pp. 994–1007, 2013.

[34] S. F. Simonsen, A. Kronstad, P. L. Arias, T. Barth, M. Oregui-Bengoechea, I. Gandarias, N. Miletić, S. F. Simonsen, A. Kronstad, P. L. Arias, and T. Barth, "Thermocatalytic conversion of lignin in an ethanol/formic acid medium with NiMo catalysts: role of the metal and acid sites," *Appl. Catal. B Environ.*, vol. 217, pp. 353–364, 2017.

[35] R. Ma, W. Hao, X. Ma, Y. Tian, and Y. Li, "Catalytic Ethanolysis of Kraft Lignin into High-Value Small-Molecular Chemicals over a Nanostructured a -Molybdenum Carbide Catalyst," *Angew. Chemie - Int. Ed.*, vol. 53, pp. 1–7, 2014.

[36] J. Zakzeski, A. L. Jongerius, P. C. a Bruijnincx, and B. M. Weckhuysen, "Catalytic lignin valorization process for the production of aromatic chemicals and hydrogen," *ChemSusChem*, vol. 5, no. 8, pp. 1602–1609, 2012.

[37] A. Kloekhorst, Y. Shen, Y. Yie, M. Fang, and H. J. Heeres, "Catalytic hydrodeoxygenation and hydrocracking of Alcell® lignin in alcohol/formic acid mixtures using a Ru/C catalyst," *Biomass and Bioenergy*, vol. 80, no. 0, pp. 147–161, 2015.

[38] S. Huang, N. Mahmood, M. Tymchyshyn, Z. Yuan, and C. (Charles) Xu, "Reductive de-polymerization of kraft lignin for chemicals and fuels using formic acid as an in-situ hydrogen source," *Bioresour. Technol.*, vol. 171, pp. 95–102, 2014.

[39] M. Grilc, B. Likozar, and J. Levec, "Hydrodeoxygenation and hydrocracking of solvolysed lignocellulosic biomass by oxide, reduced and sulphide form of NiMo, Ni, Mo and Pd catalysts," *Appl. Catal. B Environ.*, vol. 150–151, pp. 275–287, 2014.

[40] R. Rinaldi, R. Jastrzebski, M. T. Clough, J. Ralph, M. Kennema, P. C. A. Bruijnincx, and B. M. Weckhuysen, “Paving the Way for Lignin Valorisation: Recent Advances in Bioengineering, Biorefining and Catalysis,” *Angew. Chemie - Int. Ed.*, vol. 55, no. 29, pp. 8164–8215, 2016.

[41] W. Schutyser, S. Van Den Bosch, T. Renders, T. De Boe, S. Koelewijn, A. Dewaele, T. Ennaert, O. Verkinderen, B. Goderis, C. M. Courtin, and B. F. Sels, “Influence of bio-based solvents on the catalytic reductive fractionation of birch wood,” *Green Chem.*, vol. 17, pp. 5035–5045, 2015.

[42] H. Luo, I. M. Klein, Y. Jiang, H. Zhu, B. Liu, H. I. Kenttamaa, and M. M. Abu-Omar, “Total Utilization of Miscanthus Biomass, Lignin and Carbohydrates, Using Earth Abundant Nickel Catalyst,” *ACS Sustain. Chem. Eng.*, vol. 4, no. 4, pp. 2316–2322, 2016.

[43] S. Van den Bosch, W. Schutyser, R. Vanholme, T. Driessen, S.-F. Koelewijn, T. Renders, B. De Meester, W. J. J. Huijgen, W. Dehaen, C. M. Courtin, B. Lagrain, W. Boerjan, and B. F. Sels, “Reductive lignocellulose fractionation into soluble lignin-derived phenolic monomers and dimers and processable carbohydrate pulps,” *Energy Environ. Sci.*, vol. 8, no. 6, pp. 1748–1763, 2015.

[44] F. G. Calvo-Flores and J. a. Dobado, “Lignin as renewable raw material,” *ChemSusChem*, vol. 3, no. 11, pp. 1227–1235, 2010.

[45] J. H. Lora, “Industrial commercial lignins: Sources, properties and applications,” in *Monomers, Polymers and Composites from Renewable Resources*, Elsevier, 2008, pp. 225–241.

[46] E. Windeisen and G. Wegener, “Lignin as Building Unit for Polymers,” *Polym. Sci. A Compr. Ref.*, vol. 10, pp. 255–265, 2012.

[47] J. Zakzeski, P. C. A. Bruijnincx, A. L. Jongerius, and B. M. Weckhuysen, “The catalytic valorization of lignin for the production of renewable chemicals,” *Chem. Rev.*, vol. 110, no. 6, pp. 3552–3599, 2010.

[48] M. D. Kärkäs, B. S. Matsuura, T. M. Monos, G. Magallanes, and C. R. J. Stephenson, “Transition-metal catalyzed valorization of lignin: the key to a sustainable carbon-neutral future,” *Org. Biomol. Chem.*, vol. 14, no. 6, pp. 1853–1914, 2016.

[49] I. Norberg, “Carbon fibres from kraft lignin,” KTH Royal Institute of Technology, 2012.

[50] A. L. Jongerius, “Catalytic Conversion of Lignin for the Production of Aromatics,” Utrecht University, 2013.

[51] A. G. Sergeev and J. F. Hartwig, “Selective, nickel-catalyzed hydrogenolysis of aryl ethers.,” *Science*, vol. 332, no. 6028, pp. 439–443, 2011.

[52] S. Gillet, M. Aguedo, L. Petitjean, A. R. C. Morais, A. M. da Costa Lopes, R. M. Lukasik, and P. Anastas, “Lignin Transformations for High Value Applications: Towards Targeted Modifications Using Green Chemistry,” *Green Chem.*, vol. 19, pp. 4200–4233, 2017.

[53] J. L. Espinoza-Acosta, P. I. Torres-Chávez, J. L. Olmedo-Martínez, A. Vega-Rios, S. Flores-Gallardo, and E. A. Zaragoza-Contreras, “Lignin in storage and renewable energy applications: A review,” *J. Energy Chem.*, pp. 1–17, 2018.

[54] G. Gellerstedt, “The reactions of lignin during sulfite pulping,” *Sven. Papperstidning*, vol. 79, pp. 537–543, 1976.

[55] A. Duval, S. Molina-boisseau, and C. Chirat, “Fractionation of lignosulfonates: comparison of ultrafiltration and ethanol solubility to obtain a set of fractions with distinct properties,” *Holzforschung*, vol. 0, no. 0, pp. 127–134, 2014.

[56] P. Ding, M. Garrett, Ø. Loe, A. W. Nienow, and A. W. Pacek, “Generation of hydrogen gas during the catalytic oxidation of sodium lignosulfonate to vanillin: Initial results,” *Ind. Eng. Chem. Res.*, vol. 51, no. 1, pp. 184–188, 2012.

[57] K. Reknes, “The chemistry of lignosulfonate and the effect on performance of lignosulfonate base plasticizers and superplasticizerd,” in *29th Our World in Concrete and Structures (OWICs)*, 2004.

[58] J. Gierer, “Chemistry of delignification - Part 1: General concept and reactions during pulping,” *Wood Sci. Technol.*, vol. 19, no. 4, pp. 289–312, 1985.

[59] M. F. Li, S.-N. Sun, F. Xu, and R.-C. Sun, “Organosolv Fractionation of Lignocelluloses for Fuels, Chemicals and Materials: A Biorefinery Processing Perspective,” in *Biomass Conversion - The interface of Biotechnology, Chemistry and Material Science*, C. Baskar, S. Baskar, and R. S. Dhillon, Eds. 2012, pp. 381–412.

[60] X. Besse, Y. Schuurman, and N. Guilhaume, “Hydrothermal conversion of lignin model compound eugenol,” *Catal. Today*, 2015.

[61] L. Yang, K. Seshan, and Y. Li, “A review on thermal chemical reactions of lignin model compounds,” *Catal. Today*, vol. 298, pp. 276–297, 2017.

[62] C. Amen-Chen, H. Pakdel, and C. Roy, “Production of monomeric phenols by thermochemical conversion of biomass: A review,” *Bioresour. Technol.*, vol. 79, pp. 277–299, 2001.

[63] R. Rinaldi and F. Schüth, “Design of solid catalysts for the conversion of biomass,” *Energy Environ. Sci.*, vol. 2, p. 610, 2009.

[64] G. Busca, “Metal Catalysts for Hydrogenations and Dehydrogenations,” in *Heterogeneous Catalytic Materials*, 2014, pp. 297–343.

[65] J. Sehested, “Four challenges for nickel steam-reforming catalysts,” *Catal. Today*, vol. 111, pp. 103–110, 2006.

[66] X. Wang and R. Rinaldi, “Solvent effects on the hydrogenolysis of diphenyl ether with raney nickel and their implications for the conversion of lignin,” *ChemSusChem*, vol. 5, no. 8, pp. 1455–1466, 2012.

[67] S. M. G. Lama, J. Pampel, T. P. Fellinger, V. P. Beškoski, L. Slavković-Beškoski, M. Antonietti, and V. Molinari, “Efficiency of Ni Nanoparticles Supported on Hierarchical Porous Nitrogen-Doped Carbon for Hydrogenolysis of Kraft Lignin in

Flow and Batch Systems," *ACS Sustain. Chem. Eng.*, vol. 5, no. 3, pp. 2415–2420, 2017.

[68] S. Kasakov, H. Shi, D. M. Camaioni, C. Zhao, E. Baráth, A. Jentys, and J. a. Lercher, "Reductive deconstruction of organosolv lignin catalyzed by zeolite supported nickel nanoparticles," *Green Chem.*, vol. 17, pp. 5079–5090, 2015.

[69] I. Klein, B. Saha, and M. M. Abu-Omar, "Lignin depolymerization over Ni/C catalyst in methanol, a continuation: effect of substrate and catalyst loading," *Catal. Sci. Technol.*, vol. 5, no. 6, pp. 3242–3245, 2015.

[70] J. Kong, B. Li, and C. Zhao, "Tuning Ni nanoparticles and the acid sites of silica-alumina for liquefaction and hydrodeoxygenation of lignin to cyclic alkanes," *RSC Adv.*, vol. 6, no. 76, pp. 71940–71951, 2016.

[71] J. Y. Kim, J. Park, H. Hwang, J. K. Kim, I. K. Song, and J. W. Choi, "Catalytic depolymerization of lignin macromolecule to alkylated phenols over various metal catalysts in supercritical tert-butanol," *J. Anal. Appl. Pyrolysis*, vol. 113, pp. 99–106, 2015.

[72] J. Yang, L. Zhao, S. Liu, Y. Wang, and L. Dai, "High-quality bio-oil from one-pot catalytic hydrocracking of kraft lignin over supported noble metal catalysts in isopropanol system," *Bioresour. Technol.*, vol. 212, pp. 302–310, 2016.

[73] M. Nagy, K. David, G. J. P. Britovsek, and A. J. Ragauskas, "Catalytic hydrogenolysis of ethanol organosolv lignin," *Holzforschung*, vol. 63, pp. 513–520, 2009.

[74] J. a. Onwudili and P. T. Williams, "Catalytic depolymerization of alkali lignin in subcritical water: influence of formic acid and Pd/C catalyst on the yields of liquid monomeric aromatic products," *Green Chem.*, vol. 16, pp. 4740–4748, 2014.

[75] S. Jeong, G. Hun Jang, and D. H. Kim, "Decomposition of Lignin Using MO – MgAlO y Mixed Oxide Catalysts (M = Co , Ni and Cu) in Supercritical Ethanol," *Top. Catal.*, vol. 60, no. 9, pp. 637–643, 2017.

[76] L. Cattelan, A. K. L. Yuen, M. Y. Lui, A. F. Masters, M. Selva, A. Perosa, and T. Maschmeyer, "Renewable Aromatics from Kraft Lignin with Molybdenum- Based Catalysts," *ChemCatChem*, pp. 2717–2726, 2017.

[77] X. Huang, C. Atay, I. Kora, M. D. Boot, and E. J. M. Hensen, "Role of Cu − Mg − Al Mixed Oxide Catalysts in Lignin Depolymerization in Supercritical Ethanol," *ACS Catal.*, vol. 5, pp. 7359–7370, 2015.

[78] X. Huang, T. I. Korányi, M. D. Boot, and E. J. M. M. Hensen, "Ethanol as capping agent and formaldehyde scavenger for efficient depolymerization of lignin to aromatics," *Green Chem.*, vol. 17, no. 11, pp. 4941–4950, 2015.

[79] X. Huang, C. Atay, J. Zhu, S. W. L. Palstra, I. Kora, M. D. Boot, and E. J. M. Hensen, "Catalytic Depolymerization of Lignin and Woody Biomass in Supercritical Ethanol: In fluence of Reaction Temperature and Feedstock," *ACS Sustain. Chem. Eng.*, pp. 10864–10874, 2017.

[80] X. Wang and R. Rinaldi, “Bifunctional Ni catalysts for the one-pot conversion of Organosolv lignin into cycloalkanes,” *Catal. Today*, vol. 269, pp. 48–55, 2016.

[81] N. P. Vasilakos and D. M. Austgen, “Hydrogen-donor solvents in biomass liquefaction,” *Ind. Eng. Chem. Proc. Des. Dev.*, vol. 24, no. 2, pp. 304–311, 1985.

[82] R. W. Thring and J. Breau, “Hydrocracking of solvolysis lignin in a batch reactor,” *Fuel*, vol. 75, no. 7, pp. 795–800, 1996.

[83] J. He, C. Zhao, and J. a. Lercher, “Ni-catalyzed cleavage of aryl ethers in the aqueous phase,” *J. Am. Chem. Soc.*, vol. 134, no. 51, pp. 20768–20775, 2012.

[84] P. M. Mortensen, D. Gardini, H. W. P. de Carvalho, C. D. Damsgaard, J. Grunwaldt, P. a. Jensen, J. B. Wagner, and A. D. Jensen, “Stability and resistance of nickel catalysts for hydrodeoxygenation: carbon deposition and effects of sulfur, potassium, and chlorine in the feed,” *Catal. Sci. Technol.*, pp. 3672–3686, 2014.

[85] Z. Yuan, M. Tymchyshyn, and C. (Charles) Xu, “Reductive Depolymerization of Kraft and Organosolv Lignin in Supercritical Acetone for Chemicals and Materials,” *ChemCatChem*, vol. 8, no. 11, pp. 1968–1976, 2016.

[86] Z. He and X. Wang, “Hydrodeoxygenation of model compounds and catalytic systems for pyrolysis bio-oils upgrading,” *Catal. Sustain. Energy*, vol. 1, pp. 28–52, 2012.

[87] V. N. Bui, D. Laurenti, P. Afanasiev, and C. Geantet, “Hydrodeoxygenation of guaiacol with CoMo catalysts. Part I: Promoting effect of cobalt on HDO selectivity and activity,” *Appl. Catal. B Environ.*, vol. 101, no. 3–4, pp. 239–245, 2011.

[88] A. L. Jongerius, R. Jastrzebski, P. C. A. Bruijnincx, and B. M. Weckhuysen, “CoMo sulfide-catalyzed hydrodeoxygenation of lignin model compounds: An extended reaction network for the conversion of monomeric and dimeric substrates,” *J. Catal.*, vol. 285, no. 1, pp. 315–323, 2012.

[89] J. Horáček, F. Homola, I. Kubičková, and D. Kubička, “Lignin to liquids over sulfided catalysts,” *Catal. Today*, vol. 179, no. 1, pp. 191–198, 2012.

[90] A. Oasmaa, R. Alén, and D. Meier, “Catalytic hydrotreatment of some technical lignins,” *Bioresour. Technol.*, vol. 45, no. 3, pp. 189–194, 1993.

[91] C. Zhang, J. Lu, X. Zhang, K. MacArthur, M. Heggen, H. Li, and F. Wang, “Cleavage of the lignin β-O-4 ether bond via a dehydroxylation–hydrogenation strategy over a NiMo sulfide catalyst,” *Green Chem.*, vol. 18, no. 24, pp. 6545–6555, 2016.

[92] M. Oregui-Bengoechea, I. Gandarias, N. Miletic, S. F. Simonsen, A. Kronstad, P. L. Arias, and T. Barth, “Thermocatalytic conversion of lignin in an ethanol / formic acid medium with NiMo catalysts : Role of the metal and acid sites,” *Appl. Catal. B Environ.*, vol. 217, pp. 353–364, 2017.

[93] B. Yoosuk, D. Tumnantong, and P. Prasassarakich, “Unsupported MoS2 and CoMoS2 catalysts for hydrodeoxygenation of phenol,” *Chem. Eng. Sci.*, vol. 79, pp. 1–7, 2012.

[94] K. Barta and H. Jan, “Solvent free depolymerization of Kraft lignin to alkyl-phenolics using supported NiMo and CoMo catalysts,” *Green Chem.*, vol. 17, no. 11, pp. 4921–

4930, 2015.

[95] D. Meier, J. Berns, O. Faix, U. Balfanz, and W. Baldauf, “Hydrocracking of organocell lignin for phenol production,” *Biomass and Bioenergy*, vol. 7, pp. 99–105, 1994.

[96] P. M. Mortensen, J. D. Grunwaldt, P. a. Jensen, and A. D. Jensen, “Screening of catalysts for hydrodeoxygenation of phenol as a model compound for bio-oil,” *ACS Catal.*, vol. 3, no. 8, pp. 1774–1785, 2013.

[97] J. V Lauritsen, S. Helveg, E. Lægsgaard, I. Stensgaard, B. S. Clausen, H. Topsøe, and F. Besenbacher, “Atomic-Scale Structure of Co – Mo – S Nanoclusters in Hydrotreating Catalysts,” *J. Catal.*, vol. 197, pp. 1–5, 2001.

[98] F. Besenbacher, M. Brorson, B. S. Clausen, S. Helveg, B. Hinnemann, J. Kibsgaard, J. . Lauritsen, P. . Moses, J. . Nørskov, and H. Topsøe, “Recent STM , DFT and HAADF-STEM studies of sulfide-based hydrotreating catalysts : Insight into mechanistic , structural and particle size effects,” *Catal. Today*, vol. 130, pp. 86–96, 2008.

[99] G. M. Bremmer, L. van Haandel, E. J. M. Hensen, J. W. M. Frenken, and P. J. Kooyman, “Instability of NiMoS $_2$ and CoMoS $_2$ Hydrodesulfurization Catalysts at Ambient Conditions: A Quasi in Situ High-Resolution Transmission Electron Microscopy and X-ray Photoelectron Spectroscopy Study,” *J. Phys. Chem. C*, vol. 120, no. 34, pp. 19204–19211, 2016.

[100] J. V Lauritsen, J. Kibsgaard, G. H. Olesen, P. G. Moses, B. Hinnemann, S. Helveg, J. K. Nørskov, B. S. Clausen, H. Topsøe, and E. Lægsgaard, “Location and coordination of promoter atoms in Co- and Ni-promoted MoS 2 -based hydrotreating catalysts,” *Catalysis*, vol. 249, pp. 220–233, 2007.

[101] S. Texier, G. Berhault, and G. Pe, “Activation of alumina-supported hydrotreating catalysts by organosulfides or H2S : Effect of the H2S partial pressure used during the activation process,” *Appl. Catal. A-general*, vol. 293, pp. 105–119, 2005.

[102] P. M. Mortensen, D. Gardini, C. D. Damsgaard, J. Grunwaldt, P. A. Jensen, J. B. Wagner, and A. D. Jensen, “General Deactivation of Ni-MoS2 by bio-oil impurities during hydrodeoxygenation of phenol and octanol,” *"Applied Catal. A, Gen.*, vol. 523, pp. 159–170, 2016.

[103] B. Joffres, C. Lorentz, M. Vidalie, D. Laurenti, A. Quoineaud, and N. Charon, “Catalytic hydroconversion of a wheat straw soda lignin : Characterization of the products and the lignin residue,” *"Applied Catal. B, Environ.*, vol. 145, pp. 167–176, 2014.

[104] B. Joffres, M. T. Nguyen, D. Laurenti, C. Lorentz, V. Souchon, and N. Charon, “Lignin hydroconversion on MoS2 -based supported catalyst : Comprehensive analysis of products and reaction scheme,” *Appl. Catal. B Environ.*, vol. 184, pp. 153–162, 2016.

[105] A. L. Jongerius, P. C. a. Bruijnincx, and B. M. Weckhuysen, “Liquid-phase reforming and hydrodeoxygenation as a two-step route to aromatics from lignin,” *Green Chem.*,

vol. 15, no. 11, p. 3049, 2013.

[106] M. R. De Brimont, C. Dupont, A. Daudin, C. Geantet, and P. Raybaud, "Deoxygenation mechanisms on Ni-promoted MoS 2 bulk catalysts : A combined experimental and theoretical study," *J. Catal.*, vol. 286, pp. 153–164, 2012.

[107] C. R. Lee, J. S. Yoon, Y. W. Suh, J. W. Choi, J. M. Ha, D. J. Suh, and Y. K. Park, "Catalytic roles of metals and supports on hydrodeoxygenation of lignin monomer guaiacol," *Catal. Commun.*, vol. 17, pp. 54–58, 2012.

[108] E. Laurent and B. Delmon, "Study of the hydrodeoxygenation of carbonyl, carboxylic and guaiacyl groups over sulfided CoMo/[gamma]-Al2O3 and NiMo/[gamma]-Al2O3 catalysts: I. Catalytic reaction schemes," *Appl. Catal. A Gen.*, vol. 109, no. 1, pp. 77–96, 1994.

[109] R. Shu, Y. Xu, L. Ma, Q. Zhang, T. Wang, P. Chen, and Q. Wu, "Hydrogenolysis process for lignosulfonate depolymerization using synergistic catalysts of noble metal and metal chloride," *RSC Adv.*, vol. 6, no. 91, pp. 88788–88796, 2016.

[110] F. Wang, J. Xu, Q. Song, and J. Xu, "Hydrogenolysis of lignosulfonate into phenols over heterogeneous nickel catalysts w," *ChemComm*, vol. 48, no. 56, 2012.

[111] J. Horáček, J.-P. Mikkola, A. Samikannu, G. Šťávová, W. Larsson, L. Hora, and D. Kubička, "Studies on Sodium Lignosulfonate Depolymerization Over Al2O3 Supported Catalysts Loaded with Metals and Metal Oxides in a Continuous Flow Reactor," *Top. Catal.*, vol. 56, no. 9–10, pp. 794–799, 2013.

[112] S. Brand, R. F. Susanti, S. K. Kim, H. shik Lee, J. Kim, and B. I. Sang, "Supercritical ethanol as an enhanced medium for lignocellulosic biomass liquefaction: Influence of physical process parameters," *Energy*, vol. 59, pp. 173–182, 2013.

[113] S. Van den Bosch, T. Renders, S. Kennis, S.-F. Koelewijn, G. Van den Bossche, T. Vangeel, A. Deneyer, D. Depuydt, C. M. Courtin, J. M. Thevelein, W. Schutyser, and B. F. Sels, "Integrating lignin valorization and bio-ethanol production: on the role of Ni-Al2O 3 catalyst pellets during lignin-first fractionation," *Green Chem.*, vol. 19, no. 14, pp. 3313–3326, 2017.

[114] S. Brand and J. Kim, "Liquefaction of major lignocellulosic biomass constituents in supercritical ethanol," *Energy*, vol. 80, pp. 64–74, 2015.

[115] J. Yamazaki, E. Minami, and S. Saka, "Liquefaction of beech wood in various supercritical alcohols," *J. Wood Sci.*, vol. 52, no. 6, pp. 527–532, 2006.

[116] P. Ferrini and R. Rinaldi, "Catalytic Biorefining of Plant Biomass to Non-Pyrolytic Lignin Bio-Oil and Carbohydrates through Hydrogen Transfer Reactions," *Angew. Chemie Int. Ed.*, vol. 53, no. 33, pp. 8634–8639, Aug. 2014.

[117] X. Wang and R. Rinaldi, "Exploiting H-transfer reactions with RANEY® Ni for upgrade of phenolic and aromatic biorefinery feeds under unusual, low-severity conditions," *Energy Environ. Sci.*, vol. 5, no. 8, p. 8244, 2012.

[118] Z. Sun, G. Bottari, A. Afanasenko, M. C. A. Stuart, P. J. Deuss, B. Fridrich, and K.

Barta, “Complete lignocellulose conversion with integrated catalyst recycling yielding valuable aromatics and fuels,” *Nat. Catal.*, vol. 1, no. 1, pp. 82–92, 2018.

[119] Q. Xia, Z. Chen, Y. Shao, X. Gong, H. Wang, X. Liu, S. F. Parker, X. Han, S. Yang, and Y. Wang, “Direct hydrodeoxygenation of raw woody biomass into liquid alkanes,” *Nat. Commun.*, pp. 1–10, 2016.

[120] C. Li, M. Zheng, A. Wang, and Z. Tao, “One-pot catalytic hydrocracking of raw woody biomass into chemicals over supported carbide catalysts : simultaneous conversion of cellulose , hemicellulose and lignin,” *Energy Environ. Sci.*, vol. 5, pp. 6383–6390, 2012.

[121] G. E. Fredheim, S. M. Braaten, and B. E. Christensen, “Molecular weight determination of lignosulfonates by size-exclusion chromatography and multi-angle laser light scattering,” *J. Chromatogr. A*, vol. 942, no. 1–2, pp. 191–199, 2002.

[122] L. Medici and R. Prins, “The influence of chelating ligands on the sulfidation of Ni and Mo in NiMo/SiO_2 hydrotreating catalysts,” *J. Catal.*, vol. 163, no. 303, pp. 38–49, 1996.

[123] P. a Webb, “Introduction to Chemical Adsorption Analytical Techniques and their Applications to Catalysis,” *MIC Tech. Publ.*, vol. 13, no. January, pp. 1–4, 2003.

[124] A. R. Katritzky, E. S. Ignatchenko, R. A. Barcock, V. S. Lobanov, and M. Karelson, “Prediction of Gas Chromatographic Retention Times and Response Factors Using a General Quantitative Structure-Property Relationship Treatment,” *Anal. Chem*, vol. 66, no. 11, pp. 1799–1807, 1994.

[125] J. T. Scanlon and D. E. Willis, “Calculation of Flame Ionization Detector Relative Response Factors Using the Effective Carbon Number Concept,” *J. Chromatogr. Sci.*, vol. 23, pp. 333–340, 1985.

[126] S. S. J. Sun, T. Dutta, R. Parthasarathi, K. Ho Kim, N. Tolic, R. K. Chu, N. G. Isern, J. R. Cort, B. A. Simmons, “Rapid room temperature solubilization and depolymerization of polymeric lignin at high loadings,” *Green Chem.*, vol. 18, pp. 6012–6020, 2016.

[127] C. W. Lahive, P. J. Deuss, C. S. Lance, Z. Sun, D. B. Cordes, C. M. Young, F. Tran, A. M. Z. Slawin, J. G. De Vries, P. C. J. Kamer, N. J. Westwood, and K. Barta, “Advanced Model Compounds for Understanding Acid-Catalyzed Lignin Depolymerization: Identi fi cation of Renewable Aromatics and a Lignin-Derived Solvent,” *J. Am. Chem. Soc.*, no. 138, pp. 8900–8911, 2016.

[128] S. Li, N. Li, G. Li, L. Li, A. Wang, Y. Cong, X. Wang, and T. Zhang, “Lignosulfonate-based acidic resin for the synthesis of renewable diesel and jet fuel range alkanes with 2-methylfuran and furfural,” *Green Chem.*, vol. 17, no. 6, pp. 3644–3652, 2015.

[129] B. O. Myrvold, “Differences in solubility parameters and susceptibility to salting-out between softwood and hardwood lignosulfonates,” *Holzforschung*, vol. 70, no. 11, pp. 1015–1021, 2016.

[130] R. Singh, A. Prakash, S. K. Dhiman, B. Balagurumurthy, A. K. Arora, S. K. Puri, and T. Bhaskar, “Hydrothermal conversion of lignin to substituted phenols and aromatic ethers,” *Bioresour. Technol.*, vol. 165, pp. 319–322, 2014.

[131] Q. Tian, N. Li, J. Liu, M. Wang, J. Deng, J. Zhou, and Q. Ma, “Catalytic Hydrogenation of Alkali Lignin to Bio-oil Using Fullerene- like Vanadium Sulfide,” *Energy & Fuels*, vol. 29, pp. 255–261, 2015.

[132] C. S. Caetano, L. Guerreiro, I. M. Fonseca, A. M. Ramos, J. Vital, and J. E. Castanheiro, “Esterification of fatty acids to biodiesel over polymers with sulfonic acid groups,” *Appl. Catal. A Gen.*, vol. 359, no. 1–2, pp. 41–46, 2009.

[133] Q. Zhang, Y. Xu, Y. Li, T. Wang, Q. Zhang, L. Ma, M. He, and K. Li, “Investigation on the esterification by using supercritical ethanol for bio-oil upgrading,” *Appl. Energy*, vol. 160, pp. 633–640, 2014.

[134] T. Zhang, Y. Zhou, D. Liu, and L. Petrus, “Qualitative analysis of products formed during the acid catalyzed liquefaction of bagasse in ethylene glycol,” *Bioresour. Technol.*, vol. 98, pp. 1454–1459, 2007.

[135] L. Moghaddam, Z. Zhang, R. M. Wellard, J. P. Bartley, I. M. O’Hara, and W. O. S. Doherty, “Characterisation of lignins isolated from sugarcane bagasse pretreated with acidified ethylene glycol and ionic liquids,” *Biomass and Bioenergy*, vol. 70, pp. 498–512, 2014.

[136] S. Kubo, T. Yamada, K. Hashida, and H. Ono, “Grafting of Ethylene Glycol Chains in Lignin during the Solvolysis for Biomass Conversion Using Ethylene Carbonate / Ethylene Glycol System,” *Chem. Lett.*, vol. 36, no. 4, 2007.

[137] L. Mu, Y. Shi, H. Wang, and J. Zhu, “Lignin in Ethylene Glycol and Poly(ethylene glycol): Fortified Lubricants with Internal Hydrogen Bonding,” *Sustain. Chem. Eng.*, vol. 4, pp. 1840–1849, 2016.

[138] J. R. Rostrup-Nielsen, “Some principles relating to the regeneration of sulfur-poisoned nickel catalyst,” *J. Catal.*, vol. 21, no. 2, pp. 171–178, 1971.

[139] J. J. Rehr, J. J. Kas, F. D. Vila, M. P. Prange, and K. Jorissen, “Sulfur poisoning mechanism of steam reforming catalysts: an X-ray absorption near edge structure (XANES) spectroscopic study,” *Phys. Chem. Chem. Phys.*, vol. 12, no. 21, pp. 5503–5513, 2010.

[140] E. B. MAXTED, “The Poisoning of Metallic Catalysts,” *Adv. Catal.*, vol. 3, pp. 129–178, 1951.

[141] A. Q. M. Boon and J. B. Powell, “Method of extending biomass conversion catalyst life,” US15378099, 2017.

[142] Y. Hamabe, S. Jung, and H. Suzuki, “Quasi in situ Ni K -edge EXAFS investigation of the spent NiMo catalyst from ultra-deep hydro- desulfurization of gas oil in a commercial plant research papers,” *Synchrotron Radiat.*, vol. 17, pp. 530–539, 2010.

[143] J. Wadenback, D. Clapham, G. Gellerstedt, and S. Von Arnold, “Variation in content

and composition of lignin in young wood of Norway spruce," *Holzforschung*, vol. 58, pp. 107–115, 2004.

[144] J. C. Hicks, "Advances in C-O bond transformations in lignin-derived compounds for biofuels production," *J. Phys. Chem. Lett.*, vol. 2, no. 18, pp. 2280–2287, 2011.

[145] J.-L. Wen, S.-L. Sun, T.-Q. Yuan, and R.-C. Sun, "Structural elucidation of whole lignin from Eucalyptus based on preswelling and enzymatic hydrolysis," *Green Chem.*, vol. 17, no. 3, pp. 1589–1596, 2015.

[146] H. S. Yin, H. M. Liu, and Y. L. Liu, "Structural characterization of lignin in fruits and stalks of Chinese quince," *Molecules*, vol. 22, no. 6, pp. 889–902, 2017.

[147] Y. Demirel, "Energy and Energy Types," in *Energy Production, Conversion, Storage, Conservation and Coupling*, London, 2012, pp. 27–70.

[148] J. B. Nielsen, A. Jensen, C. B. Schandel, C. Felby, and A. D. Jensen, "Solvent consumption in non-catalytic alcohol solvolysis of biorefinery lignin," *Sustain. Energy Fuels*, vol. 1, no. 9, pp. 2006–2015, 2017.

[149] T. Parsell, S. Yohe, J. Degenstein, T. Jarrell, I. Klein, E. Gencer, B. Hewetson, M. Hurt, J. I. Kim, H. Choudhari, B. Saha, R. Meilan, N. Mosier, F. Ribeiro, W. N. Delgass, C. Chapple, H. I. Kenttämaa, R. Agrawal, and M. M. Abu-omar, "A synergistic biorefinery based on catalytic conversion of lignin prior to cellulose starting from lignocellulosic biomass," *Green Chem.*, vol. 17, pp. 1492–1499, 2015.

[150] M. Grilc, B. Likozar, and J. Levec, "Simultaneous Liquefaction and Hydrodeoxygenation of Lignocellulosic Biomass over NiMo/Al2O3, Pd/Al2O3, and Zeolite y Catalysts in Hydrogen Donor Solvents," *ChemCatChem*, vol. 8, no. 1, pp. 180–191, 2016.

[151] M. Castellvi Barnes, J. Oltvoort, S. R. A. Kersten, and J. Lange, "Wood Liquefaction - role of solvent," *Ind. Eng. Chem. Res.*, vol. 56, pp. 635–644, 2017.

[152] H. Nimz, "Beech Lignin—Proposal of a Constitutional Scheme," *Angew. Chemie Int. Ed. English*, vol. 13, no. 5, pp. 313–321, 1974.

[153] B. El Khaldi-hansen, M. Schulze, and B. Kamm, "Qualitative and Quantitative Analysis of Lignins from Different Sources and Isolation Methods for an Application as a Biobased Chemical Resource and Polymeric Material," in *Analytical Techniques and Methods for Biomass*, 2016, pp. 15–44.

[154] P. Sannigrahi, Y. Pu, and A. Ragauskas, "Cellulosic biorefineries-unleashing lignin opportunities," *Curr. Opin. Environ. Sustain.*, vol. 2, pp. 383–393, 2010.

[155] Ö. P. Çetinkol, A. M. Smith-Moritz, G. Cheng, J. Lao, A. George, K. Hong, R. Henry, B. A. Simmons, J. L. Heazlewood, and B. M. Holmes, "Structural and Chemical Characterization of Hardwood from Tree Species with Applications as Bioenergy Feedstocks," *PLoS One*, vol. 7, no. 12, 2012.

[156] L. Mbotchak, C. Le Morvan, K. L. Duong, B. Rousseau, M. Tessier, and A. Fradet, "Purification, Structural Characterization, and Modification of Organosolv Wheat

Straw Lignin," *J. Agric. Food Chem.*, vol. 63, pp. 5178–5188, 2015.

[157] D. Gao, H. Yin, A. Wang, L. Shen, and S. Liu, "Gas phase dehydrogenation of ethanol using maleic anhydride as hydrogen acceptor over Cu / hydroxylapatite , Cu / SBA-15 , and Cu / MCM-41 catalysts," *J. Ind. Eng. Chem.*, vol. 26, pp. 322–332, 2015.

[158] M. Zhou, P. Liu, K. Wang, J. Xu, and J. Jiang, "Catalytic hydrogenation and one step hydrogenation-esterification to remove acetic acid for bio-oil upgrading: model reaction study," *Catal. Sci. Technol.*, vol. 6, pp. 7783–7792, 2016.

Appendices

Appendix A:
Supplementary Information for Chapter 4

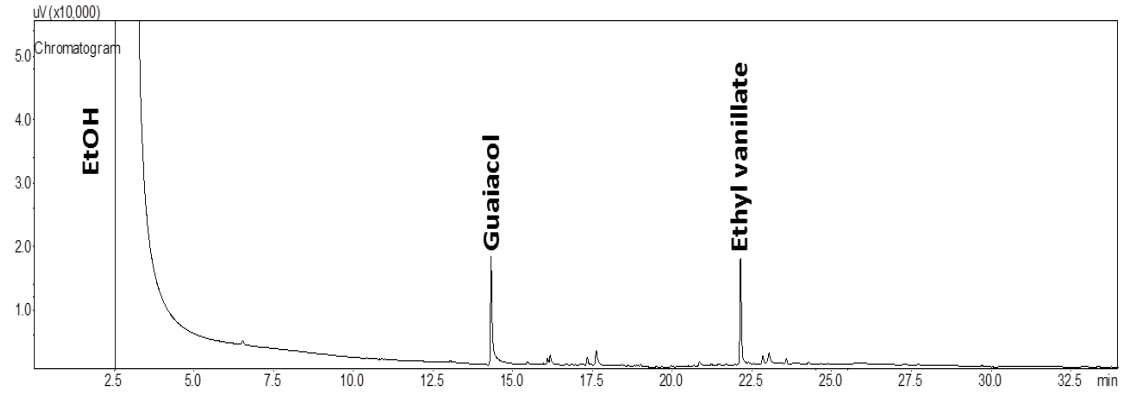

Figure A1 GC-MS analysis of the oil fraction from conversion of H-LS over Ni/SiO_2 catalyst in ethanol medium. Reaction condition: 0.75 g catalyst, 7.5 g H-LS, 75 ml solvent, initial H_2 loading of 50 bar at RT, 250 ˚C, 3 hours.

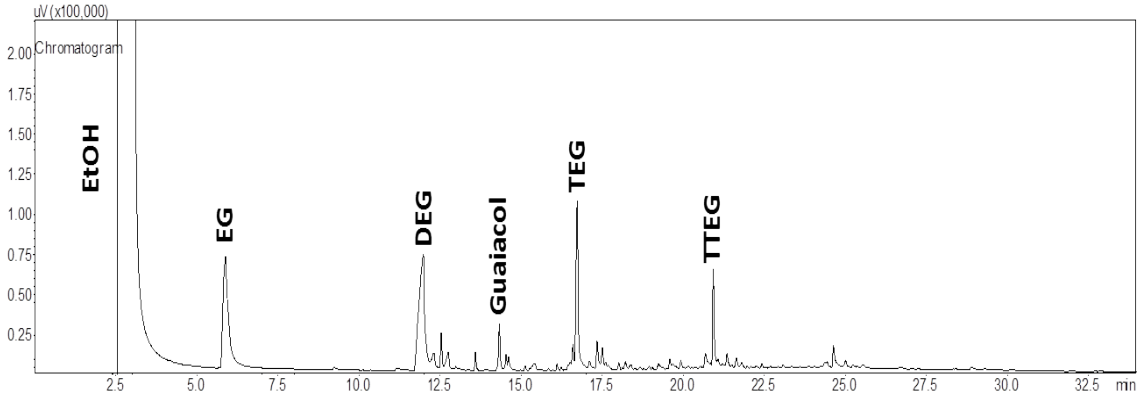

Figure A2 GC-MS analysis of the oil fraction from conversion of H-LS over Ni/SiO_2 catalyst in ethylene glycol medium. Reaction condition: 0.75 g catalyst, 7.5 g H-LS, 75 ml solvent, initial H_2 loading of 50 bar at RT, 250 ˚C, 3 hours

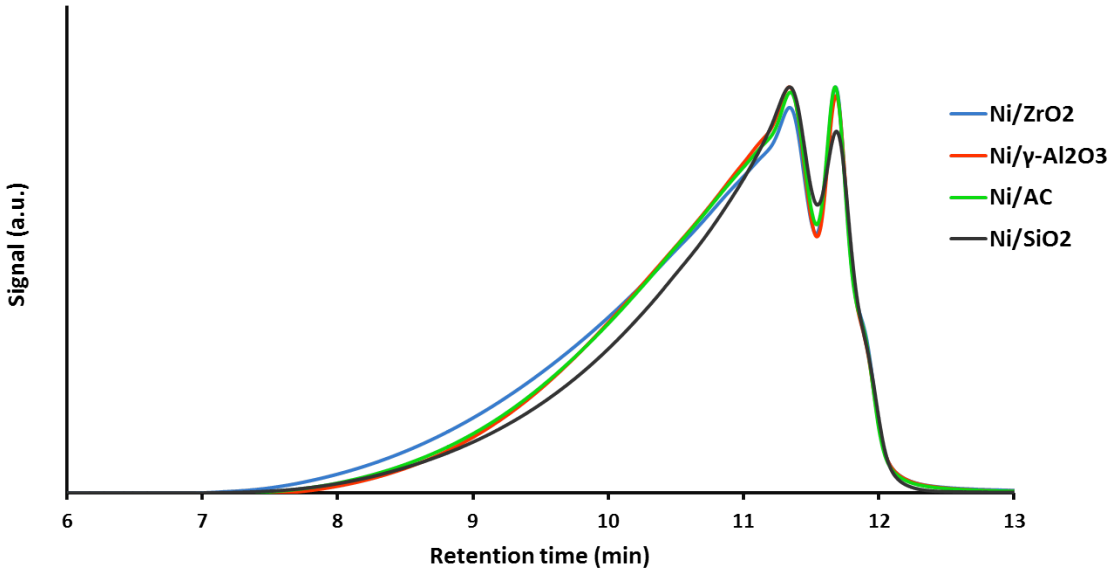

Figure A3 SEC of catalytic oil produced from conversion of H-LS in EtOH over Ni supported on SiO_2, AC, ZrO_2 and **γ**-Al_2O_3. Reaction condition: 0.75 g catalyst, 7.5 g H-LS, 75 ml solvent, initial H_2 loading of 50 bar at RT, 250 ˚C, 3 hours.

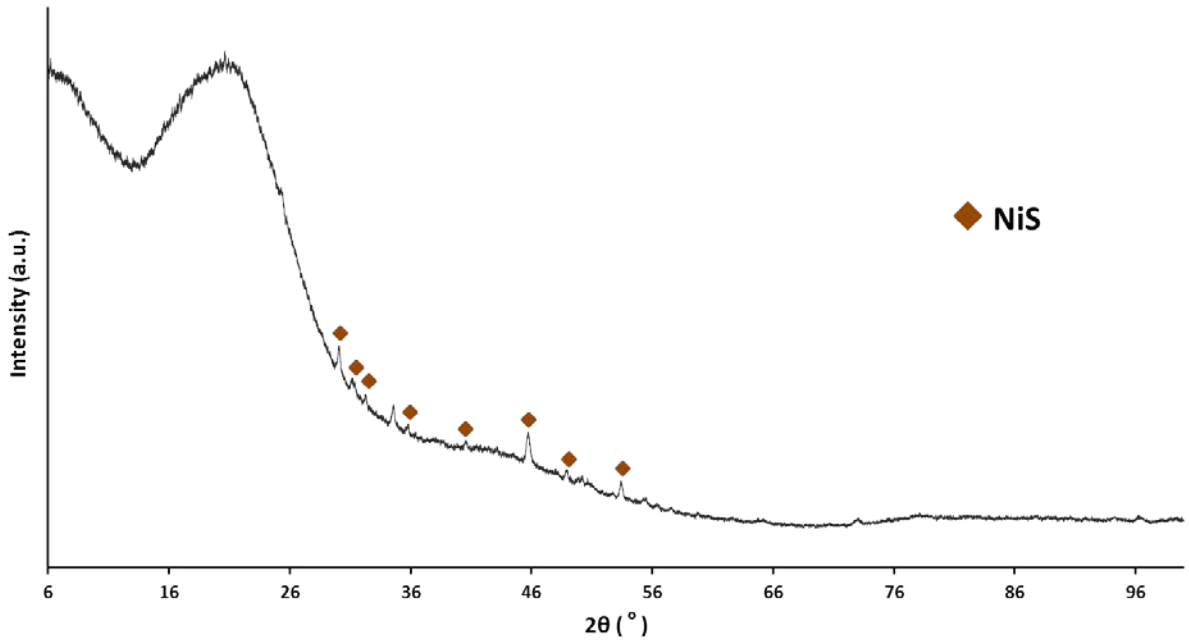

Figure A4 XRD pattern of the solid residue from conversion of H-LS over Ni/SiO_2 catalyst. The peaks for NiS are specified. Reaction condition: 0.75 g catalyst, 7.5 g lignin, 75 ml solvent, initial H_2 loading of 50 bar at RT, 250 ˚C, 3 hours.

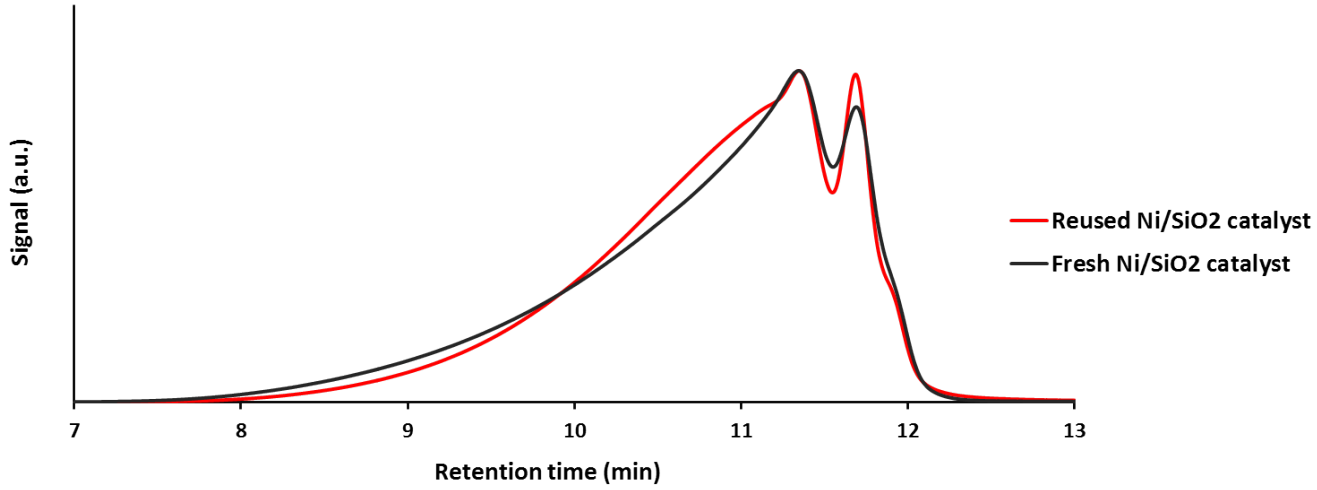

Figure A5 SEC of catalytic oil products from conversion of H-LS in EtOH over fresh and reused Ni/SiO_2 catalyst. Reaction condition: 0.75 g catalyst, 7.5 g H-LS, 75 ml solvent, initial H_2 loading of 50 bar at RT, 250 ˚C, 3 hours.

Appendix B:
Supplementary Information for Chapter 5

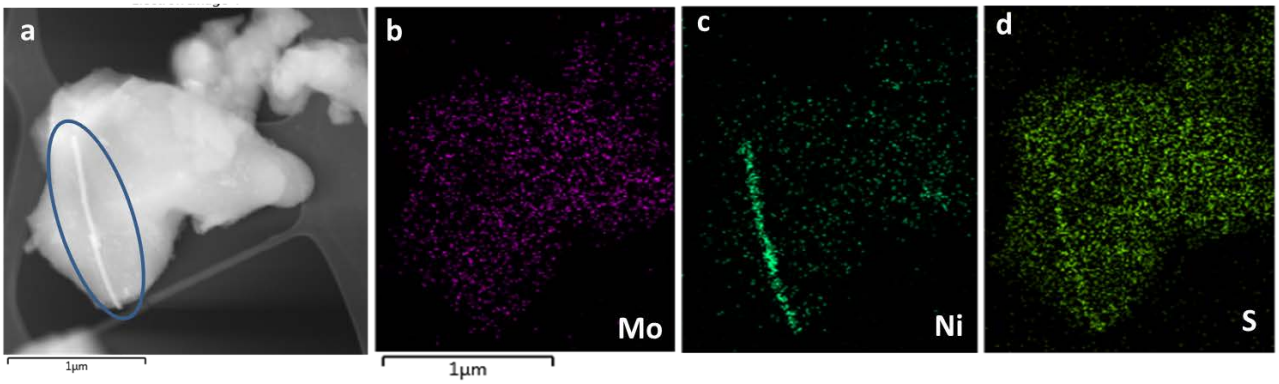

Figure B1 EDX mapping of the spent non pre-sulfided NiMo-II catalyst from reaction of H-LS at 310 ˚C: Accumulation of Ni and formation of Ni_3S_2. Reaction condition: 1 g NiMo-II catalyst, 10 g lignin, 100 ml ethanol, 26 bar H_2 (loaded at RT), 3 hours.

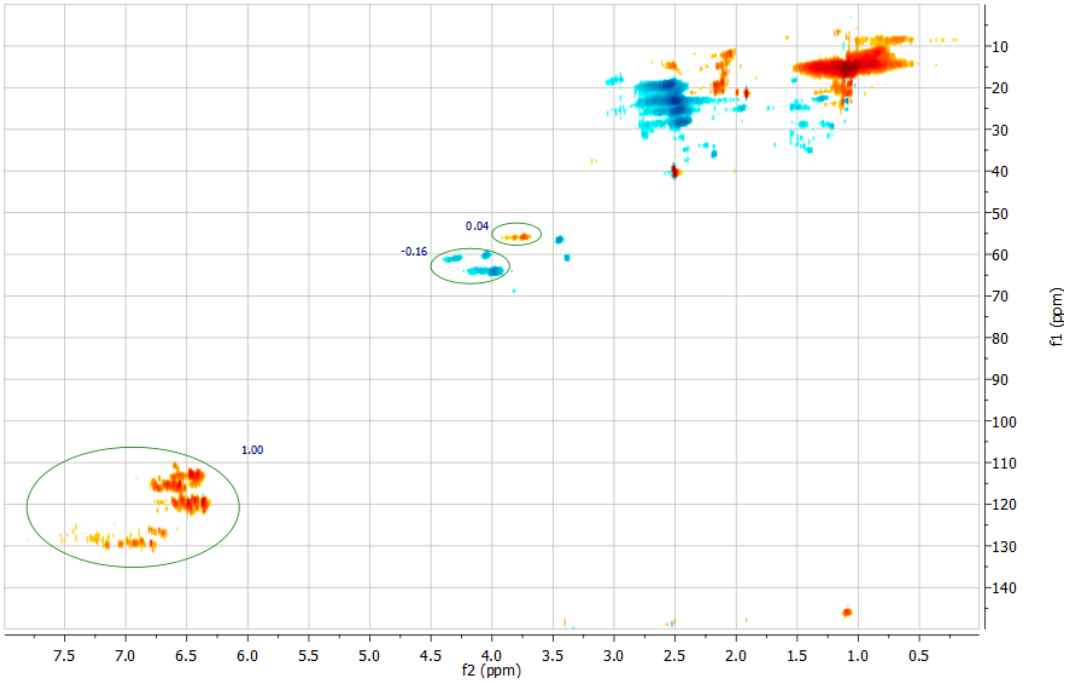

Figure B2 HSQC NMR of the oil fraction from catalytic conversion of H-LS in nitrogen atmosphere at 310 ˚C (Table 13, Entry 3). Reaction condition: 1 g catalyst, 10 g lignin, 100 ml ethanol, 8 bar N_2 (loaded at RT), 3 hours.

Figure B3 The physical appearance of the solid fractions from non-catalytic and catalytic conversion of H-LS at 310 ˚C (Table 13, Entry 1 & 2). (Right): Non catalytic solid, (Left): Catalytic solid. Reaction condition: 0/1 g catalyst: 10 g lignin: 100 ml solvent, 26 bar H_2 (loaded at RT), 3 hours.

Table B1 The selectivity of the compounds identified by GC-MS-FID analysis of the oil fractions from conversion of H-LS over non pre-sulfided and pre-sulfided NiMo-I at 310 ˚C (Table 13, Entry 7 & 8). 0.5 catalyst: 5 g lignin: 50 ml ethanol, 26 bar H_2 (loaded at RT), 3 hours.

Compound group	**Non pre-sulfided NiMo**	**Pre-sulfided NiMo**
Alkyl phenol %	36.6	39.9
Alkoxy alkyl phenol %	28.4	29.1
Alkoxy alkyl benzene %	34.9	31.0
Mono-oxygen compounds %	57.2	52.3
Di-oxygen compounds %	42.8	47.7

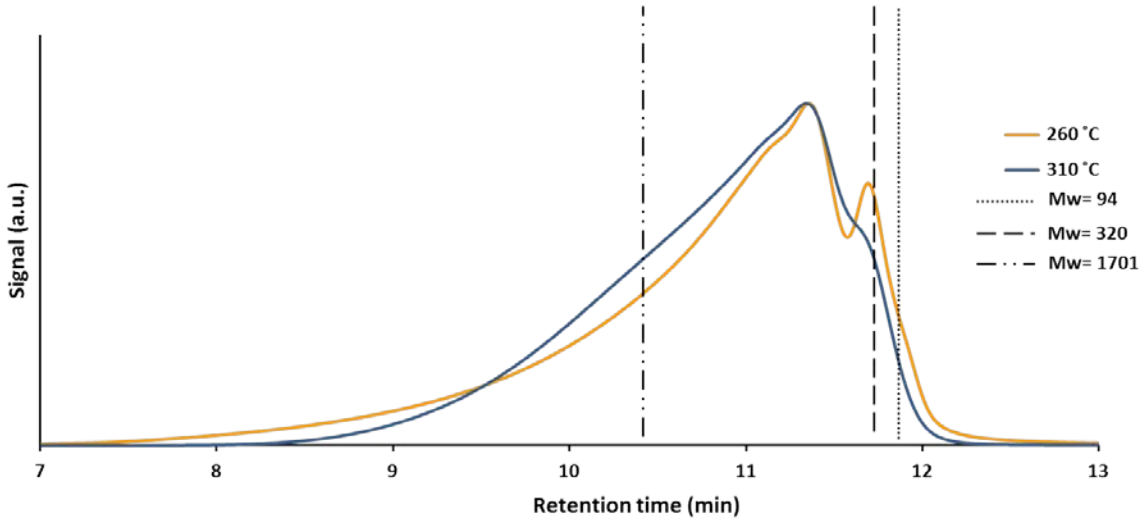

Figure B4 SEC results of the oil fractions obtained from catalytic conversion of H-LS at 260 and 310 ˚C. Loading at 260 ˚C: 1 g catalyst: 10 g lignin: 100 ml ethanol. Loading at 310 ˚C: 0.5 g catalyst: 5 g lignin: 50 ml ethanol. 26 bar H_2 (loaded at RT), 3 hours.

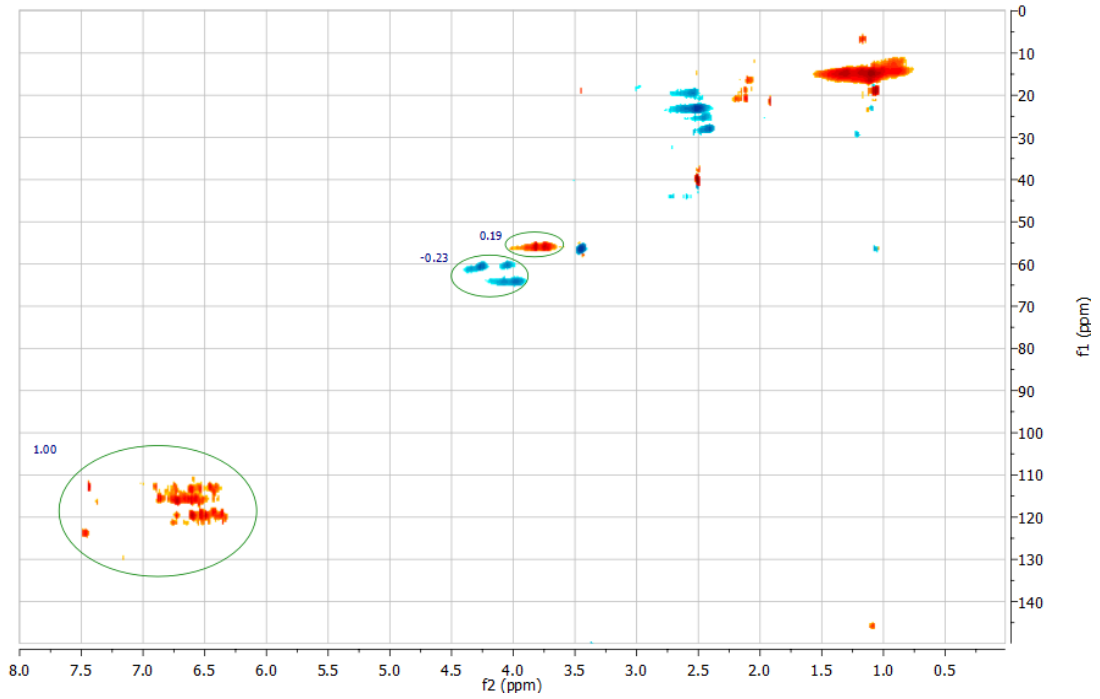

Figure B5 HSQC NMR of the oil fraction from catalytic conversion of H-LS at 310 ˚C and 1 hour reaction time. Reaction condition: 1 g catalyst, 10 g lignin, 100 ml ethanol, 26 bar H_2 (loaded at RT).

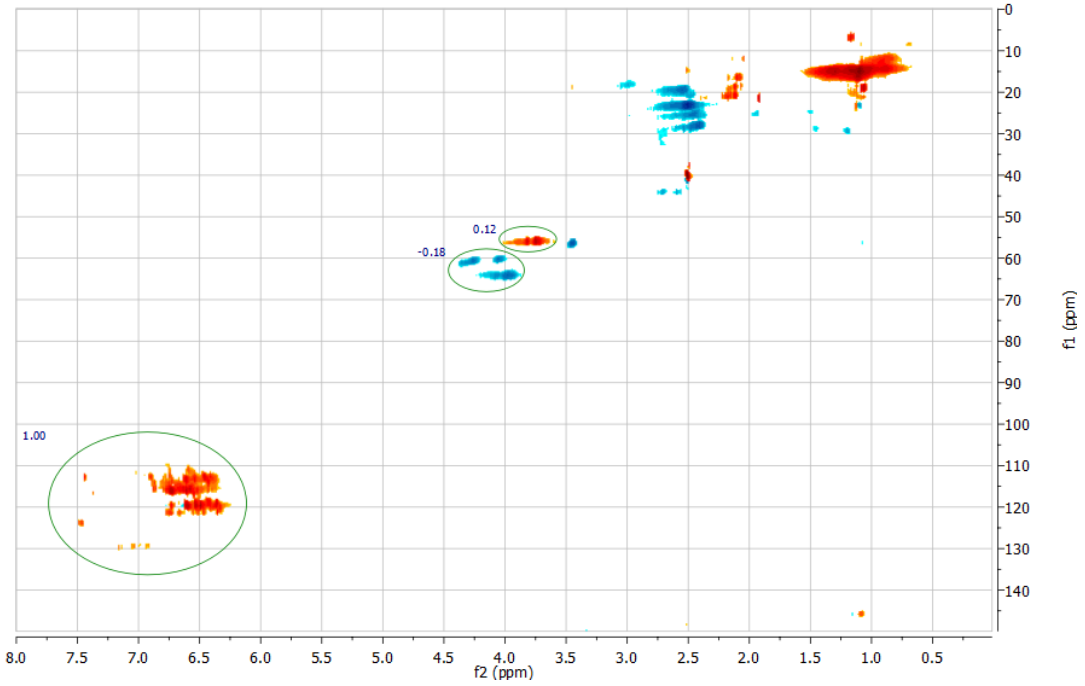

Figure B6 HSQC NMR of the oil fraction from catalytic conversion of H-LS at 310 ˚C and 2 hours reaction time. Reaction condition: 1 g catalyst, 10 g lignin, 100 ml ethanol, 26 bar H_2 (loaded at RT).

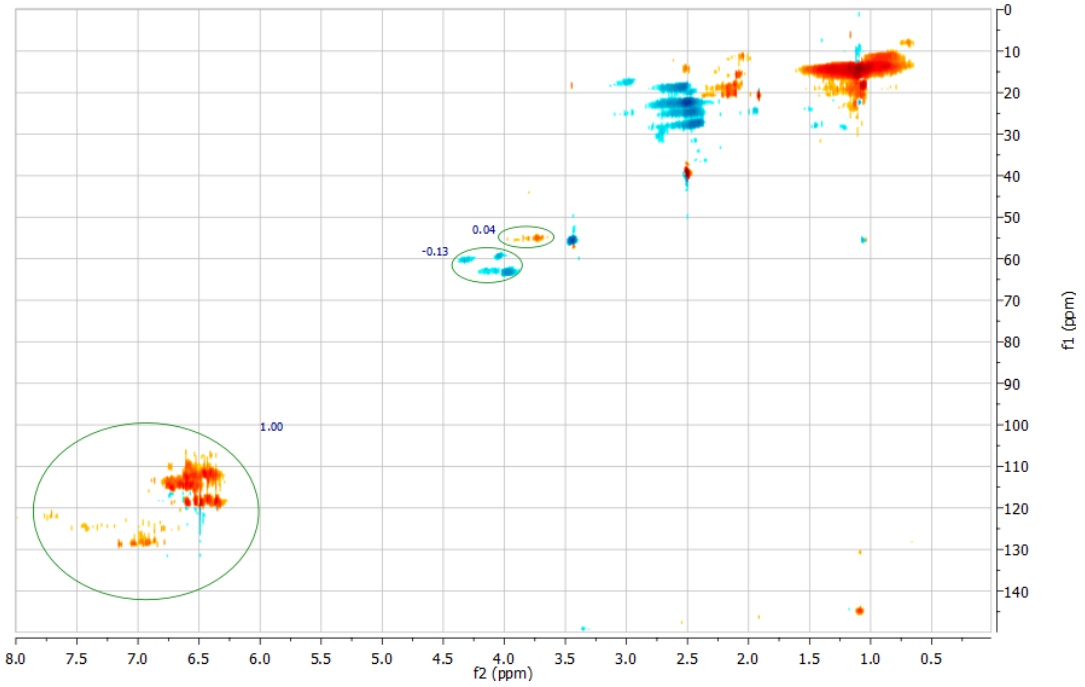

Figure B7 HSQC NMR of the oil fraction from catalytic conversion of H-LS at 310 ˚C and 4 hours reaction time. Reaction condition: 1 g catalyst, 10 g lignin, 100 ml ethanol, 26 bar H_2 (loaded at RT).

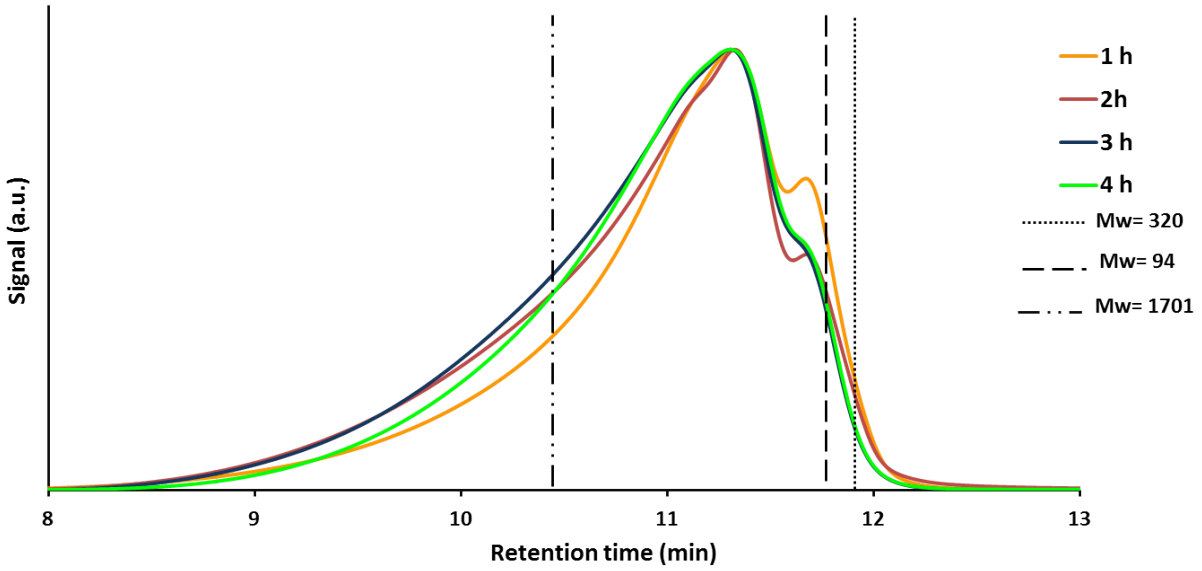

Figure B8 SEC of the oil fractions from catalytic conversion of H-LS at 310 ˚C for different reaction times. Reaction condition: 1 g catalyst, 10 g lignin, 100 ml ethanol, 26 bar H_2 (loaded at RT).

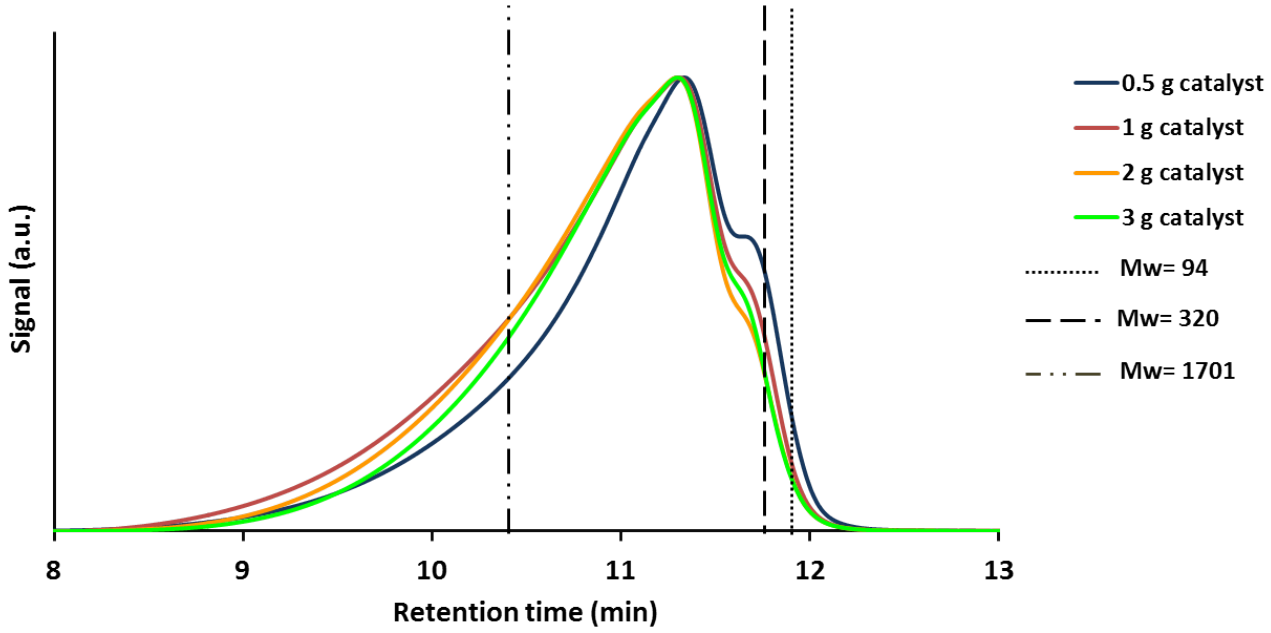

Figure B9 SEC of the oil fractions from catalytic conversion of H-LS at 310 ˚C with varied catalyst loading. Reaction condition: 0.5, 1, 2 and 3 g catalyst, 10 g lignin, 100 ml ethanol, 26 bar H_2 (loaded at RT), 3 hours.

Ethanol consumption

In order to evaluate ethanol consumption at 310 ˚C, two ethanol control tests with and without catalyst were conducted and the results were compared to the lignin conversion tests. The cold pressure after ethanol control tests in non-catalytic and catalytic conditions at 310 ˚C were 31 and 33 bar, respectively. This observation indicated continuous gas formation from degradation of ethanol and light phases, which are undesired reactions. The cold pressure in non-catalytic conversion of lignin was 26 bar, while the same number for catalytic test was 22 bar. The detailed gas phase analysis is shown in Table B2. 207 mmol of C_2^+ gases were detected form conversion of ethanol over pre-sulfided NiMo-I in control test, corresponding to 72 wt.% of the gases in the gaseous products, and equals to 12.1% of the carbons in the fed ethanol. However, in the gas phase from catalytic conversion of H-LS, 44 mmol C_2^+ was detected which was considerably lower compared to the control test.

Table B2 GC analysis of the gas phases from conversion of lignin and control tests in non-catalytic and catalytic condition. 0/1 g catalyst, 0/10 g H-LS, 100 ml ethanol, 26 bar H_2 (loaded at RT), 3 hours.

Gas	**Control tests**		**Lignin tests**	
[mmol]	Non-Catalytic	Catalytic	Non-Catalytic	Catalytic
CO	2	1	7	3
CO_2	0	9	10	10
CH_4	1	6	1	9
C_2^+	3	207	12	44
H_2	254	43	192	98

The GC-MS analysis of the light phases from non catalytic and catalytic ethanol control tests and catalytic conversion of lignin are shown in Table B3 and Figure B10. Methanol (retention time: 2.4 min) is produced *in-situ* from ethanol. Ethyl acetate (retention time: 4.1 min) may be produced from ethanol dehydrogenation [157]. Ethyl acetate can also be a product from reaction between ethanol and acetic acid. We did not detect acetic acid in the reaction products, which presumably reacted with ethanol forming ethyl acetate, or degraded to CH_4 and CO_2. These reactions are promoted over NiMo catalysts [158]. Compounds such as 1-butanol (retention time: 5.2 min) are produced via condensation reactions between two molecules of ethanol and dehydration. Formation of diethyl acetal (retention time: 6.5 min) can be through reaction of ethanol and acetaldehyde via Guerbet reactions. The esteric compounds were detected in the reaction products of ethanol, including propanoic acid ethyl ester (retention time: 6.1 min) and butanoic acid ethyl ester (retention time: 8.2 min) formed possibly through Cannizzaro/Tishchenko reactions [148]. A peak at retention time of 5.8 was detected in the light phase of catalytic tests (ethanol control test and H-LS reaction), which indicated formation of diethyl sulfide. This compound is originated from DMDS (which was added for keeping sulfidation state of catalyst) in ethanol control test, and from sulfur in lignosulfonate structure. Diethyl sulfide is known as a by-product from reaction of ethylene with H_2S over alumina based catalyst and production of ethanethiol. However, we did not detect ethanethiol in the light phase, which may have evaporated upon opening the autoclave (boiling point: 35 ˚C).

The ethanol content was considerably lower in control catalytic tests compared to non-catalytic and catalytic conversion of H-LS. Concentration of ethyl acetate increased from 0.8 % in the absence of catalyst (control test) to 6.0 % in catalytic test. However, 1.9 % ethyl acetate was detected in catalytic conversion of H-LS. Formation of esteric compounds was catalyzed over NiMo catalyst in ethanol control test, while they were detected in trace amounts in the light phase from conversion of H-LS. These observations are aligned with the results in the gas phase, which show ethanol reactions are catalyzed over NiMo catalyst, but are limited in the presence of lignin, presumably due to the coverage of the catalytic active phases with lignin derived fragments and therefore inhibiting ethanol conversion.

Table B3 GC-MS of light fractions from non-catalytic and catalytic control tests and H-LS conversion in the presence of catalyst. Reaction condition: 0/1 g catalyst, 0/10 g H-LS, 100 ml ethanol, 26 bar H_2 (loaded at RT), 3 hours.

Compound	**Retention time [min]**	**Control tests**		**Catalytic, H-LS**
		Non-Catalytic %	Catalytic %	
Methanol	2.4	0.4	0.4	0.2
Ethanol	2.9	95.6	62.5	84.3
Ethyl acetate	4.1	0.8	6.0	1.9
1-Butanol	5.2	0.1	1.1	0.1
Diethyl sulfide	5.8	-	0.4	0.2
Propanoic acid ethyl ester	6.1	-	1.3	< 0.1
Diethyl acetal	6.5	1.1	1.9	1.1
Butanoic acid ethyl ester	8.2	-	0.5	0.1
Other compounds	-	0.2	1.6	< 0.1

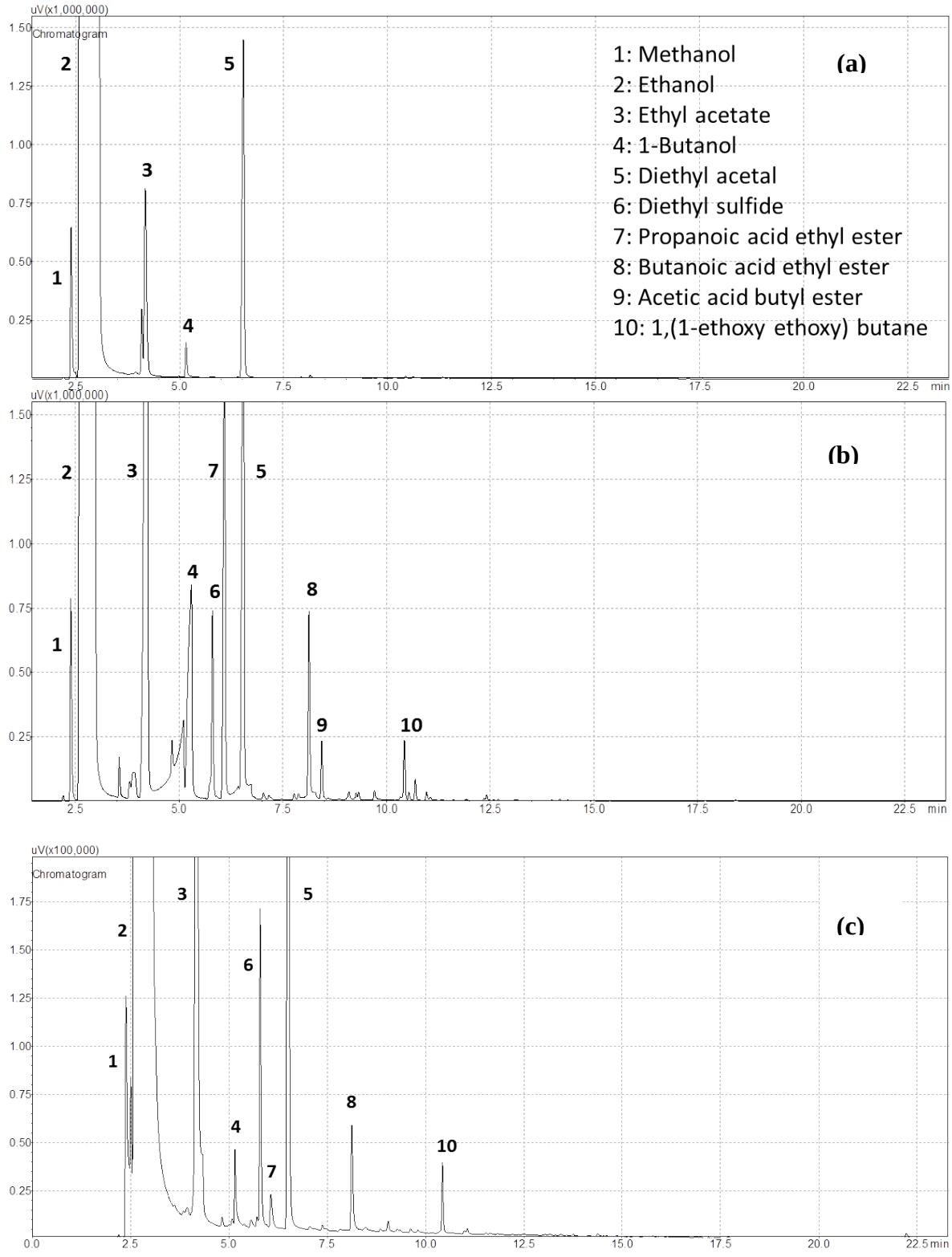

Figure B10 GC-MS analysis of the light phases from control tests and lignin conversion at 310 ˚C (a) light phase from non-catalytic control test, (b) light phase from catalytic control test, (c) light phase from catalytic conversion of lignin. Reaction condition: 0/1 g catalyst, 0/10 g H-LS, 100 ml ethanol, 26 bar H_2 (loaded at RT), 3 hours.

Appendix C:
Supplementary Information for Chapter 6

Table C1 The identified light products from conversion of beech wood over sulfided $NiMo/Al_2O_3$ at 300 ˚C. 1 g catalyst: 10 g beech wood, 100 ml ethanol, 26 bar H_2 (loaded at RT), 3 hours.

Retention time (min)	Compound	Area %	Holocellulose[a]	EtOH[a]
Alcohols				
3.56	1-Propanol	0.20	*	*
5.21	Butanol	1.01	*	*
8.44	Propylene glycol	0.06	*	*
11.37	2,4-dimethyl 1-Heptanol	0.20	*	*
12.15	1-Nonanol	0.06	*	-
Aldehydes				
2.38	Acetaldehyde	1.8	*	*
Esters				
6.05	Propanoic acid ethyl ester	0.43	*	*
8.11	Butanoic acid ethyl ester		*	*
9.68	2-Propanol, 1-(2-methylpropoxy)	0.05	*	*
10.35	Pentanoic acid ethyl ester	0.12	*	-
10.58	Acetic acid, ethoxy-, ethyl ester	0.02	*	*
Ethers				
6.16	Ethanol, 2-ethoxy	0.09	*	-
6.5	1,1-diethoxy ethane	1.13	*	*
7.09	1-ethoxy, 2-propanol	0.04	*	*
7.40	1-ethoxy, butane	0.19	*	*
8.32	2-ethoxy, butane	0.01	*	*
8.58	2-ethoxypentane	0.04	*	*
8.79	Ethylene glycol monovinyl ether	0.03	*	*
9.52	4-ethoxy 1-butanol	0.01	*	*
10.03	2-ethoxy, butane	0.03	*	-
10.41	1,1-diethoxy butane	0.07	*	*
10.52	1-ethoxy, 3-pentanol	0.02	*	*
10.68	1-(1-ethoxyethoxy), butane	0.03	*	*
10.79	2-Ethoxypentane	0.05	*	*
Ketones				
5.53	2-Pentanone	0.20	*	-
7.76	3-Hexanone	0.10	*	-
7.87	2-Hexanone	0.21	*	-
9.10	2-Methyl, cyclopentanone	0.18	*	-
9.24	3-Methyl, cyclopentanone	0.04	*	-
9.77	4-Heptanone	0.05	*	-
10.16	2-Octanone	0.03	*	-
11.29	Cyclopentanone	0.09	*	-
11.91	4-Octanone	0.02	*	-
Furans				
5.94	2,5-Dimethylfuran	0.23	*	-
13.97	Furanmethanol-tetrahydro	0.19	*	-

[a] It is specified by * whether the compounds were detected from conversion of holocellulose or ethanol

Table C2 Elemental analysis, atomic O/C and H/C ratio and high heating value of beech wood and the oil fractions from conversion of beech wood over sulfided $NiMo/Al_2O_3$. 1 g catalyst: 10 g beech wood, 100 ml ethanol, 26 bar H_2 (loaded at RT), 3 hours.

Sample	C wt%	H wt%	N wt%	S wt%	O wt%	Atomic O/C ratio	Atomic H/C ratio	HHV (MJ/kg)
Beech wood	53.0	5.8	0.1	-	41.0	0.58	1.32	18.9
Oil at 200 ˚C	59.2	7.5	0.4	2.7	30.9	0.39	1.52	25.2
Oil at 260 ˚C	59.0	7.4	0.4	1.3	31.9	0.41	1.51	24.8
Oil at 280 ˚C	61.4	8.4	0.4	-	29.8	0.36	1.64	27.4
Oil at 300 ˚C	60.9	8.2	0.3	1.0	29.6	0.36	1.61	26.9

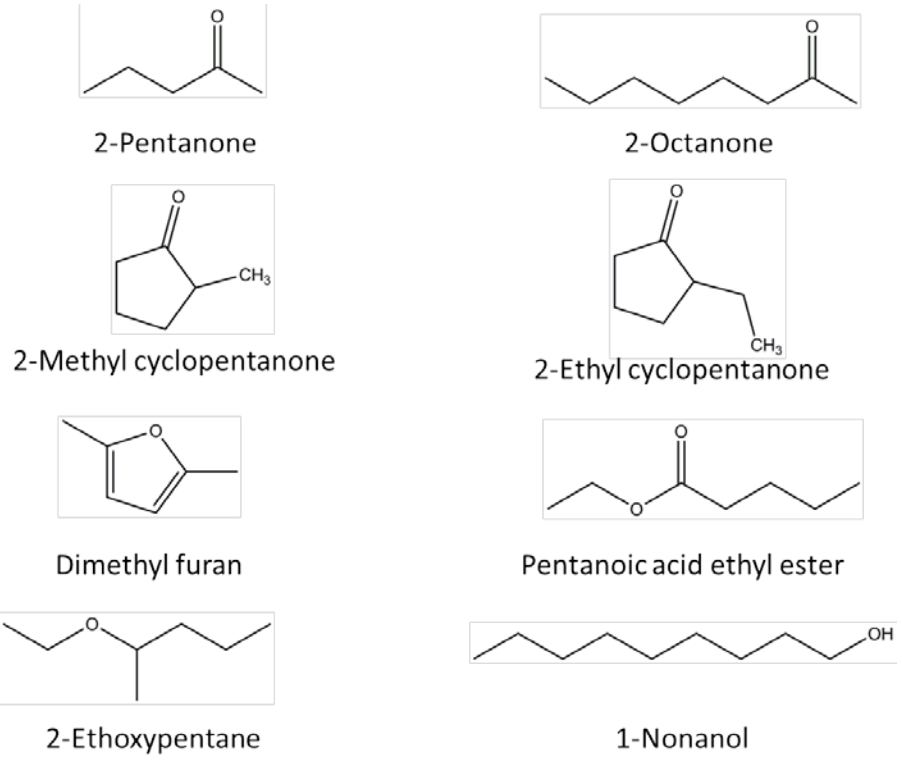

Figure C1 Structure of sugar derived compounds from conversion of beech wood over sulfided $NiMo/Al_2O_3$ in ethanol